Assimilable Organic Carbon Formation during Ultraviolet-Hydrogen Peroxide Advanced Oxidation Treatment of Surface Water

by

Mohammad Mahdi Bazri

B.Sc. Sharif University of Technology, 2008

A THESIS SUBMITTED IN PARTIAL FULFILMENT OF

THE REQUIREMENTS FOR THE DEGREE OF

MASTER OF APPLIED SCIENCE

in

The Faculty of Graduate Studies

(Chemical and Biological Engineering)

THE UNIVERSITY OF BRITISH COLUMBIA

(Vancouver)

November 2010

Abstract

Practice of UV/H_2O_2 advanced oxidation treatment has emerged as viable alternative for removing micro-pollutants and other organic contaminants from surface water. However, presence of natural organic matter (NOM) in water is problematic and hinders the efficacy of the treatment process. Indeed, NOM can undergo significant partial oxidation leading to generation of smaller more easily assimilable organic molecules (i.e., AOC). Earlier studies have found AOC as the potential cause of bacterial regrowth and other water health concerns thereof within the distribution system. Nonetheless, impact of UV/H_2O_2 process on biostability of downstream water has not gained much attention. However, a method recently developed by Hammes and Egli (2005) opened the opportunity for more accurate and relatively rapid quantification of the AOC. The main focus of this research was to modify and evaluate the protocol of Hammes and Egli (2005) for quantifying the biostability of water before and after UV/H_2O_2 process. More importantly, this research aimed to contribute substantially to the current understanding of easily assimilable organic molecules formation during UV/H_2O_2 treatment. As a result, different characterization techniques (e.g., HPSEC, UV_{254}, and TOC) were utilized to monitor transformation of NOM and to study the relationships among different NOM characteristics (e.g., molecular size distribution, UV_{254}, and AOC). Considering the concerns associated with NOM (especially when oxidation is applied in the treatment train), elimination of NOM ahead of the oxidation process can potentially increase the UV/H_2O_2 treatment efficacy as well as the finished water quality. Moreover, as the regulations become more stringent, many utilities hope to comply with them by retrofitting existing facilities and avoiding the construction of new ones. Thus, this research also focused to investigate the impact of a pre-treatment process such as coagulation to eliminate NOM prior to UV/H_2O_2 treatment. Using coagulation as pretreatment ahead of UV/H_2O_2 will be potentially of interest for those utilities that are currently applying

coagulation and hope to comply with new regulations by minimum capital investment. More importantly, this would be beneficial because of the need to improve process efficacy and also final water quality and the reduced formation of disinfection by-products (DBPs) within the distribution system.

Preface

An identical version of Appendix A has been submitted to the Journal of Environmental Engineering for the final review. My contribution to this work was writing and debugging the programming code, and providing the model predicted results. Dr. Siva Sarathy developed the model equations and collected and analyzed the data in addition to writing the manuscript.

Table of Contents

List of Tables

List of Figures

Acknowledgments

My extreme gratitude is to my supervisor, Prof. Madjid Mohseni for all his support, guidance, and companionship during the past two years. I would like to thank him for trusting me and giving me the opportunity to work and research under his supervision. Without your help and your support it was impossible to overcome so many challenges that I encountered during this project. Thank you for enlarging my vision and teaching me how to become a useful person in future.

I would like thank Drs. Gustavo Imoberdorf, Siva Sarathy, Esteban Duran, and Adrian Vega for their kind help, inputs, and guidance through this project. I am so grateful for all the instructions, feedback, penetrating questions and challenges that you provided to me.

I also would like to thank Dr. Fariborz Taghipour for letting me to use his laboratory and equipments.

I would like to acknowledge the research, development and validation center for water treatment technologies and processes (CREDEAU) (Dr. Benoit Barbeau's Lab) at Ecole Polytechnique de Montreal, in particular Jacinthe Mailly and Sebastien Charest for their kind collaboration and conducting the BDOC experiments.

A very special thank is extended to Andy Johnson at Biomedical Research Centre (BRC) at UBC for the training on the FACS machine and all his helps throughout this project.

I offer my gratitude to Ayanna Leventure for her enormous contribution in conducting many of the experiments and showing an outstanding performance in the lab.

I also would like to extend my very best regards to my best friends, Seyyed Alireza Bagherzadeh and Amir Mehdi Dehkhoda for their constant companionship, courage and friendship throughout the past years. I feel so lucky for having such good friends.

I owe a very particular and sincere thank to my family, whose continuing courage and incredible support have always been motivating for me. Your support and trust has always made me determined and confident to tackle problems.

Dedication

First and foremost, I would like to dedicate this work to The Compassionate GOD, for His generous Grace, and everlasting Mercy in every single moment of my life. I am grateful for every single breath that He allows me to take and serve His creatures.

Secondly, I would like to devote the entire of this work to the persons whom I love the most: my parents and my sisters, for their continuing support, courage, companion and absolutely everything else. The words are not enough and strong to express and convey my cordial gratefulness and respect to you.

I also would like to dedicate this work to all people around the globe whom obtaining clean drinking water is an everyday challenge for them.

1 Introduction

1.1 Importance of Safe Drinking Water

Water is the lifeblood of the planet and a key substance for human life. It is a medium through which elements interact and also circulate within the environment. Furthermore, water is an important medium to carry natural and anthropogenic harmful contaminants. The quality of drinking water is a powerful environmental determinant of health. Water related diseases impose a terrible toll on human health, as two million people die every year from diarrheal diseases (including cholera) associated with inadequate clean water supply, sanitation and hygiene. The majority are children in developing countries (WHO, 2003). Health Canada estimates that unsafe drinking water is the cause of many illnesses and deaths every year (Ecojustice, 2006). However, these problems can be largely prevented through the practice of appropriate treatment processes as well as proper protection of the water sources.

1.2 Treatment Technologies and Challenges

While the practice of conventional treatment alternatives could be satisfactory in many cases including the removal of pathogens, such treatments are known to be susceptible to failure when challenged by recalcitrant micro-pollutants. Moreover, as the water quality regulations have become more stringent, the demand for reliable and robust treatment processes has increased. So, efforts have been made to address and overcome key water quality issues.

Researchers have, over the years, studied many different alternatives for the elimination of emerging micro-pollutants. Among the options proposed, one involves the use of a very strong oxidative environment, such as advanced oxidation, in which everything could potentially be converted to carbon dioxide and water. Advanced Oxidation Processes (AOPs) typically involve the generation of the nonselective highly reactive hydroxyl radical (•OH) that performs the

oxidation and degradation of target contaminants and species. As a result, these processes have gained much attention during the past decades and their application has shown to be promising in removing very aggressive compounds and micro-pollutants (Sarathy and Mohseni, 2006).

1.3 UV-based Advanced Oxidation Processes (AOPs)

Ultraviolet (UV) based AOPs are very promising for the elimination of taste and odor compounds, a broad range of micro-pollutants, and natural organic matter (NOM) from raw drinking water (Parsons and Byrne, 2004; Sarathy and Mohseni, 2006). Among various UV-based AOPs, UV and hydrogen peroxide (UV/H_2O_2) process is the only one currently applied commercially for the removal of organic contaminants in drinking water from surface water reservoirs (Tuhkanen, 2004; Sarathy and Mohseni, 2006). It has been applied for the abatement of pesticides, pharmaceuticals, and personal care products and endocrine disrupting compounds (Kruithof et al., 2002; 2007; Swaim et al., 2008; Andreozzi et al., 1999). However, in commercial application of UV/H_2O_2 process, presence of NOM, a complex mixture of organic compounds generated from the breakdown of animals and plants body materials, in water hinders the efficacy of UV/H_2O_2 process. NOM scavenges UV irradiation and hydroxyl radicals, leading to increased energy consumption. In addition, studies have shown that the conditions applied in commercial application of UV/H_2O_2 process in drinking water treatment could lead to partial oxidation of natural and complex organic molecules, potentially producing lower molecular weight organic compounds (Sarathy and Mohseni, 2007). Earlier studies have found smaller organic carbon molecules to be assimilable by the microorganisms present in water and the potential cause of bacterial regrowth and other water health concerns thereof within the distribution system (Escobar et al., 2001; Hem and Efraimsen, 2001). Hence, proper quantification and assessment of biological stability of water and measurement of assimilable organic carbon (AOC) during treatment with AOPs is crucial. In particular, it is essential to

assess how AOC and biostability of water are altered during the UV/H_2O_2 treatment, which is currently the most widely applied AOP in drinking water and re-use applications.

1.4 Assimilable Organic Carbon (AOC) Assay

Conventional AOC assay (Clescerl et al., 1999) involves indirect estimation of AOC via enumeration of the heterotrophic bacteria after regrowth. The result is stated in terms of acetate carbon equivalent (Kasahara and Ishikawa, 2002). This process was originally developed by Van der Kooij et al. (1982, 1992), and was later improved by LeChevallier et al. (1993) via raising the incubation temperature and inoculum density. However, limited information of actual biostability due to the utilization of pure cultures, i.e., *Pseudomonas fluorescens* P-17 and *Spirillum* NOX, as well as difficult and time-demanding procedure, have made the conventional bioassay less desirable and/or practiced (Hammes and Egli, 2005; Clescerl et al., 1999; Van der Kooij et al., 1982; LeChevallier et al., 1993). A simpler, more rapid and more accurate technique has recently been developed by Hammes and Egli (2005) using flow cytometric counting of bacteria in combination with fluorescence staining of microbial cells. Despite its success as a reliable method, FC has not been used for the waters treated with UV- based AOPs, in particular UV/H_2O_2 process.

1.5 Improving the Efficacy of UV/H_2O_2 Treatment Process

Given the concerns associated with the presence of organic matter, elimination of NOM (prior to UV/H_2O_2 treatment) would be beneficial. This is not only because of the need to improve the process efficacy, but also due to the impact on final water quality and the reduced formation of Disinfection by-Products (DBPs) within the distribution system. Therefore, utilizing a pre-treatment stage upstream of the UV/H_2O_2 treatment will be desired and even necessary.

Accordingly, coagulation is considered as the viable pretreatment alternative due to its availability and well understood reaction mechanism.

This work aimed to quantify the impact of UV/H_2O_2 treatment process on biological stability of water through measurement of AOC. To do so, the rapid and accurate technique proposed by Hammes and Egli (2005) was adapted and modified to allow accurate assessment of the AOC after UV/H_2O_2 treatment. The critical step for the UV/H_2O_2 treated water was using a H_2O_2 quenching agent with minimal impact on the actual AOC. This step was indispensable since during UV/H_2O_2 a considerable portion of the dosed peroxide remains un-reacted and any residual H_2O_2 could inhibit the growth of microorganisms leading to incorrect measurement of AOC. Therefore, it was important to remove the residual H_2O_2 effectively but with the least impact on the AOC content. As a result, several (organic and inorganic) quenchers were examined and their impact on AOC was assessed.

In addition to the generation of readily biodegradable organic molecules, NOM can also reduce the efficacy of the UV/H_2O_2 treatment and potentially lead to the formation of undesirable by-products. Hence, utilizing an alternative process in order to remove NOM ahead of the UV/H_2O_2 would be beneficial not only because of the demand to improve the process efficacy, but also due to the effect on final water quality.

Alum coagulation was evaluated as pretreatment to UV/H_2O_2 process because it is being widely used and has been shown to effectively in reduce NOM. In this study, the impacts of alum coagulation on NOM removal, the performance of downstream UV oxidation process, and the quality of the finished water (e.g., AOC, TOC) were investigated for different water qualities (i.e., different TOC and alkalinity).

1.6 Presentation of the Data

The abovementioned objectives were achieved step by step throughout the project and detailed explanation of each stage is provided in the following chapters.

Chapter Two presents the literature review on one of the current issues in drinking water treatment (e.g., NOM). Through this chapter several water treatment processes are briefly explained with the main focus on the advanced oxidation process in particular UV/H_2O_2 treatment.

Chapter Three specifies the main objectives of this research and highlights the significance and the contribution of this work to the field.

Chapter Four discusses the experimental approach taken to meet the objectives of this study. Detailed explanation of each experimental procedure in addition to the NOM characterization techniques is elaborated in this chapter. More importantly, the protocols that were used for the immobilization of Catalase on two different supports (for quenching H_2O_2 after the treatment) are compared and explained in detail.

Chapter five is dedicated to present and discuss the findings that could enhance and improve the existing knowledge about the proposed method by Hammes and Egli (2005) for AOC determination. This was done since the significance of some steps (i.e. Inoculation and Pasteurization) within the procedure was not well laid out. Through the experiments valuable findings were obtained that would help to conduct the AOC test with more confidence and accuracy. Results provided in this chapter indicate the reliability of the developed biocatalyst for subsequent UV/H_2O_2 experiments in which H_2O_2 must be removed prior to the AOC analysis.

Chapter six describes the experimental results on the impact of UV/H_2O_2 process on assimilable organic carbon (AOC) of natural and synthetic waters. The method developed in chapter five

was used to assess biological stability of water. In addition, other water characteristics (UV_{254}, TOC and molecular size distribution) were monitored during the UV/H_2O_2 treatment and findings are presented, discussed, and intercorrelated. In addition to AOC measurements, BDOC of the UV/H_2O_2 treated water was also assessed in collaboration with research, development and validation center for water treatment technologies and processes (CREDEAU) (Dr. Barbeau's Lab) at Ecole Polytechnique de Montreal. Results obtained demonstrate meaningful relationship between AOC and BDOC of the treated water. This can be helpful since both AOC and BDOC can substantially enhance our understanding of biodegradable organic matter within the water.

Chapter Seven is devoted to demonstrate the effect of coagulation pretreatment ahead of the UV/H_2O_2 process on different characteristics of NOM and hence downstream water quality. It was found that using Alum as coagulant can hugely improve the UV/H_2O_2 treatment efficacy, hence reducing energy requirements as well as formation of undesirable by products.

Chapter Eight summarizes and highlights the most significant outcomes of this study and provides recommendations and suggestions for future researches.

2 Literature Review

2.1 Natural Organic Matter (NOM)

Natural organic matter (NOM) refers to a complex mixture of organic compounds, originated from the breakdown of natural species including plants and animals, usually found in many surface water sources (Leiknes et al., 2004; Frimmel, 1998). The chemical characteristics of the molecules comprising NOM are not only influenced by the nature of the source materials (allochthonous), but also by the biological processes involved in carbon cycling within the terrestrial and aquatic systems (autochthonous) (Thomson et al., 2004; Rosario-Ortiz et al., 2007). These processes include allochthonous flow of organic carbon from the watershed, autochthonous carbon fixation by aquatic plants, transformation and degradation of organic materials by heterotrophic microbial activity, transport and remobilization of particulate organic materials to the sediments, and photo-degradation by incident UV from the sun (Aiken and Cotsaris, 1995; Westerhoff et al., 1999; Rosario-Ortiz et al., 2007; Chong Soh et al., 2008).

NOM is not a well-defined chemical entity, but can be classified into a number of groups depending on source and season (Thomson et al., 2004). NOM is mainly composed of refractory humic substances, hydrophilic acids, carboxylic acids, amino acids, polysaccharides, carbohydrates, and hydrocarbons (Nishijima and Speitel, 2004; Frimmel, 1998; Nikolaou et al., 2001). Humic substances are non-biodegradable portion of NOM and may be as high as 50–90% in highly colored waters (Frimmel, 1998; Andrews and Huck, 1996). Studies have shown that polymeric molecular structure of humic substances has more contribution to the formation of disinfection by-products (DBPs) during reaction with disinfectants (Thurman, 1985; Kim and Yu, 2005). Therefore, humic substances may be the most important portion of NOM, in terms of

impact on water quality, and should be eliminated (or reduced) through drinking water treatment practices.

2.2 Current Issues with the Presence of NOM

NOM plays an important role in many different reactions and processes, thereby affects water quality during the course of treatment. It is known as precursor to most halogenated and oxygenated disinfection by-products (Chowhury et al., 2008; Sarathy and Mohseni, 2009; Leiknes et al., 2004; Kim and Yu, 2005), a suitable substrate for bacterial regrowth within the distribution systems (Chong Soh et al., 2008; Charnock and Kjønnø, 2000; Kaplan et al., 1993; Sarathy and Mohseni, 2009; Thomson et al., 2004; Hammes et al., 2005), and a complexation site for binding heavy metals (Frimmel, 1998). NOM also affects the behavior of colloidal matter by binding to the colloid surface (Chen et al., 2007; Frimmel, 1998; Singer, 1999). Therefore, the presence of NOM can deteriorate the efficacy and performance of the treatment process (Yan et al., 2007). In addition, the presence of NOM in drinking water treatment is problematic, since it consumes disinfection chemicals and causes increase in disinfectant demand (Yee et al., 2006; Chow et al., 2004(b)), competes with micro-pollutants for sites on activated carbon, consumes oxidants intended for micro-pollutant removal or microorganism inactivation, causes membrane fouling, and shields UV radiation during the UV disinfection process (Thomson et al., 2004; Sarathy and Mohseni, 2007).

Understanding and characterizing NOM are important for water utilities and operators. They help operators to modify/amend the treatment processes in order to minimize the formation of undesirable by-products (Chow et al., 1999, 2004(a), 2004(c); Drikas et al., 2003), a task which has attracted a lot of attention and research worldwide (Rosario-Ortiz et al., 2007). As a result, several techniques have been proposed/used to understand the characteristics of NOM, thereby helping to study its fate during the treatment practice and optimize the treatment process for

effective removal of organic substances (Yan et al. 2007; Nikolaou and Lekkas, 2001; Frimmel, 1998; Rosario-Ortiz et al., 2007). From the methods proposed, one can mention polarity assessment (Philibert et al., 2008;Rosario-Ortiz et al., 2007), XAD Fractionation (Chow et al., 2004(c)), High Performance Size Exclusion Chromatography (HPSEC) (Pelekani et al., 1999), along with other spectrophotometric methods that are reported elsewhere (Pelekani et al., 1999; Frimmel, 1998; Nikolaou and Lekkas, 2001).

2.3 Alternatives for NOM Removal

A range of treatment alternatives have been proposed and evaluated to remove NOM, thereby reducing its undesirable impact on the treatment process and also downstream water quality. Among these are coagulation, ion exchange, granular activated carbon (GAC), biological activated carbon (BAC), filtration processes, ozonation and advanced oxidation such as UV or ozone based oxidation processes (Chen et al., 2007; Chen ,1999; Chow et al., 2002; Cook et al., 2001; Buchanan et al., 2004). A brief discussion on each of these processes along with some of their advantages and disadvantages is provided below:

2.3.1 Coagulation

2.3.1.1 Conventional coagulation (Alum and Ferric)

Coagulation is a process in which suspended particles are agglomerated (so they can be settled or filtered more easily and faster) through neutralizing their charges mainly by adding a chemical reagent. Because of its relatively simple practical aspect and cost, this process has gained much attention during the past decades. Inorganic metal coagulants (e.g., $Al_2SO_4.18H_2O$ also known as alum and Fe^{+3} ion known as Ferric) are commonly used for the removal of color, turbidity and NOM in drinking water (Xiangli et al., 2008; Uyak and Toroz, 2007; Chong Soh et al., 2008; Drikas et al., 2003; Chow et al., 1999). However, it has been recognized that high residual

amounts of inorganic coagulants (i.e., aluminum) can potentially induce adverse health effects including Alzheimer disease (Rizzo et al., 2008; Flaten, 2001; Miller et al., 1984; McLachlan, 1996). Therefore, many recent studies have focused on modification and enhancement of the coagulation process (i.e., through optimization of pH and coagulant dose) to achieve greater removal while minimizing detrimental impact on water quality. Studies demonstrated that optimized coagulation (enhanced coagulation) will improve organic carbon removal considerably while reducing the amount of coagulant used (Chow et al., 1999; Van Leeuwen et al., 1999; Rizzo et al., 2008).

2.3.1.2 Coagulation using natural organic coagulants

Natural organic coagulants (e.g., Chitosan) are considered as viable substitute to conventional inorganic coagulants and subject of some research. The driven force behind this has been the health concerns (i.e., Alzheimer) as well as sludge formation and the related disposal problems associated with using conventional coagulants. Natural organic coagulants (NOCs) have been successfully practiced in the past several years for water and wastewater treatment applications (Selmer-Olsen et al., 1996; Diaz et al., 1999; Rizzo et al., 2008). NOCs can be classified according to the natural source that they are extracted from such as: plant seeds, plant and animal (Selmer-Olsen et al., 1996; Diaz et al., 1999). Among these, Chitosan, a linear cationic polymer of high molecular weight obtained by de-acetylation of chitin which is manufactured from the outer shell of crustaceans (particularly crabs and shrimp), has been proposed and evaluated for applications in waste and drinking water treatment processes (Rizzo et al., 2008; Selmer-Olsen et al., 1996; Diaz et al., 1999). While early research and applications showed promising results, further research is required to examine the performance and applicability of Chitosan for drinking water treatment applications and different water qualities.

2.3.2 Ion exchange process (IEX)

The ion exchange process (IEX) is a process wherein reversible exchange of an ion between a solid, insoluble resin and the surrounding water takes place (Cornelissen et al., 2008). Since NOM consists largely of negatively charged poly-electrolytes, it can be removed effectively using IEX, depending on the characteristics of NOM and properties of the water (Bolto et al., 2002 (a), 2002(b); Chen, 1999). IEX resins have been shown to perform well in comparison with other water treatment processes such as activated carbon, non-ionic resins and cationic polymers in removing small to medium molecular weight NOM (Humbert et al., 2005; Fearing et al., 2004(b); Fu and Symons, 1990).

More recently, ion exchange processes have received considerable attention with the use of a new magnetic ion exchange resin, MIEX®, which has been designed and successfully evaluated for the removal of DOC from drinking water (Singer and Bilyk, 2002; Drikas et al., 2003; Fearing et al., 2004(a); Humbert et al., 2005). Two main features make this strong anion exchange resin different from traditional ones. First, the MIEX® beads are 2-5 times smaller than those of conventional ones which allow rapid sorption kinetics. Secondly, the MIEX® backbone contains a high proportion of a magnetic iron oxide compound, helping fine resin beads agglomerate into larger and fast settling particles (Humbert et al., 2007).

2.3.3 Adsorption

Adsorption is a treatment technology often considered when removal of dissolved organics is targeted (Jacangelo et al., 1995). In water treatment, adsorption process is basically divided in two main categories, namely Granular Activated Carbon (GAC) and Powder Activated Carbon (PAC) which are widely used for taste and odor reduction (Jacangelo et al., 1995). While effective at removing NOM and DOC to some degree, adsorption process is accompanied by significant cost and GAC efficiency is limited to only hydrophobic compounds (Fabris et al.,

2004; Cook et al., 2001; Newcombe et al., 2002(a), 2002(b), 2002(c), 2002(d); Nishijima and Speitel, 2004). Despite the costs associated with GAC, its effectiveness at removing a wide range of organic compounds and disinfection by-products has placed it among the viable technologies that have received major research efforts for further optimization (Jacangelo et al., 1995).

The GAC which has biological activity on its surface and removes significant amount of DOC through biodegradation is referred to as biological activated carbon (BAC). However, standalone BAC treatment is not feasible for reducing DBP precursors (Toor, 2005; Toor and Mohseni 2007); hence, transformation of refractory NOM into biodegradable dissolved organic carbon (BDOC) ahead of BAC treatment is known to be effective for the extension of GAC service life and reducing the organic load on the carbon bed (Kim et al., 1997; Nishijima and Speitel, 2004; Toor and Mohseni, 2007).

2.3.4 Membrane processes

Recent improvements in membrane technology have made it an increasingly viable option for removing microorganisms, particulates, and organic materials from raw water (Jacangelo et al., 1995). In membrane processes, contaminants are separated based on their physical properties such as size or charge (Jacangelo et al., 1995). Depending on the molecular size (from low to high) of the substance to be removed, Reverse Osmosis (RO), Nanofiltration (NF), Ultrafiltration (UF) and Microfiltration (MF) can be used for treatment applications (Jacangelo et al., 1995). Reverse osmosis is promising at removing inorganics and small molecular size organics; however, it requires higher pressure and creates lower flux. Nanofiltration is capable of removing viruses, large portion of organic contaminants as well as hardness in water (Mijatovic et al., 2004). Ultrafiltration is efficient at reducing turbidity and suspended solids in addition to viruses. Microfiltration which has the largest molecular size cut off is utilized for removing bacteria, Giardia and Cryptosporidium (Jacangelo et al., 1995; Mijatovic et al., 2004).

Membrane filtration has the potential to achieve the highest removal of NOM, but the costs of these processes are appreciably higher than those of GAC and coagulation. On the other hand, there are still some problems associated with using membranes such as the need for pretreatment, generation of concentrated waste, fouling, and sanitary issues that demand further research (Jacangelo et al., 1995; Mijatovic et al., 2004).

2.3.5 Filtration systems

Filtration is another type of separation process in which water is treated by traveling through beds of granular materials (e.g., sand) that can remove and retain contaminants. Several configurations of these processes (i.e., slow, rapid, and conventional) have been applied to treat water for drinking purposes (LeChevallier et al., 1991; Neef et al., 1996; Logsdon et al., 2002). In the case of conventional filtration, it is combined with pre coagulation-flocculation-sedimentation where a large portion of contaminations are aggregated/settled and are eliminated when the water passes through the filter (Yao et al., 1971; Brehant et al., 2002). Slow sand filter, however, must be fed with high quality water and requires larger area in comparison with rapid sand filters (Logsdon et al., 2002).

2.3.6 Oxidation processes

2.3.6.1 Ozonation

The application of ozone in drinking-water treatment is widespread throughout the world. Ozone is utilized in various drinking water treatment applications involving disinfection, oxidation and removal of micro-pollutants, taste, odor, and color (Kruithof et al., 1999; Gottschalk et al., 2000; Graham, 1999; von Gunten, 2003(a), 2003(b); Andreozzi et al., 1999; Camel and Bermond, 1998; Ikehata et al., 2008). However, ozonation may lead to the formation of some undesired by-products, in particular bromate which is considered to be a potential human carcinogen. Bromate

is particularly problematic because unlike many other organic by-products it is not degraded in biological filters that are usually installed after the ozonation step (von Gunten, 2003(b); Collivignarelli and Sorlini, 2004; Kleiser and Frimmel, 2000).

Oxidation of organic and inorganic compounds during ozonation can occur via reaction with ozone or OH radicals or a combination thereof. Despite its high oxidation potential, ozone is selective and may not entirely oxidize some undesirable species (Kleiser and Frimmel, 2000; Volk et al., 1997). In the presence of NOM ozone decomposition is accelerated and more complex reactions take place (Glaze, 1987). Also, ozonation can breakdown larger organic compounds into more easily biodegradable ones, hence enhancing bacterial regrowth potential (Lehtola et al., 2001; Yavich et al., 2004).

To improve the effectiveness of ozonation several processes have been suggested to be used in combination with ozone to increase the oxidation potential of the process as well as the range of targeted species to be removed (Volk et al., 1997). Of these processes one can mention O_3/UV, O_3/H_2O_2 process in which nonselective OH radicals are generated (Ikehata et al., 2008; Volk et al., 1997; Hoigné and Bader, 1976). These processes are generally referred to as advanced oxidation processes (AOPs).

2.3.6.2 Advanced oxidation processes (AOPs)

AOPs provide a viable alternative for effective degradation of organic pollutants which otherwise cannot be removed by conventional treatment technologies. The main advantages of AOPs over conventional techniques is their non-selectively towards organic contaminants and their ability to degrade the pollutants without transferring them from one phase to another or concentrating them (Sarathy and Mohseni, 2006). Relying on extremely potent OH radicals (oxidation potential: 2.8 V) formed in the process; AOPs have the potential to completely and

effectively mineralize the organics (Guzzella et al., 2002; Toor and Mohseni, 2007; Anderozzi et al., 1999; Pereira et al., 2007; Stefan and Bolton, 2002, 2005; Stefan et al., 1996, 2000; Legrini et al., 1993). Hydroxyl radical generated through AOPs is extremely potent with only fluorine being more reactive (Table 2.1), and is able to degrade organics as well as other pollutants in aquatic solutions by series of reactions (Toor, 2005).

Table 2.1: Oxidation potential of various species

Species	Oxidation potential (eV)
Fluorine	3.0
OH radical	2.8
Ozone	2.4
H_2O_2	1.8
Cl	1.4
O_2	1.2

The formation of OH radicals during AOPs is often materialized through the reactions involving H_2O_2, O_3, photocatalyst (e.g., TiO_2), and UV irradiation. Currently, AOPs that are studied and developed in the literature include combinations of UV/H_2O_2, UV/O_3, UV/O_3-H_2O_2 and UV/TiO_2 (Anderozzi et al., 1999; Guzzella et al., 2002; Suty et al., 2004).

2.3.6.3 UV based advanced oxidation

UV light can be combined with other reactive species (e.g., H_2O_2, O_3) to effectively generate OH radical and remove resistant organic contaminations. The absorption of photons by H_2O_2 causes the split of the H_2O_2 molecule, generating powerful oxidizing hydroxyl radicals.

$$H_2O_2 + h\upsilon \rightarrow 2\,HO\bullet$$

Based on the pertinent literature so far, UV/H_2O_2 is the most extensively studied UV-based AOP for drinking water applications and has been shown to be promising at removing micropollutants and organics, especially aliphatic and aromatic compounds (Cater et al., 2000; Wang et al., 2000; Tuhkanen, 2004; Sarathy and Mohseni, 2006; Kruithof et al., 2007, 2002; Plumlee et al., 2008;

Kitis and Kaplan, 2007; Andreozzi et al., 1999; Swaim et al., 2008; Rosenfeldt and Linden, 2004, 2005). Besides, UV/H_2O_2 process is the only AOP that has been commercialized and implemented for drinking water treatment applications (Sarathy and Mohseni, 2006).

In the application of UV/H_2O_2 for commercial drinking water treatment two key parameters are of importance: UV fluence (i.e., irradiation time) and the initial H_2O_2 concentration (Wang et al., 2000; Stefan and Bolton, 2005), with the H_2O_2 dose being less than 15 ppm and UV dose reaching as high as up to 1400 mJ/cm^2 (Sarathy, 2009). During the practice of UV/H_2O_2 process the presence of organic matter interacts negatively with the process leading to reduction in removal efficacy (Sarathy and Mohseni, 2007). NOM scavenges OH radicals and shields the UV photons to some degree causing progressive reduction in its molecular weight, DOC and eventually to mineralization (Thomson et al., 2004; Buchanan et al., 2004). However, applied conditions in commercial scale applications of UV/H_2O_2 are not strong enough to mineralize NOM; hence, leads to its partial breakdown to lower molecular weight organic molecules (Song et al., 2008; Sarathy and Mohseni, 2007; Toor and Mohseni, 2007; Buchanan et al., 2004). The lower molecular weight NOM is more biodegradable and is considered to be a nutrient for bacteria existing within the distribution systems; therefore, its impact on water biostability is of importance (Camel and Bermond, 1998; Buchanan et al., 2004; Hem et al., 2001).

Biodegradability of organic matter is an attribute that promotes biofilm development within the treatment facility as well as in the distribution system. Bacterial regrowth and biofilm formation can mediate disinfectant decay and release cells to the aqueous phase (Angles ML. et al. 1999; Chandy and Angles. 2004; Buchanan et al., 2004; Sarathy and Mohseni, 2007). Several approaches can be taken to address the concern associated with the enhanced biodegradability of NOM after UV/H_2O_2 treatment. Some researchers have suggested implementation of a downstream BAC process after the photo-oxidation treatment to achieve higher removal of

organic matter (Toor and Mohseni, 2007, Buchanan et al., 2004). On the other hand, Sarathy and Mohseni (2007) have suggested applying a pretreatment process in order to eliminate higher molecular weight NOM from water. This can provide opportunity for more effective reaction between OH radicals and smaller organic molecules resulting in higher degradation of lower molecular weight fractions and ensuring water biostability.

2.4 Bacterial Regrowth and Biostability

The term "biologically stable" applies to potable water that does not promote growth of microorganisms within the distribution network. Bacterial regrowth mainly causes biofilm formation, resulting in increased color and turbidity of the water. Moreover, biofilm formation in pipelines in the long run causes operational problems such as biofouling and biocorrosion (Kasahara and Ishikawa, 2002; Van der Kooij et al., 2000; Liu et al., 2002) and water quality related issues (LeChevallier et al., 1987, 1990, 1996). Therefore, removing/inactivating pathogens and preventing their regrowth within the distribution system are the primary objectives of any water treatment (Van der Kooij, 1987; LeChevallier et al., 1987, 1990; Huck et al. 1991). This is indispensible since bacterial regrowth can adversely influence consumer preferences, such as taste and odor of water, or in the worst case, it can lead to potential health hazards caused by opportunistic pathogens (LeChevallier et al., 1987, 1990, 1996; Kasahara and Ishikawa, 2002; Huck, 1990). Therefore, there is a necessity to quantify the biological stability via assessing the possibility of bacterial growth within the distribution system.

2.4.1 Biological stability assessment

Measuring DOC or TOC of water has been shown to be unreliable and insufficient for predicting microbial regrowth potentials within the distribution system (Charnock and Kjønnø, 2000; Van der Kooij, 1992; Van der Kooij et al., 1982). As a result, assessing biostability of water and quantifying biodegradable portion of NOM have been the focus of much research during the past

decades (Van der Kooij et al., 1982; Servais et al., 1987, 1989; Rittmann, 1984; Lechevalier et al., 1993; Sathasivan and Ohgaki, 1999). There are generally two main methods for the measurement of biodegradable organic matter (BOM). The first is assimilable organic carbon (AOC) assay which is measured through correlating a specific organism(s) growth with assimilable organic carbon content of the water. This technique has been identified to be appropriate when measurement of bacterial regrowth potential is of concern. Previous studies have already related the concentration of AOC in water to heterotrophic regrowth (Van der Kooij, 1992; Lechevalier et al., 1993). The second technique is for measuring biodegradable dissolved organic matter (BDOC) and is based on monitoring DOC consumption over time by microorganism(s). In other words, BDOC is a measure of the biodegradable organic carbon in a sample before and after incubation (Servais et al., 1987; Block et al., 1992; Ribas et al., 1997) and becomes important when disinfectant demand or DPB formation potential is of interest (Huck, 1990; Escobar and Randall, 2001; Kaplan et al., 1994).

The relationship between the AOC or BDOC and biostability of the water are of importance when these parameters are both used to describe the biofilm formation potential. Easton (1993) suggests 20 µg/L of AOC and 200 µg/L of BDOC as thresholds for biological stability, while Van der Kooij (1992) has recommended that the limit for biostability may be below 10 µg AOC/L. Volks and LeChevallier (2000) defined AOC>100 µg/L, at 15°C, and dead-end disinfectant residuals <0.5 mg/L for free chlorine or 1.0 mg/L for chloramines as threshold values for water treatment plants (Hem and Efraimsen, 2001) .

2.4.2 Biodegradable organic carbon (BDOC) assay

The BDOC assay measures the amount of DOC that is consumed (assimilated and mineralized) by heterotrophic bacteria over a certain period of time. Several BDOC bioassays have already

been suggested even though they are practically very similar to one another. That is, all these methods involve inoculating the samples with natural microbial community for a certain period of time and considering the difference between initial and final DOCs as BDOC (Servias et al., 1987, 1989; Frias et al. 1992, 1995; Escobar and Randall, 2001; Volk et al., 1994; Kaplan and Newbold, 1995).

Several reports have tried to elaborate the BDOC results and develop correlations between the biostability of water with the amount of BDOC. For instance, Block et al. (1992), Servais et al. (1995), and Volk et al. (1994) have recommended some BDOC threshold levels (e.g., 0.16 mg/L) to maintain the biological stability of the finished water (Escobar and Randall, 2001). Kaplan et al. (1994) observed relations between AOC and BDOC with DOC and have suggested focusing on treatment systems individually to find statistical correlation among AOC, BDOC, and DOC. In contrast, Huck (1990) reported meaningless relationships among these factors. The investigation by Van der Kooij (1984) ruled out BDOC as an indication of water biostability due to its limited detection limit (i.e., 0.1-0.2 mg/L) and the fact that BDOC is both converted to biomass and CO_2 through assimilation and mineralization, respectively. Van der Kooij (1990) proposed to consider AOC/BDOC ratio as an indication of relative biodegradable organic compounds available within the water body.

2.4.3 Assimilable organic carbon (AOC) assay

AOC is a minor fraction of TOC (0.1-9%) which can be easily assimilated by the microorganisms, resulting in proliferation of microbial cells (Van der Kooij, 1990, 1992; Escobar and Randall, 2001). Although AOC usually constitutes only a small fraction of organic matter in drinking water, it has been recognized as one of the most important water quality

parameters responsible for biological instability in drinking water treatment, storage and distribution systems (van der Kooij, 1992; Escobar and Randall, 2001).

Recently, the appearance of AOC in the water treatment system and effluent of the treatment plant has attracted a lot of attention (Park et al., 2005; Bradford et al., 1994; Volk et al., 2000; Chein et al., 2007; Hem and Efraimsen, 2001). Literature reports have suggested different values for AOC concentration (e.g., 10µg/L, 100µg/L) under which no bacterial growth will occur (LeChevallier et al., 1987; Van der Kooij, 1982; Hammes and Egli., 2005). It also has been reported that variation of AOC concentration follows different patterns depending on the distribution system and the season (Bradford et al., 1994; Volk et al., 2000).

To date, several methods have been proposed/practiced for measuring AOC (Van der Kooij 1982; Jago and Stanfield, 1984; Kaplan et al., 1993; Werner, 1985, Werner and Hambsch, 1986; Frias et al. 1992, 1995) via different approaches in bacterial growth measurement and measured data interpretation. Below a brief introduction of each method is presented and drawbacks and advantages are discussed.

2.4.4 Current methods for AOC measurement

Measurements of AOC are based on bacterial counts, or proxy assays thereof and as such are theoretically closely related to the increase in heterotrophic bacteria through utilization of organic carbon. In fact, each of the AOC assays can be applied in different situations, but some limitations may confine and/or interfere with the data analysis and interpretation (Hammes, 2008).

2.4.4.1 Conventional AOC bioassay (Heterotrophic Plate Count)

The conventional AOC bioassay was first developed by Van der Kooij (1982) and later was modified by others (Kaplan et al., 1993; Lechevalier et al., 1993). Conventional plate count AOC

bioassay is based on the cultivation of pure strains (*Pseudomonas Fluorescens P17 and Spirillum NOX*) in laboratory conditions. *Pseudomonas Fluorescens P17* is able to utilize the carbon content of amino acids, hydrocarboxylic acids, carboxylic acids and carbohydrates, and *Spirillum NOX* is incorporated to utilize oxalic acid content of organic matter (Huck, 1990; Escobar and Randall, 2001; Stainfield and Jago, 1987). In this method, samples are pasteurized at 60°C for 30 minutes and then are inoculated with each strain (i.e., *P17* and *NOX*) followed by incubation at 15°C for 9 days for the bacteria to reach the stationary phase (Servais et al., 1989; Escobar and Randall, 2000, 2001). Growth is monitored by counting Colony Forming Units (CFU) and average growth N_{avg} is obtained during the incubation time and is correlated to the amount of AOC units as µg/L acetate-Carbon equivalent. It is assumed that all the utilizable organic carbon is exhausted by the microorganisms and cell counts at the stationary phase are proportional to AOC concentration in water (Hammes et al., 2005; Servias et al., 1987). Sodium acetate (or oxalate) is served as the standard reference to make up artificial assimilable carbon concentrations.

Yield coefficient, the number of cells produced per microgram of assimilable carbon, is extracted from calibration curve which is basically heterotrophic bacteria counts versus acetate-C solution with different concentrations (Escobar and Randall, 2001; Van der Kooij, 1982). Thereafter, yield coefficient is used to convert the cells counted in each sample to its pertinent AOC concentration in µg/L. However, very careful attention should be paid when obtaining yield coefficient. Van der Kooij (2002), Kaplan et al. (1993), and Hammes and Egli (2005) have found that yield coefficient can vary from one pure culture to another (i.e., from *P17* to *NOX*) and also from one organic carbon source to another (i.e., from acetate to oxalate). Moreover, yield coefficient can differ significantly when using complex organic carbon source (i.e., natural inoculum) compared to the one using pure carbon source such as acetate (Hammes and Egli,

2005). Indeed, it is uncertain whether conversion to a single simple substrate is the correct approach to reflect growth on complex organics (Hammes and Egli, 2005; Hammes, 2008).

2.4.4.2 Adenosine triphosphate (ATP) method

Adenosine Triphosphate **(**ATP)-based method is similar to the HPC technique, but performed in smaller vials (i.e., 40 mL vials) and at higher temperature and inoculum density (22°C and 10^4 CFU/mL) (Lechevallier et al., 1993). This method significantly reduces the time required for incubation (2-3 days) and also for the analysis (1 min). The ATP of the cells grown is extracted with ATP releasing agent and the sample is spiked with Luciferine-luciferase agent causing to emit a luminescence that can be detected with a luminometer. ATP luminescence units are then converted to corresponding cells concentration and AOC using standard solutions that were described earlier for AOC conventional bioassay (Lechevalier et al., 1993).

In comparison with the HPC technique, this method is shown to produce similar results but in shorter time. However, similar to the HPC, this technique is susceptible to turbidity. Moreover, the use of pure cultures (*P17* and *NOX*) brings up the question on the extent of the organic carbon utilization by these strains that can only consume a certain group and amount of organics available in the sample (Hammes and Egli, 2005; Servais et al., 1987). While it has been suggested that there is a potential to use the natural microbial community instead of pure cultures in order obtain more realistic interpretations (Lechevalier et al., 1993; Hammes et al., 2008), no such study has been reported.

2.4.4.3 Bacterial regrowth potential test

Bacterial regrowth potential (BRP) is an indicator developed to measure the ability of water to support microbiological growth. In this method, turbidity of the seeded samples is monitored through stationary phase in a specially modified turbidimeter at room temperature (Werner,

1985; Hambsch et al., 1992; Hammes et al., 2008). Thereafter, logarithm of turbidity is plotted versus incubation time and standard samples (i.e., Acetate-C solution with artificial concentration) are used to correlate turbidity to AOC. The main shortcoming of this method is its limited capacity for processing several samples at the same time (Werner, 1985; Hambsch et al., 1992; Hammes et al., 2008).

2.4.4.4 Flow cytometry and cell staining

This is a new technique recently developed in response to the shortcomings of other AOC techniques. Developed first by Hammes and Egli (2005), in this technique plating is replaced with fluorescence staining of total nucleic acids of the bacteria combined with flow cytometry (FC) as a powerful, rapid and straightforward cell enumeration and characterization technique (Hammes and Egli, 2010). This approach also allows for the detection of inactive and/or uncultivable microorganisms (Hammes and Egli, 2005; Hammes et al., 2008; Berney et al., 2008). One of the strong aspects of this method is that indigenous microbial community is used as consortium instead of conventionally used pure cultures (i.e., *P17* and *NOX*) to ensure that a broader range of organic carbons are utilized by the microorganisms. In fact, this would result in higher and more complex interactions between microbial community adapted to the water and its organic content (Hammes and Egli., 2005; Servias et al., 1987, 1989). In addition, in this method higher incubation temperature (i.e., 30°C) is used to accelerate bacterial growth and hence, reduce the incubation time required for the bacteria to reach the stationary phase. Moreover, flow-cytometric enumeration method can be used to establish complete growth curves for a natural microbial consortium growing on AOC (Hammes and Egli, 2005). Therefore, valuable kinetic data can be extracted from the growth curves to provide much clearer insight into the actual growth potential of water (Hammes and Egli, 2005). In order to better understand and

obtain clearer insight into this technique, a brief introduction of flow cytometry and its principals is given in below.

2.4.4.5 Flow cytometry (FC)

Flow cytometry (FC) is a powerful technique for cell analysis. This technique gives the ability to enumerate, sort, and measure several properties (e.g., viability, nucleic acid content) of individual cells (Hammes and Egli, 2010). The main advantage of FC is its easiness and fastness for cell characterization. In brief, individual particles and cells are suspended in a flow stream (i.e., sheath fluid) and are passed one at a time through the interrogation point where they meet an excitation light, typically a laser beam (Hammes and Egli, 2010).This process is also known as hydrodynamic focusing which allows for individual cell analysis. Laser beam is used at different wavelengths (e.g., 488 and 530 nm) to count or detect various cells. When the laser beam hits the cell, it scatters forward and also from the side. The scattered light is collected via special detectors and transformed to signals which are transmitted to the computer. Signals collected from Forward Scatter (FS) and Side Scatter (SS) provide information about cell size and granularity of the cells, respectively (Hammes and Egli, 2010). Moreover, FC technique gives the ability to differentiate various cells with different characteristics by staining the cells using special flourophore agents (e.g., SYBR GREEN). The laser beam emitted from the source, excites the flourophore dye attached to the cell to a higher energy level. The excitation lifetime is extremely short and the excited flourophore emits light at a different wavelength (i.e., longer) upon returning to its ground state energy level. Light emitted from the excited cell is then detected and collected with special detectors that produce signals which are further translated to meaningful data using computer software (Hammes and Egli, 2010).

2.4.4.6 Shortcomings of the current methods for AOC measurement

A critical shortcoming of the HPC test and other cultivation-based techniques is the significant disparity between cultivable cell counts and total cell counts (Berney et al., 2008). Moreover, total cell enumeration also fails to differentiate between live and inactive cells. Therefore, cultivation-independent methods, such as ATP based assays and/or flow cytometry combined with cell staining method have been proposed to address this concern (Berney et al., 2008; Lee et al., 2001). However, Hammes et al. (2008) have also found that ATP method is prone to interference with extracellular ATP release of cells when a huge number of them are produced during ozonation process.

Additionally, in the plate count method pure cultures (i.e., *P17* and *NOX*) are used to study the growth of bacteria on different organic compounds. However, as reported by Van der Kooij (1990) and LeChevallier et al. (1993), *P17* is not able to grow on carboxylic acids including oxalate. *NOX* strain is capable of utilizing carboxylic acids, except carbohydrates, alcohols, and aromatic acids (Van der Kooij 1984, 1990). Therefore, limited information is supplied by the utilization of pure cultures. To address this, it has been suggested that the use of a natural indigenous microbial community can provide more opportunity to utilize broader range of organics and also offer more reliable information of the actual AOC content of the sample (Hammes and Egli, 2005; Servais et al., 1987).

Conventional bioassay for AOC measurement is tedious and time-consuming (9-12 days) in comparison with FC which is relatively short and only takes 2-3 days. Hammes and Egli (2005) have compared the conventional AOC bioassay with FC and obtained more accurate, precise and reliable data when using flow cytometric enumeration (LeChevallier et al., 1993; Hammes and Egli, 2005).

2.4.5 Impact of oxidation processes on AOC and BDOC

Oxidants like chlorine, ozone, and hydroxyl radicals could break down large organic compounds into small molecules (e.g., oxalic acid), which could be easily assimilated by microorganisms leading to increases in the AOC of treated water (Lehtola et al., 2001; Liu et al., 2002; Sarathy and Mohseni, 2007, 2009; Escobar et al., 2001; Van der Kooij et al., 1984; Chien et al., 2007, 2009). Bradford et al. (1994) evaluated the impact of ozonation on AOC of ground and surface waters in southern California using two different bioassays and showed that the AOC increased substantially after ozonation. Similar study was performed by Yavich et al. (2004) looking at the impact of ozonation from mild to intense conditions followed by biofiltration on three different lake waters (i.e., three different NOM). The results showed formation of slowly and rapidly biodegradable organic carbon as a result of organic matter molecules oxidation. Analogous observation was obtained by Chien et al. (2007) in which ozonation was found to enhance formation of more biodegradable organic matter. Interestingly, Liu et al. (2002) found that for slower oxidant like chloramine, the reaction time also contributes to the AOC increment. However, the same research revealed that AOC could be consumed when travelling through the pipeline. Other observations suggest that the removal of AOC has a correlation with the decrease in concentrations of other drinking water indicators (LeChevallier, 1990; Chien et al., 2007).

During UV-based advanced oxidation processes it has been found that larger organic molecules are broken down to smaller biodegradable organic molecules as a result of photochemical oxidation and reaction with OH radical (Frimmel, 1998; Buchanan et al., 2004; Toor and Mohseni, 2007). More specifically, Toor and Mohseni (2007) have investigated the impact of UV/H_2O_2 treatment on BDOC and AOC of water and showed that the level of these indicators increased after UV/H_2O_2 demonstrating formation of more biodegradable organics, hence greater potential for bacterial regrowth. The same study reported that application of BAC after UV/H_2O_2

decreased the levels of both BDOC and AOC to the original level of the raw water. Sarathy and Mohseni (2009, 2007) have also investigated the impact of UV/H_2O_2 AOP on NOM and showed that during UV/H_2O_2 process, hydroxyl radical generated from the process preferentially reacts with larger organic molecules and oxidizes NOM into more biodegradable organic compounds such as aldehydes. This was attributed to the loss of conjugations and degradation of chromophoric NOM which can be monitored by tracking the UV absorbance at 254nm over the course of treatment (Sarathy and Mohseni, 2007, 2009; Buchanan et al., 2004; Hofbauer and Andrews, 2004). They also demonstrated that using a pretreatment process (e.g., ultrafiltration) ahead of the UV/H_2O_2 process leads to the removal of the higher molecular weight NOM, causing mineralization of lower molecular weight NOM when exposed to highly reactive OH radicals. There is a lack of detailed information in the open literature about correlating the NOM molecular weight distribution to AOC and BDOC for the UV/H_2O_2 process applied to drinking water treatment. To the best of our knowledge, a very few reports are available in the literature discussing specifically the impact of UV/H_2O_2 treatment process on downstream biological stability of water. That being said, FC has not been used as an AOC assay technique for the waters treated with UV based AOPs, in particular UV/H_2O_2 process. The critical step for UV/H_2O_2 treated water is using a H_2O_2 quenching agent with minimal impact on the original AOC of water. This step is crucial since during UV/H_2O_2 a considerable portion of the dosed peroxide will remain un-reacted. Any residual H_2O_2 inhibits the growth of microorganisms leading to incorrect measurement of AOC. Therefore, it is important to remove the residual H_2O_2 effectively but with the least impact on the original AOC content.

3 Thesis Objectives and Scope

3.1 Justification of Research

Ultraviolet (UV) based advanced oxidation processes have emerged as viable alternative technologies for removing micro-pollutants and other organic contaminants from water. Among these processes, UV/H_2O_2 is the one currently applied in commercial scale. However, in the application of UV/H_2O_2 process, presence of NOM in water is problematic and hinders the efficacy of the treatment process. During the practice of UV/H_2O_2 treatment, NOM can undergo significant partial oxidation leading to the generation of smaller easily assimilable organic molecules (i.e., AOC) (Sarathy and Mohseni, 2007). Earlier studies have found AOC as the potential cause of bacterial regrowth and other water health concerns thereof within the distribution system (Escobar et al., 2001; Hem and Efraimsen, 2001).

AOC concentration in water is conventionally assessed through time consuming and tedious bioassays (i.e., AOC assay, ATP assay). Hence, it has not been practiced widely at water treatment plants. Also, impact of UV/H_2O_2 process on biological stability of downstream water has not gained much attention in the literature. However, a method recently developed by Hammes and Egli (2005) opened the opportunity for more accurate and relatively rapid quantification of the AOC, especially for AOP treated water. As a result, this research aimed to contribute substantially to the current understanding of easily assimilable organic molecules formation during UV/H_2O_2 treatment process.

Considering the concerns and issues associated with NOM (especially when oxidation is applied is the treatment train), elimination of NOM ahead of the oxidation process can potentially increase the UV/H_2O_2 treatment efficacy as well as the finished water quality. Moreover, with regulations becoming more stringent and public concerns increasing over emerging micro-

pollutants in raw water, many utilities hope to fulfill the regulations by retrofitting existing facilities with robust treatment processes and avoiding the construction of new ones. Thus, this research also focused to investigate the feasibility and the impact of a pre-treatment process such as coagulation to eliminate NOM prior to UV/H_2O_2 treatment. This would be beneficial not only because of the need to improve process efficacy, but also due to the impact on final water quality and the reduced formation of DBPs within the distribution system.

3.2 Objectives of Research

A new method to determine biological stability of water was recently proposed by Hammes and Egli (2005). It is a rapid and straightforward method capable of detecting inactive and/or uncultivable cells. However, this method has not been used to gauge the impact of UV based AOPs (i.e., UV/H_2O_2 process) on biological stability (i.e., AOC) of water. The critical step for UV/H_2O_2 treated water is using a H_2O_2 quenching agent with least impact on the original AOC of the sample. This is necessary since any residual H_2O_2 will inhibit the growth of microorganisms and hence, interfere with the final interpretation of the AOC data. Furthermore, there are some knowledge gaps existing with the proposed protocol of Hammes and Egli (2005) and with the impact of some factors (e.g., temperature, natural inoculum) on the measured AOC data. Therefore, there is a need for further research to explore the potential utility of the FC method for UV/H_2O_2 treatment applications and to enrich the current understanding of the changes in water quality parameters, especially AOC, during the UV/H_2O_2 treatment of raw water containing NOM.

Equally important, this research aims to study the possibility of utilizing a pre-treatment step upstream of the UV/H_2O_2 process to remove NOM; hence, improving the overall treatment efficacy and the finished water quality. As a result, coagulation was selected as a viable candidate due to its well known operational aspects and effectiveness. However, the extent to

which coagulation can improve UV/H_2O_2 performance and water quality is unclear. More importantly, the type of coagulant used (i.e., organic and inorganic) for the best impact needs to be determined through experiments in order to find the best candidate in terms of organic matter removal.

Within this scope and the overall goal, the specific objectives of this research were to:

- Validate, standardize and calibrate Hammes and Egli's method (2005) for AOC determination of UV/H_2O_2 treated surface water.
- Determine and study the impact of UV/H_2O_2 treatment on the AOC profile and biological stability of raw waters from different sources.
- Examine different coagulants for their efficiency and effectiveness in terms of organic matter removal.
- Study the impact of coagulation pretreatment combined with UV/H_2O_2 on different water quality parameters (especially AOC) and UV/H_2O_2 process' efficacy.

3.3 Significance of this Work

The outcomes of this research will help to effectively and rapidly determine biological stability of water treated with UV/H_2O_2 advanced oxidation process. Having this rapid technique established and validated for the UV/H_2O_2 application, the operators and owners of the water utilities will be able to monitor the AOC profile of the treated water with confidence.

In addition to the method developed for AOC determination after UV/H_2O_2 treatment, part of this research intends to demonstrate the viability and effectiveness of using coagulation as a pre-treatment to UV and UV based oxidation processes. Coagulation was evaluated as pretreatment to UV advanced oxidation, since it is a well understood and widely used process and also effective at reducing NOM. More importantly, retrofitting existing facilities with robust

treatment alternatives such as UV/H_2O_2 is attractive to many utilities that already apply coagulation and wish to comply with new regulations, as they become more stringent, with the least possible capital investments.

4 Experimental Methodology

4.1 Introduction

This chapter provides a detailed explanation of the experimental work and analytical measurements. Moreover, comprehensive description of AOC assay, investigations related to its improvements, as well as the protocols that were used for immobilization of Catalase are elaborated. Finally, techniques used in analytical measurements in the laboratory are explained.

4.2 Experimental Procedure Overview

This study is mainly consisted of three major tasks that are briefly explained in the following.

4.2.1 Develop and validate a rapid technique for AOC measurement after UV/H_2O_2 treatment

This task intended to modify and enhance a recently proposed technique (Hammes and Egli, 2005) for AOC measurement. This was necessary since the previously existing protocol was not appropriate for UV/H_2O_2 treatment applications. Through the experiments valuable findings were obtained that could help to conduct the AOC assay with more confidence and accuracy. Catalase from bovine liver was immobilized on a polymeric support to satisfy the need for quenching H_2O_2 after the treatment with no detrimental impact on the final AOC data. Results obtained indicate the reliability of the biocatalyst developed for subsequent UV/H_2O_2 experiments in which H_2O_2 must be removed prior to the AOC assay.

4.2.2 Study the effect of UV/H_2O_2 treatment on NOM characteristics and biodegradability

In this task, impact of UV/H_2O_2 advanced oxidation treatment on organic matter from Capilano and Bowen Island waters was assessed under different reaction conditions (i.e., [H_2O_2] =10 ppm

and UV fluences of 0 to 2000 mJ/cm^2). Several variables such as TOC, UV_{254}, Apparent Molecular Weight (AMW), as well as the AOC were monitored and results are presented and discussed in the following chapter.

4.2.3 Study the impact of pretreatment using coagulation in combination with UV/H_2O_2 on natural waters

This task intended to examine the possibility of utilizing a pretreatment process (i.e., coagulation) and investigate its impact on UV/H_2O_2 process efficacy as well as the treated water quality parameters. At this stage, the best coagulant in terms of UV_{254} and TOC removal was selected (between Alum and Chitosan) and further experiments were carried out using the selected coagulant. Then, water samples underwent coagulation and UV/H_2O_2 treatment and all important parameters such as TOC, UV_{254}, AMW, and AOC were assessed in all the treatment stages.

4.3 Source Waters

Concentration of NOM as well as its composition and characteristics varies from one water source to another and also over time. Therefore, to study the effect of NOM characteristics and its concentration on the process performance and the finished water quality, two different types of water (i.e., natural surface water and synthetic water) were used in this project. Table 4.1 provides data on various water quality parameters of the water used in this study.

Table 4.1: Selected characteristics of the waters used in this study

Parameter/Water	CW Reservoir	BI water	SR NOM (5 mg/L)
TOC (ppm)	1.45±0.075	4.81±0.03	5.28±0.014
pH	6.7	6.3	7 (adjusted from the original value of 5.3)
UV_{254} (cm^{-1})	0.063± 0.002	0.185±0.003	0.220±
SUVA (L mg^{-1} m^{-1})	4.2± 0.316	3.75± 0.072	4.15± 0.05
Alkalinity (ppm)	< 5ppm	< 15ppm	NA

Two sources of surface water, originating from spring snowmelt and fall and winter runoffs were used. By using different surface water sources (i.e., Capilano water, and Bowen Island water), the impact of different NOM sources on downstream water quality was investigated. Capilano water (CW) was taken from the Capilano Reservoir, located in the Northwest of Metro Vancouver area that provides drinking water for Greater Vancouver region, British Columbia, Canada. This water contains low TOC (~1.4 ppm), turbidity and alkalinity (< 5ppm). The Bowen Island (BI) water was obtained during spring 2010 from Josephine Lake, a watershed area located in Bowen Island, British Columbia, Canada. The TOC of BI water was around 5 ppm and its alkalinity was about 15 ppm as mg/L $CaCO_3$ equivalent.

In order to investigate the impact of NOM concentration on UV/H_2O_2 process, and also to facilitate the comparison of the results with the existing data available in the literature, aquatic organic matter isolated from Suwannee River (SR) by reverse osmosis process (IHSS Corporation) was used to prepare the synthetic water solutions. The Suwannee River NOM is composed of: 48.8 %C; 3.9 %H; 39.7 %O; 1.02 %N; 0.60 %S; 0.02 %P; 7.0 % Ash (Total 101.0%, International Humic Substances Society). Given the fact that NOM cannot be measured directly with current equipments, TOC was considered as a surrogate parameter for NOM

concentration. Synthetic waters with different TOC concentrations (i.e., 5 and 10 ppm) were made by dissolving SR-NOM in Milli-Q water.

Additionally, the presence of carbonates and bicarbonates will affect the UV/H_2O_2 process, by scavenging OH radicals (Sarathy and Mohseni, 2009); therefore, synthetic water solutions with known alkalinities of 50 and 150 ppm (as $CaCO_3$ equivalent) were prepared to gauge the impact of alkalinity on the UV/H_2O_2 process. Sodium bicarbonate ($NaHCO_3$, ACS reagent, Fischer Scientific) was used to make up the desired alkalinity level.

4.4 Materials and Chemical Reagents

The chemicals that were used at various stages of this research are listed in Table 4.2. Most of the reagents were purchased from Sigma Aldrich (Ontario, Canada) and Fisher Scientific (Ontario, and Alberta, Canada).

Table 4.2: List of the chemicals used in this study

Chemical	Formula	Grade	Supplier
Hydrogen Peroxide	H_2O_2	30 %	Fischer
Ethylenediaminetetraacetic acid	$C_{10}H_{16}N_2O_8$ (EDTA)	A.C.S reagent	Fischer
SYBR GREEN I	NA	10000X	Invitrogen
Dimethyl Sulfoxide (DMSO)	$(CH_3)_2SO$	HPLC grade	Sigma Aldrich
sodium acetate	$NaCH_3CHOO$	99.99%	Sigma Aldrich
sodium chloride	NaCl	A.C.S reagent	Fisher Scientific
Benzoic Acid	C_7H_6O	A.C.S reagent	Fischer Scientific
Potassium iodide	KI	A.C.S reagent	Fisher Scientific
Potassium iodate	KIO_3	A.C.S reagent	Fisher Scientific
Potassium Hydrogen Phthalate	$KHC_8H_4O_4$ (KHP)	A.C.S reagent	Fischer Scientific
Chitosan	NA	Practical grade	Sigma Aldrich

Chemical	Formula	Grade	Supplier
Manganese dioxide granules	MnO_2	99.99+%,	Sigma Aldrich
Lead Dioxide	PbO_2	A.C.S reagent	Sigma Aldrich
Silver granule (>250 micron)	Ag	99.99%	Sigma Aldrich
SEPABEAD® EC-EP	NA	EC-EP	Resindion, Italy
Hydrochloric Acid	HCl	A.C.S reagent	Fisher Scientific
Sodium persulphate	$Na_2S_2O_8$	$\geq$98%	Sigma Aldrich
Dipotassium Phosphate	K_2HPO_4	99.99%	Sigma Aldrich
Ammonium Chloride	NH_4Cl	99.998%	Sigma Aldrich
Potassium Nitrate	KNO_3	99.999%	Sigma Aldrich
Acetone	CH_3COOCH_3	HPLC grade	Fischer Scientific
Aluminum Sulfate Octadecahydrate	Al_2 (SO4) $_3$,$18H_2O$)	A.C.S reagent	Sigma Aldrich
Ferric Oxide	Fe_2O_3 (powder <5 micron)	≥99%	Sigma Aldrich
Polysulfonate standards	7kDa, 4kDa, and 2kDa	NA	American Polymer Standards Corporation
Sodium borate	$NaBrO_3$	Laboratory grade	Fisher Scientific
Catalase from bovine liver (lyophilized powder)	NA	≥10,000 units mg^{-1} protein	Sigma Aldrich
Glass beads (1.8-2.2 mm, A series)	NA	Technical Quality Glass spheres	Potter's Industries Inc.
Hydrofluoric acid	HF	48-51% in water solution	Acros organics
3-aminopropyltriethoxy silane (3-APTES)	$CH_3CH_2O)_3Si(CH_2)_3$ NH_2	99%	Sigma Aldrich

Chemical	Formula	Grade	Supplier
Glutaraldehyde	$CH_2(CH_2CHO)_2$	25% in water Grade I	Sigma-Aldrich
Monosodium Phosphate Monohydrate	NaH_2PO_4. H_2O	A.C.S reagent	Fischer Scientific
Sodium Phosphate Dibasic Heptahydrate	Na_2HPO_4. $7H_2O$	A.C.S reagent	Fischer Scientific

4.5 Experimental Setup for UV/H_2O_2 Treatment

A collimated beam apparatus, consisting of a low-pressure high output amalgam lamp (42 W, Light Sources Inc.) along with a circular stirred reaction petri-dish (KIMAX, 60×35), were employed for the batch UV/H_2O_2 treatment studies (Figure 4.1). To maintain the ambient temperature of the UV lamp constant, a fan was positioned on the top the cylindrical tube attached to the metal closure as shown in Figure 4.1. In order to mimic the UV/H_2O_2 commercial application conditions, experiments were conducted at initial H_2O_2 concentration of 10 ppm, and UV fluences up to 2000 mJ/cm^2 (Sarathy and Mohseni, 2006).

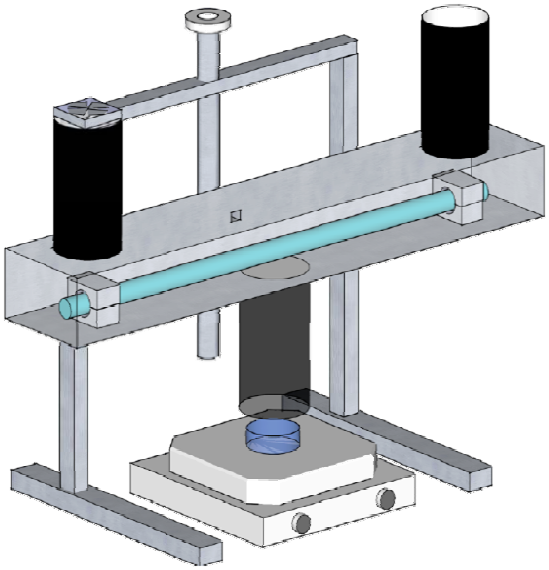

Figure 4.1: Collimated beam apparatus utilized for UV/H_2O_2 studies.

4.6 Experimental Procedure

Experiments were carried out in two main categories: UV/H_2O_2 treatment and coagulation combined with UV/H_2O_2 treatment process. These two main experimental works and their specifications are described in the two following sections.

4.6.1 UV/H_2O_2 advanced oxidation treatment

Samples were collected with volume of 70 ml in triplicate initially, after H_2O_2 dosing, and after achieving the desired fluences. In order to avoid any contamination a quartz plate was used to cover the perti-dish in all the experiments. Hydrogen Peroxide (H_2O_2 30%, Sigma Aldrich) was added initially to the water sample stock to achieve H_2O_2 concentrations of 10 mg/L. Samples were irradiated for certain treatment times calculated according to the method provided by Bolton and Linden (2003) to achieve the desired UV fluence (i.e., up to 2000 mJ/cm^2). Time required to achieve desired UV dose for the treatment process can also be determined by iodide/iodate actinometry (Rahn et al., 1997). Each experiment was carried out in triplicate and the entire water sample was used for various subsequent analyses such as UV_{254}, TOC, and High Performance Size Exclusion Chromatography (HPSEC). Given the high sensitivity of the AOC test and also to avoid any possible contamination, samples for the AOC test were prepared in separate batches and were incubated on the same day of preparation. Any sample not analyzed immediately was refrigerated at 4°C to ensure that the water quality did not change prior to the analysis. For each experiment blank and control sets were collected as well.

According to the literature (Liu et al., 2003) and also our primary findings, not all the initially dosed H_2O_2 is consumed during the course of the treatment. Indeed, a substantial amount (i.e., 80-90%) of the initial H_2O_2 remains un-reacted and may interfere with the analytical techniques. Hence, the residual H_2O_2 should be removed prior to any analysis (Liu et al., 2003). Liu et al. (2003) studied several organic and inorganic quenchers and recommended Catalase from bovine

liver with the concentration of 0.2 mg/L as a promising, fast, and effective agent for H_2O_2 removal with no impact on water characteristics such as TOC, disinfection by-product formation potential. Therefore, all UV/H_2O_2 treated water samples, except those which were used to analyze H_2O_2, were quenched from residual H_2O_2 using Catalase prior to UV_{254}, TOC, and HPSEC analyses (Sarathy and Mohseni, 2007). Quenching of residual H_2O_2 before AOC bioassay was different and will be discussed later.

4.6.2 Chemical coagulation

To study the impact of pretreatment (i.e., coagulation) on the effectiveness of UV/H_2O_2, CW and BI waters underwent coagulation treatment using two different coagulants. Chitosan (practical grade, Sigma Aldrich), a natural polymer made from marine invertebrates and Aluminum Sulfate Octadecahydrate ($Al_2(SO4)_3$,$18H_2O$, Sigma Aldrich, ACS reagent 98+%) also known as Alum, were utilized for coagulation process prior to the UV/H_2O_2 treatment. To choose between these two coagulants Jar test was carried out and characteristics (e.g., UV_{254}, TOC) of the treated water were measured for different dosages of the coagulants. The best coagulant (and dosage) in terms of TOC and UV_{254} removal was selected for subsequent experiments. To the best of our knowledge, there have been few studies concerning the use of Chitosan for drinking water treatment applications. Moreover, very little work focused on the impact of Chitosan on NOM and its characteristics.

4.6.2.1 Jar test procedure

Coagulation tests were performed according to the Jar test conditions reported by Rizzo et al. (2008) but with some slight modifications. Stock solution of Alum with the concentration of 10 g/L of Alum was made in Milli-Q water and was initially injected into the solution right before the rapid mixing to make up desired coagulant dose. In the case of Chitosan, 500 mg of Chitosan

was dissolved in 2.5 mL of 2M HCl (A.S.C reagent, Fisher Scientific) and 47.5 mL Milli-Q water and was left for 60 minutes. Then, 50 mL of Milli-Q water was added and solution was thoroughly mixed (Rizzo et al., 2008). Similar to alum, Chitosan was spiked right before the rapid mixing to make up the desired dose. The standard Jar test procedure consists of a rapid mixing at 150 rpm for 2 minutes after the addition of coagulant, followed by 30 minutes slow mixing at 60 rpm. Sixty rpm was the slowest possible speed provided by the stir plate. Following the slow mixing, flocs formed were allowed to settle for 60 min (Rizzo et al., 2008). The supernatant was then drawn and filtered through 0.45 μm membrane filter which was pre-rinsed with 1L of Milli-Q water. Filtered samples were used for subsequent analytical analyses (UV_{254}, TOC, residual aluminum, and HPSEC). All experiments were performed at room temperature and at natural pH (6.8 for Capilano water, and 6.7 for Bowen Island water) of the raw waters. To select the best dose of coagulant at which maximum removal in terms of UV_{254}, and TOC can be achieved, different dosages of coagulant from 0.5 to 5 mg/L for Chitosan, and 5 to 80 mg/L for alum were applied and the best dose and coagulant in terms of reduction of TOC, and UV_{254} was chosen for subsequent experiments.

4.6.3 Combined coagulation-UV/H_2O_2 process

Coagulation was performed according to the section 4.5.3. Then, samples were filtered through 0.45μm pre-rinsed filter and were spiked with H_2O_2 to the initial dose of 10 ppm. The rest of study was performed according the UV/H_2O_2 treatment process specifications described in section 4.5.1.

4.7 H_2O_2 Quenching for AOC Assay

A considerable amount of H_2O_2 (about 80-90%) will remain un-reacted in the solution after UV/H_2O_2 treatment and should be removed prior to further analyses. This is indispensible since

experimental results indicated that residual H_2O_2 (i.e., >0.2 ppm) inhibits bacterial regrowth, and hence deteriorates the results of the AOC assay. To the best of our knowledge there has been no information available on the literature for proper H_2O_2 removal prior to the AOC analysis. Therefore, different organic and inorganic agents were tested and compared in terms of H_2O_2 decomposition rate and their impact on the original AOC of the sample.

4.7.1 Quenching in the solution

Catalase from bovine liver (lyophilized powder, ≥10,000 units mg^{-1} protein, Sigma Aldrich) is an enzyme that has been widely used to decompose H_2O_2 into water and oxygen. For this reason, stock solution of Catalase (500 mg/L) was made in Milli-Q water and was spiked into the sample containing H_2O_2 to achieve Catalase concentrations of 0.2 mg/L as suggested by Liu et al. (2003).

Moreover, inorganic substances such as manganese dioxide granules (MnO_2, 99.99+%, Sigma Aldrich), Lead dioxide (PbO_2, 97+% ACS reagent, Sigma Aldrich), Silver granule (Ag, >250 micron 99.99%, Sigma Aldrich), and Ferric oxide (Fe_2O_3, ≥99% powder <5 micron, Sigma Aldrich) are also known to be effective at removing H_2O_2; hence, they were tested for H_2O_2 elimination.

To quench residual hydrogen peroxide, 100 mg of MnO_2, 100 mg of PbO_2, 500 mg of Fe_2O_3 and 1g of Ag were individually added to the solution containing H_2O_2 (10 ppm) with the volume of 70ml and were mixed until residual H_2O_2 reached below 0.2 ppm. Residual H_2O_2 concentration was measured by the method of Klassen et al. (1994) and the time in which H_2O_2 concentration reached below 0.2 ppm was selected as the minimum required mixing time.

4.7.2 Immobilized Catalase

Immobilized Catalase was evaluated as an effective means of quenching the residual peroxide in water. Less enzyme contamination of the product, simple recovery and reuse of the biocatalyst in addition to enhanced stability and economic benefits have made enzyme immobilization as an advantageous tool for industrial and technical applications (Sheldon, 2007; Alptekin et al., 2010).

In this research glass beads were initially chosen as support for Catalase immobilization due to their availability and lower probability of organic contamination of the sample. The following presents the procedure that was followed to immobilize Catalase on the glass bead as support.

4.7.2.1 Immobilization procedure on glass bead

The method proposed by Vasudevan and Weiland (1994) was employed for the immobilization of Catalase on glass surface with some minor modifications. Moreover, in all the steps attempts were made to avoid any possible contamination (i.e., carbon contamination) that could deteriorate the final AOC data. The following presents the procedure for the immobilization of Catalase on glass bead.

1) *Hydrofluoric Acid Treatment (etching)*: Glass beads (1.8-2.2 mm, A series Technical Quality Glass spheres, Potter's Industries Inc.) were washed with warm water and detergent and were rinsed afterward with Milli-Q water. Next, 50 mL of distilled water and 50 mL of hydrofluoric acid (48-51% in water solution, Acros organics) were added to 100 g of glass beads in a plastic container and solution was left for 1 hour. Then, hydrofluoric acid was removed and the beads were washed several times with ultrapure water. HF treatment was used to etch the surface of the glass, providing more rough surface area suitable for further treatment steps. A reduction in size of the glass beads was observed as a result of treatment with hydrofluoric acid.

In addition, after washing with distilled water, a considerable amount of the debris on the glass surface was removed.

2) *Neutralization:* 100 mL sodium hydroxide solution (10 N) was added to neutralize the glass beads and the content was heated in water bath for one hour at 80° C. Afterwards, the glass beads were washed extensively with ultrapure water and dried at 80 °C.

3) *Silanization*: Glass beads from the previous step were silanized to prepare the carrier for glutaraldehyde treatment. During silanization hydroxyl groups (OH) of glass replace the alkoxy groups (i.e., $–O-CH_2-CH_3$) of 3-aminopropyltriethoxy silane (3-APTES, $(CH_3CH_2O)_3\ Si(CH_2)_3\ NH_2$, 99% Sigma Aldrich) producing Si-O-Si bonds (Figure 4.2). This step provides amino ($–NH_2$) groups for further glutaraldehyde treatment.

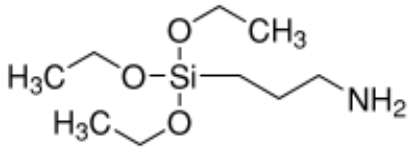

Figure 4.2: 3-aminopropyltriethoxy silane (3-APTES)

To perform silanization, 200 mL of diluted 3-aminopropyltriethoxy silane (2% v/v) in acetone (HPLC grade, Fischer Scientific) was added to the glass beads in a glass container, and the contents were left in a water bath under the fume hood at 45°C for 24 hours. Then, beads were washed thoroughly with ultrapure water and stored in refrigerator (Vasudevan and Weiland, 1994; Alptekin et al., 2010). According to the method of Vasudevan and Weiland (1994) and to enhance the stability and the activity of the immobilized enzyme, glass beads were re-silanized for an additional 24 hours and were washed extensively with ultrapure water afterward.

4) *Glutaraldehyde treatment*: Glutaraldehyde ($CH_2\ (CH_2CHO)_2$, 25% in water Grade I, Sigma-Aldrich) is an organic compound frequently used in biochemistry applications as cross-linker with two identical reactive ends (homo-bifunctional, Figure 4.3). Cross-linking agents

contain at least two reactive groups that are reactive towards numerous functional groups and can create chemical covalent bonds between two or more molecules. Functional groups that can be targeted by cross-linking agents are primary amines (-NH_2), carboxyls (-COOH), sulfhydryls (-SH), carbohydrates and carboxylic acids. Proteins have many of these functional groups and therefore, can be readily conjugated using cross-linking agents (National Institute for Occupational Safety and Health (NIOSH), http://www.cdc.gov/niosh/topics/glutaraldehyde).

Figure 4.3: chemical structure of Glutaraldehyde

In this work, 200 mL of 2.5% (v/v) aqueous solution of Glutaraldehyde (25% in water Grade I, Sigma-Aldrich) was added to the glass beads and the solution was kept for 2 hours at room temperature. Next, the beads were washed extensively with distilled water and left in the oven at 60° C to dry overnight.

Glutaraldehyde carbonyl groups react with amine (–NH_2) group of modified glass bead (with 3-APTES) according to the following reaction to create –CHO groups (Alptekin et al., 2009):

$$OHC-(CH2)3-CHO\ +\ -Si-O-Si(CH2)3NH2 \rightarrow -Si(CH2)3N=CH(CH2)3CHO$$

5) *Immobilization of Catalase*: Amine (–NH_2) functional group attached to Catalase can be readily conjugated with -CHO group created on the glass beads as a result of Glutaraldehyde treatment, according to the following reaction:

$$-\mathrm{Si(CH_2)_3N=CH(CH_2)_3CHO} + -\mathrm{NH_2} - \mathrm{Cat} \rightarrow -\mathrm{Si(CH_2)_3N=CH(CH_2)_3CH=N-Cat}$$

To immobilize Catalase, glass beads were immersed in phosphate buffer (different from Vasudevan and Weiland, 1994) solution with pH 7.0 and ionic strength 50mM containing the enzyme (1g/L). The phosphate buffer was made by dissolving 0.292 g monosodium phosphate monohydrate (A.C.S reagent, Fischer Scientific) and 0.774 g disodium phosphate heptahydrate (A.C.S reagent, Fischer Scientific) in 100 mL water. After six hours, the beads were removed and were washed with 5 liters of the same phosphate buffer solution to ensure that all the un-attached enzymes are removed and glass beads were stored in a refrigerator for further use (Vasudevan and Weiland, 1994; Alptekin et al., 2009).

4.7.2.2 Immobilization on polymeric support

Immobilization of Catalase on glass involved tedious procedure and/or working with hazardous materials, so a more user friendly technique was desired. Epoxy activated resins were suggested as providing very easy immobilization protocols, thereby attracting significant attention (Maeto et al., 2002, 2003; Torres et al., 2003; Alptekin et al., 2010). SEPABEAD® EC-EP (Resindion, Milan, Italy) is a synthetic organic resin (particle size 150-300 μm) with polymethacrylate matrix and very high superficial density of oxirane (epoxy) groups (~100 μmol/mL) on its surface, which bind to proteins (i.e., Catalase) at neutral or alkaline pH, to form covalent bonds with long-term stability within a pH range of pH 1 to 12 (Figure 4.4) (Mateo et al., 2002). The internal geometry of the support also provides good geometrical condition for very intense enzyme-support interaction (Mateo et al., 2002). These characteristics facilitate "multi-point-attachment" of the enzyme on SEPABEAD® (Sheldon, 2007).

At the time of this study there was no specific protocol available in the literature for the immobilization of Catalase on SEPABEAD®. As a result, several protocols were evaluated to

find a satisfactory condition for immobilization of Catalase, and finally a slightly modified method of Alptekin et al. (2010) was utilized. However, it should be noted that the proposed protocol by Alptekin et al. (2010) was originally applied on a different polymeric support called Eupergit-C®. Because of the similarities between the nature of Eupergit-C® and SEPABEAD®, that protocol was deemed applicable to SEPABEAD® as well.

A total of 15 g of support materials (particle size 150-300 µm) was suspended in 100 mL of 50 mg/mL Catalase solution prepared in 1 M potassium phosphate buffer (pH=7) and was mixed gently for 12 hours at room temperature in an AOC-free bottle. Then, the prepared SB was extensively washed with buffer solution to remove any residual/unattached protein.

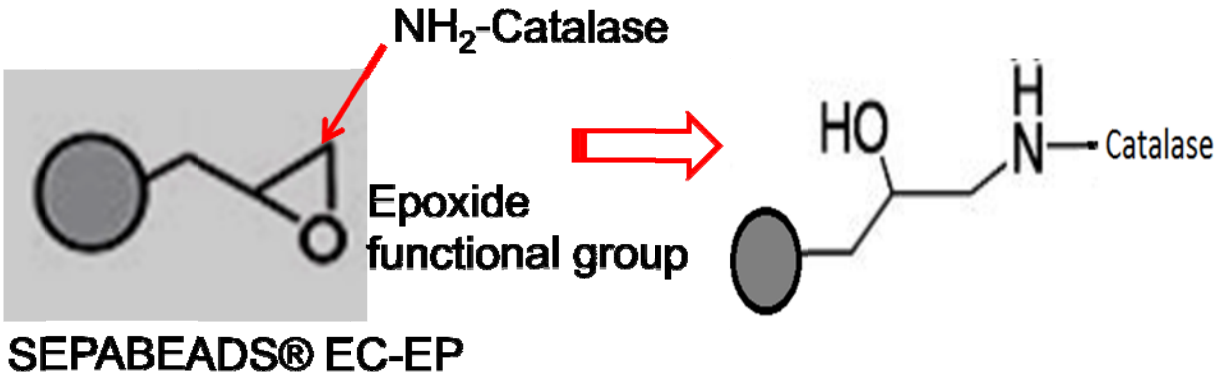

Figure 4.4: Immobilization of Catalase on SEPABEAD®

To remove H_2O_2 prior to the AOC experiments, 100 mg of SEPABEAD®, prepared according to the abovementioned protocol, was added to 70 mL of water treated with UV/H_2O_2 containing residual H_2O_2 and was allowed to mix. H_2O_2 concentration was measured during the mixing period to determine the time sufficient for peroxide removal. The residual H_2O_2 in all the samples were found to be below 0.1 mg/L. Based on the earlier tests, residual H_2O_2 with concentration of less than 0.2 mg/L was found to be satisfactory to perform the AOC assay.

4.7.2.3 Biocatalyst activity test

The efficiency of the biocatalyst made from the previous stages was evaluated in terms of rapidness and effectiveness in removing H_2O_2. Since the procedure for preparation of glass beads was time consuming and tedious, the possibility of reusing the glass beads was examined for several consequents batches.

4.8 Assimilable Organic Carbon (AOC) Measurement Using Flow Cytometry

4.8.1 General overview

The current AOC bioassay is an indirect procedure which estimates the biodegradable organic carbon through enumeration of the heterotrophic bacteria after regrowth. The result is stated in terms of acetate-carbon equivalent (Kasahara and Ishikawa, 2002). The original AOC bioassay was developed by Van der Kooij (1982, 1992) and was modified later by Lechevalier et al. (1993) by raising the incubation temperature and inoculum density. More recently, a simple, rapid and more accurate technique was developed by Hammes and Egli (2005) using flow-cytometric enumeration of bacteria. Details of this method are well described by Hammes et al, (2005, 2008), and are explained in the following sections.

4.8.2 Preparation of AOC-free glassware

This is a crucial preparation step in all the AOC bioassays because the slightest contamination can significantly influence the final data. According to the Standard Methods (SM 9217, Clescerl et al., 1999), PYREX® beakers and 40 mL borosilicate vials were washed extensively with detergent and warm water followed by rinsing with ultrapure water for at least three times. Then, glasswares were submerged overnight in 0.1 N Hydrochloric Acid (A.C.S reagent, Fisher Scientific) for at least 12 hours. Next, glasswares were rinsed with ultrapure water at least three

times and left to air dry. Glasswares were then covered with aluminum foil and heated in a muffle furnace at 550 °C for 5 hours.

According to the SM 9217 (Clescerl et al., 1999) plastic vial caps with Teflon-lined silicone septa were first washed with common detergent and warm water and rinsed with ultrapure water. Next, they were soaked in 100 g/L sodium persulphate ($Na_2S_2O_8 \geq 98\%$ reagent grade, Sigma Aldrich) solution at 80 °C for at least 1 hour to oxidize any possible contamination. Then, caps and septa were rinsed thrice with ultrapure water and left to air dry. The cleaned and dried caps were then fitted with septa and screwed tightly onto the cleaned and cooled glass vials.

For all sampling purposes, 60 mL plastic syringe (Becton, Dickinson and Company) was rinsed by flushing with ultrapure water at least 3 times before use. To ensure no possible release of organic contamination from syringe filters (0.22 μm, polyethersulfone, 33 mm filter diameter, sterilized by γ-irradiation, Millex-GP, Millipore), they were rinsed by flushing with at least 1L of ultrapure water. Sterilized pipette tips (Fisher Scientific) were used for sampling and spiking to ensure maintaining the environment AOC-free and sterilized.

4.8.3 Bacterial inactivation/removal

Cells and particulates should be removed through filtration (0.22 μm) due to their possible interference with flow cytometric detection (Hammes and Egli, 2005; Hammes et al., 2008). Note that filtration is not a sterilization step, as it has been found previously (Hammes, 2008) and also through preliminary experiments, that a percentage of cells can pass through 0.22 μm filters and are still potent to grow afterwards. Since in this method, indigenous microbial community is used as inoculum, no significant detrimental impact is expected from a few cells passing the filtration step (Hammes, 2008).

Pasteurization is another process that is applied in the conventional AOC bioassay to inactivate the bacteria. Hammes et al. (2008) have reported that pasteurization can possibly change the organic carbon and increase the AOC. This hypothesis was also investigated by analyzing water samples obtained from different treatment trains of a pilot plant. The work was done in collaboration with École Polytechnique de Montreal and samples were grabbed and analyzed at different dates during fall 2009. Samples were pasteurized at 70°C for 10 minutes and later were filtered (0.22 μm filter) and incubated. AOC of pasteurized and non-pasteurized samples were then assessed and compared to investigate the effect of pasteurization.

4.8.4 Preparation of natural microbial inoculum

The inoculum plays a key role in any biological assay like AOC. *Pseudomonas fluorescens* P17 and *Spirillum* NOX are the two organisms that are used (often in combination) in the conventional standard method (SM 9217, Clescerl et al., 1999). Using these two pure strains has the advantages of being well characterized and also showing uniform growth behavior. On the other hand, from a theoretical point of view, using natural microbial consortium offers a broader specific substrate range, compared to pure cultures (Hammes and Egli, 2005).

In this research, the method developed by Hammes and Egli (2005) was followed to prepare a natural consortium of microbes. First, 30 mL of natural water (e.g., Capilano, or Bowen Island) was filtered through 0.22 μm (pre-rinsed) syringe filter into a 40 mL AOC-free borosilicate vial to remove the bacteria and particulates. Then, the filtered sample was inoculated with 10 μL mL^{-1} of unfiltered/untreated of the same natural water, capped and vortexed, followed by incubation at 30 °C until stationary growth phase (μ=0) was reached. However, further tests were performed on filtered ultrapure water to ensure that the inoculum is AOC-free and will have minimal contribution to the final AOC measured.

It should be noted that the choice of inoculum also impacts the choice of detection method (Hammes et al., 2008). When a natural community is used, plating cannot be used for detection. Adenosine Triphosphate (ATP), scatter and flow cytometry work with both natural communities and pure cultures.

4.8.5 Incubation time

This step was necessary to ensure that bacteria reach stationary phase ($\mu=0$) and therefore, no growth will happen afterward. In this step, natural water (e.g., Capilano water) with 0, and 100 µg/L of acetate-carbon concentration underwent AOC bioassay as described in section 4.5.3 and 4.5.4. Cell concentration was measured at 24, 48, 72, 96 hours after incubation. Stationary phase ($\mu=0$) was confirmed by observing a constant cell concentration over days. The sample was assumed to be AOC-free after reaching stationary phase since it was postulated that all utilizable carbon had been consumed by the microorganisms present in water. Results obtained, indicated that stationary phase ($\mu=0$) is achieved within 48 to 72 hours of incubation; therefore, 72 hours was selected as the incubation time for subsequent experiments to ensure stationary phase is achieved.

4.8.6 Mineral addition

Addition of minerals was suggested as an optional step to ensure that carbon is not the growth-limiting compound (Hammes et al., 2007, 2008; Clescerl et al., (1999). When the water medium is carbon-limited, the absence of minerals can potentially impose no significant impact, otherwise (i.e., limited by inorganic nutrients) considerable influence is expected on the final AOC. Mineral buffer was prepared according to the recipe of Clescerl et al. (1999). The mineral buffer was made of 171 mg/L K_2HPO_4 (99.99%, Sigma Aldrich), 767 mg/L NH_4Cl (99.998%, Sigma Aldrich), and 1.44 g/L KNO_3 (99.999%, Sigma Aldrich) dissolved in filtered (0.22 µm) ultrapure water and prepared in AOC-free glassware. Three sets of natural and synthetic water

(i.e., CW, BI, and SR) were prepared with and without the addition of minerals to study the effect of minerals on the bacterial growth potential.

4.8.7 Growth of natural microbial consortium

The inoculation procedure consisted of filtering 15 mL of water sample (0.22 μm) into 40 mL AOC-free vial. Then, 2.5 μL/mL of mineral buffer/sample, prepared as previously mentioned was added to ensure that carbon was the only limiting substrate (Clescerl et al., 1999). Finally, natural inoculum prepared according to the section 4.7.4 was added to the sample. According to the method of Hammes and Egli (2005, 2007) final cell concentration in sample after inoculation and before incubation should be about 10^4 (cell/mL). Therefore, the required volume of inoculum should be calculated accordingly for each individual natural microbial community. Next, the sample was capped, vortexed, and incubated at 30 °C for 72 hours.

4.8.8 Effect of inoculum

One unreported aspect and outstanding question related to the method of Hammes and Egli (2005), is the choice of natural microbial community and it potential impact on the final outcomes of the AOC test. For this reason three different inocula were prepared from different natural water sources (i.e., Capilano, Trepanier, and Bowen Island waters) and were cultivated on three different natural waters (i.e., Capilano, Trepanier, and Bowen Island waters) and a synthetic water (with SR NOM). AOC of the waters inoculated with different inocula was assessed and information obtained was used to carry out subsequent experiments.

4.8.9 Cell staining and enumeration by flow cytometry

Because of the method used for cultivation of the bacteria (i.e., cultivation-independent, Berney et al., 2008), and according to Hammes and Egli (2005), flow cytometric enumeration was used

to count the cells grown in the sample. Using this technique has the advantage of rapid and accurate measurement of several samples within a short time (Hammes and Egli, 2005).

First, samples were taken from the incubation chamber after 72 hours and vortexed exhaustively for 30 seconds to ensure a thoroughly mixed solution. Then, 1 mL of the sample was drawn into a flow cytometer tube (Polystyrene Round-Bottom Test Tube, 5 mL, snap cap, Becton, Dickinson and Company) using sterilized pipette tip (Fisher Scientific). This sample was stained with 10 µL of EDTA (500 mM) and 10 µL SYBR Green I nucleic acid gel stain (10,000X concentrate, Invitrogen) diluted 1:100 times in dimethyl sulfoxide (DMSO, HPLC grade, Sigma Aldrich) stored at -20° C until use according to Hammes et al. (2008). The role of the SYBR GREEN was to dye the DNA of the microorganisms so they can be detectable for the flow cytometer (Lebaron et al., 2001). EDTA was used to dissociate the agglomerated cells, the case that usually happens when dealing with animal or plant cells. Hence, it was not practiced very often in this study.

The amount of SYBR GREEN and EDTA should be increased accordingly when cell concentrations exceeds 1E7 (Hammes et al., 2008, 10 µL of respectively fluorochrome and EDTA for every 1 x 10^7 cells per mL). Moreover, it is recommended the sample to be diluted to a concentration between 0.1 – 2 x 10^5 cells/mL, if the bacterial concentration in the sample exceeds 2 x 10^5 cells/mL. This step should be done after staining and just before measurement with the dilution liquid (preferably from the same solution in which the bacteria are suspended, filtered with a 0.22 µm sterile syringe filter prior to use) (Hammes et al., 2008). In addition, if the bacteria are present in clusters (can be controlled with fluorescence microscopy or evidenced through FCM light scatter data), dispersion of clustered cells can be achieved with the addition of 1% v/v of lysis buffer (comprising 10 % v/v Triton X-100, 5 % v/v Tween 20, 10 mM Tris-HCl, and 1 mM EDTA) prior to staining, coupled with vortexing or gentle sonication (Hammes

et al., 2007). This phenomenon was not observed during this study. Samples prepared in this way were stored in the dark for at least 20 minutes prior to analysis by flow cytometer (Hammes et al., 2007).

To carry out the cell analysis, a flow cytometer unit (BD FACS-Callibur System Becton, Dickinson and Company) in the Biomedical Research Centre at the University of British Columbia was used. Flow cytometer counting beads were used in preliminary analyses to obtain the cell counts, but due to significant uncertainty and low reliability which actually caused deviations in the results, their application was abandoned. However, the equipment used in this study did not have flow meter device; therefore, the equipment flow rate was measured by pipetting 1mL of ultrapure water in to a flow cytometry tube and the remaining volume was measured after 10 minutes. Change in the water sample volume divided by the time was assumed to be the flow rate of the instrument. The measurement was done after and before every analysis, and consistent results were obtained suggesting a stable flow rate for the flow cytometer. Flow cytometry instrument was configured to stop after 60 seconds. Having the flow rate known, the cell concentration in the tube and the sample vial was simply calculated. Net grown cells after incubation were correlated to the AOC content with a theoretical conversion value ($1 \times 10^7 \frac{\text{cells}}{\mu\text{g}-\text{C}}$) as suggested by Van der Kooij (2002) and Hammes and Egli (2005).

Flow cytometer (Figure, 4.5) was set with the following detector settings shown in the table 4.3. The primary threshold parameter was the side scatter channel at a value of 275 and there was no compensation.

Table 4.3: Flow Cytometer settings for cell enumeration

Channel	Voltage	Amp gain	Mode
Forward Scatter Channel (FSC)	E01	2.23	Log
Side Scatter Channel (SSC)	412	1.00	Log
Fluorescence Channel 1 (FL1)	597	1.00	Log
Fluorescence Channel 2 (FL2)	674	1.00	Log
Fluorescence Channel 3 (FL3)	520	1.00	Log

Figure 4.5: FACS Calibur BD flow cytometer

4.8.10 Control samples

Control samples were included in all the analyses. For the positive control, natural water with 100 µg/L acetate-carbon was used. The absence of growth in this sample would suggest the presence of a growth inhibitor (e.g., H_2O_2), or the absence of essential nutrients (e.g., P, N). As for the negative control, ultrapure water (or Evian water) was used to monitor any possible contamination.

4.8.11 Yield coefficient tests

With the procedure depending on microbial cells growing in the water sample, yield coefficient should be used as a conversion factor to translate cell concentration to AOC content. In other words, it has to be determined how many cells can grow within the sample as a result of a certain amount of AOC present. Moreover, it has to be examined whether the inoculum can yield linear/proportional number of cells on different concentrations of standard AOC such as sodium acetate. Note that for more simplicity and conformity with other studies (Hammes and Egli, 2005; Van der Kooij, 2002), yield coefficient tests were performed using desired concentrations of sodium acetate (i.e., 50, 100, 150 μg/L). Oxalate is another organic substrate with more complex molecular configuration which can also be used to make artificial AOC concentrations (Hammes and Egli, 2005; Van der Kooij, 2002). However complexity, concentration, and difference in nature of the organic content of water may influence final number of cells reproduced during incubation period (Hammes and Egli, 2005; Van der Kooij, 2002).

To achieve this, solutions were made using natural water (e.g., Capilano water or Evian water) with desired amount of acetate-carbon (i.e., 50, 100, and 150 μg/L acetate-C). Number of cells grown on known concentrations of acetate-C solutions were used to correlate the number of cells grown on AOC and hence, to establish the calibration curve.

To establish the calibration curve, cell concentration and AOC of the original water sample were considered as background and hence, were deducted from the total cells and the final AOC of each sample. Next, cell concentrations were correlated to the corresponding AOC values. Yield coefficient was defined as the slope of cells' number versus the acetate-C content of the solution.

4.9 Analytical Techniques and Procedures

4.9.1 pH measurement

The pH of the water samples was measured using a pH meter (Thermo Orion, model 330) before and after each treatment. When it was necessary, pH of synthetic water used in the experiments was adjusted to the ones of natural waters (6.5-7.5) using sodium hydroxide (0.1 N solution, A.C.S reagent, Fischer Scientific).

4.9.2 UV_{254} measurement

All spectrophotometric measurements were carried out using a UV-Vis spectrophotometer (Shimadzu UV-Mini 1240) with a cell path length of 1 cm. Absorbance of all water samples before and after treatment stage was measured at 254 nm. Wavelength of 254 nm was chosen since it was shown that this parameter can be used as a representative of chromophoric NOM which mainly is consisted of organic carbons with aromatic and conjugated double bounds (Sarathy, 2009).

4.9.3 Total organic carbon analysis

Total Organic Carbon (TOC) content of each water sample was analyzed in triplicate using the TOC analyzer (Shimadzu TOC-VCPH). The organic carbon is measured through the non purgeable organic carbon (NPOC) method that is based on purging volatile organic carbon of the acidified sample using an inert gas (i.e., Nitrogen). Inorganic carbon is converted to carbon dioxide through acidification and the remaining carbon content is oxidized to carbon dioxide through high temperature catalytic oxidation process.

4.9.4 High performance size exclusion chromatography (HPSEC)

Molecular weight distribution is a key bulk property of NOM, and estimating the average molecular weight of organic matter has been the focus of many studies (Pelekani et al., 1999;

Allpike et al., 2005; Sarathy and Mohseni, 2007). Recently, a method has been developed by using a tightly packed column consisting of small, uniform particles operating at high pressure to deliver fast, high-resolution chromatograms and is referred to as high performance size exclusion chromatography (HPSEC) (Pelekani et al., 1999; Allpike et al., 2005).

HPSEC technique was employed in this study to determine the Apparent Molecular Weight (AMW) distribution of NOM in raw and treated water samples. A WATERS 2695 Separation Module HPLC system equipped with a WATERS 2998 Photodiode Array Detector, set to detection at 260 nm, served as the instrument for HPSEC analysis (Figure 4.6).

Figure 4.6: Photo of the HPLC system employed for High Performance Size Exclusion Chromatography (HPSEC) analysis.

The method of Pelekani et al. (1999) was followed for the HPSEC analysis with some minor modifications along the way. Two eluents were initially used in this study to obtain the best separation and resolution of the chromatograms. Following the method described by Pelekani et al. (1999) the first eluent was Phosphate buffer 0.02 M (A.C.S reagent, Fisher Scientific); at pH 6.8 adjusted with sodium chloride (A.C.S reagent, Fisher Scientific) to 0.1M ionic strength and

the column flow-rate was set to 0.7 mL/min (Sarathy and Mohseni, 2007). The second eluent was sodium acetate 0.05 M (99% ACS Sigma Aldrich), pH= 7.5, and was used according to the method of (Matilainen et al., 2002; Murray and Parsons, 2003). However, few modifications were made to the concentration of sodium acetate to obtain the best separation and resolution (more details are provided in Appendix B). Apparent Molecular Weight was correlated to the retention time by using the calibration curve obtained from polysulfonate standards (7 kDa PSS7K, 4kDa PSS4K, 2 kDa PSS2K, American Polymer Standards Corporation), Acetone (certified A.C.S Fisher Scientific) and Benzoic Acid (certified ACS reagent, Fischer Scientific) with the concentration of 10 ppm.

4.9.5 UV fluence measurement

One of the very important parameters in UV/H_2O_2 process is UV fluence which is the total radiant power of all wavelengths emitted on an extremely small sphere (Bolton, 2000). Fluence is basically defined as the product of exposure time and UV light irradiance and is expressed as mJ/cm^2 (Bolton, 2000; Bolton and Stefan, 2002; Rahn et al., 2006).

UV fluence was determined by iodide (I^-)/iodate (IO_3^-), actinometry in which potassium iodide (A.C.S reagent, Fisher Scientific) is irradiated leading to the formation of triiodide according to the following reaction (Rahn et al., 2006):

$$8KI + KIO_3 + 3H_2O + h\nu \rightarrow 3I_3^- + 6OH^- + 9K^+$$

Triiodide (I_3^-) is measured via the spectrophotometer at λ=450 nm. Potassium iodate (A.C.S reagent, Fisher Scientific) acts as electron scavenger in this reaction, while sodium borate (Laboratory grade, Fisher Scientific) will keep the reaction pH at constant value of 9.25 (Rahn, 1997). Detailed explanation of chemical actinometry is provided in Appendix B.

A radiometer (IL1700, sensor SED240 for 254 nm, International Light Inc.) was also used as a reference to measure irradiance. Radiometer has the advantage of ease of use and rapid measurement of UV radiation. Since radiometers need periodically checking and calibration, chemical actinometers are more accurate and reproducible than physical devices (Kuhn et al., 2004).

4.9.6 H_2O_2 concentration measurement

H_2O_2 concentration was measured through the reaction with iodide catalyzed by ammonium molybdate (Klassen et al., 1994). The following reactions take place in the presence of H_2O_2 and KI resulting in the production of iodate (I_3^-) which builds the basis for the measurement of hydrogen peroxide:

$$H_2O_2 + 2I^- + 2H^+ \rightarrow I_2 + 2H_2O \qquad \text{(A)}$$

$$I_2 + I^- \leftrightarrow I_3^- \qquad \text{(B)}$$

Reaction (A) is slow and therefore is catalyzed using ammonium molybdate. Based on the Le Chatelier's principle, reaction (B) will be strongly in favor of iodate (I_3^-) at high concentration of Iodide. Iodate (I_3^-) can be detected at wavelength 351 nm. Potassium hydrogen phthalate (KHP A.C.S reagent, Fischer Scientific) was used to buffer the solution. H_2O_2 measurement technique is also elaborated in Appendix B.

4.9.7 BDOC measurements

BDOC measurements were performed at Ecole Polytechnique de Montreal, research, development and validation center for water treatment technologies and processes (CREDEAU) (Dr. Barbeau's Lab). Samples were prepared and quenched of H_2O_2 at UBC and were sent

overnight at 4°C. The method employed was similar to the one developed by Servias et al. (1987, 1989), but with some slight modifications.

In summary, water samples are filtered through a 0.45 μm membrane (Supor-450), into carbon-free 125 mL bottles (in duplicate). Then inoculum, consisting of indigenous bacteria (raw water filtered through a 2.7 μm membrane to remove protozoa), is added to the raw water (2% v/v). Next, mineral solution containing nitrogen ($(NH4)_2SO_4$) and phosphorus (KH_2PO_4) is added to the water samples to reach a final concentration of about 10 μg/L of P, and 200mg/L of N. A 40 mL-DOC aliquot is then taken from the 125 mL bottle and analyzed with the TOC analyzer (T_0) (5310C-TOC Analyzer by Sievers (GE)). The glass bottles are then incubated at 20 ° C in dark, without stirring or aeration for a period of 30 days. After 30 days, a second aliquot of 40 mL-DOC is taken again from the125 mL incubated bottles, and is analyzed (T_{30}). BDOC is the difference between the initial and final COD (BDOC= DOC T_0-DOC T_{30}).

4.9.8 Residual aluminum in the treated water

Residual aluminum in the water that undergoes coagulation by alum should be minimized since alum is suspected to be harmful to human and living organisms. Residual aluminum was measured at 167.016 nm wavelength using Inductively Coupled Plasma Optical Emission Spectroscopy technique known as ICP-OES. This technique allows determination of elements in acidified aqueous solutions. Common detection limits for most common elements is in the order of < 1μg/L. Aluminum measurements were performed using PerkinElmer 7300DV Optical Emission Spectrometer in the Environmental Engineering Laboratory at the Department of Civil and Environmental Engineering, UBC.

4.9.9 Alkalinity measurement

Alkalinity determines the capacity of water to neutralize acids by absorbing hydrogen ions without considerable change in pH. Alkalinity in water is mainly due to the presence of bicarbonates, carbonates, and hydroxide. In UV/H_2O_2 treatment applications, alkalinity (i.e., bicarbonates and carbonates ions) can compete with other target species (i.e., micro-pollutants) in scavenging OH radical, hence reducing the overall efficiency of the process. In this study, alkalinity was measured according to the Standard Method (SM 2320). Samples were titrated with standard sulfuric acid (0.02 N) to the endpoint pH equal to 4.5 (SM 2320). Alkalinity is calculated as mg/L of calcium carbonate ($CaCO_3$) equivalent according to the following equation:

$$Alkalinity\ \left(\frac{mg}{L}CaCO_3\right) = \frac{A \times N \times 50000}{mL\ samples}$$

where A is the standard acid used and N is the normality of the acid (0.02 N).

5 Development of Method for Assimilable Organic Carbon Quantification for UV/H_2O_2 Advanced Oxidation

5.1 Introduction

This chapter focuses on the results associated with modifying the method of Hammes and Egli (2005) for determining the AOC of UV/H_2O_2 treated water. The first objective was to obtain/develop the necessary skill to measure the AOC of natural waters using fluorescent staining and flow cytometric enumeration. Next, the incubation time required for the cells to reach the stationary phase was determined. To convert the number of cells grown to AOC, the yield coefficients were obtained for each natural microbial consortium by using AOC solutions artificially made with sodium acetate. The most challenging part was to find a suitable quencher for removing H_2O_2 as experimental findings showed that even a very small amount of residual H_2O_2 (0.2 ppm <) inhibits bacterial regrowth and hence, interferes with the correct estimation of AOC. However, no study reported the impact of H_2O_2 quenching agents on AOC determination. As a result, several organic and inorganic quenchers were examined and their impact on AOC was assessed.

5.2 Cell Staining and Enumeration by Flow Cytometry

Three different raw waters from Capilano Reservoir (CW), providing drinking water to the Greater Vancouver region, British Columbia (TOC~1.4 ppm), Trepanier Creek, providing water to the town of Peachland (PW), British Columbia (TOC~5 ppm), and Josephine Lake, serving water to Bowen Island (BI), British Columbia (TOC~4.8 ppm) were used in this study. The method of Hammes and Egli (2005) was applied according to Section 4.6 to assess AOC, and samples were analyzed using flow cytometer to obtain cell concentration and intensity dot plots.

Figure 5.1.a represents the density dot plot for the stained filtered CW water with SYBR GREEN I before incubation. Because of filtration with 0.22 µm filter, almost no cell was present in this sample, so all the events observed (i.e., small particulate matter in the water, not stained cells) were considered as background. As a result, the events at $<10^1$ on the fluorescence channel (FL1) were excluded accordingly, and positive stained cells were enumerated with the respective selected gate (R_1) (Figure 5.1.a). Distinguishing between background noise signals and bacteria was based on experience with the instrument and relevant controls (e.g., a water sample before and after filtration with 0.22 µm). The x-axis represents the green fluorescence intensity (FL1) and the y-axis is the side scatter channel (Figure 5.1.a) providing additional information about the relative size of the detected particles (Hammes et al., 2007). Figure 5.1.b demonstrates a typical histogram plot of the cells inside the designated gate, when sample is analyzed with flow cytometry. The y-axis shows the number of cells for the corresponding fluorescence intensity presented on the x-axis (FL1).

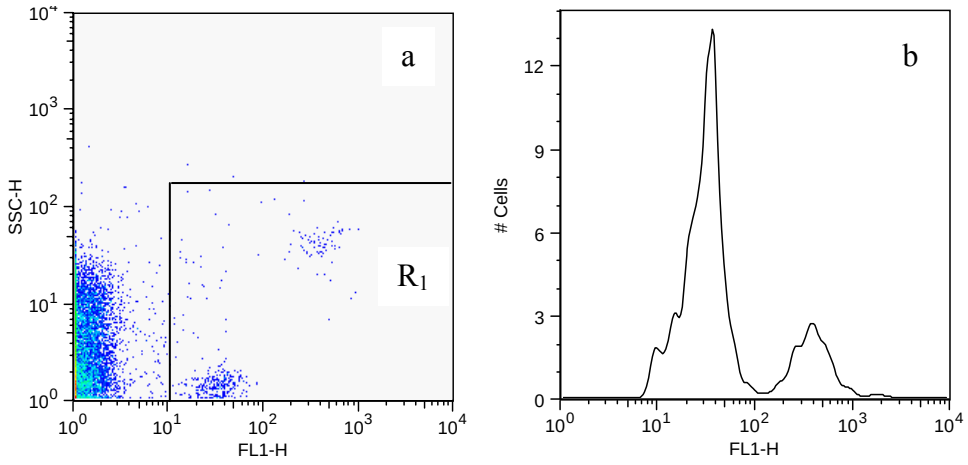

Figure 5.1: Acquisition density plot (a) and Histogram plot (b) for filtered Capilano water (0.22 µm filter)

Figure 5.2 demonstrates the cell concentration for Capilano water 72 hours after incubation. Cell concentration increased significantly over the incubation period due to the consumption of

organic carbon available in the sample. Zones with more color intensity represent higher cell density. More importantly, different cell populations can be discerned within Figure 5.2.a, with specific size and fluorescence intensity. Each colony corresponds to a particular nucleic acid content of the cells (i.e., low nucleic acid and high nucleic acid) as described by Lebaron et al. (2001) and Hammes et al. (2007). It should be noted that flow cytometry can detect total cell concentration using a DNA-targeting fluorochrome (i.e., SYBR GREEN I), and differentiation of the bacteria based on their features such as viability is very complicated and tedious (Hammes et al., 2007).

SYBR GREEN I also emits signal corresponding to the range of red fluorescence spectrum (FL3, 590-620 nm). Hence, Hammes and Egli (2005) and Hammes et al. (2007) used FL1-FL3 diagram to count the cells. This was also practiced in this study (data not shown); however, the FL3 channel intensity was compensated with a higher voltage since signals detected at this channel are about 10 times lower than the ones detected at FL1 channel (Hammes et al., 2007). Experiments were repeated three times and consistent results were obtained confirming the reproducibility of the technique and the experiments. Performing this step was necessary to obtain the skill and confidence in gaining consistent results.

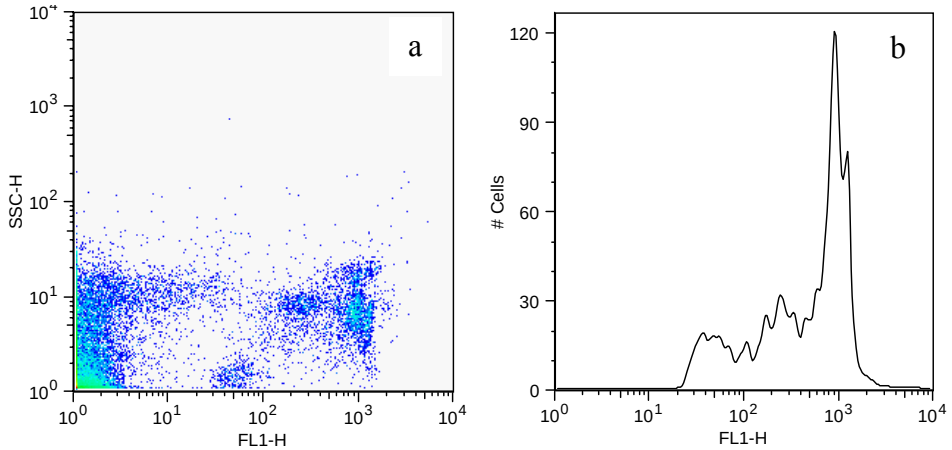

Figure 5.2: Acquisition density plot (a) and Histogram plot (b) for Capilano water after the incubation

5.3 Determination of the Incubation Time

A critical step in the AOC assay is to determine the incubation time needed for the bacteria to reach stationary phase, implying that no further growth will be taking place (μ=0) (Hammes, 2008). Raw Capilano water with zero and 100 μg/L of acetate-carbon concentration was inoculated by its indigenous consortium (prepared according to section 4.7.4) with initial cell concentration of 1E4 cells/mL followed by incubation at 30°C. Cell concentrations were measured every 24 hours after the incubation, and stationary phase was confirmed by observing a constant cell concentration over time. It is assumed that in the stationary phase all the utilizable carbon is consumed by the bacteria so the samples and the inoculum are AOC-free after reaching their stationary state (Hammes and Egli, 2005). Therefore, the number of cells grown up to the stationary phase is assumed to be controlled by the assimilable organic carbon content of the sample (Hammes and Egli, 2005).

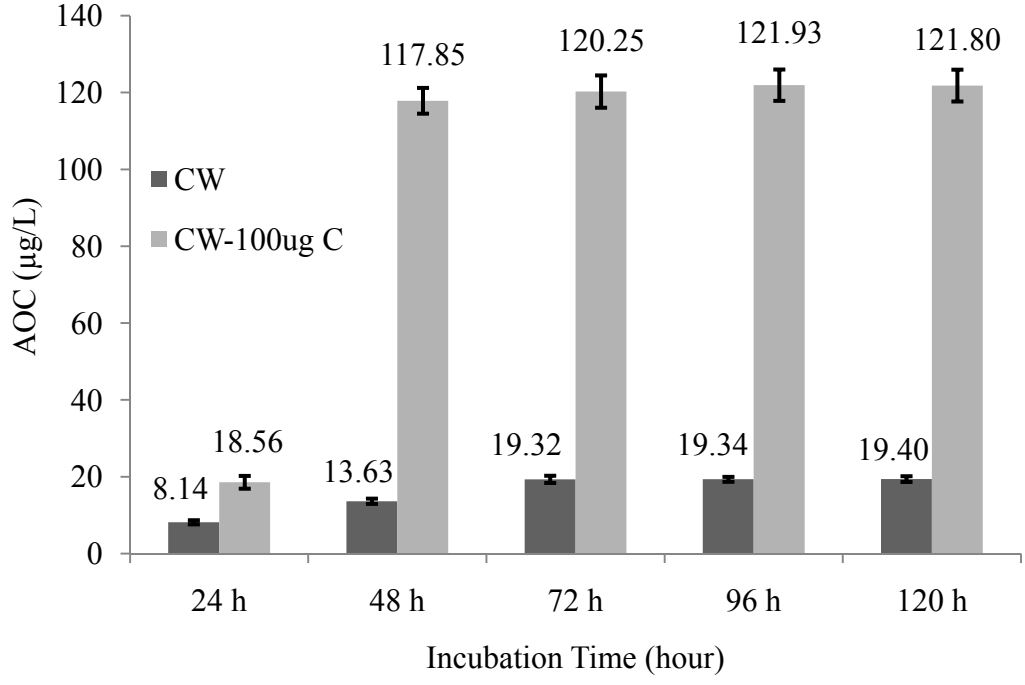

Figure 5.3: Incubation time required for CW with 0 and 100 μg/L of acetate-C to reach the stationary phase

Figure 5.3 shows the corresponding AOC data from the bacteria population growth over the incubation time for the raw Capilano water with zero and 100 µg/L acetate-C. Capilano water with artificial concentration of 100 µg/L of acetate-C reached the stationary phase within 48 hours after incubation. However, results obtained for the raw water suggests 72 hours as the sufficient time after which no growth took place. Hammes and Egli (2005) also observed that at 30 °C it takes between 24 – 48 h for a natural community to reach the stationary phase in a water sample, though this could be very different based on the type (i.e., simple or complex mixture) and concentration of the assimilable carbon available in water. Nevertheless, 72 hours was selected for subsequent experiments as the adequate incubation time for the bacteria to grow and reach stationary phase.

5.4 Determination of Yield Coefficients for Natural Inocula

Yield coefficient should be used as conversion factor to translate cell counts and concentrations to AOC content. In the other words, it has to be determined that how many cells can grow within the sample as a result of a certain amount of assimilable organic carbon available in water. Moreover, it has to be examined whether the inoculum can yield linear/proportional results on different concentrations of a standard AOC source such as acetate-C.

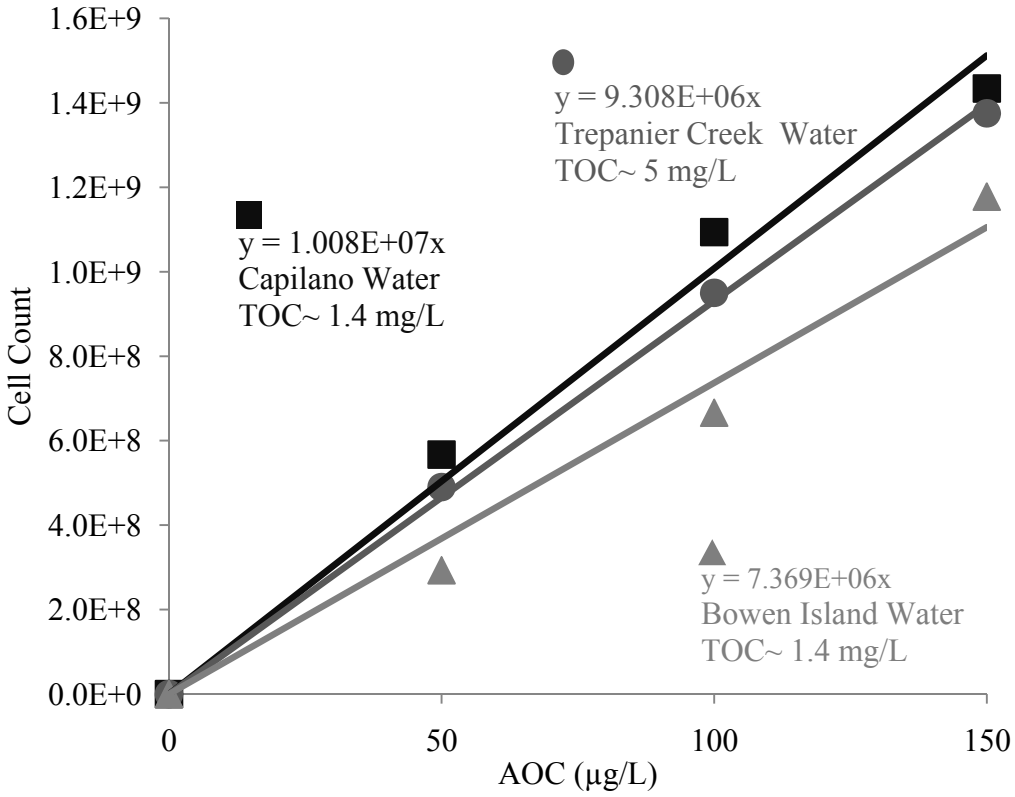

Figure 5.4: Yield coefficients obtained for three different natural waters using raw water with artificial concentration of acetate-C as AOC

Figure 5.4 demonstrates the stationary phase cell concentration versus the initial acetate-C (i.e., AOC) concentration for three different raw waters. As shown, the concentration of cells grown increased linearly as a function of acetate-C content. To obtain each curve, cell concentration of the original water was considered as background and hence, was deducted from the total cell counts. Then, the remaining cell concentration was correlated to the theoretical AOC content. With this information, yield coefficient, with unit of cells μg^{-1} acetate-C, was derived based on the following Equation:

$$Yield = \frac{[Cells] \times sample\ volume}{acetate - C\ (\mu g) \times smaple\ volume}$$

As also demonstrated in Figure 5.4, the yield coefficients obtained for Capilano and Peachland inocula were 1.01E7 and 9.31E6 cell μg^{-1} acetate-C, respectively. This agrees very well with the value (1E7 cell μg^{-1}) suggested by Hammes and Egli (2005) and Van der Kooij (2002). However, yield coefficient obtained for BI inoculum (i.e., 7.37E6 cell μg^{-1} acetate-C) shows about 27% negative deviation from the proposed value. This can be attributed to the type of NOM (i.e., complexity of organic molecules) available in BI water or to the ability/potency of the indigenous microorganisms to consume organic matter. Nonetheless, AOC values obtained for artificially made solutions are very close to their expected theoretical values for all three inocula. This confirms that AOC is directly linked to the number of grown cells up to the stationary phase. The measured yields (i.e., 1.01E7, 9.31E6, 7.37E6 cell μg^{-1} acetate-C) are about 2-times higher than the yield reported for the growth of *Pseudomonas* P17 (4.6E6 cells/µg acetate-C) but slightly lower than the one reported for *Spirillum* NOX (1.2E7 cells/µg acetate-C) reported by Hammes and Egli (2005). This difference can be attributed to the nature of the inocula used in this study (i.e., natural consortium) which can be consisted of a diverse range of microorganisms with different abilities to grow on organic carbon. This would provide broader range of microorganisms capable of consuming the AOC content of water, thereby providing a more realistic interpretation of biostability (Hammes and Egli, 2005). Further, acetate-C is the standard that is used in many other AOC assays (Clescerl et al., 1999), and therefore the findings in here can help to relate the data gathered with other AOC methods.

Given that the yield coefficients calculated from the experiments in this study were close to the proposed value of 1E7 cells μg^{-1} acetate-C (Hammes and Egli, 2005; Van der Kooij, 2002), and also for consistency in all the experiments, this yield coefficient was selected for all subsequent analyses. However, conversion is probably one of the most controversial issues in AOC assays,

since it is uncertain whether conversion to a single simple substrate is the correct approach to reflect growth on complex organics (Hammes and Egli, 2005; Hammes, 2008).

5.5 Effect of Natural Microbial Inoculum

Hammes and Egli (2007) reported that the choice of natural inoculum did not have a significant impact on the final results of the AOC bioassay. Similar observation was also reported by Servias et al. (1989) on the effect of different inocula on the final data of the BDOC test. However, in those studies it was assumed that most natural inocula would have the ability to grow on any water sample, yielding about the same cell concentrations. Nonetheless, this hypothesis was investigated through cultivating three different inocula (CW, PW, and BI) on four different waters (CW, PW, BI, and SW) to better understand the impact of the inoculum.

Figure 5.5 illustrates the results obtained using different inocula on various types of waters. It is apparent that using different microbial communities from different sources generally leads to similar results for a single water source. However, minor deviations are observed in some cases. For instance, in the case of Peachland water there is a significant (about two times) difference when using the indigenous consortium as opposed to the inocula prepared from Bowen and Capilano waters. This could be due to variability within the microbial communities and their ability in consuming different organic matters from different water media. Of important note is that, no two sources of carbon give exactly the same yield when consumed by a specific consortium, and no two bacterial species have exactly the same yield when consuming the same carbon compound (Hammes and Egli, 2005; Van der Kooij, 2002).

Despite the aforementioned results and for more conformity, one would prefer a standardized inoculum that can guarantee consistent results. This inoculum should be tested for purity (i.e., it contains no AOC and hence does not contaminate the test sample), and for growth on simple and

complex organic carbon sources. In this regard, Hammes and Egli (2007) suggested using a commercial natural mineral water (e.g., Evian water, France), which undergoes no disinfection. To obtain higher cell density, the mineral water can be spiked with known concentration of acetate-C. This approach can make an inoculum readily accessible to any user without the need for extensive pretesting (Hammes and Egli, 2005, 2007).

The results obtained in this work, nonetheless, suggest that a careful choice needs to be made when using natural consortium as inocula. That is, different inocula should be tested in order to obtain more decisive conclusions. As a result, it was preferred to use the indigenous inoculum as it was deemed that the bacteria in a specific water sample tend to be the best microorganisms adapted to the carbon source of that water.

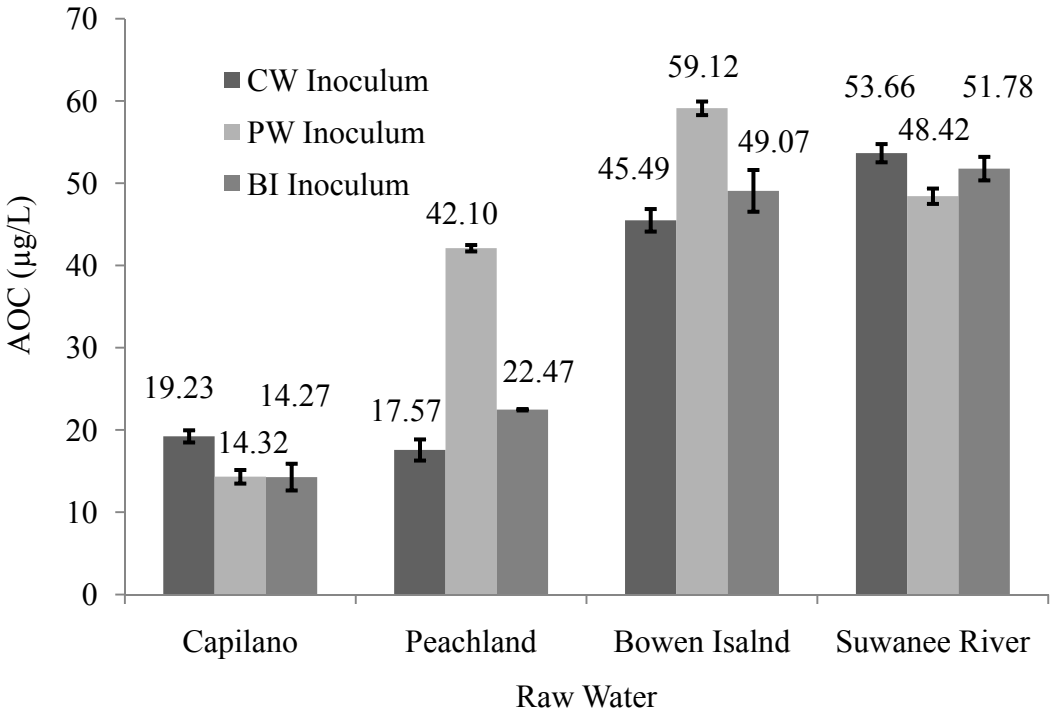

Figure 5.5: Impact of different inocula on the AOC of different natural waters.

5.6 Effect of Mineral on the Bacterial Growth

Addition of mineral buffer (Clescerl et al., 1999) is recommended for waters with low levels of phosphate and nitrate to ensure that carbon will be the only limiting substrate for bacterial growth (Hammes and Egli, 2005; Hammes, 2008). To gauge the effect of mineral addition, AOC of natural water was assessed with and without minerals added to the sample.

Figure 5.6 shows the data for two natural waters (i.e., Capilano and Peachland waters) and the synthetic water made with isolated NOM (TOC~5, pH~6.9) in the absence and presence of minerals. As illustrated, addition of minerals promoted bacterial growth in all the water samples, with the PW water showing the greatest increase (i.e., 42%) in comparison with the CW and SW waters (i.e., showing 20% and 7% increase, respectively). These variations could be due to the levels of minerals already present in these waters. With these tests showing the effect of mineral addition, all subsequent experiments were carried out with the addition of minerals to ensure that carbon was the only limiting substrate for the growth of bacteria.

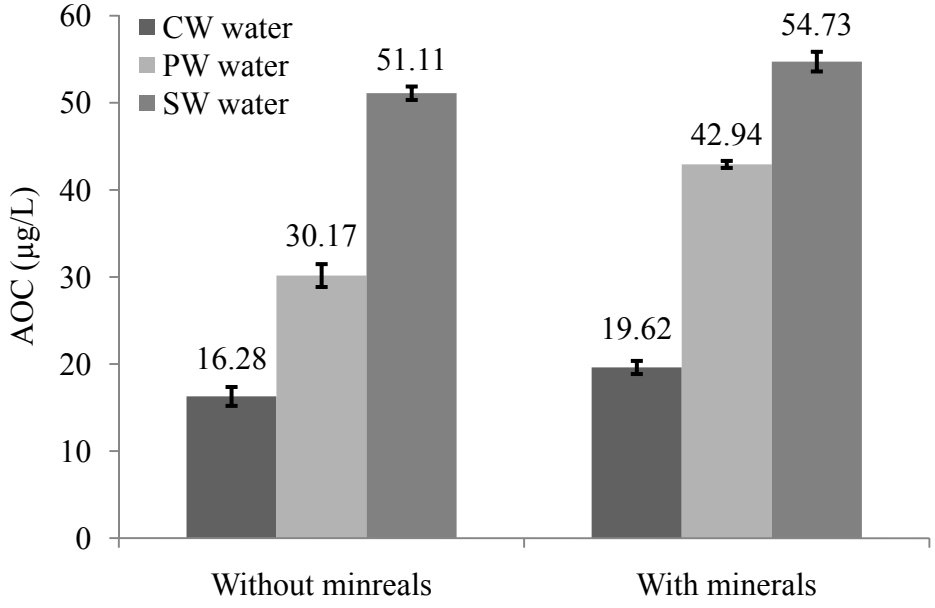

Figure 5.6: Effect of mineral addition on AOC of Capilano, Peachland, and Synthetic waters.

5.7 Effect of Pasteurization

Pasteurization step is applied in the conventional AOC bioassay to inactivate the bacteria present in the sample. This step is replaced with filtration (0.22 μm filter) in the current AOC assay. However, it should be noted that filtration is not a sterilization step, since a few cells could still pass through the filter (Hammes, 2008). Nevertheless, these cells are believed not to pose a significant impact on the final AOC results as the sample is seeded with a notably higher amount of autochthonous microbial consortium (Hammes, 2008).

The effect of pasteurization was gauged as part of a collaborative study with the drinking water research group at Ecole Polytechnique de Montreal. Two sets of samples were obtained from different stages of a pilot plant water treatment system; one set underwent pasteurization. Both sets (i.e., pasteurized and non-pasteurized) were sent to UBC overnight at 4°C for AOC analysis.

Figure 5.7 presents the AOC data obtained for pasteurized and non-pasteurized samples. As demonstrated, pasteurization generally leads to increases in the amount of AOC in all the samples. About 20% increase was observed in the AOC as a result of pasteurization. Nonetheless, no concrete conclusion was made in this regards. Hammes (2008) also reported similar observation and concluded that pasteurization can cause changes in the organic carbon structure such that it increases the AOC. Therefore, applying pasteurization step is not recommended where, filtration is used to remove bacteria and particulates.

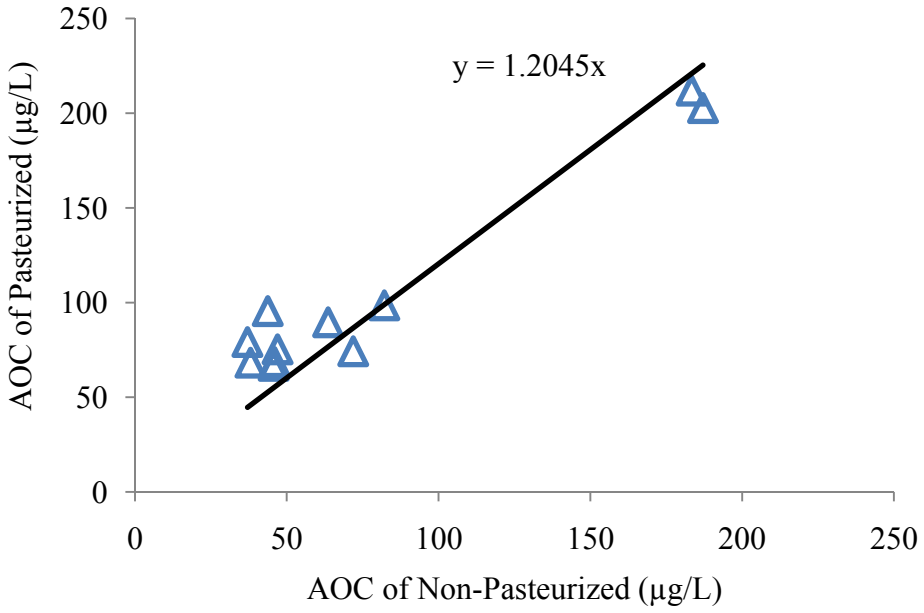

Figure 5.7: Impact of pasteurization on the AOC data for a treatment train (in collaboration with Ecole Polytechnique de Montreal)

5.8 Hydrogen Peroxide Quenching Agents

Residual H_2O_2 after the UV/H_2O_2 treatment needs to be quenched as experimental findings showed that residual H_2O_2 (> 0.2 ppm) inhibits bacterial regrowth and hence, interferes with proper/accurate estimation of AOC. Experimental data (not shown) suggested that residual H_2O_2 level must be reduced down below at least 0.2 ppm to ensure no detrimental effect on bacterial growth in the AOC assay. For this reason, different organic and inorganic reagents were utilized in this work to decompose H_2O_2 present in water samples. The candidate agents were examined and compared in terms of their ability in removing hydrogen peroxide and their effect on AOC.

5.8.1 Effect of Catalase from bovine liver

Liu et al. (2003) reported that Catalase with concentrations of up to 0.2 mg/L in water poses no negative effect when it is used to remove H_2O_2 prior to the TOC and DBPs formation potential tests. Preliminary data showed that using the minimal concentration of Catalase (0.2 ppm) can

quench 10 mg L^{-1} H_2O_2 within 30 minutes. Therefore, this information was used for further AOC experiments in which H_2O_2 was quenched using catalase.

Figure 5.8 demonstrates the impact of Catalase (0.2 ppm) on the original AOC of the raw water when it was used to remove hydrogen peroxide. As demonstrated, AOC concentration of the original raw water increased as a result of using Catalase indicating that employing even very low concentration of this enzyme will interfere with subsequent AOC analysis. The AOC increase can be attributed to the organic nature of Catalase.

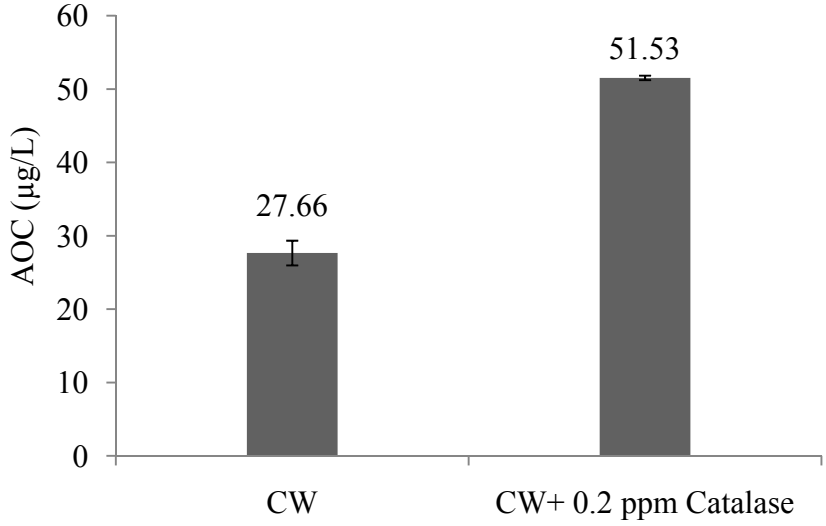

Figure 5.8: Impact of Catalase on the AOC of Capilano Water (CW) containing H_2O_2

5.8.2 Effect of pure MnO_2

Manganese dioxide (MnO_2) is known as one the most effective inorganic H_2O_2 scavengers that can accelerate H_2O_2 decomposition reaction to water and oxygen. Preliminary experiments showed that sixty minutes was appropriate for 100 mg MnO_2 to eliminate H_2O_2 (10 ppm) in 70 mL of water. Given the relatively low surface area of the pure manganese (granular form), the decomposition reaction showed to be slow and time demanding.

As shown in Figure 5.9, MnO_2 demonstrated detrimental effect on the AOC when it was used to eliminate H_2O_2 in Capilano water. Complementary tests were also performed on CW water with artificial concentrations of AOC, and the same results were obtained confirming the inhibition of bacterial growth. To ensure this, identical experiments were performed on Evian water, a commercially available mineral water, and Capilano water at Trojan Technologies, ON, by Dr. Siva Sarathy. Data obtained confirmed the previous observations for Capilano water. However, in contrast, MnO_2 was found to slightly promote bacterial growth in Evian water. The exact reason for this is unknown, but it is hypothesized that manganese is dissolved in Capilano water during the quenching process due to the relatively low pH (pH = 6.8) or the low alkalinity (< 5 mg/L as $CaCO_3$) of Capilano water. On the other hand, Evian water contains significant buffer capacity (i.e., pH 7.18, Calcium (Ca) 78, Chloride (Cl^-) 2.2, Bicarbonate (HCO_3) 357, Magnesium (Mg) 24, Nitrate (NO_3) 3.8, Potassium (K) 0.75, Sodium (Na) 5, Sulfates (SO) 10, all units in ppm). The residual concentration for MnO_2 was measured for both water media and data obtained showed a considerably higher level of residual Mn in CW water in comparison with that in Evian water (i.e., 0.228 ppm vs. 0.005 ppm). Nonetheless, no concrete conclusion was drawn for this phenomenon, so the application of MnO_2 was ruled out due to the variability in its function and unpredictable impact on AOC.

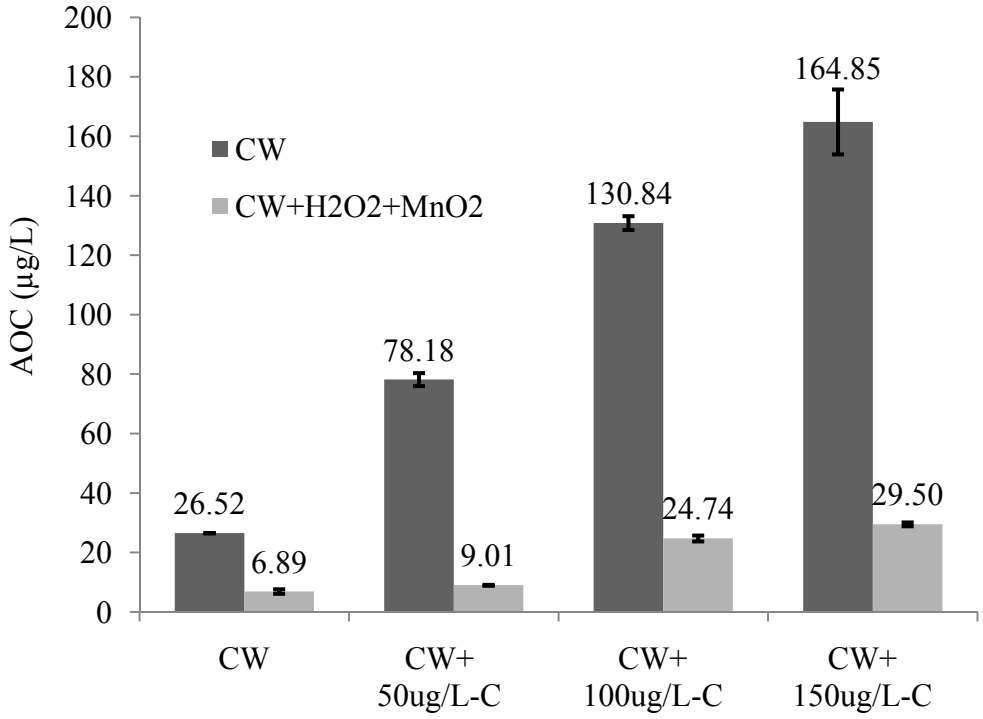

Figure 5.9: Impact of MnO_2 on AOC of Capilano water containing H_2O_2

5.8.3 Effect of 85% MnO_2

Pure manganese in the granular form had lower surface area and therefore it required a relatively long time to decompose H_2O_2. To resolve this, manganese dioxide (80-85% Sigma-Aldrich) was used in the powder from. This caused H_2O_2 to decompose more rapidly leading to shorter time for quenching. However, similar to the pure agent, inhibition of growth was observed for powdered MnO_2 (see Table 5.1).

5.8.4 Effect of PbO_2

Lead dioxide (PbO_2) is another oxidizing agent used for the decomposition of H_2O_2 to hydrogen and oxygen. H_2O_2 showed faster decomposition (in comparison with MnO_2) in the presence of PbO_2 (10 minutes). As shown in Table 5.1, data obtained from the AOC assay after H_2O_2 quenching indicated that using PbO_2 also inhibits bacterial growth within the sample. One possible explanation for this could be the dissolution of Pb/PbO_2 in water sample during H_2O_2

removal procedure. PbO_2 is known to have strong oxidizing nature, which can severely impede bacterial growth. However, measurement of residual Pb/PbO_2 can provide more insight into this hypothesis; however, this was not investigated since it was not a priority and was outside the scope of the research.

5.8.5 Effect of Fe_2O_3

Hydrogen peroxide can react with Fe^{+2} and oxidize it to Fe^{3+} as in the following reaction:

$$Fe^{2+} + H_2O_2 + 2H^+ \rightarrow 2Fe^{+3} + 2H_2O$$

OH radical can also be generated as the result of H_2O_2 and Fe^{+2} in a process known as Fenton reaction:

$$H_2O_2 + Fe^{+2} \rightarrow Fe^{+3} + OH^- + HO^{\cdot}$$

As a result, hydroxyl radicals generated from this reaction can oxidize the organic species leading to potential AOC increase. This hypothesis was confirmed with experiments and the results are shown in Table 5.1. Therefore, using ferric oxide was also ruled out as a possible alternative for H_2O_2 elimination.

5.8.6 Effect of Silver (Ag)

This alternative was also examined to remove hydrogen peroxide. The results obtained on AOC assay after hydrogen peroxide quenching clearly illustrated the detrimental impact of Ag on bacterial growth in the water sample (Table 5.1). This was potentially expected since Silver has been used for drinking water disinfection and other antimicrobial purposes especially when limitations exist in using chlorine (Silvestry-Rodriguez et al., 2007). Therefore, having even a small amount of dissolved Ag in water can certainly hinder bacterial growth and reproduction.

Similar to the case of PbO_2, assessing the residual silver in the solution was not investigated even though it could provide deeper insight into this phenomenon.

Table 5.1: Effect of different inorganic H_2O_2 quenching agents on AOC

Substrate	**Purity (%)**	**Initial [H_2O_2]**	**Original AOC**	**AOC measured**
Manganese dioxide (MnO_2)	85%	10 ppm	18 µg/L	LDL[1]
Lead dioxide (PbO_2)	99.99%	10 ppm	18 µg/L	LDL
Ferric Oxide (Fe_2O_3)	97%	10 ppm	18 µg/L	50 µg/L
Silver (Ag)	99.99%	10 ppm	18 µg/L	LDL

5.8.7 Sodium thiosulfate as H_2O_2 quenching agent

Sodium thiosulfate is another H_2O_2 scavenger that has been suggested in SM 9217 to remove chlorine and also has been used widely for quenching ozone prior to AOC determination (Clescerl et al., 1999; MacLean et al., 1996). However, its viability as H_2O_2 quencher has not been reported in the literature.

Sodium thiosulfate reacts with H_2O_2 according to the following reaction:

$$2Na_2S_2O_3 + H_2O_2 \rightarrow Na_2S_4O_6 + 2\ NaO$$

The concentration of thiosulfate applied to remove H_2O_2 should at least be the stoichiometric equivalent or more. MacLean et al. (1996) reported thiosulfate to have detrimental effect on the BDOC analysis. The authors correlated this to the production of sulfuric acid as a result of bacterial activities metabolizing the residual thiosulfate; hence, changing the pH and the heterotrophic activity of the microorganisms. Similar observation was reported by Sarathy

[1] Detection limit of the AOC is 10 µg/L as reported by Hammes and Egli., 2005

(2009) who used thiosulfate to eliminate H_2O_2 prior to AOC assay and showed thiosulfate to inhibit microorganisms growth. The author hypothesized that tetrathionate, the product of the reaction between H_2O_2 and sodium thiosulfate, may potentially inhibit microbial growth. However, this hypothesis was not investigated. The other possible explanation for this could be due to the pH change as a result of NaOH production, which affects the heterotrophic activity of the microorganisms. Therefore, it is hypothesized that the buffer capacity of the water can potentially play an important role in affecting the bacterial growth in the water. Taking into account all the aforementioned uncertainties, thiosulfate was not considered a feasible alternative; hence, was not investigated in this study.

5.8.8 Effect of immobilized Catalase on glass beads

The characteristics of immobilized enzyme preparations are governed by the properties of both the enzyme and the carrier material (Sheldon, 2007). Several methods have been proposed for Catalase immobilization on various types of supports for different applications (Lohmann and Legge, 2006; Sheldon 2007; Vasudevan and Weiland, 1994; Betancor et al., 2003; Tukel and Alptekin., 2004; Vera-Avila et al., 2004; Yoon et al., 2007; Alptekin et al., 2010). In general, three established methods can be employed for enzyme immobilization (Sheldon, 2007):

1) Support binding which can be physical (such as hydrophobic and van der Waals interactions), ionic, or covalent. The support can be a synthetic resin, a biopolymer or an inorganic polymer such as (mesoporous) glass-bead or a zeolite (Sheldon, 2007).
2) Encapsulation via entrapping of an enzyme in a non-prefabricated polymer net such as an organic polymer or a silica sol-gel (Sheldon, 2007).
3) Cross-linking of enzyme aggregates or crystals, using a bi-functional reagent, to prepare carrier-less macro-particles.

Glass beads prepared according to the procedure explained in Section 4.6.2.1 were used to eliminate H_2O_2 from the water sample. Figure 5.10 shows the impact of glass beads on the AOC of water. As demonstrated the AOC of the raw waters increased after the elimination of H_2O_2 with glass beads immobilized with Catalase. This increase was attributed to the release of the immobilized enzyme with weak attachment to the surface of the glass bead.

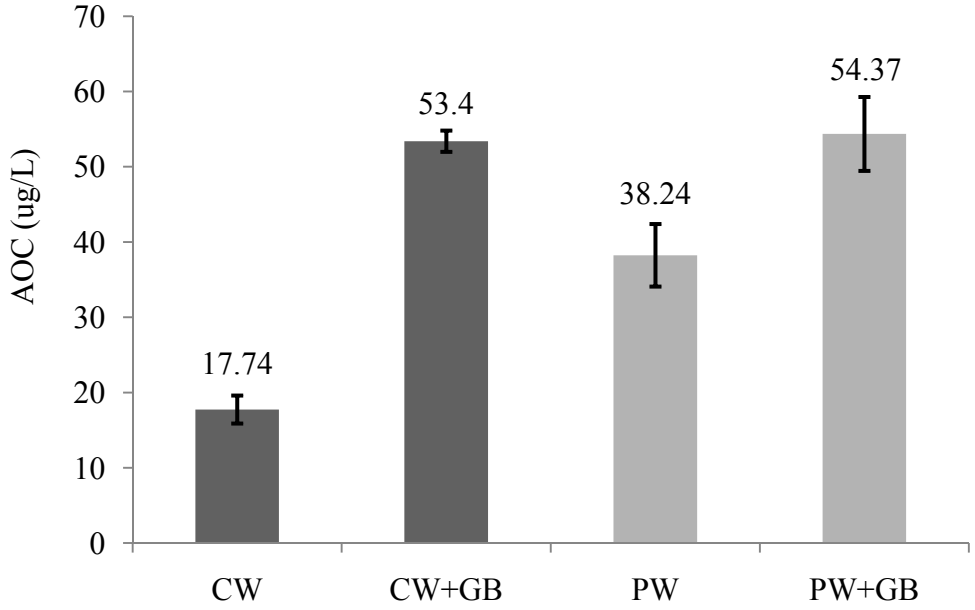

Figure 5.10: Impact of Catalase immobilized on glass bead (GB) on natural waters (i.e., CW and PW)

The reuse of GB for repeated peroxide quenching applications has been investigated. This was particularly of interest because of the tedious nature of the work involved in the immobilization of enzyme on the glass surface. Glass beads were recovered and re-used after each quenching step. Quenching was continued for 60 minutes and H_2O_2 concentration was measured every 15 minutes. Figure 5.11 demonstrates the activity of the biocatalyst at removing H_2O_2 for five subsequent batches. As shown in Figure 5.11, the initial H_2O_2 degradation rate decreased as the number of recycles increased, indicating that the performance of the biocatalyst in decomposing

H_2O_2 decreased as it was used for subsequent experiments. One possible explanation is mainly attributed to the release of the immobilized Catalase into the solution as a result of instability of the enzyme on the glass surface.

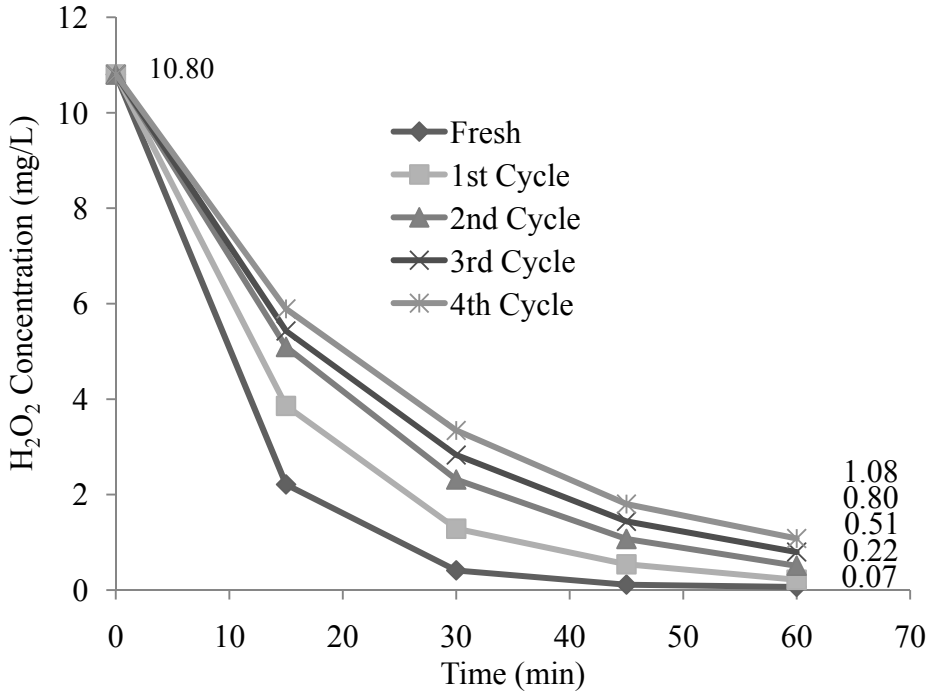

Figure 5.11: Effectiveness of the immobilized GB for the repeated quenching H_2O_2

5.8.9 Effect of immobilized Catalase on SEPABEAD®

SEPABEAD® EC-EP, an epoxy activated resin, with very easy immobilization protocol was tested for H_2O_2 removal. The application of this polymeric substrate was of particular interest when compared to GB because of the tedious nature and hazardous materials used for immobilization on GB. Hydrogen peroxide elimination was observed to be fast and effective when using SEPABEAD (10 ppm of H_2O_2 reduced to below 0.1 ppm within 20 minutes). Figure 5.12 compares the results for the AOC of Peachland and Capilano waters after removing H_2O_2 with SEPABEAD and GB. As demonstrated, SEPABEAD showed promising results with minimal detrimental impact on the AOC of the original sample. This confirms the strong multi-point attachment between the enzyme and the epoxy groups, on the surface of PS, as reported by

Mateo et al. (2002). The biocatalyst prepared in this work, can be kept in AOC-free glassware in the fridge for up to two months without losing any activity or stability of the immobilized enzyme. In fact, this was expected since the physical property and internal geometry of the PS lead to multi-point attachment of the enzyme to the support, thereby providing stable and strong immobilized enzyme. Therefore, Catalase immobilized on the polymeric support was selected for subsequent experiments.

It should be noted that finding the best immobilization protocol on SEPEABEAD was not the primary objective in this study and therefore the procedure used in this work was deemed to be satisfactory for our application. Nonetheless, finding the optimal condition to enhance stability and activity of the immobilized Catalase on the polymeric support can be very valuable for future researches.

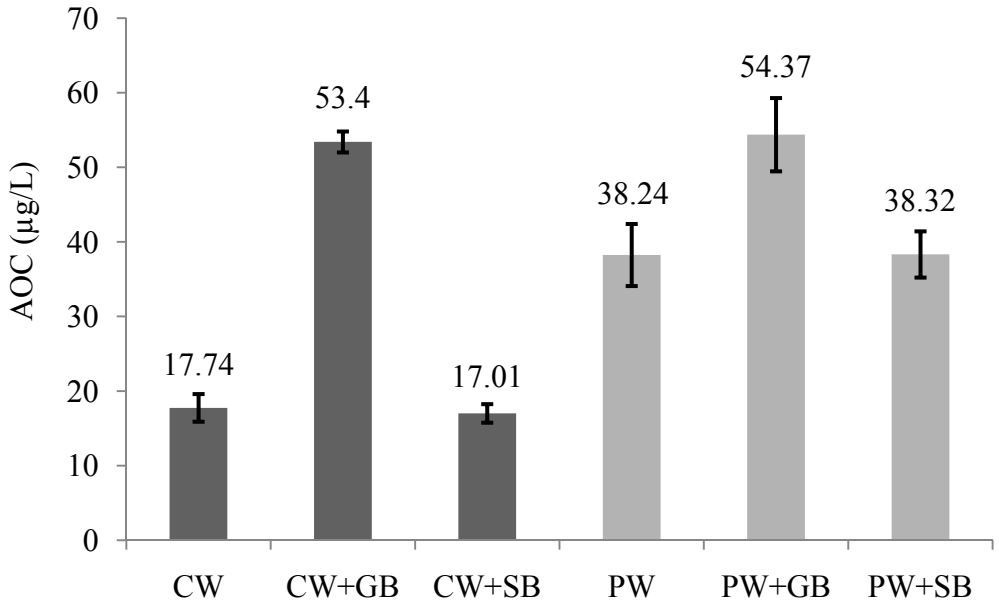

Figure 5.12: Comparison of the impact of Catalase immobilized on SB and GB (used to remove H_2O_2) on the AOC of natural water.

5.9 Highlights and Remarks

A previously developed method by Hammes and Egli (2005) for AOC determination was modified for UV/H_2O_2 treatment applications. The critical step for UV/H_2O_2 treated water was using a H_2O_2 quenching agent with minimal impact on the actual AOC. After examining several candidates, Catalase immobilized on SEPABEAD® was chosen to remove H_2O_2 for subsequent experiments studying the impact of UV/H_2O_2 on the AOC profile of natural waters. However, when applying this method to assess biological stability of water, one should note to some key aspects that could potentially influence the results of the assay.

1. *Inoculum*: Natural microbial consortium can potentially exhibit different utilization of AOC compared to pure cultures (i.e. *P17* and *NOX*). Moreover, AOC results may also vary for a single inoculum depending on the organic substrates available (Hammes and Egli, 2005). Moreover, the choice of the natural inoculum can also play an important role in the outcome of the AOC assay.

2. *Conversion values:* Of important point to note is that, AOC of natural water was assessed through cultivating a natural indigenous consortium and cells were counted via flow cytometry. This would provide broader range of substrate capable of consuming the AOC content of water, thereby providing a more realistic interpretation of biological stability (Hammes and Egli, 2005). However, conversion is probably one of the most controversial issues in AOC assays, since it is uncertain whether conversion to a single simple substrate is the correct approach to reflect growth on complex organics (Hammes and Egli, 2005; Hammes, 2008).

3. *Contamination prevention*: AOC assay is highly sensitive and susceptible to many sources of organic carbon contamination. Therefore, it requires strong operator skills to identify problematic points. Nonetheless, for any given set of experiments, it is strongly recommended to

include positive and negative controls in order to be aware of any inhibition and/or contamination affecting bacterial growth within the sample (Sarathy, 2009).

6 Impact of UV/H_2O_2 Advanced Oxidation Process on Water Quality Parameters

6.1 Introduction

Two different types of water (i.e., natural and synthetic waters) were used in this study. Synthetic water was made from Suwannee River (SR) isolated NOM at two different TOC concentrations of 5 ppm and 10 ppm. Table 6.1 represents the selected characteristics of the waters used in this study.

Table 6.1: Selected characteristics of the waters used in this study

Parameter/Water	CW Reservoir	BI water	SR NOM (5 mg/L)
TOC (ppm)	1.45±0.075	4.81±0.03	5.28±0.014
pH	6.7	6.3	7 (adjusted from the original value of 5.3)
UV_{254} (cm^{-1})	0.063± 0.002	0.185±0.003	0.220
SUVA (L mg^{-1} m^{-1})	4.2± 0.316	3.75± 0.072	4.15± 0.05
Alkalinity (ppm)	< 5ppm	< 15ppm	NA

Specific UV absorbance (SUVA) defined as the ratio of UV_{254} to DOC was monitored in all the experiments. Given that UV_{254} is a surrogate parameter for aromaticity, employing SUVA helps to represent the relative amount of aromatic carbon in NOM (Singer, 1999; Sarathy, 2009).

6.2 Impact of UV/H_2O_2 Process on Physiochemical Properties of Waters

6.2.1 Impact of UV/H_2O_2 treatment process on Capilano water

Figure 6.1 illustrates changes observed in UV_{254}, TOC, and SUVA profiles for Capilano water (CW) treated with UV/H_2O_2 process. Experiments were conducted with initial H_2O_2 dosage of 10 ppm and different UV exposure times. The portion of NOM that absorbs UV at 254nm is defined as chromophoric NOM (CNOM) (Sarathy, 2009; Sarathy and Mohseni, 2007). Therefore, a change (i.e., reduction) in the UV_{254} of water indicates a change (i.e., loss) in the aromatic and conjugated double bond structures of NOM (Sarathy, 2009).

As demonstrated in Figure 6.1, a similar linear reduction was observed for both UV_{254} and SUVA profiles. This is because, TOC was reduced about 25% over the course of the treatment, and most of the reduction in SUVA (i.e., 35%) was due to the loss (i.e., 50%) of aromatic and conjugated double bonded portion of NOM measured as UV254 absorbing species. This phenomenon was also observed and reported by other researchers (Speitel et al., 2000; Thomson et al., 2004; Toor, 2005; and Sarathy, 2009) for various initial H_2O_2 concentrations and different UV exposures. In fact, SUVA can be used as a very useful surrogate to monitor the structural changes of NOM during the treatment. Toor (2005) and Sarathy (2009) reported that the change in SUVA was correlated to the changes in biodegradability of organic matter as well as the DBPs formation potential.

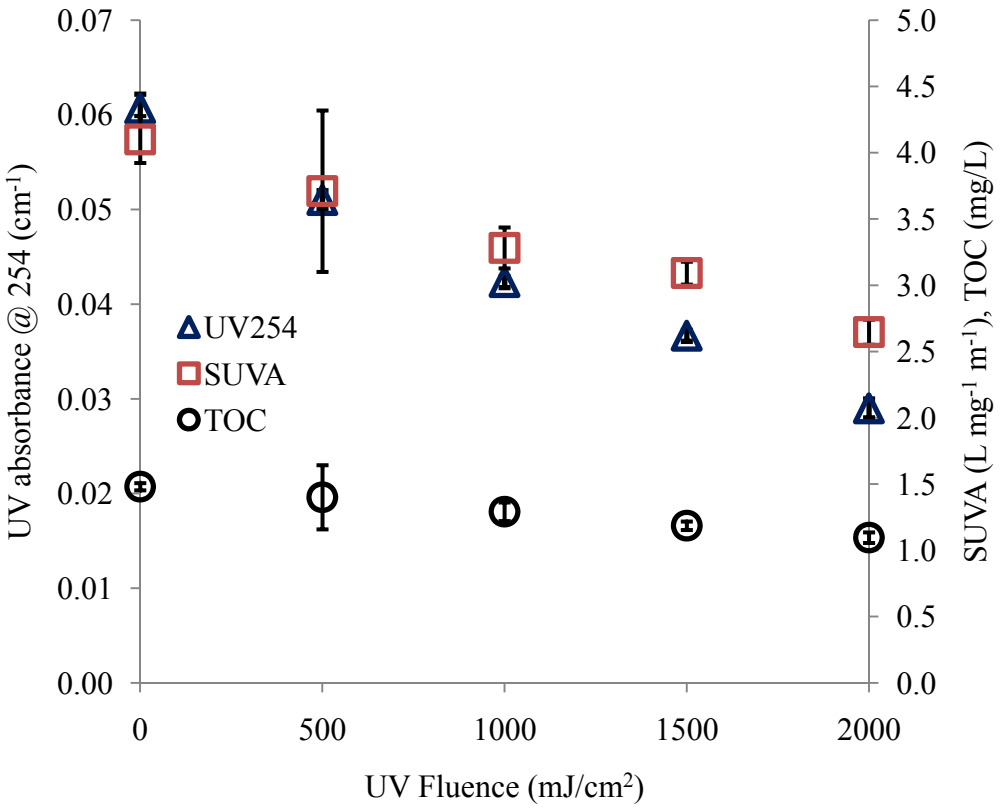

Figure 6.1: Impact of UV/H_2O_2 treatment on the physiochemical characteristics of Capilano Water (CW).

6.2.2 Impact of UV/H_2O_2 treatment process on Bowen Island water

Bowen Island water (BI) underwent the identical UV/H_2O_2 treatment as Capilano water and the same analyses were performed in order to assess the impact of the treatment process on water quality characteristics. Figure 6.2 demonstrates changes in physiochemical characteristics of Bowen Island water. Total organic carbon was observed to reduce by about 12% during the treatment and UV_{254} reduced by 38% from its initial value, indicating the transformation of aromatic constituents of NOM into aliphatic molecules (Sarathy and Mohseni, 2007, 2009; Song et al., 2008). Similar to the case of Capilano water, TOC reduction was less significant in comparison with that of UV absorbance, indicating the dominant effect of UV_{254} on the trends observed for the SUVA profile.

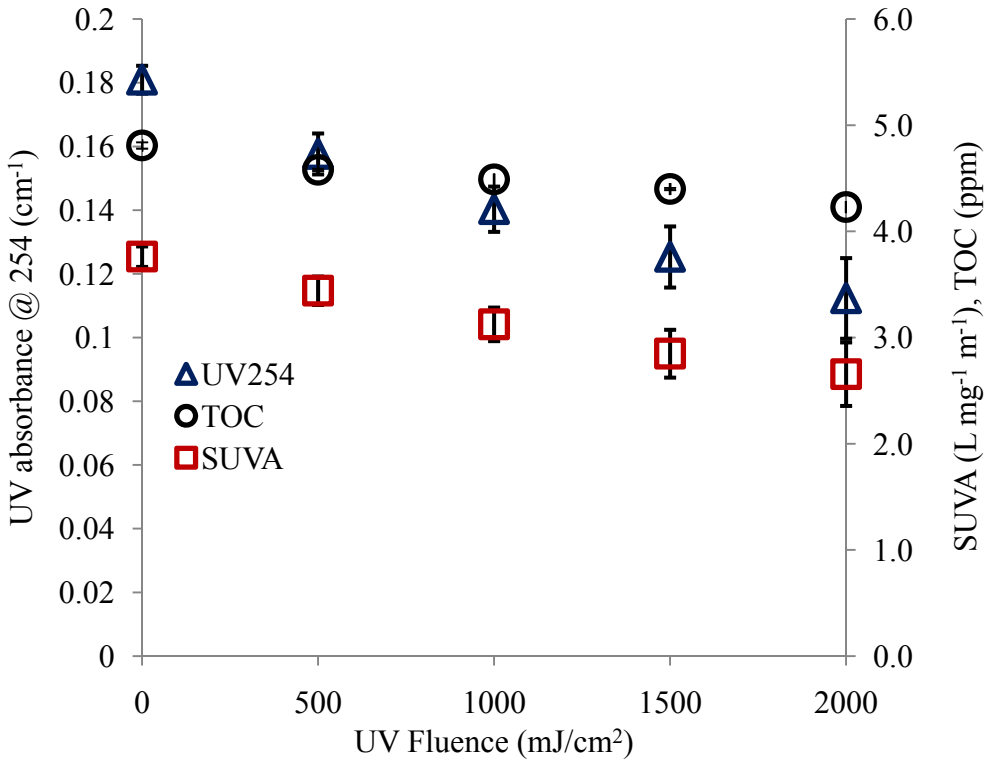

Figure 6.2: Impact of UV/H_2O_2 treatment on physiochemical characteristics of Bowen Island (BI) water.

Table 6.2 summarizes the reduction of TOC and UV_{254} for the Capilano and Bowen Island waters after UV/H_2O_2 treatment with a UV fluence of 2000 mJ/cm^2. The percentage reductions of UV_{254} and TOC are higher for CW than BI water. However, the net change (or reduction) in both parameters are greater for the BI water. To explain this, one should note that the required time to reach identical UV fluence in BI water is almost twice as the one required for CW water. Therefore higher amount of photons will be absorbed by the organic matter in BI water. This leads to greater number of organic molecules being converted, however the fractional change would be smaller than that in Capilano water. Moreover from the kinetic point of view, the degradation of CNOM has been reported to be in the form of $r_{CNOM} = -k[CNOM][HO^{\cdot}]$ (See Appendix A). Assuming that the concentration of OH radical to be the same in both systems therefore the change in CNOM can be expressed as:

$$\Delta\, CNOM = CNOM_0(1 - e^{-kt})$$

Therefore time (t) and the nature of the organic matter (k) also affect the degradation profile of CNOM. It is important to realize that the characteristics of NOM which can affect its reaction rate with OH radical can be very different from one water source to another. For instance higher SUVA value of the CW water indicates higher amount of aromatic compounds prone to react with OH radical. Moreover, according to the equation 11 in Appendix A the absorbance of the water also affects the degradation of H_2O_2, thereby generation rate of OH radical. Therefore to better understand and predict the CNOM profile over the UV/H_2O_2 treatment, on should take into account all the considerations and the factors that can affect the concentration of species in the system.

Table 6.2: Comparison of the Impact of UV/H_2O_2 on Capilano and Bowen Island waters

Water	UV_{254} reduction (%)	UV_{254} reduction (absolute)	TOC reduction (%)	TOC reduction (absolute)
Capilano	50%	0.032	25%	0.384
BI	38%	0.069	12%	0.580

6.3 Impact of UV/H_2O_2 Treatment on Synthetic Water

Isolated NOM was used in this study at two different concentrations (i.e., 5 and 10 ppm as TOC) to investigate the impact of NOM concentration on UV/H_2O_2 process performance. Suwannee River (SR) NOM was used because it is a well characterized and widely studied NOM. The pH of the solution decreased after dissolving SR NOM in Milli-Q water due to dissolution of humic and fulvic acids present in NOM. As a result, pH was adjusted to neutral range (about 7) by using NaOH (0.1 N). Alkalinity was also amended by adding sodium bicarbonate.

6.3.1 Impact of NOM concentration

Figure 6.3 shows the UV_{254} profile of SR water at two different TOC concentrations (i.e., 5 and 10 ppm) during the UV/H_2O_2 treatment. The results indicate that UV absorbance for the synthetic water with 10 ppm TOC decreased about 27%, while this parameter showed about 33% reduction for SR water with 5 ppm TOC for the same treatment condition (i.e., [H_2O_2]~10 ppm and UV fluence up to 2000 mJ/cm^2). However, the absolute change of UV_{254} for the SR water with 10 ppm TOC (0.122) is 1.67 times higher than that for the SR water with 5 ppm TOC (0.073). This observation is similar to the previous data on the natural waters where higher amount of CNOM degradation was observed for the water with higher initial CNOM, while percentage reduction was lower in comparison with the water with lower initial CNOM. Of important note is the smaller difference in UV_{254} percentage reduction for SR water at two different concentrations compared to the one between CW and BI waters. This can be attributed to the effect of nature of CNOM on its degradation profile.

According to the abovementioned pseudo first order kinetic expression, and because of the similarity in the CNOM nature of SR water used, one may expect to observe proportional reduction in for the synthetic waters. However, predicting the real impact of a single parameter in a complex reaction environment such as UV/H_2O_2 is not straightforward. The change in the initial UV absorbance at 254 nm will affect the generation of OH radicals. Moreover, CNOM competes with H_2O_2 in scavenging UV; therefore, lower levels of CNOM leads to greater photolysis of H_2O_2 and thereby OH radical generation. On the other hand, more organic molecules get the chance to react with OH radicals and the UV (Sarathy et al., 2009). Therefore, a complex combination of these impacts will determine the final CNOM (i.e., UV_{254}) profile change.

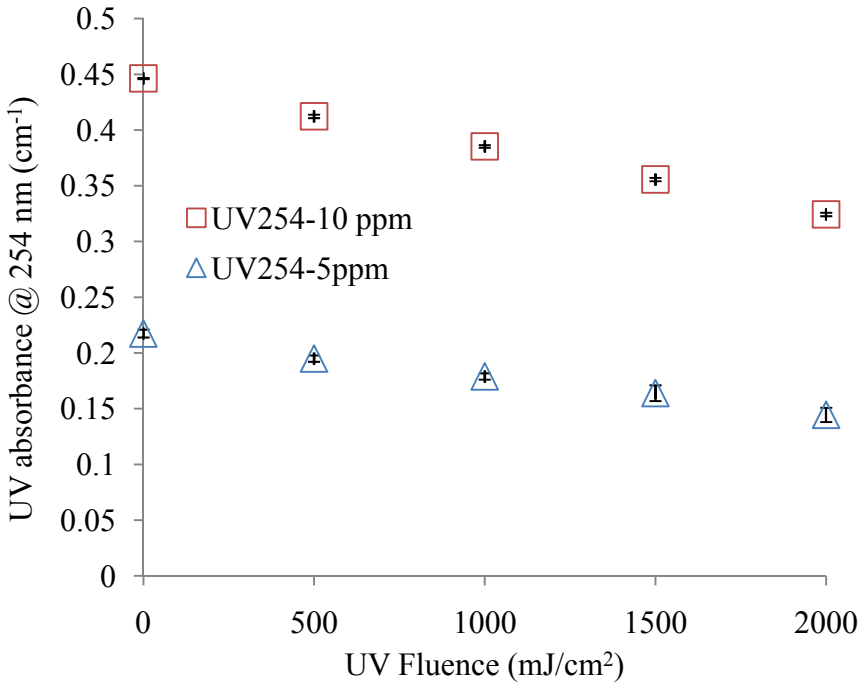

Figure 6.3: Impact of UV/H_2O_2 treatment on UV_{254} profile of SR water with different TOC concentrations.

Figure 6.4 demonstrates the effect of UV/H_2O_2 treatment process on the TOC profile of the synthetic water. As illustrated, TOC did not show considerable reduction during the course of the treatment for both concentrations of NOM. This is consistent with previous data of CW and BI water as well as the data in the literature (Sarathy, 2009). In fact, organic carbon is partially oxidized within the applied condition of UV/H_2O_2 treatment; hence no significant reduction in TOC is expected. The synthetic water with 10 ppm TOC showed 10% reduction, while the SR water with lower concentration (i.e., 5 ppm) showed 20% reduction in TOC over the treatment time. This is in agreement with the previous data on UV_{254} profile indicating reduction in the efficacy of the process as the NOM concentration increases. Increase in UV_{254} of water results in stronger UV shielding effect that in turn leads to lower break down of H_2O_2, and hence lower generation of OH radicals.

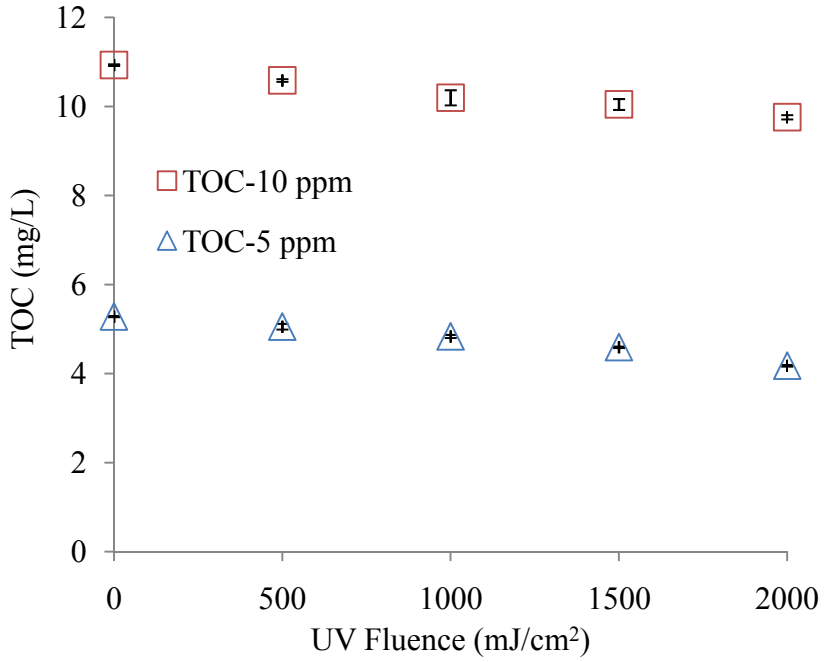

Figure 6.4: Impact of UV/H_2O_2 treatment on TOC profile of SR water with different TOC concentrations.

6.3.2 Impact of alkalinity

To examine the effect of alkalinity, SR water with 5 and 10 ppm TOC was amended with additional alkalinity (i.e., 50 and 150 ppm) and underwent UV/H_2O_2 treatment. The pH did not need to be adjusted as it was within the natural range as a result of $NaHCO_3$ dissociation. Figure 6.5 shows the impact of UV/H_2O_2 treatment on UV_{254} profile of SR water with TOC of 5 ppm at different alkalinities (0, 50 and 150 as mg/L of $CaCO_3$) and initial H_2O_2 dose of 10 ppm.

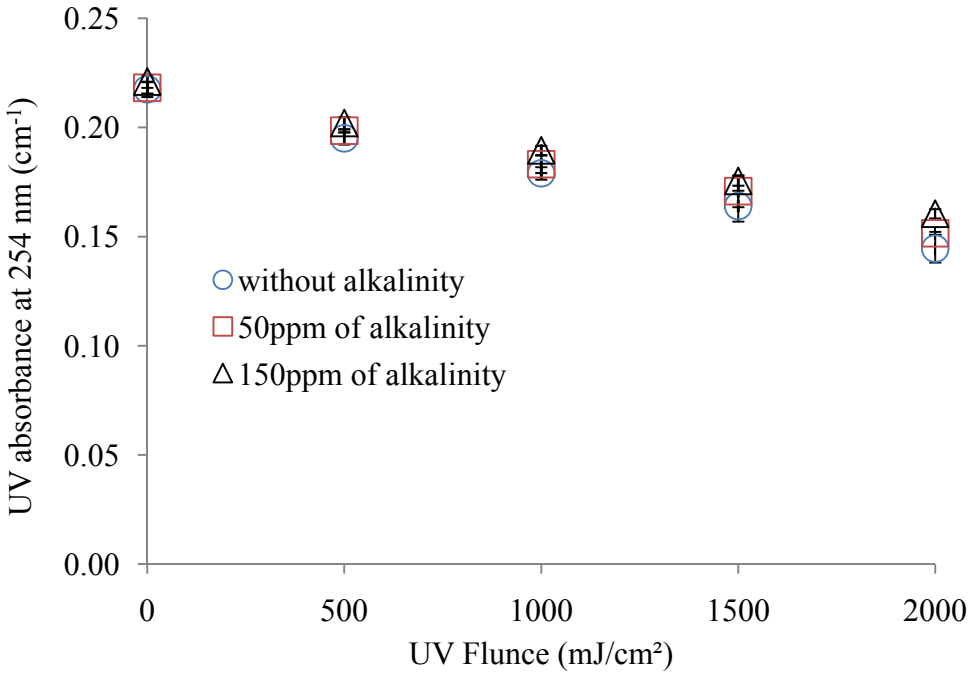

Figure 6.5: UV_{254} profile of SR water during UV/H_2O_2 treatment, $[H_2O_2]$ ~10 ppm.

As demonstrated, a slightly smaller reduction of CNOM was observed for the synthetic water as alkalinity increased. This is because the presence of alkalinity (mostly carbonate species) competes with organic molecules in scavenging OH radicals. However, the overall scavenging impact of carbonate species is not substantial. The reduction in UV_{254} is 33% for raw SR water while it is 30% and 26% for SR water with alkalinities of 50 and 150 ppm (equivalent $CaCO_3$). This difference may be explained based on the concentrations of organic matter and carbonates as well as their reaction rate constants with OH radical. Buxton et al. (1988) reported the rate constant for the reaction between CO_3^{-2} and OH radical as 3.9E8 L $mol^{-1}s^{-1}$ (6.5E3 L $mg^{-1}s^{-1}$) and Westerhoff et al., (2007, 1999) and Goldstone (2002) have reported the reaction rate between OH radical and TOC to be about 1.5E4 L $mg^{-1}s^{-1}$. Therefore, in addition to the governing concentration of NOM, its reaction rate with OH radicals is also 10 times higher in comparison with carbonate species. Therefore, concentration of NOM and its reaction rate constant with OH radicals have the influential impact on the CNOM degradation profile.

One notable point is the distinction between the CNOM results with and without alkalinity at higher UV fluences. This can be correlated to the degradation of CNOM during the treatment hence, providing more opportunity for other species to react with OH radicals. This magnifies the effect of alkalinity as there will be less organics for them to compete with in scavenging OH radicals.

Figure 6.6 demonstrates the TOC results for SR water with TOC~5ppm at different alkalinities. The presented data also agree with the findings for the UV_{254} profile. As expected TOC does not change significantly over the treatment and the presence of alkalinity diminishes the TOC reduction rate. The TOC of the SR water without alkalinity showed 24% reduction during the treatment while SR water with alkalinities of 50 and 150 ppm showed 22% and 20% reduction, respectively. This observation confirms the role of alkalinity in scavenging OH radicals, thereby reducing the efficacy of the process.

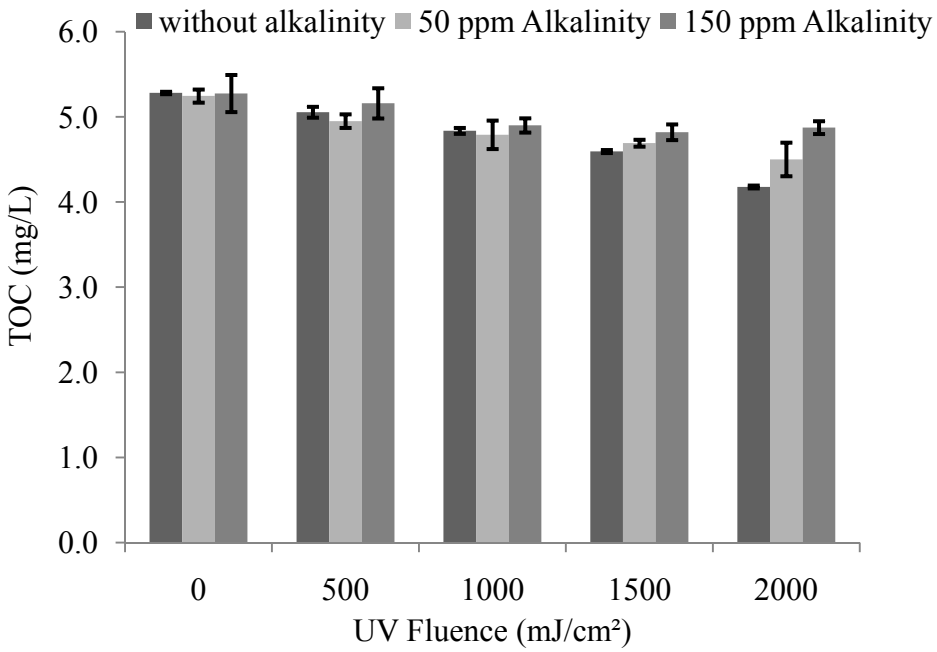

Figure 6.6: Impact of alkalinity on the TOC profile of SR water with $[TOC]_0$ ~5ppm

6.3.3 Impact of UV/H_2O_2 process on molecular weight distribution of CW NOM

Figure 6.7 demonstrates the impact of UV/H_2O_2 treatment on the AMW distribution of organic matter present in Capilano water. As illustrated, the original HPSEC chromatogram of CW with no treatment (i.e., UV fluence 0 mJ/cm^2) consists of a large, early peak followed by smaller, later eluting peaks indicating the molecular weight distribution of the organic matter. As the UV irradiation progressed (i.e., UV fluence increased), the leading edge and the first peak reduced in size significantly while the second peak reduces to a lesser extent. The third peak seemed to increase slightly in size at fluences between 500 and 1500 mJ/cm^2, followed by a decrease at fluences greater than 1500 mJ/cm^2. Finally, the last two peaks representing lower molecular weight organics increase in size after UV/H_2O_2 treatment at all UV fluences. The increase in the latter peaks is correlated with the production of smaller organic molecules (i.e., AMW < 500 Da). As can be seen, the total area under the HPSEC chromatograms decreased with the extent of the UV/H_2O_2 treatment. This was represented earlier by the reduction in UV_{254} (Figure 6.1) and therefore, has not been reported here. Sarathy and Mohseni (2007) also demonstrated that reduction in aromaticity (i.e., UV_{254}) is accompanied by reduction in the amount of higher molecular weight NOM, that in turn leads to the formation of smaller organic molecules such as aldehydes, ketones, and carboxylic acids (Thomson et al., 2004; Sarathy, 2009).

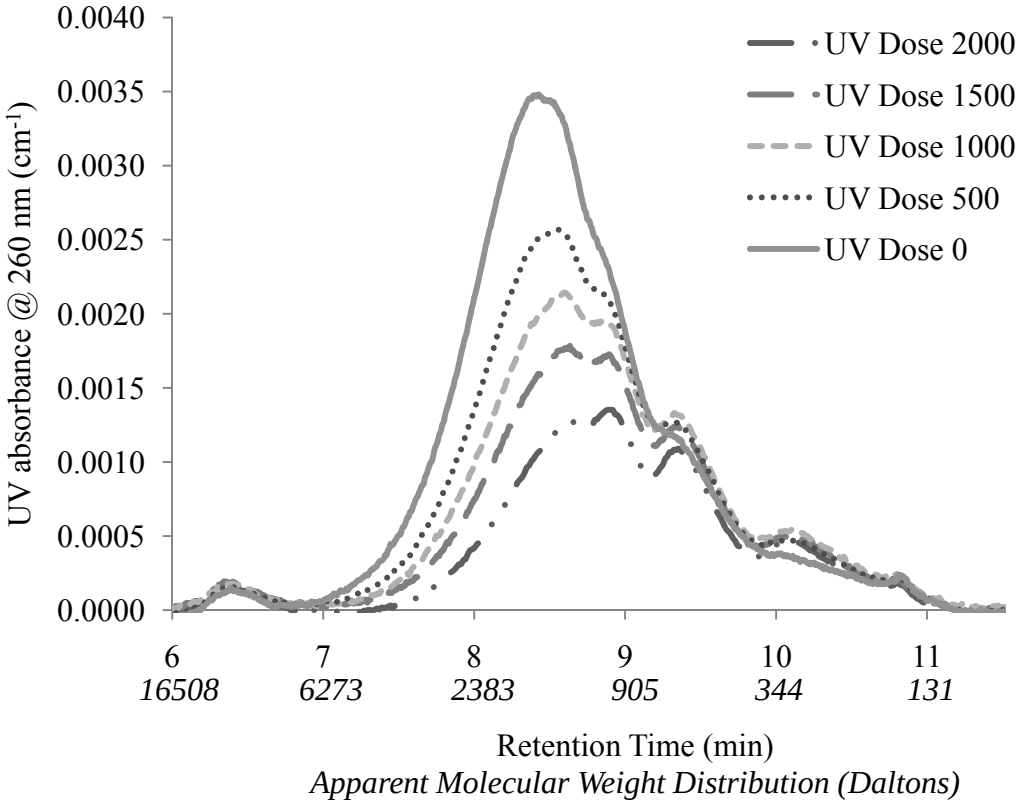

Figure 6.7: HPSEC chromatogram of AMW of NOM for UV/H_2O_2 treated Capilano water

Figure 6.7 demonstrates a typical HPSEC chromatogram of CNOM consisted of aggregation of peaks without a clear resolution. In order to quantify the changes in the apparent molecular weight, the observed chromatograms were deconvoluted into a number of Gaussian peaks using PeakFit v4.12 software in a similar fashion presented by Sarathy and Mohseni (2007). HPSEC data were imported into PeakFit and were deconvoluted using the settings presented in the Table 6.3.

Table 6.3: Settings used in deconvolution of HPSEC chromatograms

Parameter	**Function/Value**
Deconvolution	Autofit Peak III Deconvolution
Peak type	extreme value 4 parameter tailed (Eval4)
Gaussian response width	20 seconds
Frequency domain filter	60%
Rejection threshold	3%
R2 of the fit	≥0.97

These settings were selected based on the R^2 of the fit and yielded a $R^2 > 0.97$ for all peak fitted chromatograms. Afterward, the areas and the average retention times of the resolved peaks were used along with a calibration equation, obtained from the standards (see Appendix B) to quantify the changes in the molecular weight distribution of organics during each set of analyses.

The analysis revealed that 49% of the Capilano water NOM consisted of organic molecules with AMW greater than 1500 Da, while organic molecules with molecular weight less than 500 Da made up only 11% of the total. As shown in Figure 6.8, with an initial H_2O_2 concentration of 10 mg/L, as the UV exposure (i.e., fluence) increased, a large reduction in higher AMW CNOM (i.e. AMW> 1500 Da) was observed: 36%, 54%, 65% and, 75% reductions in for the UV fluences of 500, 1000, 1500, and 2000 mJ/cm^2,respectively. Similar reduction trends were observed for other molecular weight categories with AMW larger than 500 Da. Meanwhile, smaller AMW CNOM (AMW< 500 Da) increased in concentration: 17%, 22%, and 12% increase for fluences up to 1500mJ/cm^2. However, at fluences greater than or equal to 1500 mJ/cm^2, AMW was further reduced. This reduction is also demonstrated in Figure 6.7 where later peaks of the chromatograms for fluences larger than 1000 mJ/cm^2 start to reduce in size. This reduction in higher molecular weight organics and associated formation of smaller organic

molecules led to a shift in molecular size distribution from the one with a majority of large species to a more even smaller molecular weight distribution after UV/H_2O_2 treatment (Sarathy, 2009). Therefore, from the HPSEC chromatograms and the quantified graph, it was observed that •OH, generated within the UV/H_2O_2 treatment, preferentially react with larger molecular weight CNOM resulting in increase in lower molecular weight organics (Figures 6.7 and 6.8). This also could be attributed to CW NOM high aromatic character as indicated by the high SUVA of about 4.2 L mg^{-1} m^{-1} and its considerable reduction (i.e., 35%) during the treatment.

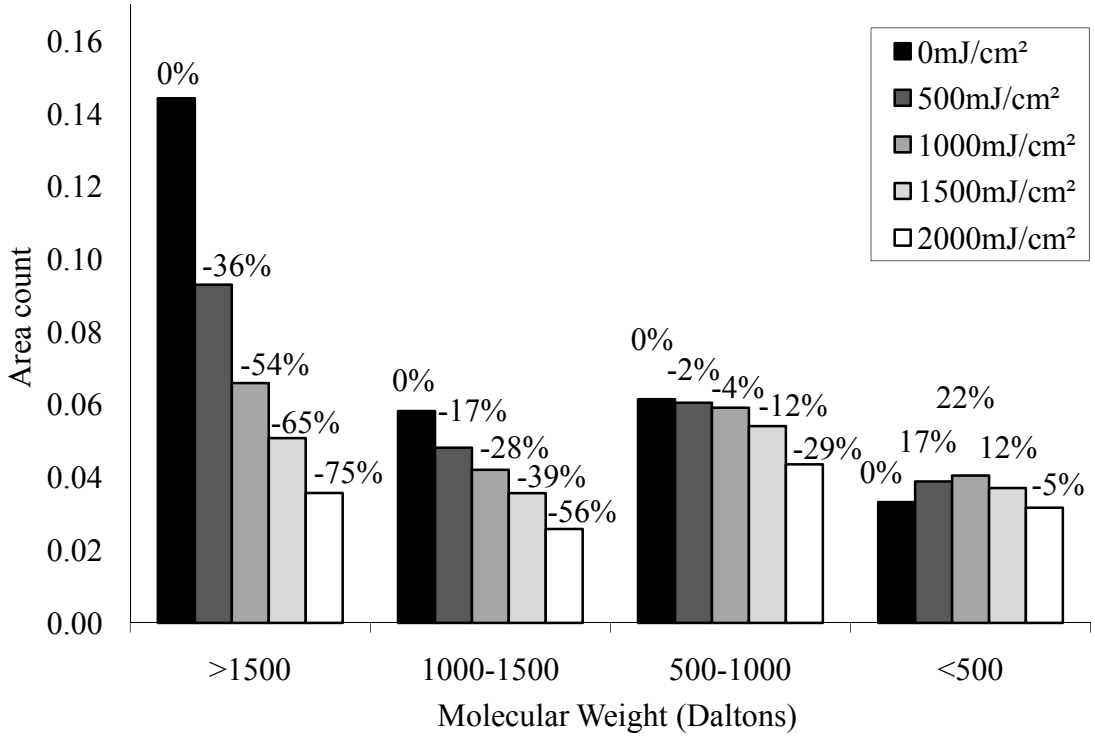

Figure 6.8: Impact of UV/H_2O_2 treatment on apparent molecular weight distribution of NOM in Capilano water.

6.3.4 Impact of UV/H_2O_2 on molecular weight distribution of BI NOM

Figure 6.9 shows the impact of UV/H_2O_2 treatment process on molecular weight distribution of the organic matter present in Bowen Island water. Similar to CW water, a decrease in the areas

under the chromatograms was observed as the UV/H_2O_2 treatment progressed. This observation is in agreement with the change in the UV_{254} profile (See Figure 6.2).

As shown in Figure 6.9, the original HPSEC chromatogram of BI with no treatment (i.e., fluence 0) consists of a large, single early peak followed by relatively smaller, aggregation of peaks. The early large single peak was found to be recalcitrant to the applied treatment conditions (i.e., [H_2O_2] = 10 ppm, UV fluence up to 2000 mJ/cm^2). To further assess the nature of molecules associated with this peak, extended treatment (i.e., UV fluence up to 8000 mJ/cm^2, data not shown) was applied on BI water sample. As a result, the early large peak was removed with the extended UV/H_2O_2 treatment indicating the organic nature for the molecules associated with the abovementioned peak. For the other organic constituents in BI water, UV fluences greater than or equal to 500mJ/cm^2 resulted in increasing the peaks associated with the smaller size organics (i.e., AMW < 500 Da) increased slightly in size, illustrating the generation of smaller molecules within the treatment process.

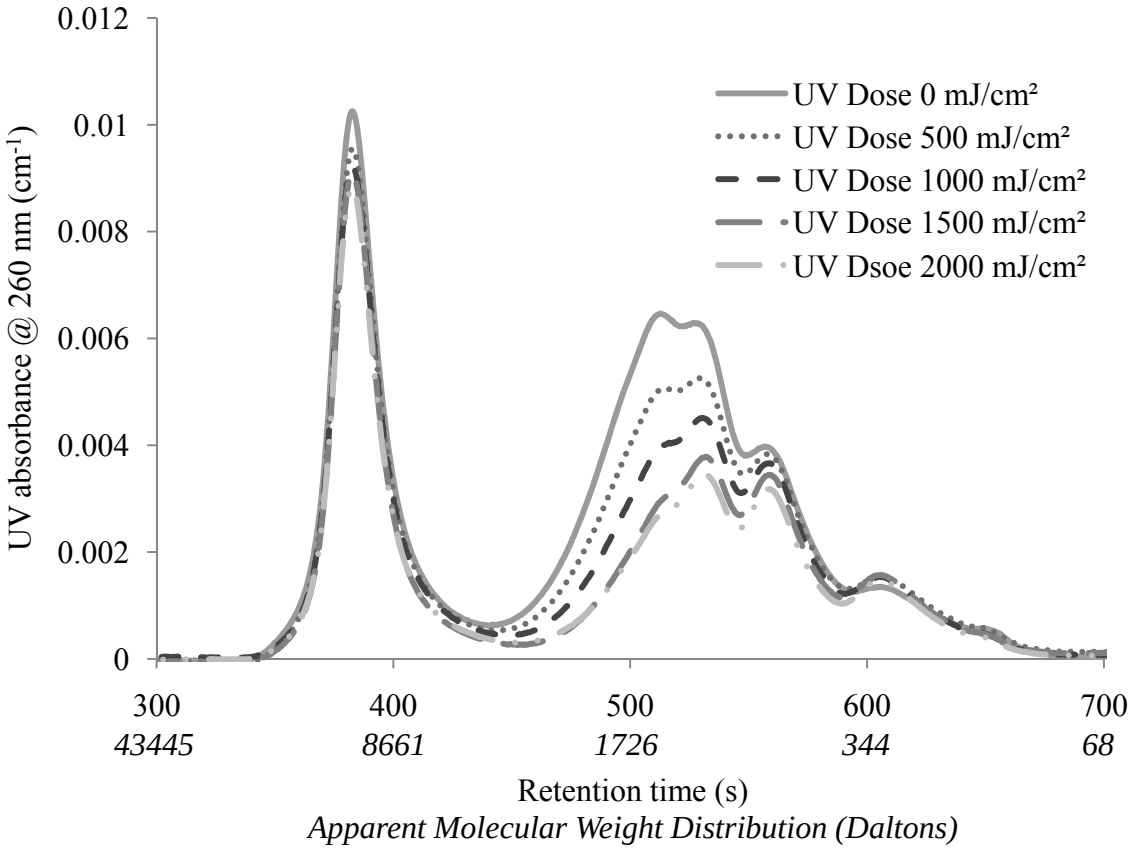

Figure 6.9: Impact of UV/H_2O_2 treatment on the molecular weight distribution of Bowen Island NOM.

Similar to CW water, PeakFit software was used to disintegrate the chromatograms into single peaks in order to better investigate and quantify the impact of the UV/H_2O_2 treatment on the molecular weight distribution of NOM. Identical settings to the one applied for the CW water was used and the results are shown in Figure 6.10.

As demonstrated in Figure 6.10, the highest reduction is seen for the portion related to molecules with 1000-1500 Da which corresponds to the second largest peak in the HPSEC chromatogram. The data representing organics with AMW > 1500 Da are mainly related to the large single peak, which was found to be recalcitrant to UV/H_2O_2 treatment. This could also be seen from the low reduction in the amount of organics as presented in Figure 6.10. For the smaller organic molecules (AMW < 500 Da), it is observed that with further treatment (i.e., UV fluence > 500

mJ/cm^2) the reaction rate with OH radicals leads to the production of smaller molecules; hence, little reduction is observed for smaller organic molecules.

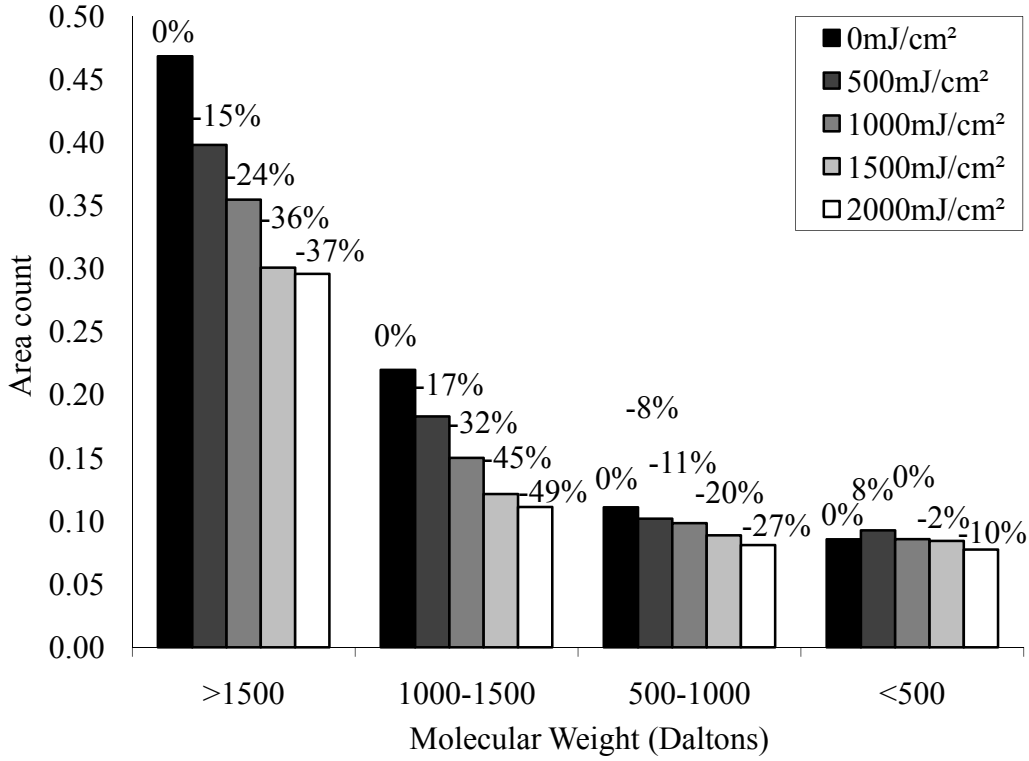

Figure 6.10: Impact of UV/H_2O_2 treatment on molecular weight distribution of BI water.

6.3.5 Impact of UV/H_2O_2 on molecular weight distribution of SR NOM

Figure 6.11 shows the HPSEC chromatograms obtained for the synthetic water with 5ppm TOC. One notable point is the molecular weight distribution of SR NOM which mostly consists of high molecular weight organic compounds. Therefore, OH radicals generated in the process will be reacting primarily with larger organics to breakdown the conjugated double bounds. As can be seen, a significant reduction was observed for the UV260 nm absorbing compounds, especially for those with higher molecular weight. The peaks appearing at longer retention time, and representing relatively lower molecular weight organics increased during the UV/H_2O_2

treatment. This again indicates the breakdown of larger organic molecules to relatively smaller organic molecules.

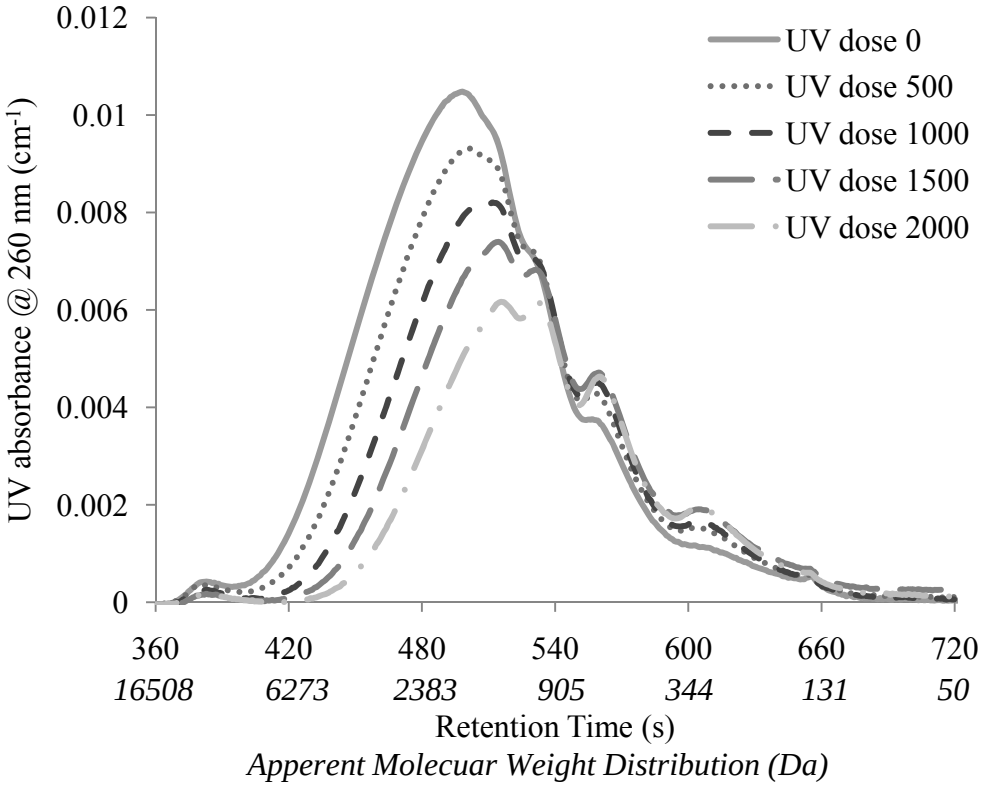

Figure 6.11: HPSEC chromatograms for the SR NOM (5ppm TOC) treated with UV/H_2O_2 process.

Figure 6.12 shows the HPSEC chromatograms for the same SR water (i.e., 5 ppm TOC) with added alkalinity (to 50 and 150 ppm as $CaCO_3$). The obtained chromatograms clearly demonstrate the effect of alkalinity on the removal of CNOM (in particular high molecular weight CNOM) during UV/H_2O_2 treatment. As shown, species comprising alkalinity (mostly carbonate species) scavenge OH radicals leading to lower degradation of CNOM during the treatment. This will in turn lead to lower generation of smaller organic molecules. Similar results were obtained for SR with higher TOC (i.e., 10 ppm) and are presented in Appendix C. As can be seen, there is no significant difference between the chromatograms representing SR water with 50 and 150 ppm of alkalinity. This is in agreement with previous data for UV_{254} and TOC

where no tangible difference was observed with the increase of alkalinity. This can be mainly attributed to the dominant influence of NOM concentration and its reaction rate with OH radicals in controlling the overall CNOM degradation rate.

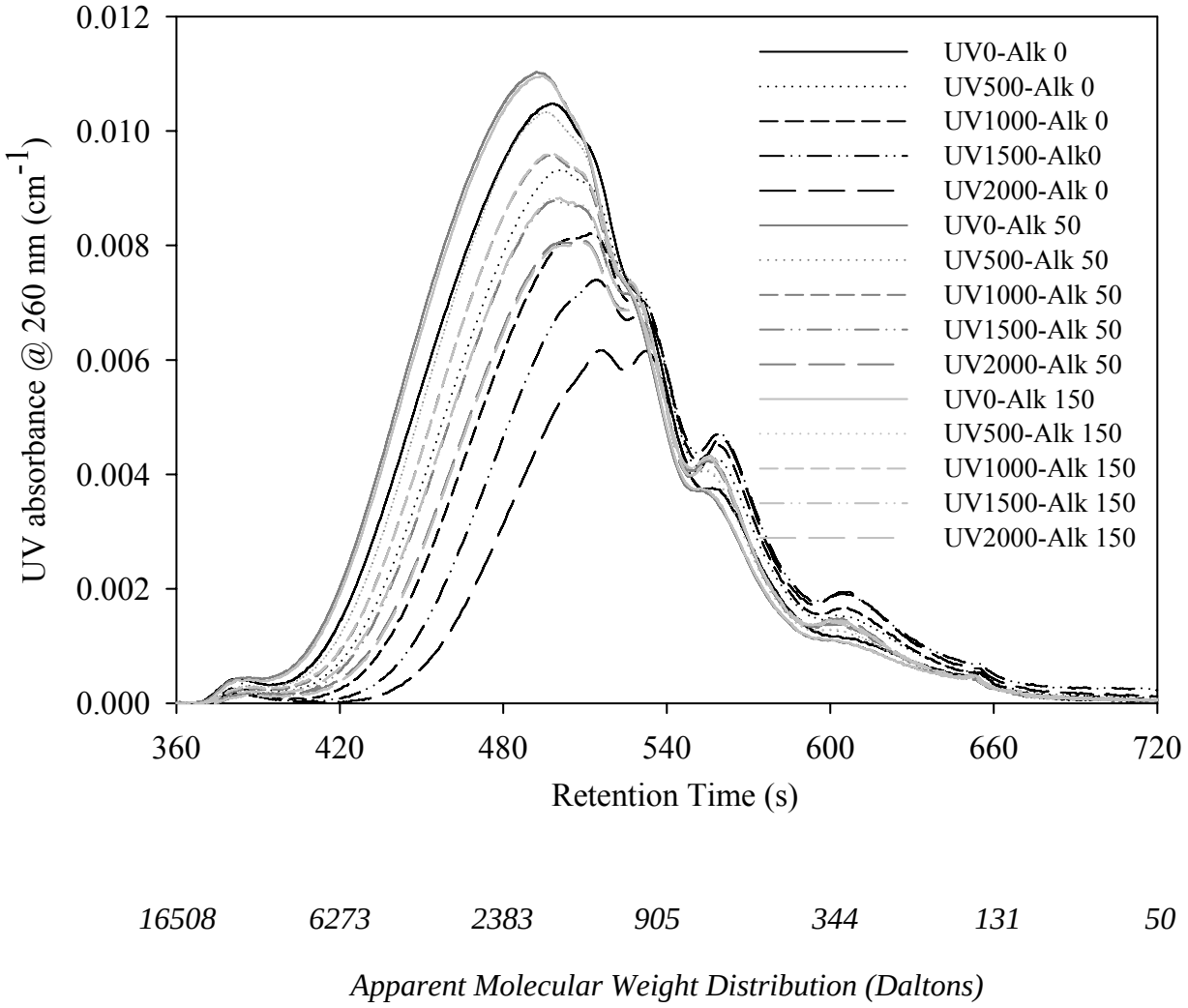

Figure 6.12: HPSEC chromatograms for SR water with TOC~5 ppm and different alkalinities

Figure 6.13 shows the data obtained after deconvoluting the HPSEC chromatograms of the SR water with initial TOC of 5 ppm and no alkalinity over the course of treatment with UV/H_2O_2. As previously mentioned, a large portion of the organic molecules in SR NOM belongs to the

higher molecular weight organic category. As a result, significant reduction is observed in almost all the AMW categories except for AMW< 500 (Da) where some increases were observed for the organic molecules, further supporting the formation of smaller organic molecules. This is in agreement with the data shown earlier on natural waters, confirming that OH radicals preferentially react with larger organics leading to the formation of smaller ones. Moreover, it can be concluded that, at higher fluences of UV (i.e., extended treatment) smaller molecules also start to decrease indicating that their rate of consumption dominates their rate of production.

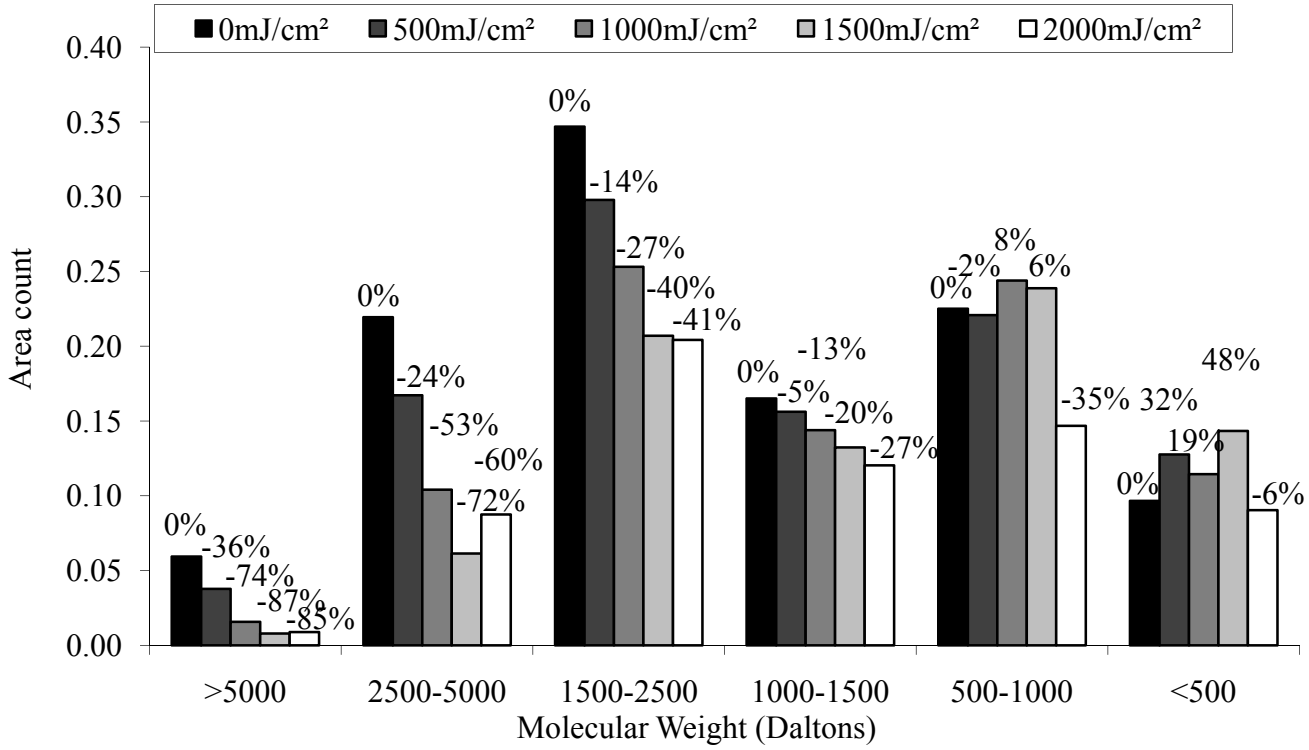

Figure 6.13: Impact of UV/H_2O_2 treatment process on molecular weight distribution of SR NOM (TOC~5ppm, no alkalinity).

6.4 Impact of UV/H_2O_2 Process on AOC of Natural Waters

The modified assimilable organic carbon (AOC) bioassay, presented in Chapter 5, was used to study the change in the AOC profile of water during the UV/H_2O_2 treatment. Residual H_2O_2 was

removed from the UV/H_2O_2 treated water using Catalase immobilized on SEPABEAD® and subsequent steps were applied to prepare the samples and analyze them for AOC.

Figure 6.14 shows the average AOC measured after each UV/H_2O_2 treatment for three independent experiments for both Capilano (CW) and Bowen Island (BI) waters.

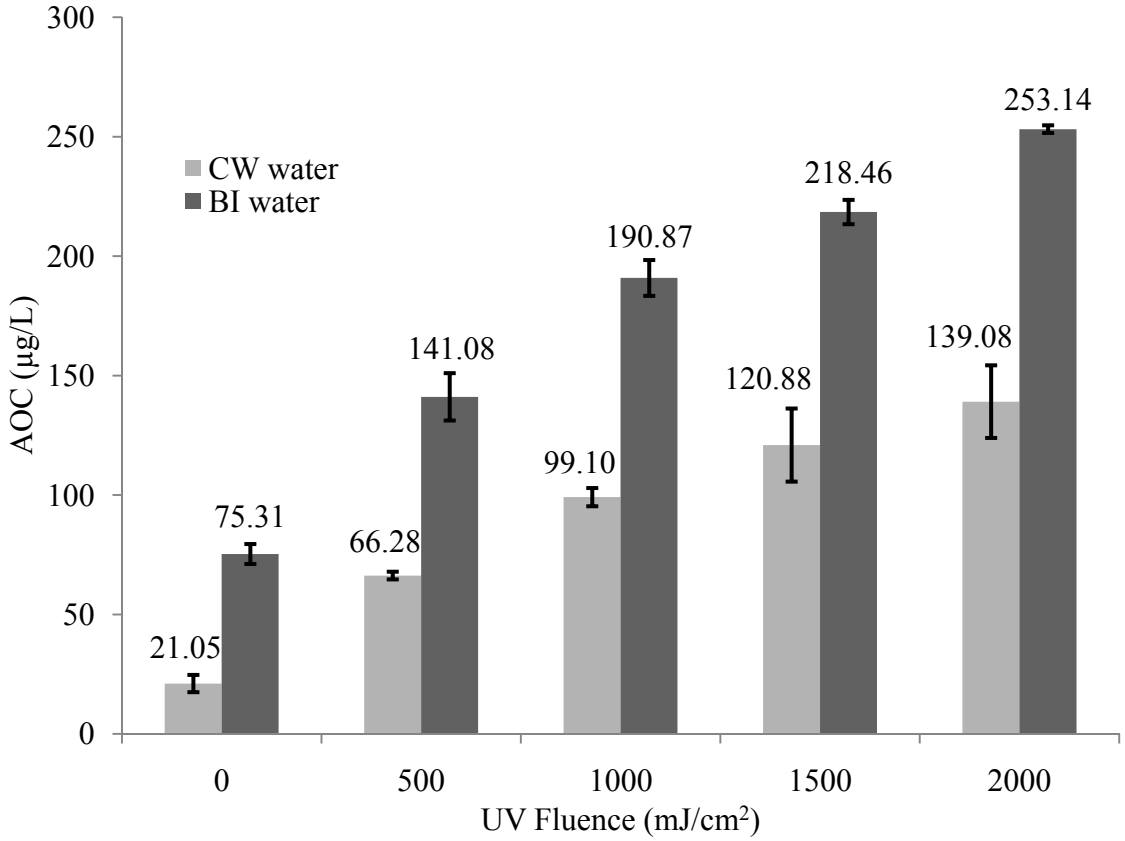

Figure 6.14: Impact of UV/H_2O_2 treatment on the AOC profile of Capilano and Bowen Island waters.

For both CW and BI waters, the amount of AOC increased as the UV/H_2O_2 treatment progressed. This indicates the production of more readily available organic molecules for degradation/consumption by bacteria. Raw Bowen Island water showed to have a higher AOC in comparison with Capilano water. This can be attributed to the higher TOC of Bowen Island (i.e., ~5 ppm). Moreover, AOC has increased about 5.6 and 2.36 times for Capilano and Bowen Island waters, respectively, over the course of treatment, indicating the formation of more

biodegradable organics during the UV/H_2O_2 treatment of Capilano water. The findings on the SUVA profile of these waters (i.e. CW and BI) as demonstrated in Figure 6.15 could be used to explain the data on AOC. SUVA of CW showed to decrease 35.5% from its initials value whereas data on BI water indicated 29.5% reduction in the amount of SUVA over the course of treatment. This indicates higher fractional conversion of aromatic double bounded compounds in the CW NOM than the ones in BI NOM. Therefore, it is hypothesized that SUVA and AOC data from the UV/H_2O_2 treatment could have a positive but inverse correlation.

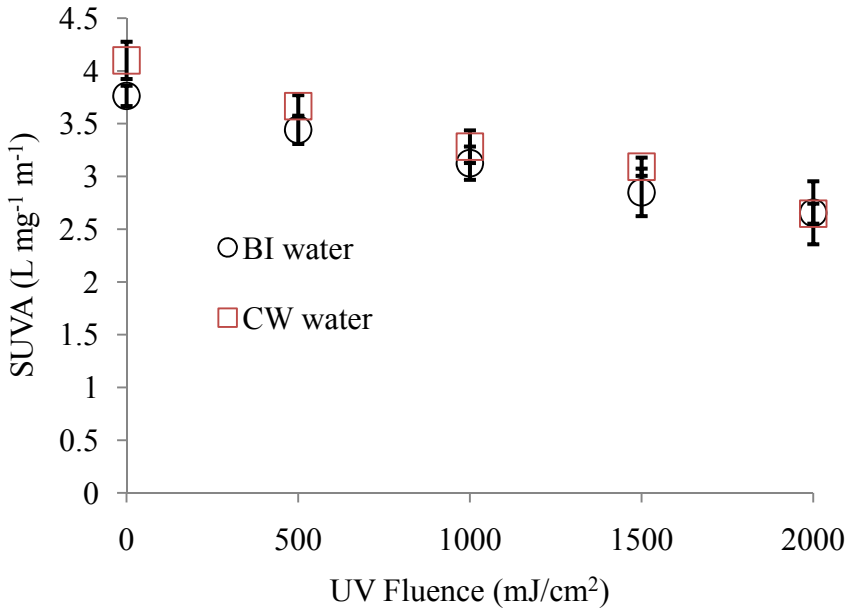

Figure 6.15: SUVA profile of natural waters during UV/H_2O_2 treatment

A general and interesting observation is that the overall AOC trend shows increment throughout the UV/H_2O_2 treatment process. As previously demonstrated in Figures 6.8 and 6.10, at UV fluence of 2000 mJ/cm^2, the entire molecular weight categories show reduction; however, from the data presented in Figure 6.14, AOC still shows increment even at this fluence. This observation can be attributed to two major reasons. First, parameters indicating physiochemical properties such as UV_{254} or HPSEC chromatograms cannot provide accurate prediction/indication on biological degradability of organic matter. Second, there are some

biodegradable small molecules/species present in water which cannot be detected by HPSEC or other techniques relying on spectrophotometric properties of water. HPSEC depends entirely on the absorption of organic molecules at UV 260 nm, so it would not detect organics that do not absorb light at this wavelength.

Data presented in Figures 6.8 and 6.10 indicate a reduction in all the molecular weight categories, except the fraction with AMW< 500 Da, after the UV fluence of 500 mJ/cm^2. However, as shown in Figure 6.14 the amount of AOC increased considerably (by about 2-3 times) for both Capilano and Bowen Island water at UV fluence of 500 mJ/cm^2. This indicates that smaller organic molecules are not the only portion of NOM contributing to AOC formation. This is in agreement with the observation reported by Hem and Efraimsen (2001) who reported that organic molecules from all size categories contribute to the overall AOC formation, even though smaller molecules may play a more dominant role. Therefore, it can be concluded that the biodegradability of organic matter increases with the extent of UV/H_2O_2 treatment. Similar observation has also been reported by Toor (2005) where it was found that application of AOPs enhances the biodegradability of organic matter over the course of treatment.

To better understand the fate of AOC over the course of treatment with UV/H_2O_2, extended treatment was applied to CW and BI waters and biodegradability of NOM was examined. Figure 6.16 shows the AOC for Capilano and Bowen Island waters under the extended UV/H_2O_2 treatment. As demonstrated, AOC profile for both waters reached a plateau for UV fluences between 2000 mJ/cm^2 and 4000 mJ/cm^2. This likely indicates equilibrium between the rates generation and degradation of smaller organic molecules with OH radicals. For UV fluences higher than 3000 mJ/cm^2, AOC profiles of both waters started to decline, indicating the overall net degradation of smaller organics. However, further treatment (i.e., beyond 4000 (mJ/cm^2)) needs to be studied to investigate the fate of AOC profile over the treatment.

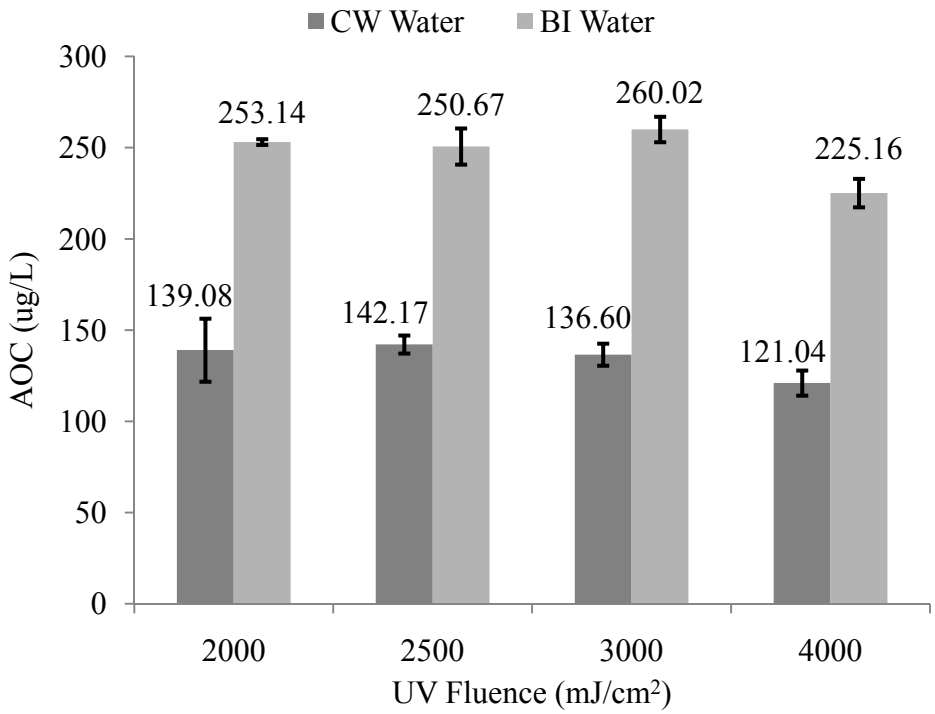

Figure 6.16: Impact of extended UV/H_2O_2 treatment on AOC profile of natural waters.

6.5 Impact of UV/H_2O_2 Process on AOC of Synthetic Waters

Synthetic water was used with different NOM concentrations and alkalinities to better understand the AOC trend over the UV/H_2O_2 treatment. Figure 6.17 shows the AOC results for synthetic water at two different NOM concentrations (5 and 10 ppm as TOC) treated with initial [H_2O_2] ~10ppm and UV fluences up to 2000 mJ/cm^2. The pH of the original synthetic water was 5.3 and 3.68 for TOC of 5 and 10 ppm, respectively. Preliminary experiments showed inhibition in bacterial growth at acidic pH. Therefore, pH was amended to 6.9~7 by adding NaOH to the synthetic water sample. Note that this step was not necessary when alkalinity (i.e., $NaHCO_3$) was added, since dissolution of $NaHCO_3$ led pH to stabilize in the neutral range (7.0-7.5).

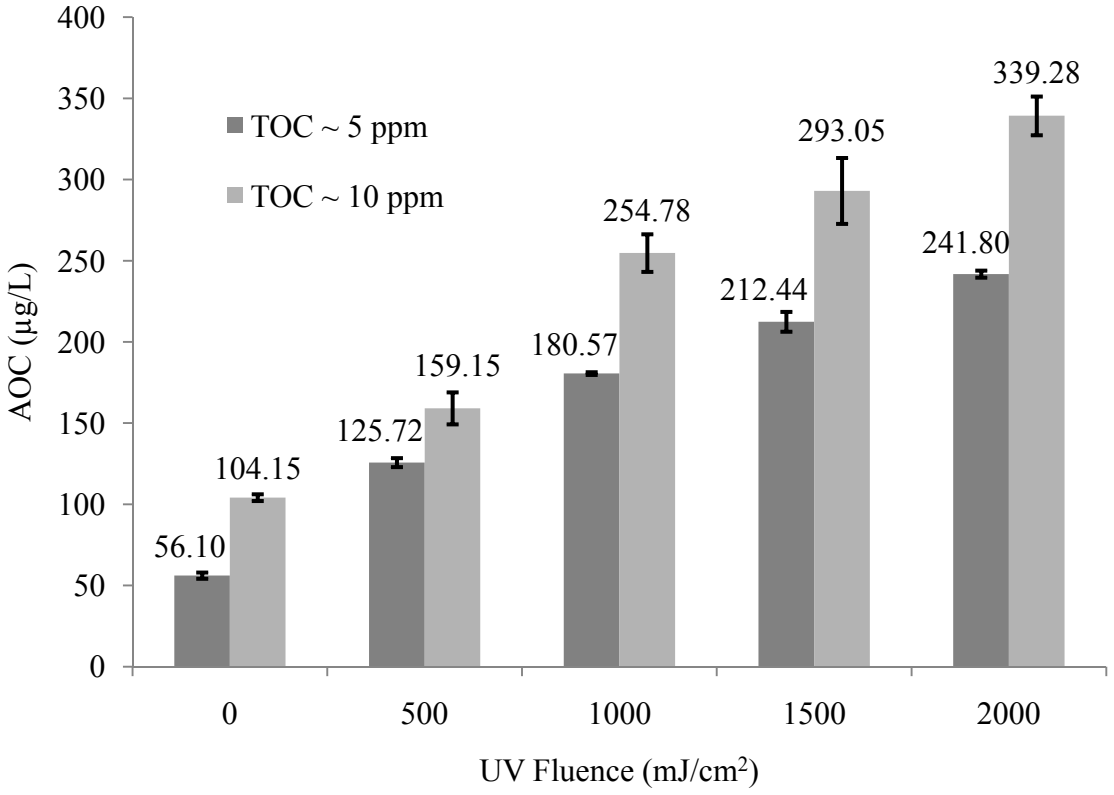

Figure 6.17: AOC formation for synthetic water (with SR NOM) during the treatment with UV/H_2O_2 at two different initial TOC concentrations.

As demonstrated in Figure 6.17, the initial AOC values measured for the synthetic water are proportional to their relevant TOC amount. The AOC of the synthetic water with TOC~ 5 ppm was increased about 4.3 times from its initial value while the SR water with TOC~ 10 ppm showed 3.3 fold increases from its original amount. This is similar to the AOC data on the natural waters as was presented in Figure 6.14. Therefore, one could attribute the lower percentage increase in the SR water with higher NOM concentration to the shielding and scavenging effects of NOM which reduces the number of generated OH radicals as well as interactions/reactions between OH radical and organic matter. This would in turn affect the percent conversation of organics and the formation of AOC.

However, despite the similarities between SUVA values of the CW and SR, they did not show similar behavior in AOC increase when underwent UV/H_2O_2 treatment. To better explain this phenomenon one should look at the AMW distribution of NOM in both waters. As was demonstrated in Figures 6.7 and 6.11, the SR NOM is mainly consisted of very large organic molecules (AMW > 2000 Da) whereas; CW NOM is comprised of relatively medium to small organics (AMW~ 1500-500 Da). Therefore, it is hypothesized that the AMW distribution of organic matter can potentially affect the formation of AOC during the treatment. OH radicals generated within the process are mainly scavenged by larger organic molecules leading to their breakdown into smaller species. Therefore, depending on how large the primary organic molecules are, the AOC profile can be influenced.

Figure 6.18 illustrates the effect of alkalinity on the AOC profile of the SR water with initial TOC~ 5ppm. As previously mentioned, the pH of SR increased to the neutral range (i.e., 7.0-7.5) as a result of dissolving $NaHCO_3$, thus the solution was not amended at this stage. For a given level of UV/H_2O_2 treatment, lower values of AOC were formed in the presence of alkalinity. Also, the higher was the alkalinity; the lower was the amount of AOC formed. The findings here were expected since carbonate species comprising alkalinity compete with NOM in scavenging OH radicals, thereby lower the amount of smaller organic molecules formed during the UV/H_2O_2 treatment. It is of course difficult to accurately describe/predict the behavior of a complex system such as the UV/H_2O_2 process which involves many reactions and the influencing parameters (See Table 3, Equations 1-10 in Appendix A). Nevertheless, it is sufficed to say that, a proportional change would not be expected with changes in alkalinity, because the process involves various reactions which are linked together. Additional data obtained with the SR water with 10 ppm showed similar findings (data are presented in Appendix C).

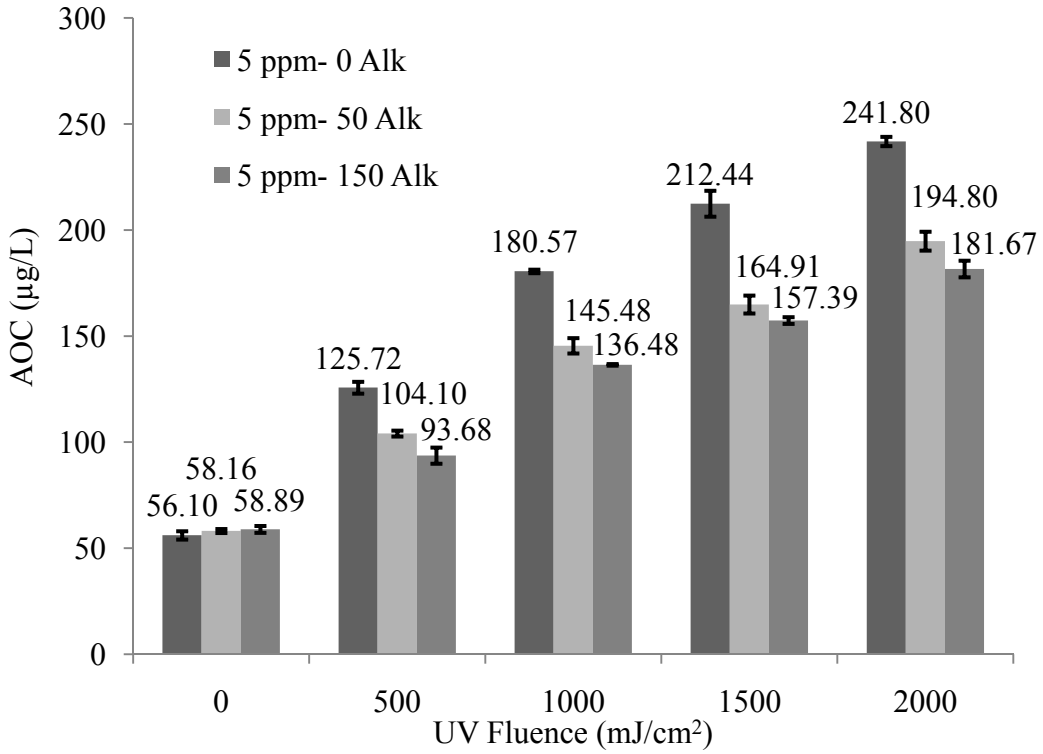

Figure 6.18: Impact of UV/H_2O_2 on AOC of SR water with TOC~ 5 ppm and different alkalinities.

6.6 Biodegradable Organic Carbon (BDOC) versus AOC after UV/H_2O_2 Treatment of Natural Waters

Huck et al., (1990) suggested utilizing AOC as an indicator of bacterial regrowth and BDOC as an indicator of disinfection by-product formation potential. Servias et al. (1995) and Volk et al. (1994) proposed BDOC as a factor indicating biological stability of water. Hence, it is a frequent practice for water utilities, monitoring biostability of water, to measure both AOC and BDOC (Escobar and Randall, 2001). However, it would be far more desirable to only use one technique to quantify biological stability of water, so that significant saving could be made on time and resources associated to run both assays.

As a result, some experiments were carried out to measure BDOC on the UV/H_2O_2 treated natural waters (i.e., CW and BI) to investigate the relationship between AOC and BDOC.

UV/H_2O_2 treatment experiments were performed at UBC and samples were quenched of H_2O_2 and then were sent over night @ 4°C to Ecole Polytechnique de Montreal for BDOC analysis. BDOC tests were performed at research, development and validation center for water treatment technologies and processes (CREDEAU) (Dr. Barbeau's lab).

Figures 6.19 and 6.20 demonstrate the correlations between BDOC and AOC profiles for Capilano and Bowen Island waters over the course of the treatment. As is observed, the results obtained for both waters indicate meaningful correlations between AOC and BDOC (R^2=0.96 and 0.98). However, different correlations are attained for the two waters examined in here. This can be attributed to the difference in the nature of the NOM that undergoes UV/H_2O_2 treatment. Therefore, further research on various type of water quality will be value to better understand the correlation between AOC and BDOC.

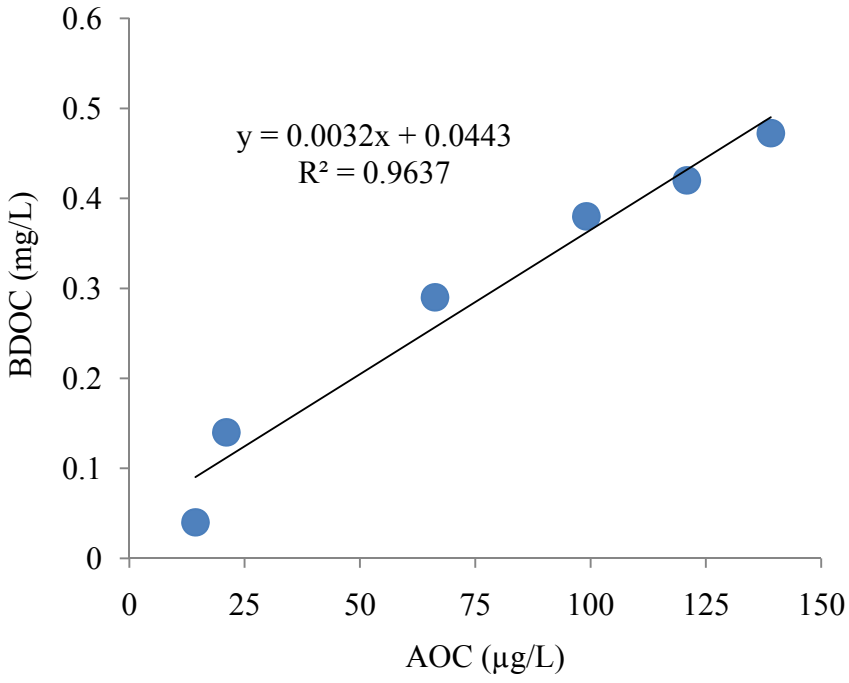

Figure 6.19: BDOC vs. AOC for UV/H_2O_2 treated Capilano water.

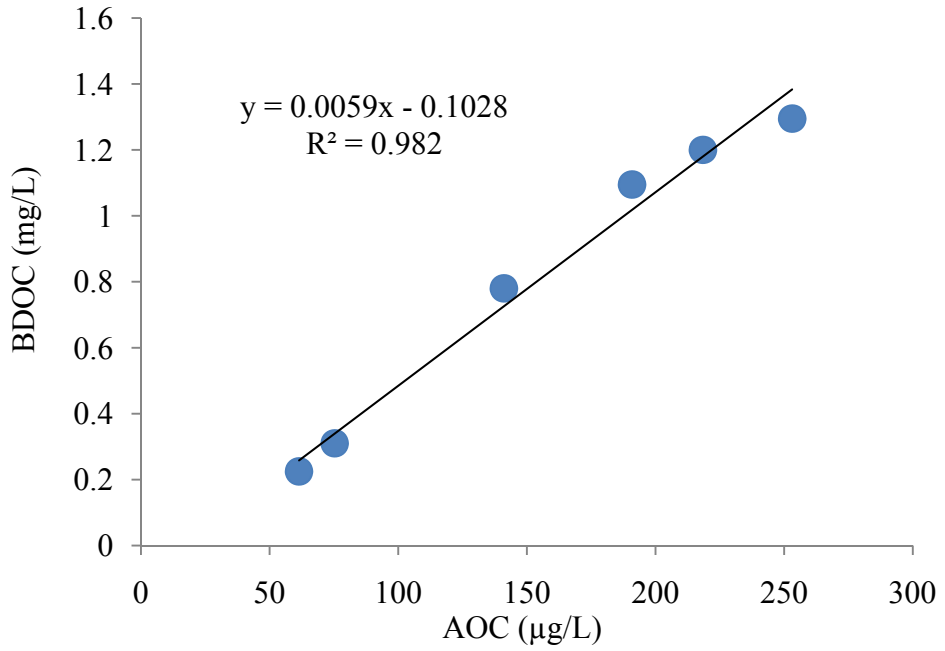

Figure 6.20: BDOC vs. AOC for UV/H_2O_2 treated Bowen Island water.

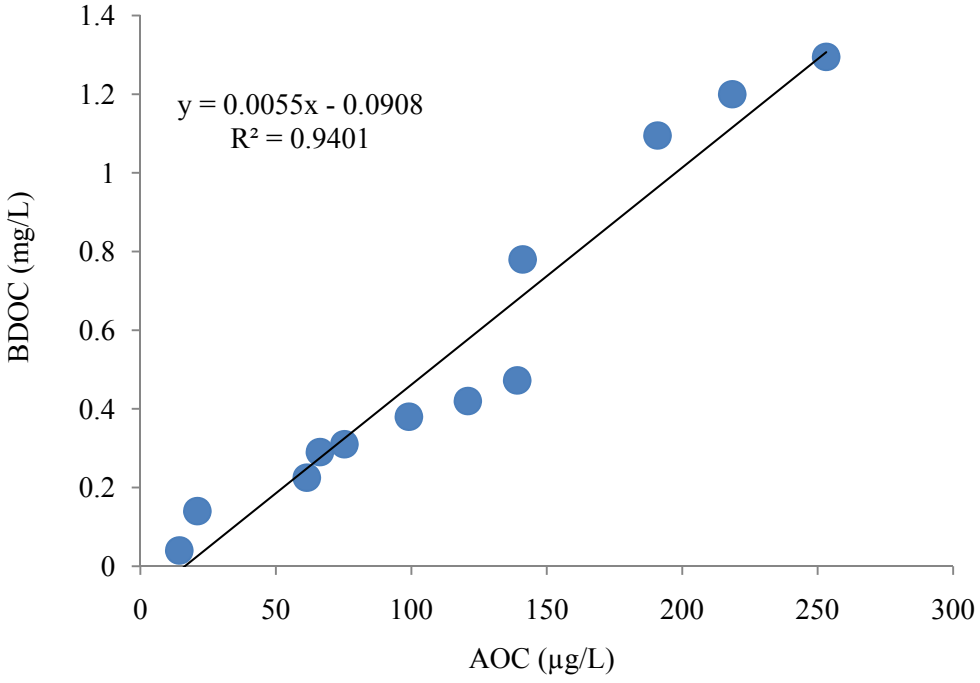

Figure 6.21: BDOC vs. AOC for UV/H_2O_2 treated natural water (CW and BI).

Figure 6.21 presents all the data showing the relationship between AOC and BDOC for both waters. Overall, there is clear and direct correlation between AOC and BDOC for the waters that

underwent UV/H_2O_2 treatment. One possible explanation can be the similarity in the nature of the assays employed in this study (i.e. BDOC and AOC) in which natural consortium is used as the inoculum. However, the incubation time, incubation temperature and the measurement techniques are different. Of course examining different waters under different treatment strategies will help to collect more data and to draw a more concrete conclusion about any possible correlation between BDOC and AOC. However, the question remains whether such correlation could be extrapolated to other waters with different NOM, especially because there has been little prior data reported in the literature. On the contrary, Kaplan et al. (1994) and Escobar and Randall (2001), investigating the profile of AOC and BDOC for different waters and also for different treatment alternatives, concluded that no clear correlation could be extracted for AOC and BDOC. Escobar and Randall (2001) recommended that both AOC and BDOC be evaluated in monitoring biological stability of water. It should be noted that AOC is a more sensitive parameter directly indicating the regrowth potential whereas BDOC is a less sensitive (lower detection limit) parameter used to quantify biodegradable carbon available for bacterial regrowth. Given the initial results obtained in this research, it is recommended that more AOC and BDOC data be gathered on other source waters undergoing treatment with UV/H_2O_2 oxidation, before any final conclusion could be drawn.

In this regard, and to better understand the relationship between AOC and BDOC another set of experiments were conducted in collaboration with Ecole Polytechnique de Montreal, studying the AOC profile of a river water undergoing multistage treatment in a pilot plant, consisting of GAC filtration, Ozonation and Membrane filtration. Samples were sent to UBC overnight @ 4°C and were analyzed for AOC the next day. The results were then compared with those obtained for UV/H_2O_2 treated water.

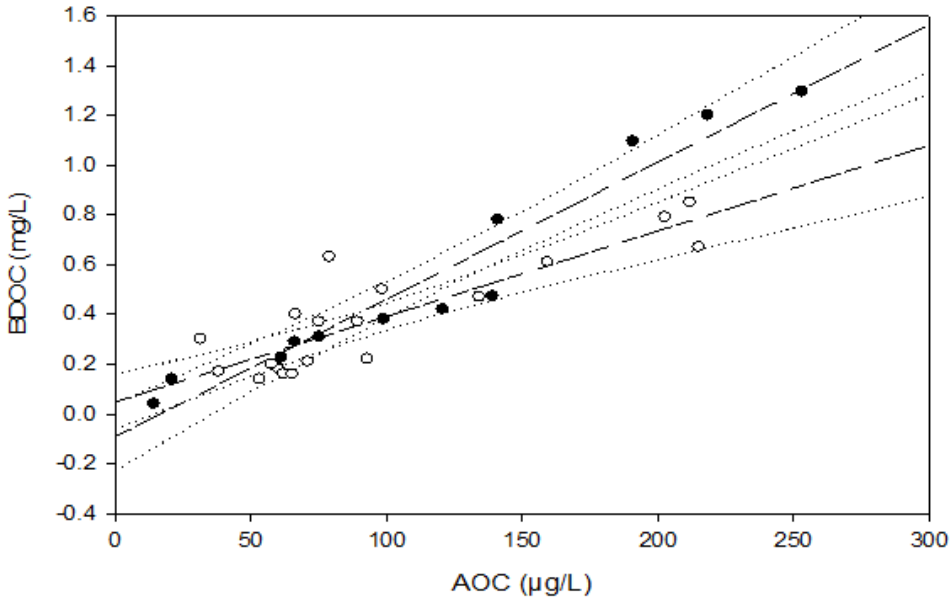

Figure 6.22: Comparison of BDOC vs. AOC for UV/H_2O_2 treated water and pilot plant study; (•) UV/H_2O_2 treated water, (○) pilot plant treated water.

Figure 6.22 shows the results for UV/H_2O_2 treated water along with the data obtained from the pilot plant study. For each set of scattered data, there is a positive and meaningful correlation between AOC and BDOC; however, the correlations are statistically different from one another. The dashed lines represent the linear regression between the data, and the dotted lines show the 95% confidence intervals for the regression equation. To examine the statistical differences of these two trends, the errors associated with the estimation of the coefficients with 95% of confidence are presented in Table 6.4.

Table 6.4: Coefficients of the linear regression equations for the correlation between BDOC and AOC correlation (**BDOC=a × AOC +b**, Errors represent ± 95% confidence limits).

Treatment/ Coefficient	a	b
Pilot treatment plant	0.0034±0.0010	0.0485±0.1038
UV/H_2O_2 treatment	0.0055±0.0008	-0.0908±0.1212

According to Table 6.4, no overlap was observed for the slopes of the regression lines for the two different studies. Hence, it can be concluded that these two correlations are significantly different from one another at 95% confidence level. However, the b coefficients did show overlapped as it is also demonstrated in the figure 6.22. Further statistical calculations also demonstrated that b values are not statistically significant from zero (See Appendix D). Therefore, one can argue that the correlation between BDOC and AOC can be in the form of BDOC=a*AOC rather than BDOC=a*AOC+b. More information regarding the correlation between AOC and BDOC (considering b=0) is provided in Appendix D.

Overall, meaningful correlations were observed between AOC and BDOC in all the cases. This is in contrast with the previous reports by Kaplan et al. (1994) and Escobar and Randall (2001).

6.7 Highlights and Remarks

This chapter investigated the impact of UV/H_2O_2 treatment process on AOC and BDOC of waters with different qualities.

AOC was shown to increase within the commercial UV/H_2O_2 treatment conditions (i.e., UV fluence up to 2000 mJ/cm^2). However, with further treatment AOC reached a plateau and started to decline afterward. That being said, further experiments with more extended time are required to obtain a complete profile of fate of AOC during UV/H_2O_2 treatment.

Smaller organic molecules were found as the portion most contributing to AOC. However, data obtained indicated that other molecular weight categories also support the bacterial growth.

One interesting observation was regarding the AOC profile of BI and SR waters with similar TOC contents. Although the initial AOC values were in the same range for both water but different AOC trends were obtained when they underwent UV/H_2O_2 treatment. This

phenomenon can mainly be attributed to the AMW distribution of NOM in these waters. SR water is mainly consisted of very large organic molecules which are relatively harder to breakdown by OH radicals. As a result, lower degradation of organic matter takes place in SR water in comparison with BI water.

Presence of alkalinity was shown to compete with NOM in scavenging OH radicals hence diminishing the production of smaller molecules, and AOC.

Positive and meaningful correlations were observed between BDCO and AOC of different water that underwent different treatments. However, the correlations obtained in this study were shown to be statistically different, and further data is required to improve the conclusion.

7 Coagulation as a Pre-treatment Alternative for UV/H_2O_2 Advanced Oxidation Applications

7.1 Introduction

This chapter presents the findings on the impact of Chitosan and Alum coagulations on the efficacy of UV/H_2O_2 treatment as well as the finished water quality. NOM behaviour was studied at different treatment stages by monitoring its physical properties. Also the effect of coagulation on AOC of finished water after the UV/H_2O_2 treatment was investigated.

7.2 Selection of the Coagulant

Chitosan and Alum were tested to find the most effective coagulant in terms of TOC and UV_{254} removal. Figure 7.1 shows the performance of different doses of Chitosan in removing organic matter. As can be observed, Chitosan was not effective at reducing TOC and UV_{254}. In fact, by using Chitosan higher amount of TOC and UV_{254} (except one point) was measured for all the doses investigated. This can be attributed to the organic nature of the Chitosan which can result in increase in TOC and UV absorbance of water. According to these results Chitosan was found to be not suitable for removing organic matter and hence, its application was ruled out from this work.

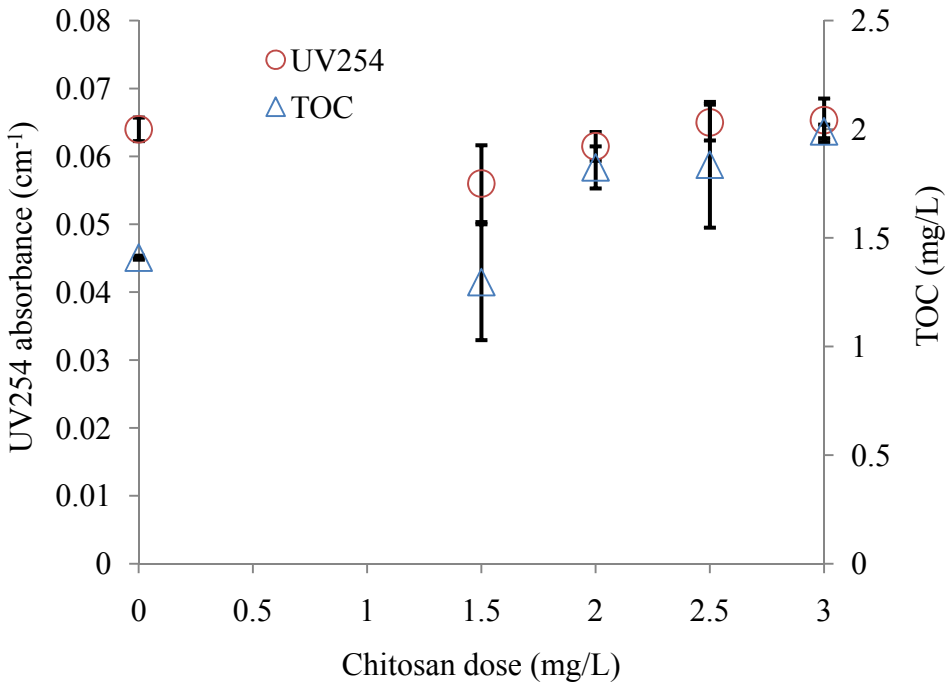

Figure 7.1: Effect of Chitosan applied at different doses on UV_{254} and TOC of Capilano water

Aluminum sulphate Octadecahydrate ($Al_2(SO_4)_3.18H_2O$) also known as Alum, has been used widely in water and wastewater treatment facilities and its reaction mechanism is well understood. In this study, different doses of Alum were applied to Capilano and Bowen Island waters and TOC and UV_{254} were measured after each treatment. Coagulation was performed according to the section 4.5.3. Total organic carbon and UV_{254} profile were plotted versus the Alum dose used for both CW and BI waters in Figures 7.2 and 7.3, respectively.

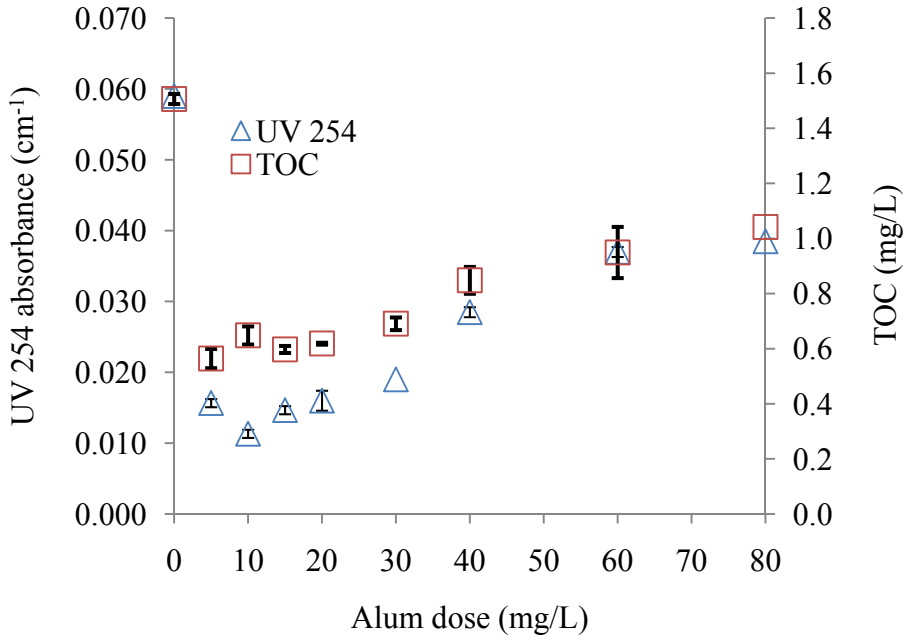

Figure 7.2: Impact of Alum Coagulation on UV_{254} and TOC of Capilano water.

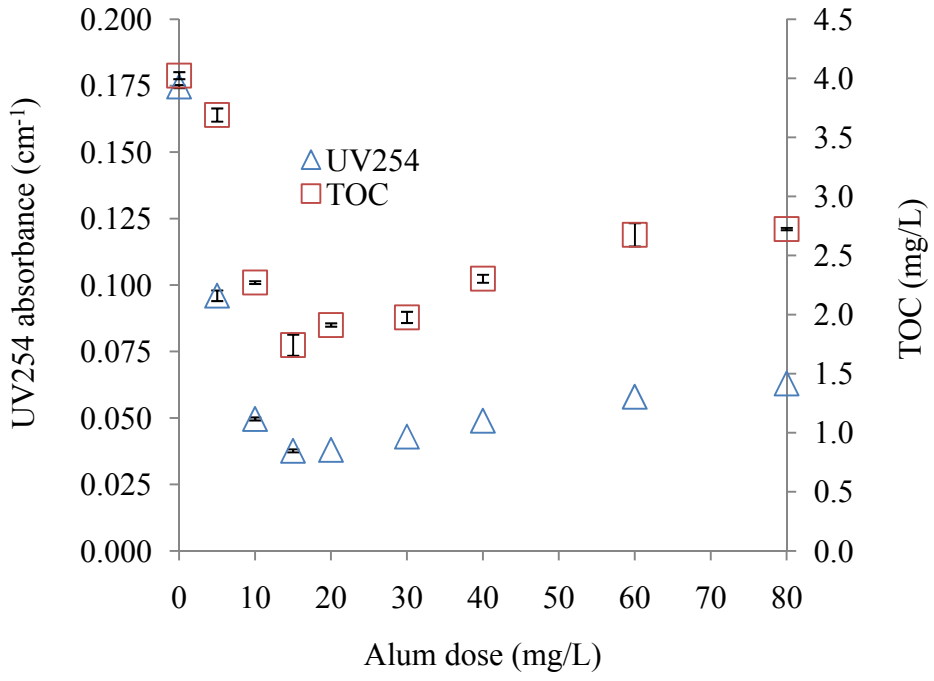

Figure 7.3: Impact of Alum coagulation on UV_{254} and TOC of Bowen Island water.

The application of alum dramatically decreased the UV_{254} and TOC for both natural waters. From Figure 7.2 it can be seen that alum had a significant impact on CW and that alum doses of

5, 10, and 15 ppm show similar performance in removing organic matters. Given the economical considerations and the proximity of the amount of UV_{254} and TOC removed, the alum dose of 5 ppm was selected for further coagulation experiments on Capilano water. The application of alum with an alum dose of 5 ppm resulted in about 62% and 75% removal of TOC and UV_{254}, respectively.

In the case of Bowen Island, alum doses of 10, and 15 ppm showed similar performance in removing UV_{254} (71% and 78% removal, respectively). However, 15 ppm alum showed to be more effective at removing TOC (56%) in comparison with the removal achieved from dosing 10 ppm of alum (43%). Hence, alum dose of 15 ppm was selected for subsequent coagulation experiments on Bowen Island water.

Residual aluminum was measured to ensure that the residual aluminum from application of alum does not exceed the standard limits (i.e., 0.2 ppm, EPA 2006 Edition of the Drinking Water Standards and Health Advisories). The concentration of residual aluminum was measured after coagulation using inductively coupled plasma (ICP) spectroscopy technique and the results for both waters are presented in Figure 7.4. For Capilano water the residual aluminum exceeds the standard level for all the applied doses except for 5 ppm (i.e., residual aluminum~0.055 mg/L). For BI water the residual aluminum after coagulation with 15 ppm of alum was 0.082 ppm that is below the regulation limits. Therefore, alum doses of 5 and 15 ppm were considered safe in terms of final aluminum residual and were used for subsequent coagulation experiments on CW and BI waters.

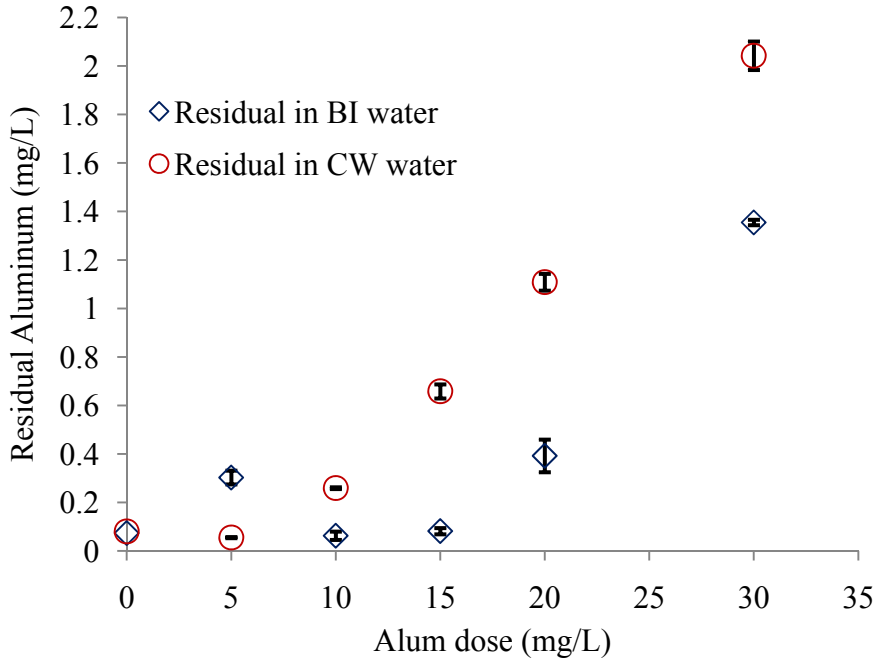

Figure 7.4: Residual Aluminum in Capilano and Bowen Island waters after the coagulation with alum using ICP spectroscopy.

7.3 Impact of Alum Coagulation on Molecular Weight Distribution of NOM

Effect of alum coagulation on molecular weight distribution of NOM was studied for Capilano and Bowen Island waters using size exclusion chromatography. Figures 7.5 and 7.6 compare the original raw water chromatograms versus the ones for treated with alum coagulation at different doses of alum.

Both Figures 7.5 and 7.6 show that, alum coagulation resulted in a significant removal of organic matter mostly in the large to medium (>500 Da) range of molecular weight organics. However, a slight decrease was also observed for the small size organic molecules (AMW <500 Da). Results presented in Figure 7.6 also confirm that alum dose of 15 ppm shows the best performance in removing organic matter. Moreover, the sharp single front peak present in the BI water was completely removed after coagulation, confirming the organic nature of the peak. More interestingly, at very high doses of alum, no further NOM removal was obtained in both waters indicating the presence of portions of NOM recalcitrant to removal by coagulation. As shown

there was no tangible reduction in the size of the chromatograms after 10 ppm and 15 ppm doses of alum used to treat Capilano and Bowen Island, respectively.

These observations are consistent with the findings reported in the literature for the application of alum. Chong Soh et al., (2008), Van Leeuwen et al. (1999), Drikas et al. (2003), and Chow et al. (1999) studied the impact of alum coagulation on NOM character and biodegradability, and concluded that alum removed more of the hydrophobic and higher molecular weight fraction of NOM, but less of neutral hydrophilic fraction and lower molecular weight organics. Moreover, it has been found that there is a preferential removal of NOM that absorbs UV indicating the aromatic NOM.

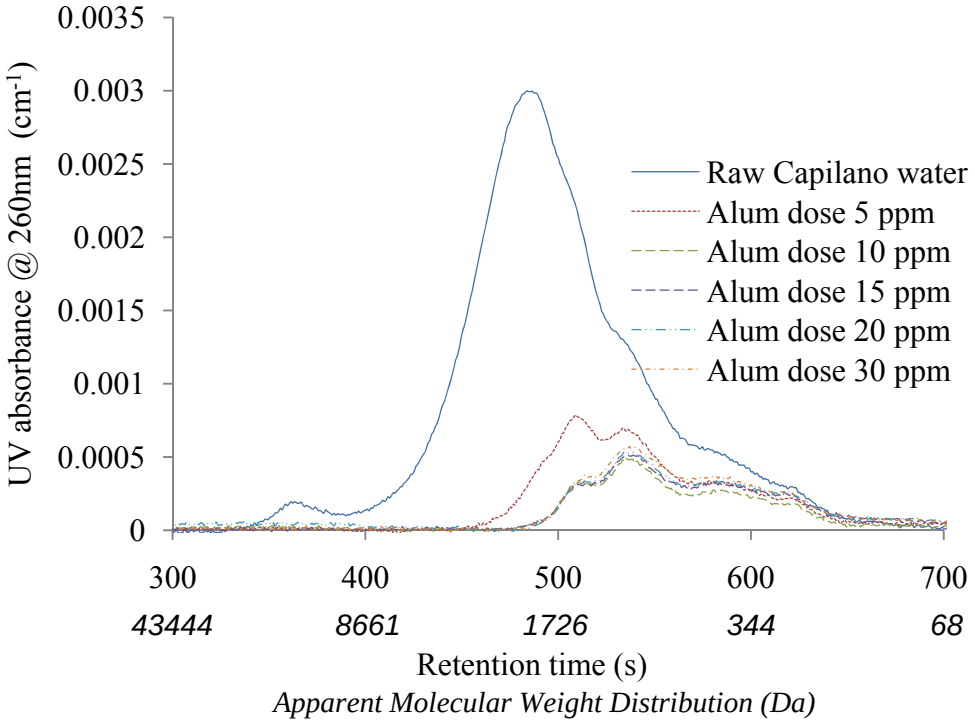

Figure7.5: HPSEC chromatogram for Capilano water treated with different doses of alum.

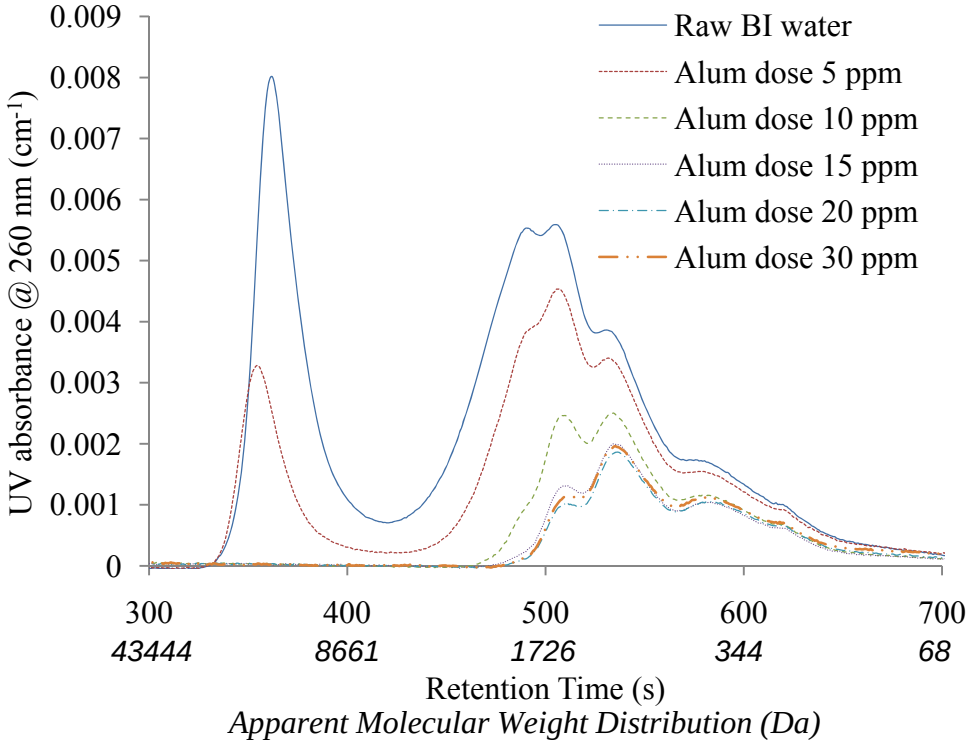

Figure 7.6: HPSEC chromatogram for Bowen Island water treated with different doses of alum.

7.4 Combined Alum-UV/H_2O_2 Treatment of Natural Waters

Capilano and Bowen Island waters were filtered (0.45 μm) and underwent alum coagulation using the alum doses determined as part of the work presented in section 7.2. After settling, alum treated water was filtered (0.45 μm) and underwent UV/H_2O_2 treatment and UV_{254}, TOC, molecular weight distribution, and AOC were measured.

Figures 7.7 and 7.8 compare UV/H_2O_2 process with combined alum-UV/H_2O_2 treatment for Capilano and Bowen Island waters, respectively. As illustrated in Figure 7.7, alum coagulation significantly reduces the amount of organic matter present in Capilano water by removing about 50% of the TOC and 73% of the UV254 absorbing organic compounds. In addition, application of alum resulted in 63% TOC and 80% UV_{254} reductions for Bowen Island water (Figure 7.8).

Applying UV/H_2O_2 process after alum coagulation decreased further, however slightly, the amount of remaining organics. As can be seen in Figures 7.7 and 7.8, the amount of UV_{254} and TOC did not change significantly during the oxidation process. This indicates the presence of recalcitrant organics that cannot be removed easily within the applied condition of UV/H_2O_2 process. However, one should note that the relative fraction of UV254 absorbing species eliminated in both treatments (i.e. UV/H_2O_2 and alum-UV/H_2O_2) is larger than that of TOC removed in the same process. This implies that OH radical generated, preferentially reacts with UV254 absorbing compounds. Alum coagulation removes a considerable portion of NOM mainly from large to medium molecular weight organics. Therefore, the remainder portion of NOM is mainly smaller organics that are more susceptible to react with OH radicals. Given that, one can expect larger reduction in UV_{254} as a result of absence of lager organics. However, interestingly lower reduction in the amount of TOC is observed for the alum treated water when it underwent UV/H_2O_2 process. The reason of this phenomenon was not concluded. That being said, one can still hypothesize that the structure of NOM after coagulation is mainly consisted of

UV254 absorbing compounds with very small molecular weights. Therefore, the change in the amount of UV_{254} has a lower contribution to the TOC.

Table 7.1 compares the amount of TOC and UV_{254} removal within each of UV/H_2O_2 and combined processes for two natural waters used in this study.

Table 7.1: Comparison of the effectiveness of UV/H_2O_2 and combined Alum-UV/H_2O_2 processes.

	Capilano Water			Bowen Island Water		
	UV Reduction	TOC Reduction	SUVA Reduction	UV Reduction	TOC Reduction	SUVA reduction
UV/H_2O_2	52%	26%	35.4%	38%	12%	29.4%
Alum-UV/H_2O_2	66%	18%	58.4%	52%	8%	46.8%

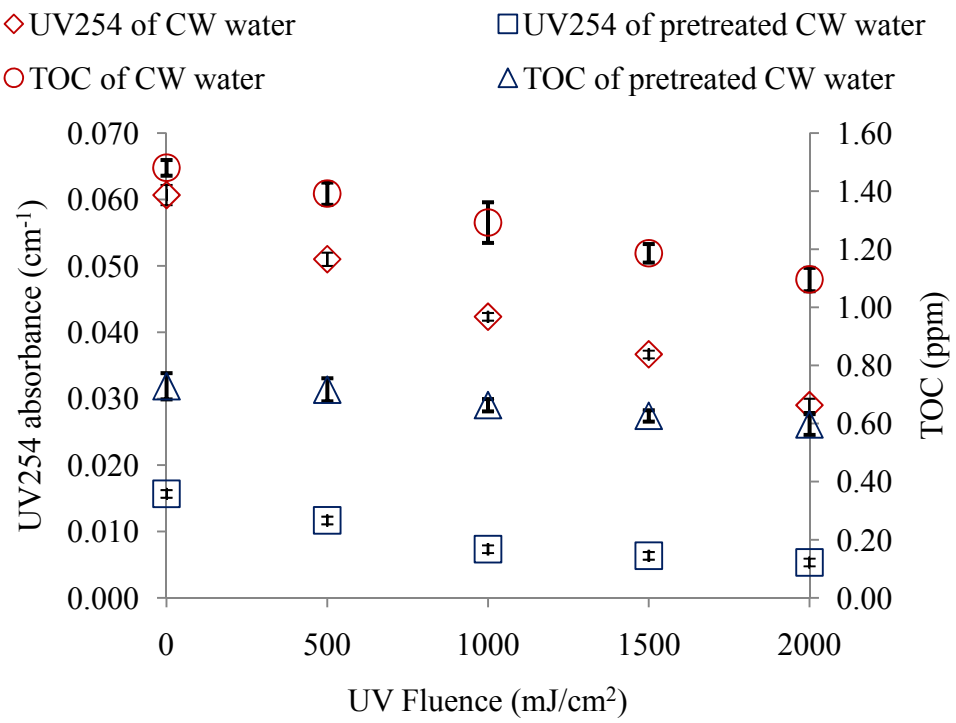

Figure 7.7: Impact of the pretreatment process on the efficacy of the UV/H_2O_2 treatment process.

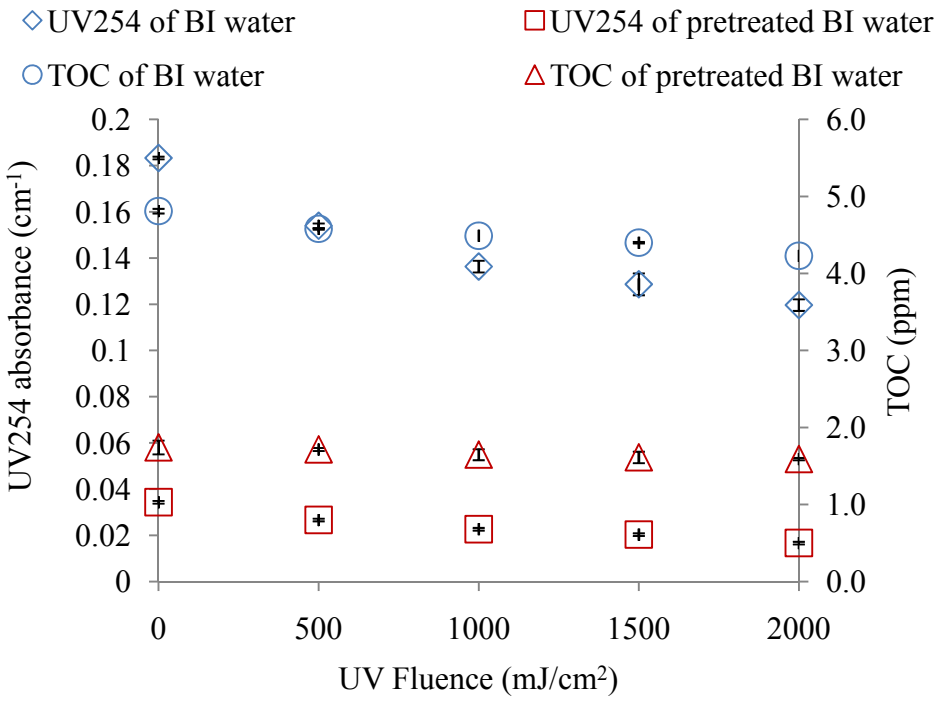

Figure 7.8: Impact of the pretreatment process on the efficacy of UV/H_2O_2 treatment process.

Figures 7.9 and 7.10 demonstrate the impact of combined alum-UV/H_2O_2 treatment on the molecular weight distribution of NOM for two natural waters (i.e., CW and BI) used in this study. As demonstrated, the extent of UV/H_2O_2 treatment beyond the UV fluence of 500 (mJ/cm^2) was not beneficial when alum coagulation was applied ahead of the oxidation process. That is, no significant reduction in the size of the peaks was observed for UV fluences greater than 500 (mJ/cm^2). This observation confirms the previous data on TOC and UV_{254} profiles, indicating the presence of recalcitrant organic matters that could not be eliminated within the range of applied UV fluences of up to 2000 mJ/cm^2. Nonetheless, it is important to highlight the lower amount of the energy required to achieve a certain level of target contaminant removal because of the absence of NOM scavenging effect. In other words, the higher quality of water allows for better utilization of OH radicals towards target contaminants in water. Therefore, pretreatment could be potentially influential in preserving energy while improving the overall removal efficiency.

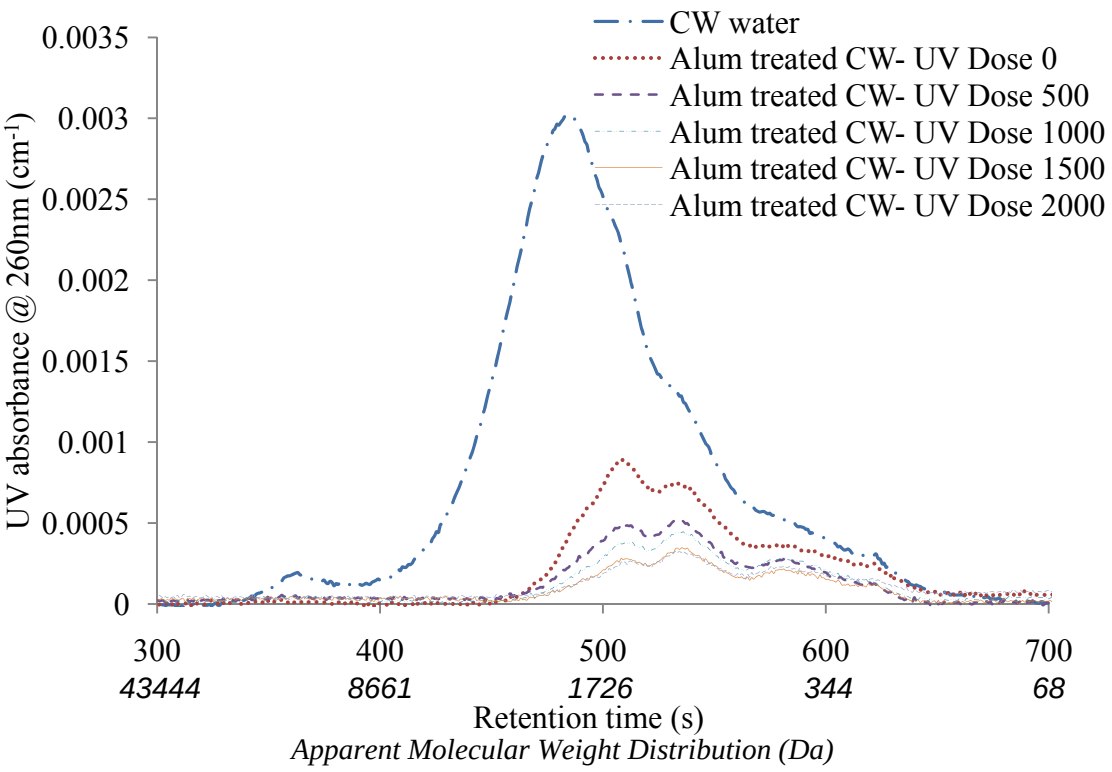

Figure 7.9: Impact of combined Alum-UV/H_2O_2 treatment on AMW of CW NOM

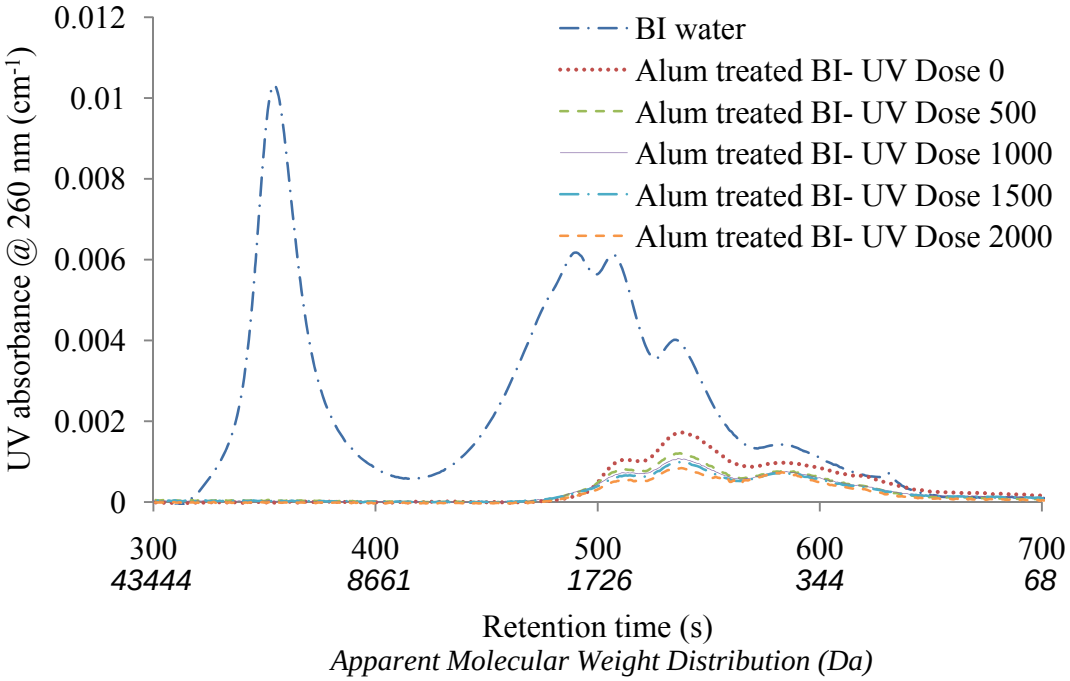

Figure 7.10: Impact of Alum-UV/H_2O_2 combined treatment on AMW of BI NOM

7.5 Impact of Alum Pre-treatment on the Efficacy of the UV/H_2O_2 Treatment

Data obtained from UV/H_2O_2 treatment along with those of the combined treatment clearly indicated that the application of alum significantly reduces the concentration of high molecular weight NOM, and improves the efficacy of the UV/H_2O_2 process. This in turn reduces the concerns associated with the formation of by-products during the oxidation process (i.e., DBPs, aldehydes, etc.). With the concentration of NOM and hence, less scavenging of OH radicals, target compounds can be removed more effectively with little concerns associated with the generation of undesirable by-products. More importantly, this helps conserve considerable amount of electrical energy used by the UV energy. Another economical benefit is the lower consumption of hydrogen peroxide which is an expensive reagent during the treatment (Toor, 2005). However, one may argue that the overall cost of coagulation (coagulation, flocculation, and sedimentation) is also high. Although it should be noted that the findings in here can be potentially of interest for those facilities that are have coagulation process in place. Therefore, applying UV/H_2O_2 process can be a viable alternative to increase their water quality.

Table 7.2 compares the amount of H_2O_2 consumed during the UV/H_2O_2 process (up to the UV fluence of 2000 mJ/cm^2) with the initial H_2O_2 concentration of 10 ppm. As demonstrated, utilizing alum coagulation resulted in significant reductions in the amount of H_2O_2 consumed during the UV/H_2O_2 treatment (i.e., by about 37.5% for CW and 50% for BI).

Table 7.2: H_2O_2 consumption during UV/H_2O_2 treatment with and without pretreatment.

	H_2O_2 consumption	
Source water	**Without pre-treatment**	**With pre-treatment**
Capilano Water	16%	10%
Bowen Island Water	36%	18%

7.6 Impact of Combined Alum-UV/H_2O_2 Treatment on AOC of Natural Waters

Application of alum was effective at removing a significant portion of organic matter mainly in the range of lager to medium size organic molecules. Therefore, utilization of alum ahead of the UV/H_2O_2 treatment could potentially reduce the amount of organics that react with OH radicals, generating smaller more biodegradable organic molecules.

To examine the impact of coagulation on the AOC profile of downstream water, experiments were performed with the combined alum-UV/H_2O_2 process. To avoid any organic contamination, alum stock solution was also prepared in an AOC free bottle. Alum treated water was filtered (0.45 μm pre-rinsed filter) and underwent different UV treatments (fluences of up to 2000 mJ/cm^2) with initial H_2O_2 concentration of 10 ppm.

Figures 7.11 and 7.12 demonstrate the effect of coagulation on the AOC profile of Capilano and Bowen Island waters. As expected, the AOC of CW and BI waters decreased significantly as a result of alum treatment. The reduction was more significant for the Bowen Island water, this being largely ascribed to the elimination of the large single eluting peak that represent high molecular size organics in the HPSEC chromatogram. Nonetheless, the application of UV/H_2O_2 on the pretreated water still showed to increase the AOC. This indicates that the portion of NOM (mostly of lower molecular weight nature) not removable by coagulation has the potential to support microbial growth. Similar observations were also reported by Chong Soh et al. (2008) and Liang and Ma, (2009) in which biodegradability of the alum treated water were assessed after alum coagulation.

One notable point in Figures 7.11 and 7.12 is the rate of AOC change for alum treated waters over the course of UV/H_2O_2 treatment. After UV fluence of 1000 mJ/cm^2, the AOC profile shows a lower increment and approaches a plateau. This can be attributed to the equilibrium in

the rates of production of smaller biodegradable organic molecules and their degradation with OH radical. Figure 7.11 also shows that AOC of CW starts to reduce slightly after the UV fluence of 1500 mJ/cm^2. A likely and plausible explanation is that at this fluence, the degradation rate of organic molecules dominates the production rate; hence, an overall decrease in the amount of small biodegradable organic molecules is observed.

As demonstrated in Figures 7.11 and 7.12, both alum treated CW and BI waters showed higher percentagewise increase in the amount of AOC in comparison with raw waters. This is similar to the previous data that was presented in chapter 6. As discussed earlier, this can be mainly attributed to higher number of interactions between OH radicals and organic molecules at lower concentration of NOM, thereby higher AOC production. Another noteworthy point is related to the greater potency of the remainder BI NOM in supporting microbial growth than the CW NOM. As can be seen, AOC of the pretreated CW water increased by about 7 times up to UV fluence of 2000 mJ/cm^2 and then started to decline afterwards. However, the AOC of pretreated BI water showed increases of about 12 times from its initial value over the course of the treatment. This can be attributed to the presence of more susceptible organic molecules to react with OH radicals, in the pretreated BI water. Therefore, the remaining NOM can easily breakdown into smaller organic molecules readily assimilable by the bacteria, during the UV/H_2O_2 treatment.

Figure 7.13 shows the molecular weight distribution of NOM for raw CW and BI waters, alum treated water, and after UV fluence of 2000 (mJ/cm^2). As demonstrated, alum treated BI water has a higher amount of organic molecules in the range of low-medium molecular weights (AMW < 1000 Da) in comparison with alum treated CW. This might explain the higher amount of AOC generated during UV/H_2O_2 treatment of alum treated BI compared to alum treated CW. Indeed, it is hypothesized that the availability of higher amounts of smaller organic molecules in alum

treated BI lead to generation of higher amount of AOC. Moreover, the nature of BI and CW NOM are different from one another and hence different behaviors could be observed with respect to their biodegradability at identical conditions.

That being said, as it was discussed earlier in this chapter, HPSEC chromatograms cannot ideally reflect all the characteristics of NOM. Therefore more extended investigation on various types of waters is required to better understand the fate of AOC with respect to the organic carbon concentration and its molecular weight distribution.

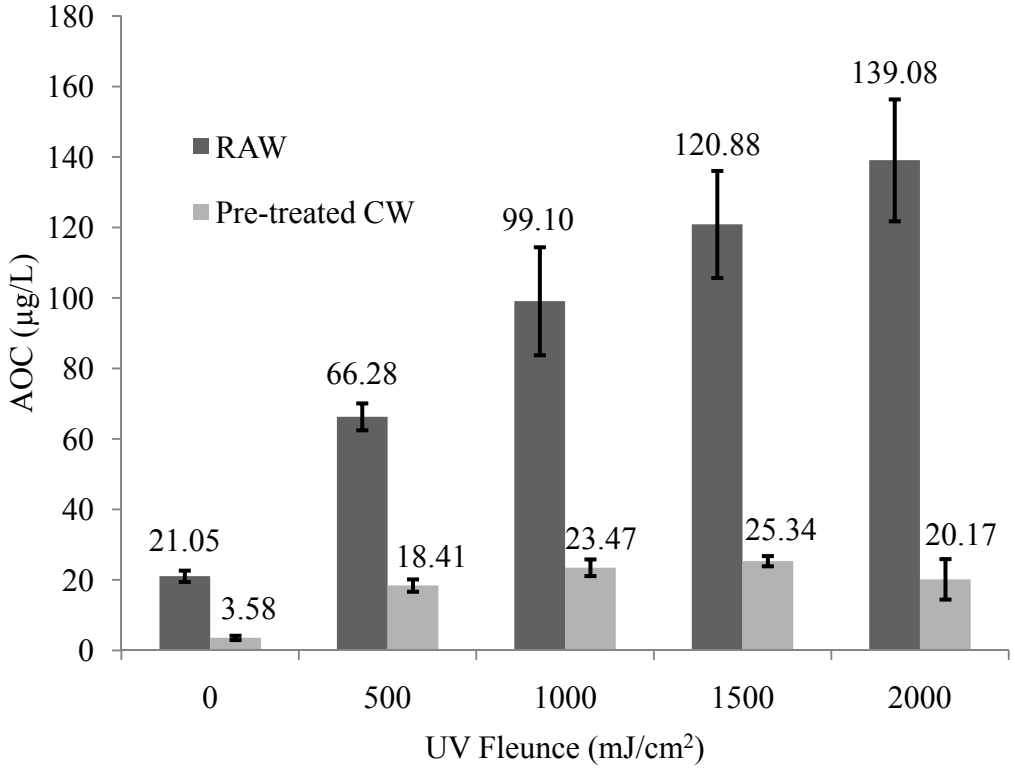

Figure 7.11: Effect of alum coagulation and combined treatment on AOC of CW water

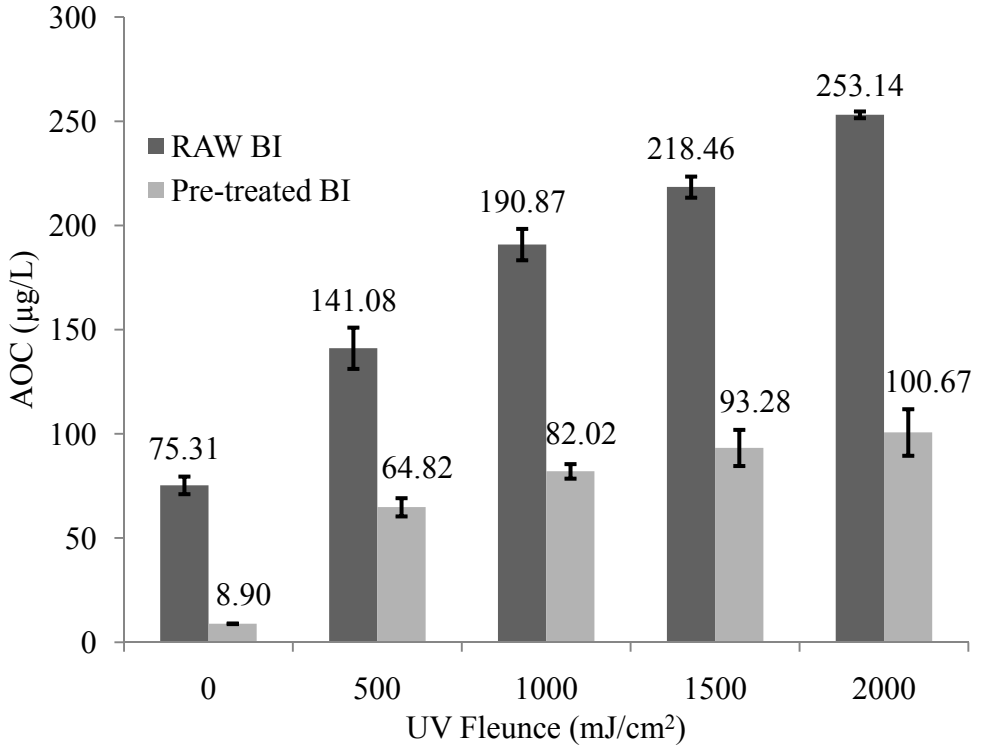

Figure 7.12: Effect of alum coagulation and combined treatment on AOC of BI water

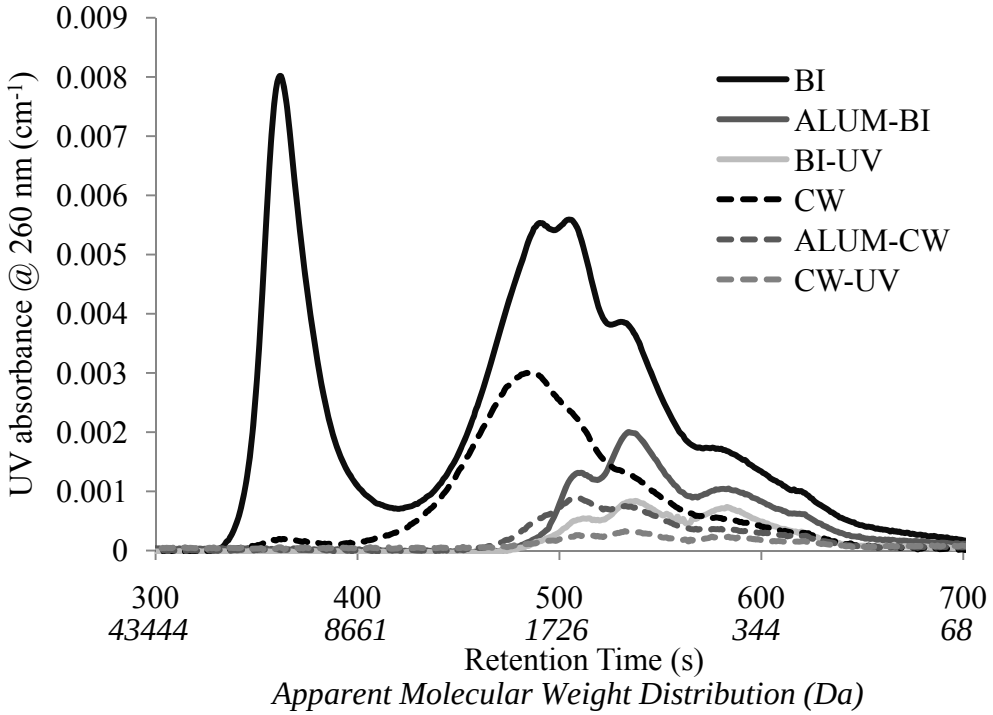

Figure 7.13: Comparison of AMW distribution of NOM for CW and BI waters at different treatment stages

7.7 Highlight and Remarks

The potential of using a pre-treatment process ahead of the UV/H_2O_2 treatment was evaluated in this chapter.

Alum coagulation was shown to be effective in removing a substantial portion of large to medium weight organic molecules. This in turn leads to a considerable increase in the efficacy of the UV/H_2O_2 process in elimination of the target compounds. Moreover, significant (about 75%) electrical energy can be preserved and concerns with undesirable by-products can be reduced.

Elimination of a large portion of NOM by application of alum ahead of the UV/H_2O_2 treatment showed to be very effective in reducing the AOC to about 15-20% of the original value. However, application of the oxidation process (i.e. UV/H_2O_2) still showed to be raising the amount of biodegradable organic molecules. The amount of increase in AOC can vary depending on the nature of the NOM and the treatment conditions.

8 Conclusions and Recommendations for Future Work

8.1 Conclusions

This work investigated the impact of UV/H_2O_2 treatment on biostability of natural and synthetic waters. This goal was achieved by adapting and modifying a previously developed method for AOC quantification and making it applicable to UV/H_2O_2 applications. Further, improving the efficacy of the UV/H_2O_2 treatment was examined by removing NOM ahead of the UV/H_2O_2 process through coagulation. This strategy will not only be beneficial in enhancing the performance of the UV/H_2O_2 treatment, but also lead to a better quality for the finished water.

According to the experimental work and the findings obtained in this study, the following conclusions have been made:

8.1.1 Development of the method for AOC determination of UV/H_2O_2 treated water

1. The flow cytometric method developed by Hammes and Egli (2005) to quantify Assimilable Organic Carbon (AOC) is rapid, straightforward and accurate in enumeration of the bacteria proliferated in water.
2. Residual H_2O_2 (>0.2 ppm) after the UV/H_2O_2 treatment was found to inhibit microorganisms growth leading to incorrect assessment of AOC. Therefore, Immobilized Catalase on SEPABEAD® was used in this study to rapidly and effectively remove H_2O_2 with minimal impact on the original AOC.
3. Inoculum plays a key role in all the AOC bioassays. Utilization of pure cultures (i.e., *P17* and *NOX*) in determination of AOC has been around for the past two decades however, it may result in erroneous estimation of AOC. Therefore, employing a natural consortium obtained from the water will provide a broader range of microorganisms capable of utilization the organic carbon content. The choice of the natural inoculum is also

important, as it may affect the outcome of the AOC bioassay. Results obtained in this study showed that different natural inocula generally yield similar results when they are seeded on an identical water sample. However, variations in AOC determination of some natural waters were observed. Therefore, it is suggested to use an indigenous natural consortium as it is deemed that the bacteria in a specific water sample tend to be the best microorganisms adapted to the carbon source of that water.

4. Addition of mineral buffer solution consisted of phosphate, nitrate, and ammonium ions was found to be instrumental in the bacterial growth. Applying this step is recommended to ensure that carbon is the only substrate limiting the bacterial growth.
5. The buffer capacity of the water was also shown to influence the AOC results. For instance data from using MnO_2 for H_2O_2 removal in Capilano water clearly showed its inhibitory impact on the bacterial growth. However contrary findings were obtained when Evian water was used.

8.1.2 Impact of UV/H_2O_2 process on AOC profile of water

6. Application of UV/H_2O_2 was found to increase the AOC during the commercially applied treatment conditions. This is mainly attributed to the breakdown of larger organic molecules into more small biodegradable organic molecules.
7. Biodegradable Organic Carbon (BDOC) and AOC showed to have correlation in their profiles. However, results obtained in this study indicated slightly different correlations between these two parameters. Therefore, performing more experiments on various water qualities under different treatment processes can help to collect more data and draw more concrete conclusions.
8. Alum coagulation was shown to be effective in removing a substantial portion of large to medium weight organic molecules. This in turn leads to a considerable increase in the

efficacy of the UV/H_2O_2 process in elimination of the target compounds. Moreover, significant (about 75%) electrical energy can be preserved and concerns with undesirable UV/H_2O_2 treatment by-products can be reduced.

9. Alum coagulation showed to be very effective in reducing the AOC to about 15-20% of the original value. However, the portion of NOM recalcitrant to coagulation was found to be still able to support microbial growth.
10. Application of the oxidation process (i.e., UV/H_2O_2) on the pre-treated water still showed to be raising the amount of biodegradable organic molecules. The amount of increase in AOC can vary depending on the nature of the NOM and the treatment conditions.
11. High performance size exclusion chromatography was not inappropriate to predict the biodegradability profile of the organic matter. This can be attributed to the inability of this method in detecting non-UV absorbing small organic species that can potentially promote bacterial activity in water.
12. AOC was found to have a positive direct correlation with the total organic carbon. Waters with higher TOC showed to have higher proportional AOC values.
13. Presence of alkalinity resulted in lower degradation of organic molecules hence lower production of AOC. This is attributed to the scavenging effect of carbonate species representing alkalinity leading to lower degradation of organic molecules.
14. pH was found to have an instrumental effect on the activity and metabolism of microorganisms. Bacteria showed no growth at acidic (pH~5) or basic (pH~ 9.5) solutions artificially made with SR NOM.
15. Chitosan, an organic coagulant from crab shell, was found to be ineffective for removing organic matter in surface water. On the other hand, application of alum showed to be promising in removing a substantial portion of NOM.

8.2 Recommendations for the Future Works

1. Employing a natural consortium as inoculum however results in more realistic interpretation of the AOC but can potentially introduce deviations into the AOC analysis. Therefore, one would prefer to use a standardized natural inoculum that can be accessible worldwide. As suggested in this work and also by Hammed and Egli (2007), Evian mineral water can be used as the reference inoculum. However, more experiments with different water sources around the world should be conducted in order to investigate the diversity in the inoculum and he variance that it may cause in the results of the AOC assay.
2. Pure cultures (i.e., *P17* and *NOX*) could also be used as the standard inoculum in combination with flow cytometry technique. Flow cytometry can be used to enumerate the cells grown when these pure strains are used. Therefore, comparison between the results obtained from the natural inoculum with those from the pure strains when FC is used as the numeration technique will be extremely valuable. Using FC will result in more accurate and rapid enumeration of the cells grown in water.
3. Alum was used in this study as a well established/understood coagulation agent to eliminate organics before UV/H_2O_2 treatment process. Therefore examination of other coagulants such as ploy aluminum chloride (PAC) can provide a better understanding of the NOM behaviour and removal during the coagulation process.
4. Examination of other pre-treatment alternatives can be of interest. For example ion exchange resins and processes may offer suitable pre-treatment alternatives that can remove certain (smaller) fractions of organic matter. This would be of particular interest since it was found that smaller organic molecules are mainly responsible for the formation of AOC during the course of treatment. Therefore, investigating the

performance of ion exchange resins known to effectively remove organics, mainly from medium to small molecular weights, could be valuable.

5. Instead of pre-treatment, application of a post-treatment step could also be effective in increasing the overall efficacy of the process. For instance, filtration processes have a great potential to be implemented ahead and/or after the UV/H_2O_2 treatment. However, feasibility of these processes as pre or post treatment alternatives needs be fully examined and understood.
6. Robustness and flexibility of the combined treatment (i.e., UV/H_2O_2 with pre or post treatment) in removing NOM could be investigated under different water qualities. The findings can be extremely valuable especially when the inlet water quality can be very different for a variety of end-users. Therefore, this can help to design a combined treatment tolerant and flexible to the diversity available in the water quality across the country.
7. Robust calculations and analyses can be performed in order to clearly quantify the impact of combined treatment on the energy consumption of the UV/H_2O_2 treatment process. Moreover, economical analysis should be performed to compare the cost of the combined process where lower energy is used with UV/H_2O_2 process where a single process is operating.

Bibliography

1. Aiken G, Cotsaris E. Soil and hydrology: their effect on NOM: Natural organic matter. *Journal-American Water Works Association*. 1995;87(1):36–45.

2. Allpike BP, Heitz A, Joll CA, et al. Size Exclusion Chromatography To Characterize DOC Removal in Drinking Water Treatment. *Environmental Science & Technology*. 2005;39(7):2334-2342.

3. Alptekin Ö, Tükel SS, YIldIrIm D, Alagöz D. Immobilization of catalase onto Eupergit C and its characterization. *Journal of Molecular Catalysis B: Enzymatic*. 2010;64(3-4):177-183.

4. Alptekin Ö, Tükel SS, YIldIrIm D, Alagöz D. Characterization and properties of catalase immobilized onto controlled pore glass and its application in batch and plug-flow type reactors. *Journal of Molecular Catalysis B: Enzymatic*. 2009;58(1-4):124-131.

5. Andreozzi R, Caprio V, Insola A, Marotta R. Advanced oxidation processes (AOP) for water purification and recovery. *Catalysis Today*. 1999;53(1):51-59.

6. Andrews SA, Huck PM. Using fractionated natural organic matter to study ozonation by-product formation. *Minear, Roger A.; Amy, Gary L.. Disinfection by-products in water treatment: the chemistry of their formation and control. Boca Raton, Lewis Publishers, 1996, p. 411-47 Ilus., tab.* 1996.

7. Angles ML, Chandy J, Kastl G, Jegatheesan V, Cox P, Fisher I. Biofilms in drinking water: influence of organic carbon and disinfection. *Water.* 1999;26:30-33.

8. Berney M, Vital M, Hülshoff I, et al. Rapid, cultivation-independent assessment of microbial viability in drinking water. *Water Research*. 2008;42(14):4010-4018.

9. Betancor L, Hidalgo A, Fernández-Lorente G, et al. Preparation of a stable biocatalyst of bovine liver catalase using immobilization and postimmobilization techniques. *Biotechnol. Prog*. 2003;19(3):763-767.

10. Block J, Mathieu L, Servais P, Fontvieille D, Werner P. Indigenous bacterial inocula for measuring the biodegradable dissolved organic carbon (BDOC) in waters. *Water Research*. 1992;26(4):481-486.

11. Bolto B, Dixon D, Eldridge R, King S, Linge K. Removal of natural organic matter by ion exchange. *Water Research*. 2002;36(20):5057-5065.

12. Bolto B, Dixon D, Eldridge R, King S. Removal of THM precursors by coagulation or ion exchange. *Water Research*. 2002;36(20):5066-5073.

13. Bolton JR. Calculation of ultraviolet fluence rate distributions in an annular reactor: significance of refraction and reflection. *Water Research*. 2000;34(13):3315-3324.

14. Bolton JR, Linden KG. Standardization of Methods for Fluence (UV Dose) Determination in Bench-Scale UV Experiments. *J. Envir. Engrg.* 2003;129(3):209-215.

15. Bolton JR, Stefan MI. Fundamental photochemical approach to the concepts of fluence (UV dose) and electrical energy efficiency in photochemical degradation reactions. *res chem intermed*. 2002;28(7):857-870.

16. Bradford SM, Palmer CJ, Olson BH. Assimilable organic carbon concentrations in Southern California surface and groundwater. *Water Research*. 1994;28(2):427-435.

17. Brehant A, Bonnelye V, Perez M. Comparison of MF/UF pretreatment with conventional filtration prior to RO membranes for surface seawater desalination. *Desalination*. 2002;144(1-3):353-360.

18. Buchanan W, Roddick F, Porter N, Drikas M. Enhanced biodegradability of UV and VUV pre-treated natural organic matter. *Water Science & Technology: Water Supply*. 2004;4(4):103–111.

19. Buxton GV, Greenstock CL, Helman WP, Ross AB. Critical review of rate constants for reactions of hydrated electrons, hydrogen atoms and hydroxyl radicals. *Phys. Chem. Ref. Data*. 1988;17:513–886.

20. Camel V, Bermond A. The use of ozone and associated oxidation processes in drinking water treatment. *Water Research*. 1998;32(11):3208-3222.

21. Cater SR, Stefan MI, Bolton JR, Safarzadeh-Amiri A. UV/H2O2 Treatment of Methyl tert-Butyl Ether in Contaminated Waters. *Environmental Science & Technology*. 2000;34(4):659-662.

22. Chandy JP, Angles ML. Factors Influencing the Development of Biofilms Under Controlled Conditions, CRC for Water Quality and Treatment Research Report No. 20, Sydney Australia. 2004.

23. Charnock C, Kjønnø O. Assimilable organic carbon and biodegradable dissolved organic carbon in Norwegian raw and drinking waters. *Water Research*. 2000;34(10):2629-2642.

24. Chen PH. Removing aquatic organic substances by anion-exchange resin and activated carbon. *Environment International*. 1999;25(5):655-662.

25. Chen C, Zhang X, He W, Lu W, Han H. Comparison of seven kinds of drinking water treatment processes to enhance organic material removal: A pilot test. *Science of The Total Environment*. 2007;382(1):93-102.

26. Chien C, Kao C, Dong C, Chen T, Chen J. Effectiveness of AOC removal by advanced water treatment systems: a case study. *Desalination*. 2007;202(1-3):318-325.

27. Chien CC, Kao CM, Chen CW, Dong CD, Chien HY. Evaluation of biological stability and corrosion potential in drinking water distribution systems: a case study. *Environmental monitoring and assessment*. 2009;153(1):127–138.

28. Chong Soh Y, Roddick F, van Leeuwen J. The impact of alum coagulation on the character, biodegradability and disinfection by-product formation potential of reservoir natural organic matter (NOM) fractions. *Water Science & Technology*. 2008;58(6):1173.

29. Chow CWK, Fabris R, Drikas M, Holmes M. The Impact of Organic Character on Water Treatment Plant Performance. *NOM research: Innovations and Applications for Drinking Water Treatment*, Victor Harbor, Australia (2004).

30. Chow CWK, Fitzgerald F, Holmes M. The Impact of Natural Organic Matter on Disinfection Demand - A Tool to Improve Disinfection Control. *AWA Enviro*, Sydney 2004.

31. Chow CWK, Fabris R, Drikas M. A Rapid Fractionation Technique to Characterise Natural Organic Matter for the Optimisation of Water Treatment Processes. *J Water SRT – Aqua*. 2004; 53(2): 85-92.

32. Chow CWK, Van Leeuwen JA, Drikas M, et al. The impact of the character of natural organic matter in conventional treatment with alum. *Water Science and Technology*. 1999;40(9):97–104.

33. Chow C, Cook D, Drikas M. Evaluation of magnetic ion exchange resin (MIEX®) and alum treatment for formation of disinfection by-products and bacterial regrowth. *Water science and technology: water supply*. 2002:267–274.

34. Clescerl, L.S., Greenberg, A.E., Eaton, A.D. Standard Methods for Examination of Water & Wastewater. American Public Health Association (1999).

35. Collivignarelli C, Sorlini S. AOPs with ozone and UV radiation in drinking water: contaminants removal and effects on disinfection byproducts formation. *Water Sci. Technol*. 2004;49(4):51-56.

36. Cook D, Chow C, Drikas M. Laboratory Study of Conventional Alum Treatment versus MIEX Treatment for Removal of Natural Organic Matter. In: *Proceedings of the 19th Federal AWA Convention, April*.Vol 14.; 2001.

37. Cornelissen ER, Moreau N, Siegers WG, et al. Selection of anionic exchange resins for removal of natural organic matter (NOM) fractions. *Water Res*. 2008;42(1-2):413-423.

38. Crittenden JC, Hu S, Hand DW, Green SA. A kinetic model for H2O2/UV process in a completely mixed batch reactor. *Water research*. 1999;33(10):2315–2328.

39. Christensen, R. Ecojustice's second investigative report into the state of drinking water in Canada, October 2006.

40. Diaz A, Rincon N, Escorihuela A, et al. A preliminary evaluation of turbidity removal by natural coagulants indigenous to Venezuela. *Process Biochemistry*. 1999;35(3-4):391-395.

41. Drikas M, Chow CW, Cook D. The impact of recalcitrant organic character on disinfection stability, trihalomethane formation and bacterial regrowth: An evaluation of magnetic ion exchange resin(MIEX registered) and alum coagulation. *Aqua- Journal of Water Supply: Research and Technology*. 2003;52(7):475–488.

42. Easton J. Measurement and significance of assimilable organic carbon. Report no. FR 0373, Foundation for Water Research, GB, 1993.

43. Escobar IC, Randall AA. Sample storage impact on the assimilable organic carbon (AOC) bioassay. *Water Research*. 2000;34(5):1680-1686.

44. Escobar IC, Randall AA. Assimilable organic carbon (AOC) and biodegradable dissolved organic carbon (BDOC): complementary measurements. *Water Research*. 2001;35(18):4444-4454.

45. Escobar IC, Randall AA, Taylor JS. Bacterial Growth in Distribution Systems: Effect of Assimilable Organic Carbon and Biodegradable Dissolved Organic Carbon. *Environmental Science & Technology*. 2001;35(17):3442-3447.

46. Fabris R, Chow CWK, Drikas M. Practical application of a combined treatment process for removal of recalcitrant NOM- alum and PAC. *Water Science & Technology: Water Supply*. 2004;4(4):89–94.

47. Fearing D, Banks J, Wilson D, et al. NOM control options: the next generation. *Water Science & Technology: Water Supply*. 2004;4(4):139–145.

48. Fearing DA, Banks J, Guyetand S, et al. Combination of ferric and MIEX® for the treatment of a humic rich water. *Water Research*. 2004;38(10):2551-2558.

49. Flaten TP. Aluminium as a risk factor in Alzheimer's disease, with emphasis on drinking water. *Brain Research Bulletin*. 2001;55(2):187-196.

50. Frías J, Ribas F, Lucena F. A method for the measurement of biodegradable organic carbon in waters. *Water Research*. 1992;26(2):255-258.

51. Frías J, Ribas F, Lucena F. Comparison of methods for the measurement of biodegradable organic carbon and assimilable organic carbon in water. *Water Research*. 1995;29(12):2785-2788.

52. Frimmel FH. Characterization of natural organic matter as major constituents in aquatic systems. *Journal of Contaminant Hydrology*. 1998;35(1-3):201-216.

53. Fu PL, Symons JM. Removing aquatic organic substances by anion exchange resins. *Journal-American Water Works Association*. 1990;82(10):70–77.

54. Glaze WH. Drinking-water treatment with ozone. *Environmental Science & Technology*. 1987;21(3):224-230.

55. Glaze WH, Lay Y, Kang JW. Advanced oxidation processes. A kinetic model for the oxidation of 1, 2-dibromo-3-chloropropane in water by the combination of hydrogen

peroxide and UV radiation. *Industrial & Engineering Chemistry Research*. 1995;34(7):2314–2323.

56. Goldstone JV, Pullin MJ, Bertilsson S, Voelker BM. Reactions of hydroxyl radical with humic substances: Bleaching, mineralization, and production of bioavailable carbon substrates. *Environ. Sci. Technol*. 2002;36(3):364–372.

57. Gottschalk C, Libra JA, Saupe A. Ozonation of water and waste water. *Willey-VCH Verlag GmbH, D-69469 Weinheim*. 2000.

58. Graham NJ. Removal of humic substances by oxidation/biofiltration processes -- A review. *Water Science and Technology*. 1999;40(9):141-148.

59. Guzzella L, Feretti D, Monarca S. Advanced oxidation and adsorption technologies for organic micropollutant removal from lake water used as drinking-water supply. *Water Research*. 2002;36(17):4307-4318.

60. Hambsch B, Werner P, Frimmel FH. Bacterial Growth Measurements in Treated Waters from Different Origins (Bakterienvermehrungsmessungen in aufbereiteten Wassern verschiedener Herkunft). *Acta Hydrochimica et Hydrobiologica(Berlin) AHCBAU,* 1992;20(1).

61. Hammes F. A comparison of AOC methods used by the different TECHNEAU partners. *TECHNEAU 06, Deliverable 3.3.10*, June 2008.

62. Hammes FA, Egli T. New Method for Assimilable Organic Carbon Determination Using Flow-Cytometric Enumeration and a Natural Microbial Consortium as Inoculum. *Environmental Science & Technology*. 2005;39(9):3289-3294.

63. Hammes F, Berney M, Vital M, Egli T. A protocol for the determination of total cell concentration of natural microbial communities in drinking water with FCM. *TECHNEAU Report Deliverable 3.3.7*. 2007.

64. Hammes F, Egli T. Cytometric methods for measuring bacteria in water: advantages, pitfalls and applications. *Anal Bioanal Chem*. 2010;397(3):1083-1095.

65. Hammes F, Berney M, Wang Y, et al. Flow-cytometric total bacterial cell counts as a descriptive microbiological parameter for drinking water treatment processes. *Water Research*. 2008;42(1-2):269-277.

66. Hem LJ, Efraimsen H. Assimilable organic carbon in molecular weight fractions of natural organic matter. *Water Research*. 2001;35(4):1106-1110.

67. Hofbauer DEW, Andrews SA. Influence of UV irradiation and UV/hydrogen peroxide oxidation process on natural organic matter fluorescence characteristics. *Water Science & Technology: Water Supply*. 2004;4(4):41–46.

68. Hoigné J, Bader H. The role of hydroxyl radical reactions in ozonation processes in aqueous solutions. *Water Research*. 1976;10(5):377-386.

69. Huck, P.M., Measurement of biodegradable organic matter and bacterial growth in drinking water. J. Am. Water Works Assoc. 1990;82(7):78–86.

70. Huck P, Fedorak P, Anderson W. Biodegradation of aquatic organic matter with reference to drinking water treatment. *Science of The Total Environment*. 1992;117-118:531-541.

71. Humbert H, Gallard H, Suty H, Croué J. Performance of selected anion exchange resins for the treatment of a high DOC content surface water. *Water Research*. 2005;39(9):1699-1708.

72. Humbert H, Gallard H, Jacquemet V, Croué J. Combination of coagulation and ion exchange for the reduction of UF fouling properties of a high DOC content surface water. *Water Research*. 2007;41(17):3803-3811.

73. Ikehata K, El-Din MG, Snyder SA. Ozonation and Advanced Oxidation Treatment of Emerging Organic Pollutants in Water and Wastewater. *Ozone: Science & Engineering: The Journal of the International Ozone Association*. 2008;30(1):21.

74. Jacangelo JG, DeMarco J, Owen DM, Randtke SJ. Selected processes for removing NOM: an overview: Natural organic matter. *Journal-American Water Works Association*. 1995;87(1):64–77.

75. Jago P.H., G. Stanfield, Application of ATP determination to measurement of growth potential in water. Water Res. Centre Report. October 1984.

76. Jürgen-Lohmann DL, Legge RL. Immobilization of bovine catalase in sol-gels. *Enzyme and Microbial Technology*. 2006;39(4):626-633.

77. Kaplan LA, Newbold JD. Measurement of streamwater biodegradable dissolved organic carbon with a plug-flow bioreactor. *Water Research*. 1995;29(12):2696-2706.

78. Kaplan LA, Bott TL, Reasoner DJ. Evaluation and simplification of the assimilable organic carbon nutrient bioassay for bacterial growth in drinking water. *Applied and environmental microbiology*. 1993;59(5):1532.

79. Kaplan LA, Reasoner DJ, Rice EW. A survey of BOM in US drinking wateers. *Journal-American Water Works Association*. 1994;86(2):121–132.

80. Kasahara S, Ishikawa M. Evaluation of assimilable organic carbon in the Yodo River and the effect of coagulation on its control. *Water science and technology: water supply*. 2002:465–472.

81. Kim H, Yu M. Characterization of natural organic matter in conventional water treatment processes for selection of treatment processes focused on DBPs control. *Water Research*. 2005;39(19):4779-4789.

82. Kim WH, Nishijima W, Shoto E, Okada M. Competitive removal of dissolved organic carbon by adsorption and biodegradation on biological activated carbon. *Water Science and Technology*. 1997;35(7):147-153.

83. Kitis M, Kaplan S. Advanced oxidation of natural organic matter using hydrogen peroxide and iron-coated pumice particles. *Chemosphere*. 2007;68(10):1846-1853.

84. Klassen NV, Marchington D, McGowan HC. H2O2 determination by the I3-method and by KMnO4 titration. *Analytical chemistry*. 1994;66(18):2921–2925.

85. Kleiser G, Frimmel FH. Removal of precursors for disinfection by-products (DBPs) -- differences between ozone- and OH-radical-induced oxidation. *The Science of The Total Environment*. 2000;256(1):1-9.

86. Kruithof JC, Masschelein WJ. State-of-the-Art of the Application of Ozonation in BENELUX - Drinking Water Treatment. *Ozone: Science & Engineering: The Journal of the International Ozone Association*. 1999;21(2):139.

87. Kruithof J, Kamp P, Belosevic M. UV/H2O2-treatment: the ultimate solution for pesticide control and disinfection. *Water Supply*. 2002;2(1):113–122.

88. Kruithof JC, Kamp PC, Martijn BJ. UV/H2O2 Treatment: A Practical Solution for Organic Contaminant Control and Primary Disinfection. *Ozone: Science & Engineering: The Journal of the International Ozone Association*. 2007;29(4):273.

89. Lebaron P, Servais P, Agogue H, Courties C, Joux F. Does the High Nucleic Acid Content of Individual Bacterial Cells Allow Us To Discriminate between Active Cells and Inactive Cells in Aquatic Systems? *Appl. Environ. Microbiol.* 2001;67(4):1775-1782.

90. LeChevallier MW. Coliform regrowth in drinking water: a review. *Journal-American Water Works Association*. 1990;82(11):74–86.

91. LeChevallier MW, Babcock TM, Lee RG. Examination and characterization of distribution system biofilms. *Appl. Environ. Microbiol.* 1987;53(12):2714-2724.

92. LeChevallier MW, Norton WD, Lee RG. Giardia and Cryptosporidium spp. in filtered drinking water supplies. *Appl. Environ. Microbiol.* 1991;57(9):2617-2621.

93. LeChevallier MW, Norton WD, Lee RG. Occurrence of Giardia and Cryptosporidium spp. in surface water supplies. *Appl. Environ. Microbiol.* 1991;57(9):2610-2616.

94. LeChevallier MW, Shaw NE, Kaplan LA, Bott TL. Development of a Rapid Assimilable Organic Carbon Method for Water. *Appl Environ Microbiol*. 1993;59(5):1526-1531.

95. LeChevallier M, Welch N, Smith D. Full-scale studies of factors related to coliform regrowth in drinking water. *Appl. Environ. Microbiol.* 1996;62(7):2201-2211.

96. Legrini O, Oliveros E, Braun AM. Photochemical processes for water treatment. *Chemical Reviews*. 1993;93(2):671-698.

97. Lehtola MJ, Miettinen IT, Vartiainen T, Myllykangas T, Martikainen PJ. Microbially available organic carbon, phosphorus, and microbial growth in ozonated drinking water. *Water research*. 2001;35(7):1635–1640.

98. Leiknes T, Ødegaard H, Myklebust H. Removal of natural organic matter (NOM) in drinking water treatment by coagulation-microfiltration using metal membranes. *Journal of Membrane Science*. 2004;242(1-2):47-55.

99. Liang T, Ma J. Impacts of Assimilable Organic Carbon During the Coagulation by Aluminum in Drinking Water. In: *2009 3rd International Conference on Bioinformatics and Biomedical Engineering*. Beijing, China; 2009:1-4.

100. Liu W, Andrews SA, Stefan MI, Bolton JR. Optimal methods for quenching H2O2 residuals prior to UFC testing. *Water Research*. 2003;37(15):3697-3703.

101. Liu W, Wu H, Wang Z, et al. Investigation of assimilable organic carbon (AOC) and bacterial regrowth in drinking water distribution system. *Water research*. 2002;36(4):891–898.

102. Logsdon G, Kohne R, Abel S, LaBonde S. Slow sand filtration for small water systems. *J. Environ. Eng. Sci.* 2002;1(5):339-348.

103. Maclean RG, Prévost M, Coallier J, Duchesne D, Mailly J. Thiosulfate interference in the biodegradable dissolved organic carbon assay. *Water Research*. 1996;30(8):1858-1864.

104. Mateo C, Abian O, Fernandez-Lorente G, et al. Epoxy Sepabeads: A Novel Epoxy Support for Stabilization of Industrial Enzymes via Very Intense Multipoint Covalent Attachment. *Biotechnol. Prog.* 2002;18(3):629-634.

105. Mateo C, Torres R, Fernández-Lorente G, et al. Epoxy-Amino Groups: A New Tool for Improved Immobilization of Proteins by the Epoxy Method. *Biomacromolecules*. 2003;4(3):772-777.

106. Matilainen A, Lindqvist N, Korhonen S, Tuhkanen T. Removal of NOM in the different stages of the water treatment process. *Environment International*. 2002;28(6):457-465.

107. McLachlan DRC, Bergeron C, Smith JE, Boomer D, Rifat SL. Risk for neuropathologically confirmed Alzheimer's disease and residual aluminum in municipal drinking water employing weighted residential histories. *Neurology*. 1996;46(2):401.

108. Mijatovic I, Matosic M, Hajduk Cerneha B, Bratulic D. Removal of natural organic matter by ultrafiltration and nanofiltration for drinking water production. *Desalination*. 2004;169(3):223-230.

109. Miller RG, Kopjleer FC, Kelty KC, Stober JA, Ulmer NS. The occurrence of aluminum in drinking water. *ilj*. 1984;186:205.

110. Murray CA, Parsons SA. Removal of NOM from drinking water: Fenton's and photo-Fenton's processes. *Chemosphere*. 2004;54(7):1017-1023.

111. Neef A, Zaglauer A, Meier H, et al. Population analysis in a denitrifying sand filter: conventional and in situ identification of Paracoccus spp. in methanol-fed biofilms. *Appl. Environ. Microbiol.* 1996;62(12):4329-4339.

112. Newcombe G, Cook D. Influences on the removal of tastes and odours by PAC. *Aqua*. 2002;51:463–474.

113. Newcombe G, MORISON J, Hepplewhite C, Knappe DRU. In the (adsorption) competition between NOM and MIB, who is the winner, and why? *Water science and technology: water supply*. 2002:59–67.

114. Newcombe G, Morrison J, Hepplewhite C, Knappe DRU. Simultaneous adsorption of MIB and NOM onto activated carbon:: II. Competitive effects. *Carbon*. 2002;40(12):2147–2156.

115. Newcombe G, Morrison J, Hepplewhite C. Simultaneous adsorption of MIB and NOM onto activated carbon. I. Characterisation of the system and NOM adsorption. *Carbon*. 2002;40(12):2135–2146.

116. Nikolaou AD, Lekkas TD. The role of natural organic matter during formation of chlorination by-products: A review. *Acta hydrochimica et hydrobiologica*. 2001;29(2-3):63–77.

117. Nishijima W, Speitel GE. Fate of biodegradable dissolved organic carbon produced by ozonation on biological activated carbon. *Chemosphere*. 2004;56(2):113-119.

118. Park N, Kwon B, Sun M, et al. Application of various membranes to remove NOM typically occurring in Korea with respect to DBP, AOC and transport parameters. *Desalination*. 2005;178(1-3):161-169.

119. Parsons, S.A. and Byrne, A. Water treatment applications. In: Advanced Oxidation Processes for Water and Wastewater Treatment. Parsons, S. (Ed.). IWA. 2004.

120. Pelekani C, Newcombe G, Snoeyink VL, et al. Characterization of Natural Organic Matter Using High Performance Size Exclusion Chromatography. *Environmental Science & Technology*. 1999;33(16):2807-2813.

121. Pereira VJ, Linden KG, Weinberg HS. Evaluation of UV irradiation for photolytic and oxidative degradation of pharmaceutical compounds in water. *Water Research*. 2007;41(19):4413-4423.

122. Philibert M, Bush S, Rosario-Ortiz F. Advances in the characterization of the polarity of DOM under ambient water quality conditions using the polarity rapid assessment method. 2008.

123. Plumlee MH, López-Mesas M, Heidlberger A, Ishida KP, Reinhard M. N-nitrosodimethylamine (NDMA) removal by reverse osmosis and UV treatment and analysis via LC-MS/MS. *Water Res*. 2008;42(1-2):347-55.

124. Rahn RO. Potassium Iodide as a Chemical Actinometer for 254 nm Radiation: Use of Iodate as an Electron Scavenger. *Photochemistry and Photobiology*. 1997;66(4):450–455.

125. Rahn RO, Bolton J, Stefan MI. The Iodide/Iodate Actinometer in UV Disinfection: Determination of the Fluence Rate Distribution in UV Reactors. *Photochemistry and photobiology*. 2006;82(2):611–615.

126. Ribas F, Frías J, Huguet JM, Lucena F. Efficiency of various water treatment processes in the removal of biodegradable and refractory organic matter. *Water Research*. 1997;31(3):639-649.

127. Rittmann BE. Achieving biologically stable drinking water. *Journal of the American Water Works Association*. 1984;76(10):106.

128. Rizzo L, Di Gennaro A, Gallo M, Belgiorno V. Coagulation/chlorination of surface water: A comparison between chitosan and metal salts. *Separation and Purification Technology*. 2008;62(1):79–85.

129. Rosario-Ortiz FL, Snyder S, Suffet IH. Characterization of the polarity of natural organic matter under ambient conditions by the polarity rapid assessment method (PRAM). *Environ. Sci. Technol*. 2007;41(14):4895–4900.

130. Rosenfeldt EJ, Linden KG. Degradation of endocrine disrupting chemicals bisphenol A, ethinyl estradiol, and estradiol during UV photolysis and advanced oxidation processes. *Environ. Sci. Technol*. 2004;38(20):5476–5483.

131. Rosenfeldt EJ, Melcher B, Linden KG. UV and UV/H2O2 treatment of methylisoborneol (MIB) and geosmin in water. *Journal of water supply: research and technology. AQUA*. 2005;54(7):423–434.

132. Sarathy, S.R., Effect of UV/H_2O_2 Advanced Oxidation on Physical and Chemical Characteristics of Natural Organic Matter in Raw Drinking Water Sources, A thesis submitted in partial fulfillment of the requirements for the degree of Doctor of Philosophy in the faculty of graduate studies (chemical and biological engineering), University of British Columbia. 2009.

133. Sarathy, S.R.; Mohseni, M. An overview of UV-based advanced oxidation processes for drinking water treatment. *IUVA News*. 2006; 8: 16-27.

134. Sarathy SR, Mohseni M. The Impact of UV/H2O2 Advanced Oxidation on Molecular Size Distribution of Chromophoric Natural Organic Matter. *Environmental Science & Technology*. 2007;41(24):8315-8320.

135. Sarathy S, Mohseni M. The fate of natural organic matter during UV/H2O2 advanced oxidation of drinking water. *Canadian Journal of Civil Engineering*. 2009;36(1):160–169.

136. Sathasivan A, Ohgaki S. Application of new bacterial regrowth potential method for water distribution system - a clear evidence of phosphorus limitation. *Water Research*. 1999;33(1):137-144.

137. Selmer-Olsen E, Ratnaweera H, Pehrson R. A novel treatment process for dairy wastewater with chitosan produced from shrimp-shell waste. *Water Science and Technology*. 1996;34(11):33-40.

138. Servais P, Billen G, Hascoët M. Determination of the biodegradable fraction of dissolved organic matter in waters. *Water Research*. 1987;21(4):445-450.

139. Servais P, Anzil A, Ventresque C. Simple Method for Determination of Biodegradable Dissolved Organic Carbon in Water. *Appl. Environ. Microbiol.* 1989;55(10):2732-2734.

140. Servais P, Barillier A, Garnier J. Determination of the biodegradable fraction of dissolved and particulate organic carbon in waters. In: *Annales de Limnologie-International Journal of Limnology*.Vol 31.; 1995:75–80.

141. Sheldon RA. Enzyme immobilization: the quest for optimum performance. *Advanced Synthesis & Catalysis*. 2007;349(8-9):1289–1307.

142. Silvestry-Rodriguez N, Sicairos-Ruelas EE, Gerba CP, Bright KR. Silver as a disinfectant. *Reviews of environmental contamination and toxicology*. 2007:23–45.

143. Singer PC. Humic substances as precursors for potentially harmful disinfection by-products. *Water Science and Technology*. 1999;40(9):25–30.

144. Singer PC, Bilyk K. Enhanced coagulation using a magnetic ion exchange resin. *Water Research*. 2002;36(16):4009-4022.

145. Song W, Ravindran V, Pirbazari M. Process optimization using a kinetic model for the ultraviolet radiation-hydrogen peroxide decomposition of natural and synthetic organic compounds in groundwater. *Chemical Engineering Science*. 2008;63(12):3249-3270.

146. Speitel GE, Symons JM, Mialaret JM, Wanielista MM. AOP/biofilm processes for DOX precursors. *Journal-American Water Works Association*. 2000;92(10):59–73.

147. Stainfield G., Jago P. H. The development and use of a method for measuring the concentration of assimilable organic carbon in water. WRC Environment Report, RU 1628-M, Manheim, UK. 1987.

148. Stefan M, Bolton J. UV Direct Photolysis of N-Nitrosodimethylamine (NDMA): Kinetic and Product Study. *HCA*. 2002;85(5):1416.

149. Stefan MI, Bolton JR. Fundamental approach to the fluence-based kinetic and electrical energy efficiency parameters in photochemical degradation reactions: polychromatic light. *J. Environ. Eng. Sci.* 2005;4(S1):S13-S18.

150. Stefan MI, Hoy AR, Bolton JR. Kinetics and mechanism of the degradation and mineralization of acetone in dilute aqueous solution sensitized by the UV photolysis of hydrogen peroxide. *Environ. Sci. Technol*. 1996;30(7):2382–2390.

151. Stefan MI, Mack J, Bolton JR. Degradation pathways during the treatment of methyl tert-butyl ether by the UV/H2O2 process. *Environ. Sci. Technol*. 2000;34(4):650–658.

152. Suty H, De Traversay C, Cost M. Applications of advanced oxidation processes: present and future. *Water Science and Technology*. 2004;49(4):227–233.

153. Swaim P, Royce A, Smith T, et al. Effectiveness of UV - Advanced Oxidation for Destruction of Micro-Pollutants. *Ozone: Science & Engineering: The Journal of the International Ozone Association*. 2008;30(1):34.

154. Thomson J, Parkinson A, Roddick FA. Depolymerization of Chromophoric Natural Organic Matter. *Environmental Science & Technology*. 2004;38(12):3360-3369.

155. Thurman EM. *Organic geochemistry of natural waters*. Springer; 1985.

156. Toor, R., UV/H_2O_2 based advanced oxidation of drinking water for disinfection by-product control, A thesis submitted in partial fulfillment of the requirements for the degree of Master of Applied Science in the faculty of graduate studies (chemical and biological engineering), University of British Columbia. 2005.

157. Toor R, Mohseni M. UV-H2O2 based AOP and its integration with biological activated carbon treatment for DBP reduction in drinking water. *Chemosphere*. 2007;66(11):2087-2095.

158. Torres R, Mateo C, Fernandez-Lorente G, et al. A Novel Heterofunctional Epoxy-Amino Sepabeads for a New Enzyme Immobilization Protocol: Immobilization-Stabilization of β-Galactosidase from Aspergillus oryzae. *Biotechnol. Prog.* 2003;19(3):1056-1060.

159. T.A. Tuhkanen, UV/H_2O_2 processes. In: S. Parsons, Editor, Advanced Oxidation Processes for Water and Wasterwater Treatment, IWA Publishing, London, UK (2004), pp. 86–110.

160. Tukel S, Alptekin O. Immobilization and kinetics of catalase onto magnesium silicate. *Process Biochemistry*. 2004;39(12):2149-2155.

161. Uyak V, Toroz I. Disinfection by-product precursors reduction by various coagulation techniques in Istanbul water supplies. *Journal of Hazardous Materials*. 2007;141(1):320-328.

162. Van der Kooij D. Assimilable organic carbon (AOC) in drinking water. In: McFeters GA, editor. *Drinking Water Microbiology*. New York: Springer; 1990: 57–87.

163. Van der Kooij D. Assimilable organic carbon as an indicator of bacterial regrowth. *Journal of the American Water Works Association*. 1992;84(2):57–65.

164. Van der Kooij D. Effect of Treatment on Assimilable Organic Carbon in Drinking Water. 1987.

165. Van der Kooij D. Biological stability: a multidimensional quality aspect of treated water. *Water, Air, & Soil Pollution*. 2000;123(1):25–34.

166. Van der Kooij, D. Assimilable Organic Carbon (AOC) in Treated Water: Determination and Significance. *In Encyclopedia of Environmental Microbiology*; Bitton, G., Ed.; John Wiley & Sons: Hoboken, NJ, 2002; 312-327.

167. Van der Kooij D, Hijnen WAM. Substrate Utilization by an Oxalate-Consuming Spirillum Species in Relation to Its Growth in Ozonated Water. *Appl. Environ. Microbiol.* 1984;47(3):551-559.

168. Van der Kooij D, Visser A, Hijnen WAM. Determining the concentration of easily assimilable organic carbon in drinking water. *Journal American Water Works Association*. 1982;74(10):540–545.

169. Van Leeuwen, J., Chow, C., Fabris, R., Drikas, M., Spark, K. Enhanced Coagulation for Dissolved Organic Carbon Removal in Conventional Treatment with Alum, *Proceedings of the 18th Federal Convention*, April 11-14, 1999, AWWA, Adelaide.

170. Vasudevan P, Weiland R. Studies on the morphology of immobilized catalase. *The Chemical Engineering Journal and the Biochemical Engineering Journal*. 1994;55(1-2):B41-B45.

171. Vera-Avila L, Morales-Zamudio E, Garcia-Camacho M. Activity and Reusability of Sol-Gel Encapsulated -Amylase and Catalase. Performance in Flow-Through Systems. *Journal of Sol-Gel Science and Technology*. 2004;30(3):197-204.

172. Volk CJ, LeChevallier MW. Assessing biodegradable organic matter. *Journal American Water Works Association*. 2000;92(5):64–76.

173. Volk C, Renner C, Robert C, Joret JC. Comparison of two techniques for measuring biodegradable dissolved organic carbon in water. *Environmental Technology*. 1994;15(6):545.

174. Volk C, Roche P, Joret J, Paillard H. Comparison of the effect of ozone, ozone-hydrogen peroxide system and catalytic ozone on the biodegradable organic matter of a fulvic acid solution. *Water Research*. 1997;31(3):650-656.

175. von Gunten U. Ozonation of drinking water: part I. Oxidation kinetics and product formation. *Water Res*. 2003;37(7):1443-1467.

176. von Gunten U. Ozonation of drinking water: part II. Disinfection and by-product formation in presence of bromide, iodide or chlorine. *Water Res*. 2003;37(7):1469-1487.

177. Wang G, Hsieh S, Hong C. Destruction of humic acid in water by UV light--catalyzed oxidation with hydrogen peroxide. *Water Research*. 2000;34(15):3882-3887.

178. Werner, P. Eine Methode zur Bestimmumg der Verkeimungsneigung von Trinkwasser, Vom Wasser. 1985;65, 257-270.

179. Werner P., Hambsch B. Investigations on the growth of bacteria in drinking water, *Wat. Supply*. 1986;4:227–232.

180. Westerhoff P, Aiken G, Amy G, Debroux J. Relationships between the structure of natural organic matter and its reactivity towards molecular ozone and hydroxyl radicals. *Water Research*. 1999;33(10):2265-2276.

181. Westerhoff P, Mezyk SP, Cooper WJ, Minakata D. Electron pulse radiolysis determination of hydroxyl radical rate constants with Suwannee River fulvic acid and other dissolved organic matter isolates. *Environ. Sci. Technol*. 2007;41(13):4640-4646.

182. Xiangli Q, Zhenjia Z, Nongcun W, et al. Coagulation pretreatment for a large-scale ultrafiltration process treating water from the Taihu River. *Desalination*. 2008;230(1-3):305-313.

183. Yao K, Habibian MT, O'Melia CR. Water and waste water filtration. Concepts and applications. *Environmental Science & Technology*. 1971;5(11):1105-1112.

184. Yavich AA, Lee K, Chen K, Pape L, Masten SJ. Evaluation of biodegradability of NOM after ozonation. *Water Research*. 2004;38(12):2839-2846.

185. Yee LF, Abdullah MP, Ata S, Ishak B. Dissolved Organic Matter and its impact on the chorine demand of treated water. *Malaysian Journal of Analytical Sciences*. 2006;10(2):243–250.

186. Yoon D, Won K, Kim Y, et al. Continuous removal of hydrogen peroxide with immobilised catalase for wastewater reuse. *Water Science & Technology*. 2007;55(1-2):27.

Appendix A Modeling the Transformation of Chromophoric Natural Organic Matter during UV/H_2O_2 Advanced Oxidation

An identical version of the following appendix A has been submitted to the Journal of Environmental Engineering for the final review. My contribution to this work was writing and debugging the programming code, and providing the model predicted results. Dr. Siva Sarathy developed the model equations and collected and analyzed the data in addition to writing the manuscript.

Authors: Siva R. Sarathy[2], Mohammad M. Bazri[3], and Madjid Mohseni[4]

This research developed a dynamic kinetic model to predict the partial degradation of natural organic matter (NOM) during ultraviolet plus hydrogen peroxide (UV/H_2O_2) advanced oxidation treatment. The absorbance of 254nm UV, representing chromophoric NOM (CNOM) was used as a surrogate to track the degradation of NOM. To obtain reaction rate constants not available in literature, i.e., reactions between hydroxyl radical ($^{\bullet}OH$) and NOM, experiments were conducted with "synthetic" water using isolated Suwannee River NOM and parameter estimation was applied to obtain the unknown model parameters. The model was evaluated on two natural waters to predict the degradation of CNOM and H_2O_2 during UV/H_2O_2 treatment. Model predictions of CNOM degradation agreed well with the experimental results for UV/H_2O_2 treatment of the natural waters, with errors up to 6%. For the natural water with additional alkalinity, the model also predicted well the slower degradation of CNOM during UV/H_2O_2 treatment, due to scavenging of $^{\bullet}OH$ by carbonate species. The model, however, under predicted the degradation of H_2O_2 suggesting that, when NOM is present, mechanisms besides the photolysis of H_2O_2 contribute appreciably to H_2O_2 degradation.

Subject headings: water treatment, surface water, drinking water, models, ultraviolet radiation, hydrogen peroxide

[2] - Research Scientist, Trojan Technologies, London, ON N5V 4T7 Canada; ssarathy@trojanuv.com
[3] - MASc Candidate, Department of Chemical and Biological Engineering, University of British Columbia, 2360 East Mall, Vancouver, BC V6T 1Z3 Canada; mbazri@chbe.ubc.ca
[4] - Professor, Department of Chemical and Biological Engineering, University of British Columbia, 2360 East Mall, Vancouver, BC V6T 1Z3 Canada; mmohseni@chbe.ubc.ca

Introduction

Designing a UV/H_2O_2 system for a practical application necessitates the prediction of H_2O_2 concentration and fluence requirements to achieve the desired levels of contaminant removal (Tühkanen 2004). There are a number of mathematical models describing the UV/H_2O_2 advanced oxidation (Glaze et al. 1995; Liao and Gurol 1995; Crittenden et al. 1999; Stefan et al. 2000; Sharpless and Linden 2004; Song et al. 2008). Some of these models use a pseudo-steady-state assumption for the concentration of hydroxyl radicals ($^{\bullet}OH$), assuming that the net formation of $^{\bullet}OH$ is zero (Glaze et al. 1995; Liao and Gurol 1995; Stefan et al. 2000), while others assume all species, including radicals, to be dynamic (Crittenden et al. 1999; Song et al. 2008). While the pseudo-steady-state assumption is a safe simplification, since $^{\bullet}OH$ reacts rapidly with many species and the concentration of $^{\bullet}OH$ is very low and will not accumulate over time (Linden et al. 2007), a dynamic model is a better descriptor of actual system behavior.

Some of the existing models incorporate the $^{\bullet}OH$ scavenging potential of natural organic matter (NOM) (Liao and Gurol 1995; Crittenden et al. 1999; Sharpless and Linden 2004) while only one models the degradation of NOM (Song et al. 2008). However, Song et al. (2008) primarily targeted the mineralization of NOM and so, did not address the partial degradation of NOM that occurs under practical operating conditions. In commercial drinking water UV/H_2O_2 applications, the oxidation conditions (i.e., fluence and/or H_2O_2 concentration) are not strong enough to mineralize NOM. Instead, partial oxidation of NOM takes place, leading to constantly changing water characteristics that in turn affect process efficacy and water quality (Sarathy and Mohseni 2007, 2009). For example, reduction in the absorbance of water at 254nm UV would lead to the increased photolysis of H_2O_2, thereby increasing the rate of $^{\bullet}OH$ production.

The focus of this research was to develop a dynamic kinetic model that predicts partial degradation of NOM by incorporating a surrogate parameter, the absorbance of 254nm UV, representing structural transformation of NOM attributable to $^{\bullet}OH$ attack. The portion of NOM that absorbs at 254nm has been defined as chromophoric NOM (CNOM). The model was developed using literature obtained reaction schemes and kinetic rate constants. To obtain reaction rate constants not available in the literature (i.e., reactions between $^{\bullet}OH$ and NOM), experiments were conducted with "synthetic" water using isolated Suwannee River NOM and parameter estimation was applied to obtain the unknown model parameters. Subsequently, the model, using the literature and estimated rate constants, was evaluated on two natural waters in order to predict the degradation of CNOM and H_2O_2 during UV/H_2O_2 treatment. Further, the

natural waters were amended with additional alkalinity and treated in order to elucidate the impact of alkalinity on CNOM and H_2O_2 degradation.

Materials and Methods

Waters.

"Synthetic" water was created to empirically estimate model parameters. Suwannee River Aquatic NOM (SRNOM-aquatic) (International Humic Substance Society) was added to ultrapure water (Millipore) at varying concentrations. A detailed description of the source of SRNOM-aquatic isolate as well as its chemical properties and the isolation method are available from the International Humic Substances Society. Total organic carbon (TOC) concentration was used as a surrogate to quantify NOM. Table A.1 summarizes the properties of the synthetic waters prepared.

The source of the first surface water, Capilano Water (CW), was the Capilano Reservoir which serves the Greater Vancouver Region, British Columbia, Canada. The second source, Trepanier Water (TW), originated from Trepanier Creek, providing drinking water for the town of Peachland, British Columbia, Canada. The alkalinity of both CW and TW was modified by the addition of sodium bicarbonate (ACS Grade, Fisher Scientific). The characteristics of raw CW and TW are provided in Table A.1.

Advanced Oxidation Treatment.

A collimated beam apparatus, exactly as described in Sarathy and Mohseni (2007) was employed for the batch UV/H_2O_2 studies. The water was irradiated and samples were taken at various intervals from 0 to 150 minutes, corresponding to a fluence range up to 2000 mJ cm^{-2}. H_2O_2 (30%, Fisher Scientific) was added initially to the water at the desired concentrations. H_2O_2 containing samples were quenched of H_2O_2 using 0.2 mg L^{-1} bovine liver catalase (lyophilized powder, ≥10,000 units mg^{-1} protein, Sigma Aldrich) prior to absorbance and TOC measurements.

Analytical Methods.

The incident fluence rate (E_P°) was determined using iodide/iodate actinometry exactly as described in Sarathy and Mohseni (2007). In some cases, a calibrated radiometer (IL1700, sensor SED240 for 254nm, International Light Inc.) was used to determine E_P° following the standardized method for fluence determination (Bolton and Linden, 2003). H_2O_2 concentration

was measured by reaction with iodide catalyzed by molybdate (Klassen et al. 1994). TOC was measured using a TOC analyzer (Shimadzu TOC-VCPH or Sievers 900). Absorbance measurements were determined using a UV-Vis spectrophotometer (Shimadzu UV-Mini 1240 or Cary 100) with 1cm quartz cuvette (Hellma). Alkalinity was measured according to the Standard Method 2320 (Clescerl et al. 1999).

4-chloro-benzoic acid (pCBA) was detected using a Waters 600-MS HPLC equipped with Waters 996 photodiode array detector, Waters 717 plus autosampler, and Supelcosil LC-18 column. The eluent consisted of 0.5% H_2PO_4 and acetonitrile, at a ratio of 52%:48%, and was run at a column flowrate of 1.5 mL min^{-1}. The quantification wavelength for pCBA was at 238 nm.

The procedure for hydrophobic/hydrophilic fractionation was based on the rapid fractionation technique published by Chow et al. (2004). Two resins, Supelite DAX-8 (Supelco) and Amberlite XAD-4 (Supelco) were used in series to separate the NOM into three fractions: (i) very hydrophobic acids (VHA), (ii) slightly hydrophobic acids (SHA), and (iii) charged plus neutral hydrophilic (CHA+NEU).

Kinetic Modeling Approach, Reaction Scheme, and Governing Rate Expressions.

A dynamic kinetic model for the UV/H_2O_2 process was developed for predicting CNOM changes over time, H_2O_2/HO_2^-, carbonate species (HCO_3^-/CO_3^{2-}), pCBA (the ·OH probe employed), and radical species (·OH, $O_2^{\cdot-}/HO_2^{\cdot}$, $CO_3^{\cdot-}$). The approach taken closely followed that of UV/H_2O_2 models developed previously by other researchers (Glaze et al. 1995; Liao and Gurol 1995; Crittenden et al. 1999; Stefan et al. 2000; Sharpless and Linden 2003; Song et al. 2008). Table A.2 provides a summary of the reactions defined for the system along with the literature reaction rate constants used. Based on the reactions in Table A.2, the overall kinetic rate expressions were defined by the ordinary differential equations given in Table A.3.

The first term in Equation [1] (Table A.3) represents the rate of photolysis of H_2O_2 which is dependent on the primary quantum yield of H_2O_2, $\Phi_{H_2O_2,\cdot OH}$, in Reaction 1 equal to 0.5 and the specific rate of light absorption by H_2O_2 at 254 nm, $k_{a,H_2O_2,254}$ (Es mol^{-1}). The specific rate of light adsorption by H_2O_2 is defined by Equation [A1] (Sharpless and Linden 2003).

$$[\boldsymbol{A1}] \qquad \boldsymbol{k_{a,H_2O_2,254} = \frac{E_P^{\circ}\varepsilon_{H_2O_2(254)}[1 - 10^{-A_{total,254}z}] \times 1000}{A_{total,254}z}}$$

$$[A2] \qquad A_{total,254} = [\mathbf{H_2O_2}]\varepsilon_{H_2O_2,254} + [\mathbf{CNOM}]\varepsilon_{CNOM}$$

In Equation [A1], E_P° is the incident photon fluence rate (Es cm^{-2} s^{-1}), z is the path-length, and $A_{total,254}$ is the total water absorption coefficient at 254 nm (cm^{-1}). $A_{total,254}$ is defined by Equation [A2] where $\varepsilon_{H_2O_2,254}$ is the decadic molar absorption coefficient of H_2O_2 at 254 nm (19.6 L^{-1} mol^{-1} cm^{-1}), and ε_{CNOM} is the decadic molar absorption coefficient of CNOM. By definition CNOM only absorbs UV at 254 nm, so the absorption coefficient for CNOM, A_{CNOM} (cm^{-1}), is defined by Equation [A3].

$$[A3] \qquad A_{CNOM} = [\mathrm{CNOM}]\varepsilon_{CNOM}$$

As with the models developed by Crittenden et al. (1999) and Song et al. (2008), the model developed in this study was dynamic for all radical species present within the system as defined by Equations [3-6] (Table A.3). In Equation [3], the first ten terms represent the scavenging of $^{\bullet}OH$ in the system. All the major scavengers have been incorporated including NOM (represented as TOC), carbonates, H_2O_2, and pCBA. Note that although the model included the reaction between CNOM and $^{\bullet}OH$ (Reaction 26), CNOM need not be included in Equation [3] as one of the scavenging terms since CNOM is a subset of NOM. The last three terms in Equation [3] represent the generation of $^{\bullet}OH$.

Species contributing to alkalinity, namely bicarbonate and carbonate, are present in most natural waters and are major scavengers of $^{\bullet}OH$ (Reactions 4 and 5), thus these reactions have been included in the model by Equations [7] and [8].

In Equation [9] pCBA, the $^{\bullet}OH$ probe, could be substituted with any organic contaminant. Further, additional organic contaminants could be added to this model easily. pCBA is predominantly degraded by $^{\bullet}OH$ so its reaction with other species is neglected. Also, the direct photolysis of pCBA at 254 nm is negligible so is not included in this model. Of course, if pCBA was substituted with another compound that is photolyzed at 254 nm and/or reacts with other free radicals, the kinetic rate expressions would require modification to include the necessary terms.

As defined by Reaction 26 and Equation [10], CNOM was assumed to be degraded by $^{\bullet}OH$ only. Direct photolysis of CNOM was neglected since prior experimental results demonstrated that when treatment was conducted in the absence of H_2O_2 (i.e., only UV irradiation), there was

no reduction in CNOM (Sarathy and Mohseni 2007). Thus, under the irradiation conditions (i.e., incident photon fluence rate and irradiation time) implemented in this study, degradation of CNOM by photolysis is negligible.

As mineralisation of raw water TOC had previously not been observed under the irradiation conditions implemented in this study (Sarathy and Mohseni 2007, 2009), this model assumes TOC was constant over the duration of the treatment.

Experimental Approach for Parameter Estimation.

Controlled experiments were conducted to gather data for estimating the two unknown reaction rate constants, $k_{\cdot OH,CNOM}$ (L mg^{-1} s^{-1}) and $k_{\cdot OH,TOC}$ (L mol^{-1} s^{-1}). Experiments were conducted with SRNOM-aquatic synthetic water with TOC levels of 1.33, 2.21, and 3.08 mg L^{-1} and initial H_2O_2 concentration levels of approximately 5 and 15 mg L^{-1}. For each experiment E_P° was 6.42E-10 Es cm^{-2} s^{-1} and pCBA was added initially at a concentration of approximately 200 µg L^{-1}. The water was then irradiated for 150 minutes with measurements of pCBA taken every 15 minutes and measurements of H_2O_2 and CNOM taken every 30 minutes.

In these experiments, pCBA served as an $^{\bullet}OH$ probe so, by monitoring the concentration of pCBA, competition kinetics was used to estimate the reaction rate constant for the reaction between $^{\bullet}OH$ and TOC, $k_{\cdot OH,TOC}$. Thus, experimentally monitored was the relationship represented in Equation [A4] where k'_{pCBA} is the apparent reaction rate constant for the reduction of pCBA (s^{-1}).

$$[A4] \qquad \frac{d[\mathrm{pCBA}]}{dt} = -k'_{\mathrm{pCBA}}[\mathrm{pCBA}]$$

pCBA only reacted with $^{\bullet}OH$ so Equation [A4] can be written as Equation [9] (Table A.3). As $k_{\cdot OH,pCBA}$ was known, 5E9 L mol^{-1} s^{-1} (Neta and Dorfman 1968), the $^{\bullet}OH$ concentration was responsible for the measured k'_{pCBA}. Thus, the unknown component in Equation [3], i.e., $k_{\cdot OH,TOC}$, could be estimated based on the experimental measurement of pCBA.

Since it was not possible to measure the molar concentration of CNOM and ε_{CNOM} is unknown, A_{CNOM} was measured as it was the absorbance coefficient of the water at 254 nm after H_2O_2 was quenched. A_{CNOM} was used for the estimation of $k_{\cdot OH,CNOM}$. Thus, experimentally monitored was the relationship represented by Equation [A5] where $k'_{A_{CNOM}}$ is the apparent reaction rate constant for the reduction in A_{CNOM} (s^{-1}).

$$[A5] \qquad \frac{dA_{CNOM}}{dt} = -k'_{A_{CNOM}} A_{CNOM}$$

By definition in Equation [A3] A_{CNOM} is directly proportional to the molar concentration of CNOM by an unknown factor of ε_{CNOM}. Therefore, Equation [A5] can be written as Equation [A6].

$$[A6] \qquad \varepsilon_{CNOM} \frac{d[\text{CNOM}]}{dt} = -k'_{CNOM}[\text{CNOM}]\varepsilon_{CNOM}$$

Equation [A6] simplifies to Equation [A7] where k'_{CNOM} is the apparent reaction rate constant for the reduction of CNOM (s^{-1}).

$$[A7] \qquad \frac{d[\text{CNOM}]}{dt} = -k'_{CNOM}[\text{CNOM}]$$

Finally, given the assumption that CNOM is only degraded by $^{\bullet}$OH, Equation [A7] can be written as Equation [10] (Table A.3). Thus, the experimental data for A_{CNOM} could be used to determine $k_{.OH,CNOM}$.

Numerical Solution of Governing Rate Expressions and Parameter Estimation.

The MATLAB function ode15s was used to solve the system of stiff differential equations (program code available upon request). $k_{.OH,CNOM}$ and $k_{.OH,TOC}$ were estimated by maximum likelihood estimation with a weighted least squares objective function (OF) given by Equation [A8] where i represents a measurement made at some point in time, $\text{CNOM}_{\text{expt}}$ is the experimental measurement at i, $\text{CNOM}_{\text{model}}$ is the model prediction at i, $\text{pCBA}_{\text{expt}}$ is the experimental measurement at i, $\text{pCBA}_{\text{model}}$ is the model prediction at i, and σ_{CNOM} and σ_{pCBA} are weighting parameters to compensate for error due to measurement. σ_{CNOM} was set equal to 0.002 cm^{-1} in order to represent the typical standard deviation observed when making absorbance measurement and σ_{pCBA} was set equal to 5 μg L^{-1} in order to represent the typical standard deviation observed when making pCBA measurements.

$$[A8] \qquad \text{OF} = \sum_{i=1}^{N} \left\{ \frac{\left(\text{CNOM}_{\text{expt}} - \text{CNOM}_{\text{model}}\right)_i^2}{\sigma_{\text{CNOM}}^2} + \frac{\left(\text{pCBA}_{\text{expt}} - \text{pCBA}_{\text{model}}\right)_i^2}{\sigma_{\text{pCBA}}^2} \right\}$$

MATLAB's *fminsearch* function was used to find values of $k_{.OH,CNOM}$ and $k_{.OH,TOC}$ that minimized the OF, in effect estimating the parameters that best fit model predictions to

experimental data. The standard error for the parameters was determined by calculating the Fisher Information Matrix followed by determination of the covariance/sensitivity matrix (according to calculation procedure described by Englezos & Kalogerakis (2001). From the calculated standard errors, the 95% confidence intervals of each parameter were calculated and are reported.

Experimental Approach for UV/H_2O_2 Treatment of Natural Waters.

The model was evaluated by comparing the model predicted concentrations for H_2O_2 and CNOM to experimental data collected during UV/H_2O_2 treatment of the two raw waters, CW and TW, as well as these waters with additional alkalinity. CW was treated with initial H_2O_2 concentrations between 5 and 20 mg L^{-1} and an E_P° between 2.54E-10 and 2.84E-10 Es cm^{-2} s^{-1}. Further, CW was adjusted to alkalinities of approximately 50, 100, and 150 mg $CaCO_3$ L^{-1} and was treated with initial H_2O_2 concentrations ranging from 5 to 15 mg L^{-1} and an E_P° between 8.59E-10 and 9.72E-10 Es cm^{-2} s^{-1}. TW and TW adjusted to alkalinities of 100 and 150 mg $CaCO_3$ L^{-1} were treated with initial H_2O_2 concentrations ranging from 5 to 20 mg L^{-1} and an E_P° between 9.03E-10 and 9.52E-10 Es cm^{-2} s^{-1}.

Results and Discussion

The model proposed here was unique in that it considered the change in the absorption coefficient of water at 254nm, $A_{total,254}$, that occurred during UV/H_2O_2 treatment as a result of H_2O_2 and CNOM degradation. It was deemed necessary to consider the change in $A_{total,254}$ since the kinetics of UV/H_2O_2 system inherently depend on $A_{total,254}$ (Equations [1] and [3] in Table A.3). Thus, including the change in $A_{total,254}$ provided a more complete characterization of the UV/H_2O_2 system.

Synthetic Water Experimental Observations and Model Parameter Estimation.

Results from UV/H_2O_2 treatment of SRNOM-aquatic synthetic water are presented in Figures A.1-A.3. Using these experimental data and the set of kinetic rate expressions in Tables A.2 and A.3, the two unknown rate parameters, $k_{\cdot OH,CNOM}$ and $k_{\cdot OH,TOC}$, were estimated simultaneously by minimizing the weighted least squares between model predictions and experimental data. Figures A.1-A.3 also include the model predictions using the estimated rate parameters.

Hydroxyl Radical Scavenging by Natural Organic Matter. Figure A.1 shows that the observed rate of degradation of pCBA increased with increasing the initial H_2O_2 concentration. On the other hand, the observed degradation rate of pCBA decreased with increasing the concentration of TOC. Both these phenomena were expected since an increase in H_2O_2 yielded a greater concentration of $^{\bullet}OH$, thus increasing the degradation rate of the $^{\bullet}OH$ probe. Also, an increased concentration of TOC led to increased scavenging of $^{\bullet}OH$ by TOC, consequently yielding less $^{\bullet}OH$ to react with pCBA.

The optimal reaction rate constant for the reaction between $^{\bullet}OH$ and TOC, $k_{.OH,TOC}$, was estimated at 1.14±0.10E4 L mg^{-1} s^{-1}. There have been no previous studies reporting $k_{.OH,TOC}$ for the SRNOM-aquatic used in this study; however, past literature reports are available for $k_{.OH,TOC}$ of the Suwannee River NOM fulvic acid (SRNOM-fulvic), Suwannee River NOM humic acid (SRNOM-humic) and NOM from other sources (Table A.4). SRNOM-aquatic was preferred in this study since it was considered to be more representative of the NOM found in natural waters, rather than fulvic or humic fraction isolates. Nonetheless, the $k_{.OH,TOC}$ estimated in this study for SRNOM-aquatic agreed reasonably well with the literature on $k_{.OH,TOC}$ for SRNOM-fulvic, SRNOM-humic, and NOM from other sources (Table A.4). The estimated value, 1.14±0.10E4 L mg^{-1} s^{-1}, was within error of the value reported for SRNOM-fulvic (Westerhoff et al., 2007) using pulse radiolysis with competition kinetics and direct transient growth (1.33±0.20E4 L mg^{-1} s^{-1}). The variation between reported $k_{.OH,TOC}$ values (Table A.4) demonstrates that estimation of the parameter is subject to the method used for $^{\bullet}OH$ production (i.e., ozonation, UV/H_2O_2, pulse radiolysis, γ-radiolysis, etc.), as well as the type of NOM employed (i.e., aquatic isolate, fulvic or humic isolates, or non-isolated/whole water). Yet, regardless of the $^{\bullet}OH$ production method or the type of NOM employed, $k_{.OH,TOC}$ has been reported to be around 2E4 L mg^{-1} s^{-1} (Reisz et al. 2003). As the $k_{.OH,TOC}$ estimated in this work agreed well with other literature values, it was deemed acceptable.

Degradation of Chromophoric Natural Organic Matter.

Figure A.2 illustrates the experimental data for A_{CNOM} for UV/H_2O_2 treatment of SRNOM-aquatic synthetic water. There was a marked reduction in CNOM as irradiation time increased, as was observed by Sarathy and Mohseni (2007, 2009). Further, as the initial H_2O_2 concentration was increased, the observed rate of degradation of CNOM increased, also as expected and

observed by Sarathy and Mohseni (2007). For $k_{\cdot OH,CNOM}$ the optimum value was estimated at 3.04±0.33E8 L mol^{-1} s^{-1}. Literature estimates of $k_{\cdot OH,CNOM}$ were non-existent at the time of publication so it could not be compared.

Prediction of the change in CNOM was regarded valuable since in the UV/H_2O_2 system CNOM would often be the major absorber of photons. Any change in A_{CNOM} would have an impact on $A_{total,254}$ (Equation [A2]), the photolysis of H_2O_2 (Equation [1] in Table A.3), and subsequently the concentration of $^{\bullet}OH$ (Equation [3] in Table A.3). A reduction in A_{CNOM} would lead to greater absorption of photons by H_2O_2, thus increasing photolysis of H_2O_2 and $^{\bullet}OH$ production. Therefore, by considering the change in CNOM, prediction of H_2O_2 degradation would be more accurate.

Degradation of Hydrogen Peroxide.

Similar to the UV/H_2O_2 models presented in the literature, the model presented here considered photolysis to be the main pathway for H_2O_2 degradation. As an improvement to past models, this model also included the change in CNOM, thereby improving the modeling of H_2O_2 degradation. Despite improving model predictions to some extent, the model developed here, as have past models, under predicted the measured H_2O_2 concentrations (Figure A.3).

Interestingly, the observed maximum extent of degradation of H_2O_2 increased as the concentration of TOC increased, from about 15-20% at a TOC concentration of 1.33 mg L^{-1} to about 20-25% at a TOC concentration of 3.08 mg L^{-1} (Figure A.3). Had photolysis been the primary pathway for H_2O_2 degradation, an increased concentration of TOC would have led to slower degradation of H_2O_2 since higher levels of TOC would result in higher CNOM and greater water absorbance and screening of UV. Consequently, there would be a reduction in the number of photons absorbed by H_2O_2 thereby impeding H_2O_2 degradation. In fact, this phenomenon was predicted by the model but was not supported by the experiments (Figure A.3). The model predicted best when the conditions were closest to pure water (RMSE < 0.035 for 1.33 mg L^{-1} TOC concentration) and worst when the TOC concentration was the highest. This demonstrated that the assumption of photolysis being the predominant mechanism for H_2O_2 degradation may be true only for water with very low amounts of NOM, but when NOM is present at even moderately low levels, other mechanisms, besides photolysis and reaction with radical species, contribute to H_2O_2 degradation.

Earlier modeling efforts by Song et al. (2008) and Liao and Gurol (1995) also showed that model predictions for H_2O_2 degradation deviated from the experimental data, with the model under predicting experimental measurements. Song et al. (2008) speculated this under prediction could be due to H_2O_2 reacting with NOM. Our experimental results did not support this hypothesis and showed that when NOM was in water with H_2O_2 and no irradiation (i.e., dark reaction), there was no measurable reduction in H_2O_2 over several hours (data not shown). Thus, it is unlikely that the raw NOM reacts with H_2O_2 at a significant rate.

It is more plausible that H_2O_2 reacts readily with the products of the NOM and $^{\bullet}OH$ reaction. $^{\bullet}OH$ reacts with NOM either by $^{\bullet}OH$ addition to a carbon-carbon double bond or by abstraction of a carbon bound hydrogen (von Sonntag 1997). Both mechanisms result in the formation of carbon-centered radicals (von Sonntag 1997). These carbon-centered radicals quickly react with dissolved oxygen forming peroxyl radicals which, via various reactions, go on to form low molecular weight carbonyls such as aldehydes, ketones, carboxylic acids and eventually carbon dioxide. Alternatively, the carbon-centered radicals could react with H_2O_2. Neta et al. (1996) reported the reaction rate constants for reactions between carbon-centered radicals with oxygen were generally in the range of 10^8 to 10^{10} L mol^{-1} s^{-1} versus 10^4 to 10^6 L mol^{-1} s^{-1} for reactions between carbon-centered radicals and H_2O_2. Even though the dominant reaction for carbon-centered radicals is with oxygen, their reaction with H_2O_2 cannot be ignored and this could explain the additional degradation, beyond photolysis, of H_2O_2. Further research is required to define expressions to more accurately model H_2O_2 degradation during UV/H_2O_2 treatment of water in which NOM is present.

Surface Water Experimental Observations and Model Validation.

Results from UV/H_2O_2 treatment of CW and TW along with model predictions, given as lines, are presented in Figures A.4 and A.5. Also, provided are the root mean square errors (RMSE) of each model prediction, an indicator of the model's accuracy.

Degradation of Chromophoric Natural Organic Matter in Capilano Water and Trepanier Water.

For both CW and TW, CNOM was degraded as irradiation time increased (Figure A.4). Note that for TW experiments, E_P° was over three times greater than that for the CW experiments. Therefore, the extent of degradation of CNOM at a specific time should not be directly compared. Nevertheless, a slower degradation over time was observed for TW since TW had a

greater TOC concentration and A_{CNOM} than CW (Table A.1). The higher A_{CNOM} resulted in lower photolysis of H_2O_2 and thus less $^{\bullet}OH$ generation, thereby reducing the rate of CNOM degradation. Further, TW also had alkalinity at 47 mg $CaCO_3$ L^{-1} which has impeded the rate of CNOM degradation (further results and discussion on the impact of alkalinity are provided below). As was observed for SRNOM-aquatic synthetic water (Figure A.2), there was a clear link between the extent of degradation of CNOM and the initial H_2O_2 concentration for CW and TW (Figure A.4).

In general, the model predictions of CNOM degradation agreed well with the experimental results for UV/H_2O_2 treatment of CW and TW. For CW, the model predicted very well the degradation of CNOM both as a function of irradiation time and initial H_2O_2 concentration. The RMSE ranged from 0.004 to 0.058 with an average of 0.040 indicating a percentage error of about 4% on average. Since both irradiation time and initial H_2O_2 concentration affect the level of $^{\bullet}OH$ exposure, this agreement between model predictions and experimental observations reinforces the model's assumption that CNOM is mainly degraded by $^{\bullet}OH$. For TW, model predictions were also accurate for initial H_2O_2 concentrations of approximately 15 mg L^{-1} (RMSE = 0.028) and 5 mg L^{-1} (RMSE = 0.052) (Figure A.4).

Impact of Alkalinity on Degradation of Chromophoric Natural Organic Matter.

An increase in alkalinity resulted in lower degradation of CNOM for CW with approximately 10 or 15 mg L^{-1} initial H_2O_2 concentration (Figure A.5). The model's prediction was also in agreement with the observed behavior of CW, that is increasing alkalinity resulted in less degradation of CNOM. This was caused by the scavenging of $^{\bullet}OH$ by bicarbonate (Reaction 4 in Table A.2) and carbonate (Reaction 5 in Table A.2) which resulted in fewer $^{\bullet}OH$ available for reaction with CNOM (Equation [3] in Table A.3).

Degradation of Hydrogen Peroxide.

As was observed with SRNOM-aquatic synthetic water, there was an apparent degradation of H_2O_2 during UV/H_2O_2 of CW and TW. The maximum extent of H_2O_2 degradation for CW was 24% and 19% with initial H_2O_2 concentrations of 5 and 15 mg L^{-1}, respectively (Table A.5). When alkalinity was added to CW at different concentrations, the maximum extent of H_2O_2 degradation remained at around 19%, irrespective of the initial H_2O_2 or alkalinity (Table A.5). Similarly for TW, additional alkalinity did not considerably impact the maximum extent of

H_2O_2degradation, which was between 15% and 23% (Table A.5). Therefore, experimental results did not demonstrate that change in alkalinity considerably affected the observed degradation of H_2O_2. On the contrary, the model predicted that additional alkalinity resulted in greater degradation of H_2O_2, bringing the model predictions closer to the experimental results (Table A.5). This increased H_2O_2 degradation predicted by the model can be explained by the presence of the carbonate radical, formed as a result of $^{\bullet}OH$ reaction with bicarbonate (Reaction 4 Table A.3) and carbonate (Reaction 5 Table A.3). The formed carbonate radical can react with H_2O_2 (Reaction 15 Table A.3) thus contributing to excess H_2O_2 degradation. The RMSE between model predictions and experimental observations ranged from 0.012 to 0.041 for CW with alkalinity present compared to RMSE of 0.036 and 0.082 for raw CW (Table A.5). Similarly, for TW model predictions were noticeably better with increasing the alkalinity, as indicated by the lower RMSE values (Table A.5). It is apparent that despite the improved performance of the model in predicting the degradation of H_2O_2 as alkalinity increased, the model still under predicted the experimentally observed degradation of H_2O_2 during UV/H_2O_2 treatment of CW and TW. This again can be explained by the hypothesis that reactions between H_2O_2 and carbon-centered radicals are important and contribute to the overall H_2O_2 degradation.

Implications of Natural Organic Matter Characteristics.

NOM varies widely and its composition is largely dependent upon the autochthonous and allochthonous influences of a particular source. Subsequently, the characteristics of NOM can vary from one source to another. In this study, model parameters were obtained based on an isolated NOM dissolved in pure water and were applied to predict the degradation of CNOM during UV/H_2O_2 treatment of natural waters. It is plausible that this approach yielded satisfactory results due to the characteristics of three NOMs used in this study. As shown in Table A.1, the values of specific ultraviolet absorbance (SUVA), a measure of the aromatic character of NOM (Nikolaou and Lekkas, 2001), were quite similar for the three NOMs. In terms of hydrophobic/hydrophilic fractionation, all three NOMs were composed of predominantly hydrophobic acids, from 80% to 86% VHA and SHA combined. These resemblances in characteristics may have contributed to the observed similarities in the way these three NOMs reacted with $^{\bullet}OH$. The results may not have been as satisfactory had the characteristics of the NOM been very different, so future research should broaden the study to a range of NOMs that cover more diverse characteristics.

Highlights of this Model and Potential Applications. This model incorporated unique features by accounting for the changes in water absorbance as well as the reduction in H_2O_2 concentration. By including these features and considering all species dynamic, it came closer to ideal characterization of the UV/H_2O_2 system. As residual H_2O_2 is present in all UV/H_2O_2 applications, and requires costly removal, accurate prediction is of high value for system design as well as cost reduction. The model can also be applied to predict the degradation of organic micro-pollutants.

The model tracked the transformation of NOM by the surrogate parameter, CNOM. Changes in CNOM have been correlated with changes in water quality parameters such as assimilable organic carbon (AOC) concentration during various stages of treatment including ozonation, carbon filtration, and slow sand filtration (van den Broeke et al. 2008). Thus, this model could also be modified to predict changes in water quality by using empirical correlations linking degradation of CNOM to changes in water quality parameters.

CNOM could be used in actual process operation to track the transformation of NOM as well as to approximate the $^{\bullet}OH$ concentration. In practice this would involve simple monitoring of CNOM upstream and downstream of the UV/H_2O_2 process. Since changes in CNOM may correlate with changes in AOC, monitoring of CNOM would provide an indication of possible changes in biological stability of water after treatment. Further, given that the reduction in CNOM is dependent on $^{\bullet}OH$ concentration, variations in CNOM reduction would indicate a change in $^{\bullet}OH$ concentration. As $^{\bullet}OH$ concentration impacts the removal of target contaminants, this simple method has the potential to improve process performance.

Acknowledgments

The authors acknowledge Anaig Rosmorduc and Steve McDermid for assisting with experimental and analytical work. We thank Ted Mao, Mihaela Stefan, Bill Cairns, Alan Royce, Gustavo Imoberdorf, Esteban Duran, and Bhushan Gopaluni for all the valuable discussions. National Science and Engineering Research Council of Canada and Trojan Technologies are acknowledged for financial support.

Table A.1: Select characteristics of waters used in UV/H_2O_2 experiments. Table values are averages of numerous measurements.

Parameter	Suwannee River Natural Organic Matter Synthetic Water	Capilano Water [(i)]	Trepanier Water [(ii)]
Alkalinity (mg $CaCO_3$ L^{-1})	none added	none detected	47
Total organic carbon (mg L^{-1})	1.33/2.21/3.08	2.45	5.12
pH	5.5-5.8	6.5-6.8	7.5-7.7
A_{CNOM} (cm^{-1})	0.049/0.065/0.108	0.089	0.214
SUVA (L mg^{-1} m^{-1})	3.4	3.6	4.2
VHA (%)	80	66	76
SHA (%)	4	20	5
CHA+NEU (%)	16	14	19

SUVA – specific ultraviolet absorbance; VHA – very hydrophobic acids; SHA – slightly hydrophobic acids; CHA+NEU – charged plus neutral hydrophilic.

(i) Collected May 2006
(ii) Collected May 2008 (water shed was experiencing elevated levels of colour and TOC due to the spring snow melt)

Table A.2: The series of reactions used in the kinetic model of the UV/H_2O_2 system.

	Reaction	Rate constant	Reference
1	$H_2O_2 + h\nu \rightarrow 2{\cdot}OH$	$\Phi_{H_2O_2,\cdot OH}$ = 0.5 (primary quantum yield)	Baxendale and Wilson 1957
2	$\cdot OH + H_2O_2 \rightarrow O_2^{\cdot-} + H_2O + H^+$	k_2 = 2.7E7 L mol^{-1} s^{-1}	Buxton et al. 1988
3	$\cdot OH + HO_2^- \rightarrow O_2^{\cdot-} + H_2O$	k_3 = 7.5E9 L mol^{-1} s^{-1}	Buxton et al. 1988
4	$\cdot OH + HCO_3^- \rightarrow H_2O + CO_3^{\cdot-}$	k_4 = 8.5E6 L mol^{-1} s^{-1}	Buxton et al. 1988
5	$\cdot OH + CO_3^{2-} \rightarrow OH^- + CO_3^{\cdot-}$	k_5 = 3.9E8 L mol^{-1} s^{-1}	Buxton et al. 1988
6	$\cdot OH + HO_2^{\cdot} \rightarrow H_2O + O_2$	k_6 = 6.6E9 L mol^{-1} s^{-1}	Buxton et al. 1988
7	$\cdot OH + O_2^{\cdot-} \rightarrow OH^- + O_2$	k_7 = 8.0E9 L mol^{-1} s^{-1}	Buxton et al. 1988
8	$\cdot OH + \cdot OH \rightarrow H_2O_2$	k_8 = 5.5E9 L mol^{-1} s^{-1}	Buxton et al. 1988
9	$\cdot OH + CO_3^{\cdot-} \rightarrow OH^- + CO_3^{2-}$	k_9 = 3.0E9 L mol^{-1} s^{-1}	Holcman et al. 1987
10	$O_2^{\cdot-} + H_2O_2 \rightarrow \cdot OH + OH^- + O_2$	k_{10} = 0.13 L mol^{-1} s^{-1}	Bielski et al. 1985
11	$O_2^{\cdot-} + CO_3^{\cdot-} \rightarrow O_2 + CO_3^{2-}$	k_{11} = 6.5E8 L mol^{-1} s^{-1}	Eriksen et al. 1985
12	$O_2^{\cdot-} + HO_2^{\cdot} + H_2O \rightarrow H_2O_2 + OH^- + O_2$	k_{12} = 9.7E7 L mol^{-1} s^{-1}	Buxton et al. 1988
13	$HO_2^{\cdot} + HO_2^{\cdot} \rightarrow H_2O_2 + O_2$	k_{13} = 8.6E5 L mol^{-1} s^{-1}	Weinstein and Bielski 1979
14	$HO_2^{\cdot} + H_2O_2 \rightarrow \cdot OH + H_2O + O_2$	k_{14} = 3.7 L mol^{-1} s^{-1}	Bielski et al. 1985
15	$CO_3^{\cdot-} + H_2O_2 \rightarrow HCO_3^- + O_2^{\cdot-} + H^+$	k_{15} = 8.0E5 L mol^{-1} s^{-1}	Neta et al. 1988
16	$CO_3^{\cdot-} + HO_2^- \rightarrow HCO_3^- + O_2^{\cdot-}$	k_{16} = 3.0E7 L mol^{-1} s^{-1}	Neta et al. 1988
17	$CO_3^{\cdot-} + CO_3^{\cdot-} \rightarrow 2CO_3^{2-}$	k_{17} = 2.0E7 L mol^{-1} s^{-1}	Neta et al. 1988
18	$H_2O_2 \rightarrow H^+ + HO_2^-$	k_{18} = 0.0356 s^{-1}	Ershov and Gordeev 2008
19	$H^+ + HO_2^- \rightarrow H_2O_2$	k_{19} = 2.0E10 L mol^{-1} s^{-1}	Ershov and Gordeev 2008
20	$HO_2^{\cdot} \rightarrow H^+ + O_2^{\cdot-}$	k_{20} = 7.0E5 s^{-1}	Ershov and Gordeev 2008
21	$H^+ + O_2^{\cdot-} \rightarrow HO_2^{\cdot}$	k_{21} = 4.5E10 L mol^{-1} s^{-1}	Ershov and Gordeev 2008
22	$HCO_3^- \rightarrow H^+ + CO_3^{2-}$	k_{22} = 0.2 s^{-1}	Brezonik 1994
23	$H^+ + CO_3^{2-} \rightarrow HCO_3^-$	k_{23} = 3.99E9 L mol^{-1} s^{-1}	Brezonik 1994
24	$\cdot OH + pCBA \rightarrow products$	$k_{\cdot OH,pCBA}$ = 5E9 L mol^{-1} s^{-1}	Neta and Dorfman 1968
25	$\cdot OH + TOC \rightarrow products$	$k_{\cdot OH,TOC}$ = ? L mg^{-1} s^{-1}	Present work
26	$\cdot OH + CNOM \rightarrow products$	$k_{\cdot OH,CNOM}$ = ? L mol^{-1} s^{-1}	Present work

Table A.3: The mathematical model's system of ordinary differential equations.

Equation	
[1]	$\frac{d[H_2O_2]}{dt} = -k_{a,H_2O_2,254}\Phi_{H_2O_2,\cdot OH}[H_2O_2] - k_2[\cdot OH][H_2O_2] - k_{10}[O_2^{\cdot-}][H_2O_2] - k_{14}[HO_2^{\cdot}][H_2O_2] - k_{15}[CO_3^{\cdot-}][H_2O_2] - k_{18}[H_2O_2] + k_8[\cdot OH]^2 + k_{12}[O_2^{\cdot-}][HO_2^{\cdot}] + k_{13}[HO_2^{\cdot}]^2 + k_{19}[H^+][HO_2^-]$
[2]	$\frac{d[HO_2^-]}{dt} = -k_3[\cdot OH][HO_2^-] - k_{16}[CO_3^{\cdot-}][HO_2^-] - k_{19}[H^+][HO_2^-] + k_{18}[H_2O_2]$
[3]	$\frac{d[\cdot OH]}{dt} = -k_2[\cdot OH][H_2O_2] - k_3[\cdot OH][HO_2^-] - k_4[\cdot OH][HCO_3^-] - k_5[\cdot OH][CO_3^{2-}] - k_6[\cdot OH][HO_2^{\cdot}] - k_7[\cdot OH][O_2^{\cdot-}] - k_8[\cdot OH]^2 - k_9[\cdot OH][CO_3^{\cdot-}] - k_{.OH,TOC}[\cdot OH]\mathrm{TOC} - k_{.OH,pCBA}[\cdot OH][\mathrm{pCBA}] + 2k_{a,H_2O_2}\Phi_{H_2O_2,\cdot OH}[H_2O_2] + k_{10}[O_2^{\cdot-}][H_2O_2] + k_{14}[HO_2^{\cdot}]H_2O_2$
[4]	$\frac{d[O_2^{\cdot-}]}{dt} = -k_7[\cdot OH][O_2^{\cdot-}] - k_{10}[O_2^{\cdot-}][H_2O_2] - k_{11}[O_2^{\cdot-}][CO_3^{\cdot-}] - k_{12}[O_2^{\cdot-}][HO_2^{\cdot}] - k_{21}[H^+][O_2^{\cdot-}] + k_2[\cdot OH][H_2O_2] + k_3[\cdot OH][HO_2^-] + k_{15}[CO_3^{\cdot-}][H_2O_2] + k_{16}[CO_3^{\cdot-}][HO_2^-] + k_{20}[HO_2^{\cdot}]$
[5]	$\frac{d[HO_2^{\cdot}]}{dt} = -k_6[\cdot OH][HO_2^{\cdot}] - k_{12}[O_2^{\cdot-}][HO_2^{\cdot}] - k_{13}[HO_2^{\cdot}]^2 - k_{14}[HO_2^{\cdot}][H_2O_2] - k_{20}[HO_2^{\cdot}] + k_{21}[H^+][O_2^{\cdot-}]$
[6]	$\frac{d[CO_3^{\cdot-}]}{dt} = -k_9[\cdot OH][CO_3^{\cdot-}] - k_{11}[O_2^{\cdot-}][CO_3^{\cdot-}] - k_{15}[CO_3^{\cdot-}][H_2O_2] - k_{16}[CO_3^{\cdot-}][HO_2^-] - k_{17}[CO_3^{\cdot-}]^2 + k_4[\cdot OH][HCO_3^-] + k_5[\cdot OH][CO_3^{2-}]$
[7]	$\frac{d[HCO_3^-]}{dt} = -k_4[\cdot OH][HCO_3^-] - k_{22}[HCO_3^-] + k_{15}[CO_3^{\cdot-}][H_2O_2] + k_{16}[CO_3^{\cdot-}][HO_2^-] + k_{23}[H^+][CO_3^{2-}]$
[8]	$\frac{d[CO_3^{2-}]}{dt} = -k_5[\cdot OH][CO_3^{2-}] - k_{23}[H^+][CO_3^{2-}] + k_9[\cdot OH][CO_3^{\cdot-}] + k_{11}[O_2^{\cdot-}][CO_3^{\cdot-}] + 2k_{17}[CO_3^{\cdot-}]^2 + k_{22}[HCO_3^-]$
[9]	$\frac{d[\mathrm{pCBA}]}{dt} = -k_{.OH,pCBA}[\cdot OH][\mathrm{pCBA}]$
[10]	$\frac{d[\mathrm{CNOM}]}{dt} = -k_{.OH,CNOM}[\cdot OH][\mathrm{CNOM}]$

Table A.4: Empirically calculated reaction rate constants for the reaction between hydroxyl radical and natural organic matter.

NOM Source	$k_{.OH,TOC}$ (L mg^{-1} s^{-1})	Determination Method	Reference
Suwannee River Aquatic NOM	1.14E4	UV/H_2O_2 - competition kinetics	Present work
Suwannee River Fulvic Acid	1.33±0.2 E4	Pulse radiolysis - competition kinetics and direct transient growth	Westerhoff et al. 2007
Suwannee River Fulvic Acid	3.08E4	Ozonation - competition kinetics	Westerhoff et al. 1999
Suwannee River Fulvic Acid	2.70±0.05 E4	γ-radiolysis - competition kinetics	Goldstone et al. 2002
Suwannee River Humic Acid	1.90±0.05 E4	γ-radiolysis - competition kinetics	Goldstone et al. 2002
Fluka Humic Acid	1.60E4	UV/H_2O_2 - numerical parameter estimation	Liao and Gurol 1995
Average of six NOM isolates	2.54E4	Pulse radiolysis - competition kinetics and direct transient growth	Westerhoff et al. 2007
Average of sixteen NOM isolates	3.00±0.45 E4	Ozonation - competition kinetics	Westerhoff et al. 1999
Average of five surface waters	2.30±0.77 E4	Nitrate-induced solar driven photolysis	Brezonik & Fulkerson-Brekken 1998

Table A.5: Experimentally observed and model predicted extent of hydrogen peroxide degradation ($[H_2O_2]_{final}/[H_2O_2]_0$) for CW and TW over alkalinity and H_2O_2 concentrations.

		CW			TW		
Approximate $[HCO_3^-]_0$ (L mg^{-1})	**Approximate $[H_2O_2]_0$ (L mg^{-1})**	**Observed**	**Predicted**	**RMSE**	**Observed**	**Predicted**	**RMSE**
0	5	24	13	0.082	-	-	-
	15	19	14	0.036	-	-	-
50	5	19	13	0.041	23	9	0.125
	15	19	16	0.031	19	10	0.075
100	5	18	14	0.012	16	11	0.054
	15	20	15	0.018	16	8	0.063
150	5	-	16	-	21	10	0.066
	15	-	17	-	15	10	0.037

RMSE – root mean square error; $[HCO_3^-]_0$ – initial bicarbonate concentration; $[H_2O_2]_0$ – initial hydrogen peroxide concentration; CW – Capilano Water; TW – Trepanier Water

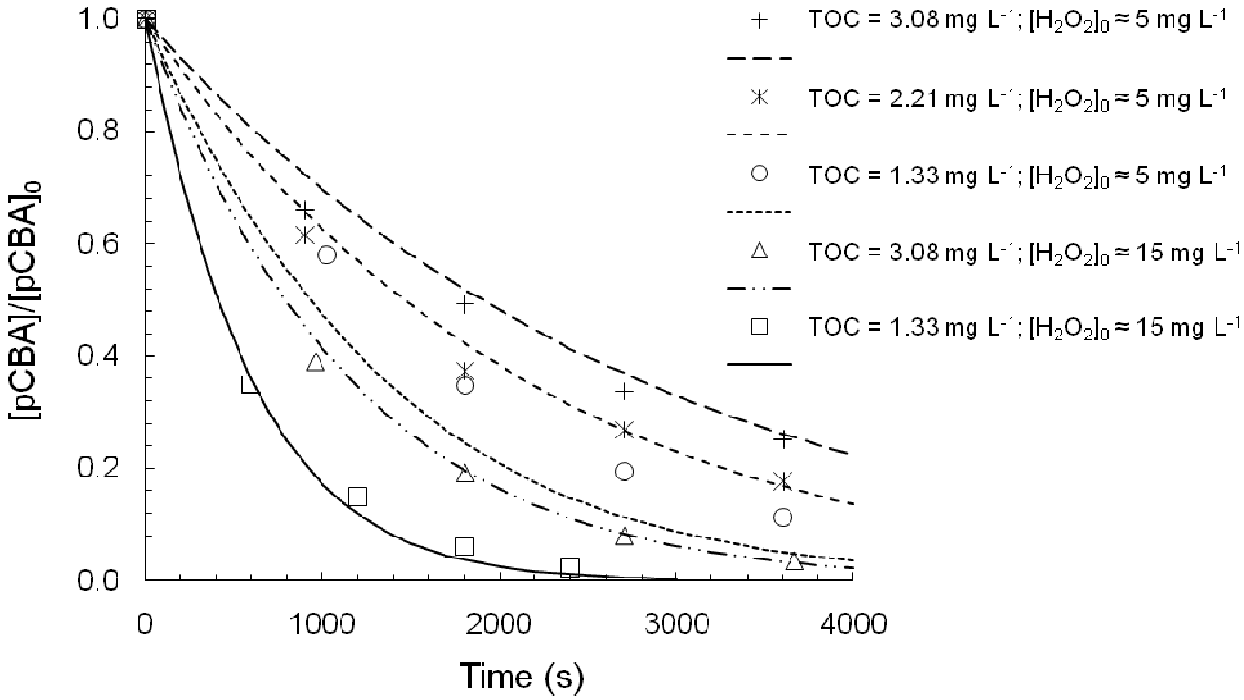

Figure A.1: Degradation of pCBA during the UV/H_2O_2 treatment of SRNOM-aquatic synthetic water at an E_P° of 6.42E-10 Es cm^{-2} s^{-1} and varying levels of TOC and initial H_2O_2 concentration. Points represent experimental measurements and lines represent model predictions.

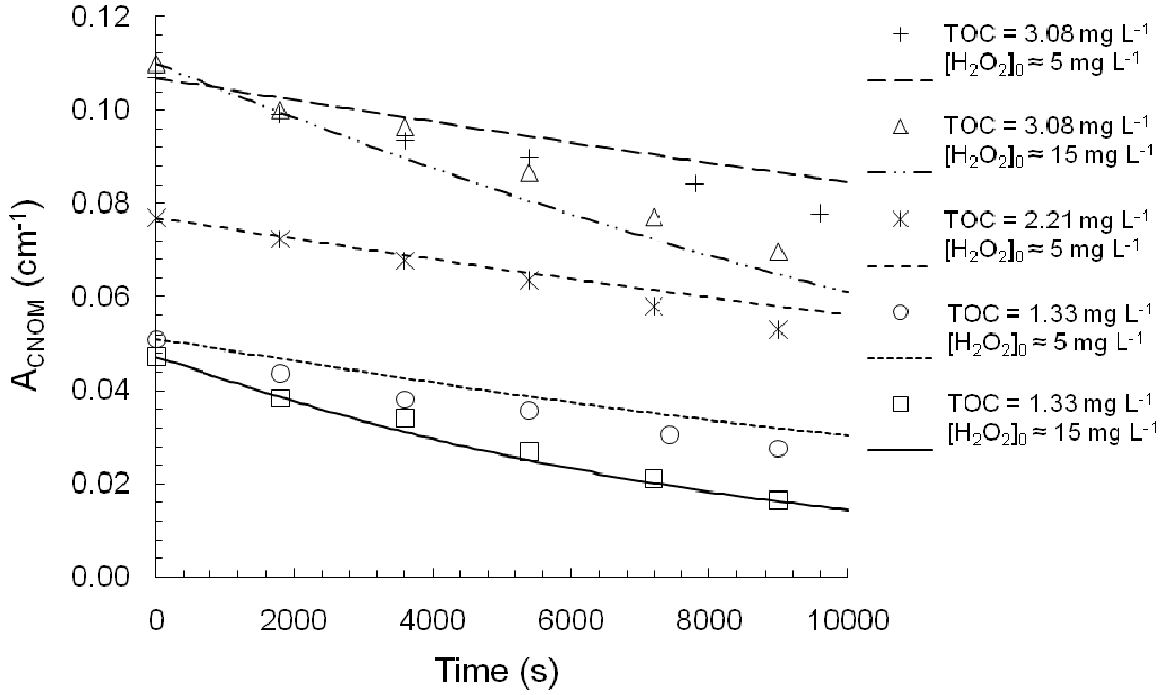

Figure A.2: Degradation of CNOM during the UV/H_2O_2 treatment of SRNOM-aquatic synthetic water at an $\boldsymbol{E_P^\circ}$ of 6.42E-10 Es cm^{-2} s^{-1} and varying levels of TOC and initial H_2O_2 concentration. Points represent experimental measurements and lines represent model predictions.

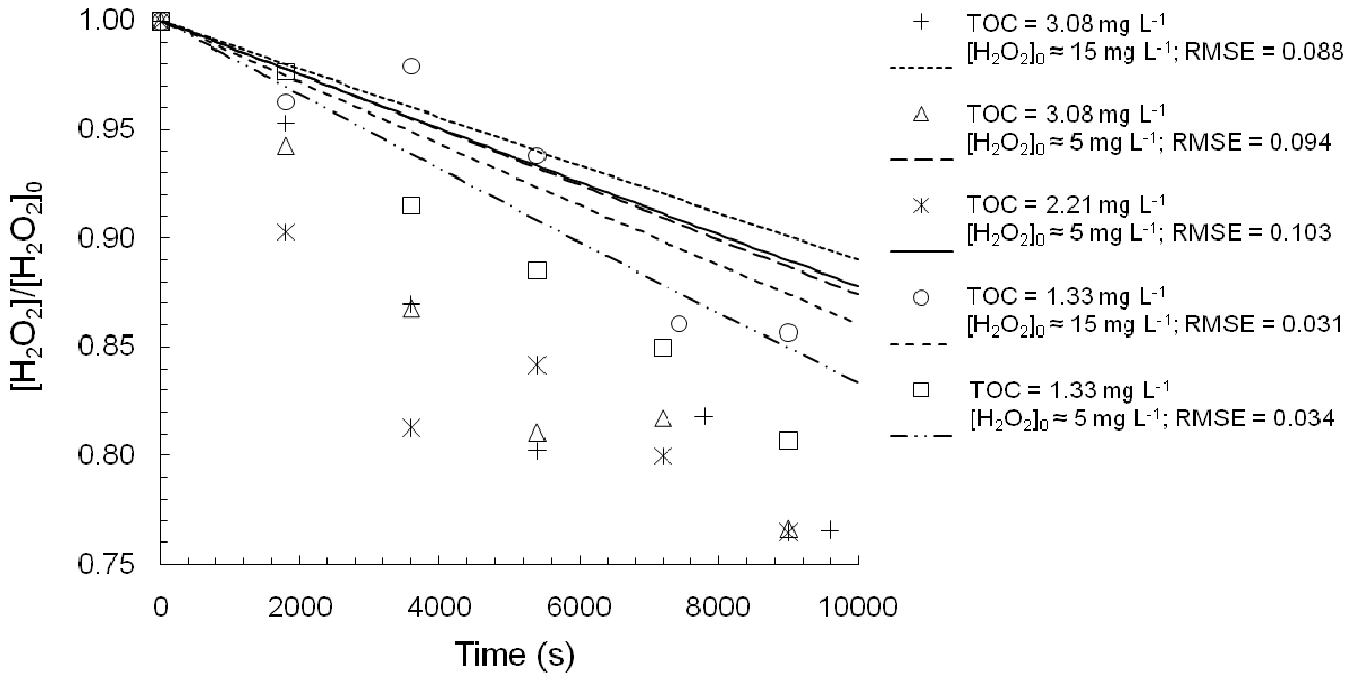

Figure A.3: Degradation of H_2O_2 during the UV/H_2O_2 treatment of SRNOM-aquatic synthetic water at an $\boldsymbol{E_P^\circ}$ of 6.42E-10 Es cm^{-2} s^{-1} and varying levels of TOC and initial H_2O_2 concentration. Points represent experimental measurements and lines represent model predictions.

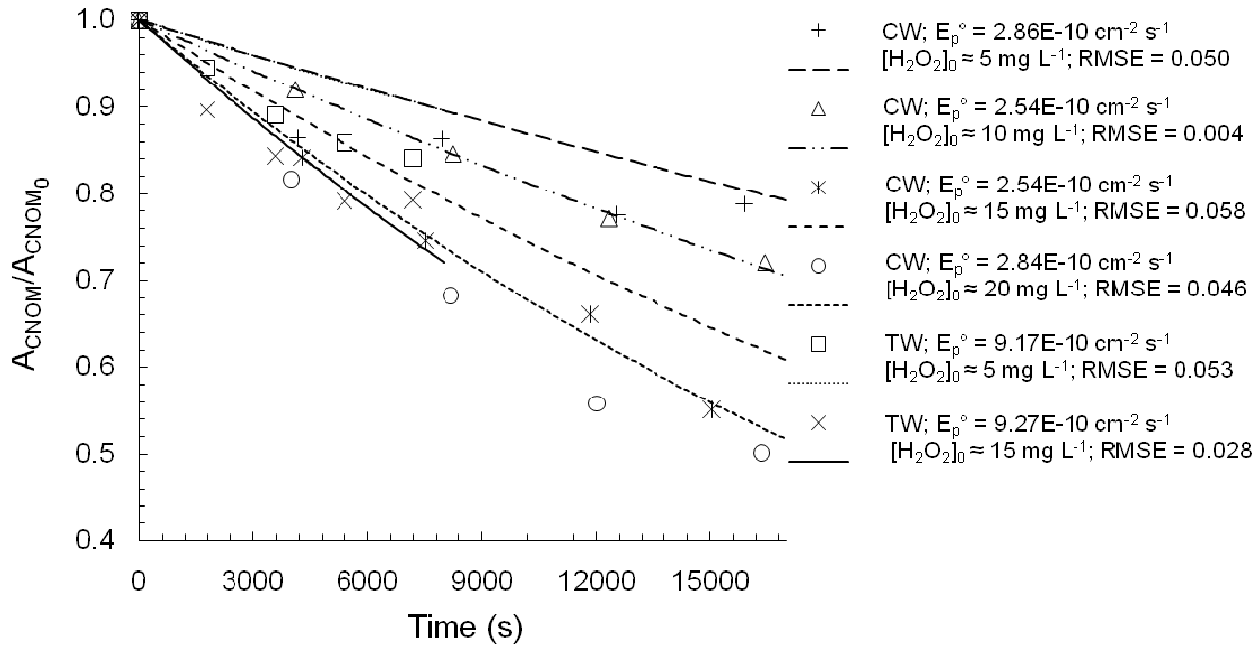

Figure A.4: Degradation of CNOM during the UV/H_2O_2 treatment of CW and TW at varying levels of initial H_2O_2 concentration. Points represent experimental measurements and lines represent model predictions.

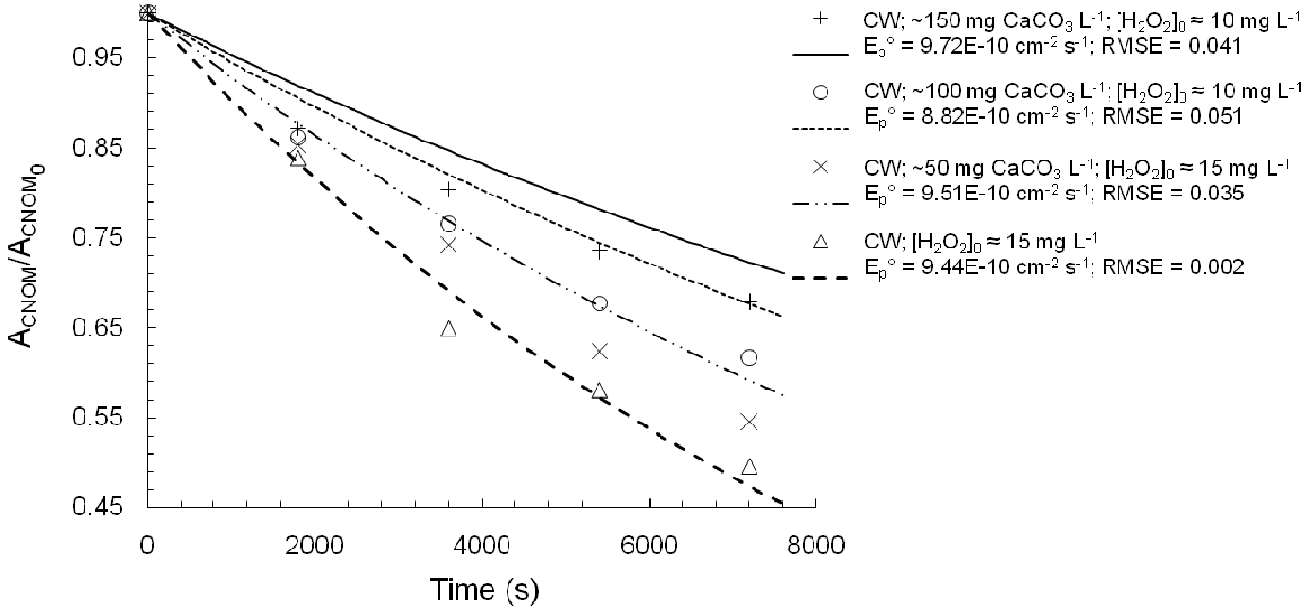

Figure A.5: Degradation of CNOM during the UV/H_2O_2 treatment of CW at an initial H_2O_2 concentration of 10 or 15 mg L^{-1} and varying levels of alkalinity. Points represent experimental measurements and lines represent model predictions.

References

Baxendale, J.H. and Wilson, J.A. (1957). Photolysis of hydrogen peroxide at high light intensities. *Trans. Faraday Society*, 53, 344-356.

Bielski, B., Cabelli, D., Arudi, R., and Ross, A. (1985). Reactivity of HO_2/O_2^- radicals in aqueous-solution. *Journal of Physical and Chemical Reference Data*, 14, 1041-1100.

Bolton, J.R. and Linden, K.G. (2003). Standardization of methods for fluence (UV dose) determination in bench-ccale UV experiments. *Journal of Environmental Engineering*, 129, 209-215.

Brezonik, P.L. and Fulkerson-Brekken, J. (1998). Nitrate-Induced photolysis in natural waters: Controls on concentrations of hydroxyl radical photo-intermediates by natural scavenging agents. *Environmental Science & Technology*, 32, 3004-3010.

Buxton, G.V., Greenstock, C.L., Helman, W.P. & Ross, A.B. (1988) Critical review of rate constants for reactions of hydrated electrons, hydrogen atoms and hydroxyl radicals ($^{\cdot}OH/^{\cdot}O^-$) in aqueous solution. *Journal of Physical and Chemical Reference Data*, 17, 513-886.

Chow, C.W.K., Fabris, R., and Drikas, M. (2004). A rapid fractionation technique to characterise natural organic matter for the optimisation of water treatment processes. *Journal of Water Supply: Research and Technology - AQUA*, 53, 85-92.

Clescerl, L. S., Greenberg, A. E., and Eaton, A. D., eds. (1999). *Standard Methods for Examination of Water & Wastewater*, 20th edition, American Public Health Association, 1999.

Crittenden, J.C., Hu, S., Hand, D.W., and Green, S.A. (1999). A kinetic model for H_2O_2/UV process in a completely mixed batch reactor. *Water Research*, 33, 2315-2328.

Englezos, P. and Kalogerakis, N. (2001). *Applied parameter estimation for chemical engineers*. Marcel Dekker, Inc., New York.

Eriksen, T.E., Lind, J., and Merényi, G. (1985). On the acid-base equilibrium of the carbonate radical. *Radiation Physics and Chemistry*, 26, 197-199.

Ershov, B. and Gordeev, A. (2008). A model for radiolysis of water and aqueous solutions of H_2, H_2O_2 and O_2. *Radiation Physics and Chemistry*, 77, 928-935.

Glaze, W.H., Lay, Y., and Kang, J. (1995). Advanced oxidation processes. A kinetic model for the oxidation of 1,2-dibromo-3-chloropropane in water by the combination of hydrogen peroxide and UV radiation. *Industrial & Engineering Chemistry Research*, 34, 2314-2323.

Goldstone, J. V., Pullin, M. J., Bertilsson, S., and Voelker, B. M. (2002). Reactions of hydroxyl radical with humic substances: Bleaching, mineralization, and production of bioavailable carbon substrates. *Enviromental Science Technol*ogy, *36*, 364-372.

Holcman, J., Bjergbakke, E., and Sehested, K. (1987). The importance of radical-radical reactions in pulse radiolysis of aqueous carbonate/bicarbonate. *Proceedings of the Sixth Tihany Symposium on Radiation Chemistry*. pp. 149-153. Academic Kiado Publishing, Budapest, Hungary.

Klassen, N.V., Marchington, D., and McGowan, H.C.E. (1994). H_2O_2 determination by the I_3^- method and by $KMnO_4$ titration. *Analytical Chemistry*, 66, 2921-2925.

Liao, C. and Gurol, M.D. (1995). Chemical oxidation by photolytic decomposition of hydrogen peroxide. *Environmental Science & Technology*, 29, 3007-3014.

Linden, K. G., Rosenfeldt, E. J., and Kullman, S. W. (2007). UV/H_2O_2 degradation of endocrine-disrupting chemicals in water evaluated via toxicity assays. *Water Science & Technology*. *55*, 313-319.

Neta, P. and Dorfman, L. (1968). Pulse radiolysis studies. 13. Rate constants for reaction of hydroxyl radicals with aromatic compounds in aqueous solutions. *Advances in Chemistry Series*, 222-230.

Neta, P., Grodkowski, J., and Ross, A.B. (1996). Rate constants for reactions of aliphatic carbon-centered radicals in aqueous solution. *Journal of Physical and Chemical Reference Data*, 25, 709-1050.

Neta, P., Huie, R.E., and Ross, A.B. (1988). Rate Constants for Reactions of Inorganic Radicals in Aqueous Solution. *Journal of Physical and Chemical Reference Data*, 17, 1027-1284. Nikolaou, A.D. and Lekkas, T.D. (2001). The role of natural organic matter during formation of chlorination by-products: a review. *Acta Hydrochimica et Hydrobiologica*, 29, 63-77.

Reisz, E., Schmidt, W., Schuchmann, H., and von Sonntag, C. (2003). Photolysis of ozone in aqueous solutions in the presence of tertiary butanol. *Environmental Science & Technology*, 37, 1941-1948.

Sarathy, S.R. & Mohseni, M. (2007). The impact of UV/H_2O_2 advanced oxidation on molecular size distribution of chromophoric natural organic matter. *Environmental Science & Technology*, 41, 8315-8320.

Sarathy, S.R. & Mohseni, M. (2009). The fate of natural organic matter during UV/H_2O_2 advanced oxidation of drinking water. *Canadian Journal of Civil Engineering*, 36, 160-169.

Sharpless, C.M. and Linden, K.G. (2003). Experimental and model comparisons of low- and medium-pressure Hg lamps for the direct and H2O2 assisted UV photodegradation of N-nitrosodimethylamine in simulated drinking water. *Environmental Science & Technology*, 37, 1933-1940.

Song, W., Ravindran, V., and Pirbazari, M. (2008). Process optimization using a kinetic model for the ultraviolet radiation-hydrogen peroxide decomposition of natural and synthetic organic compounds in groundwater. *Chemical Engineering Science*, 63, 3249-3270.

Stefan, M.I., Mack, J., and Bolton, J.R. (2000). Degradation pathways during the treatment of methyl tert-butyl ether by the UV/H2O2 process. *Environmental Science & Technology*, 34, 650-658.

Tühkanen, T. (2004). "UV/H_2O_2 processes." *Advanced oxidation processes for water and wastewater treatment,* Parsons, S., ed., IWA Publishing: London, UK, 356.

van den Broeke, J., Ross, P. S., van der Helm, A. W. C., Baars, E. T., and Rietveld, L. C. (2008). Use of online UV/Vis-spectrometry in the measurement of dissolved ozone and AOC concentrations in drinking water treatment. *Water Science & Technology*, *57*, 1169-75.

von Sonntag, C., Dowideit, P., Fang, X., Mertens, R., Pan, X., Schuchmann, M.N., and Schuchmann, H. (1997). Fate of peroxyl radicals in aqueous solution. *Water Science & Technology*, 35, 9-15.

Weinstein, J. and Bielski, B. (1979). Kinetics of the interaction of HO_2 and O_2^- radicals with hydrogen peroxide - Haber-Weiss reaction. *Journal of the American Chemical Society*, 101, 58-62.

Westerhoff, P., Aiken, G., Amy, G., and Debroux, J. (1999). Relationships between the structure of natural organic matter and its reactivity towards molecular ozone and hydroxyl radicals. *Water Research*, 33, 2265-2276.

Westerhoff, P., Mezyk, S.P., Cooper, W.J., and Minakata, D. (2007). Electron pulse radiolysis determination of hydroxyl radical rate constants with Suwannee River Fulvic Acid and other dissolved organic matter isolates. *Environmental Science & Technology*, 41, 4640-4646.

Appendix B Analytical Methods

Iodide/Iodate Actinometry

Iodide irradiated by UV leads to the linear formation of triodide, which is used to determine the lamp output based on photochemical theory. Iodate acts as an electron scavenger and prevents the back reaction of the free electron with the iodine atom following UV excitation of KI.

PROCEDURE

1.) Prepare 0.01M sodium borate buffer(1, 2)
   - 0.381g $Na_2B_4O_7.10H_2O$ per 100 mL distilled water

2.) Measure pH of solution (pH ~ 9.25)
3.) Prepare 0.1M potassium iodate in borate buffer
   - 2.14g KIO_3 per 100mL borate buffer

   - This solution can be stored for several weeks in an opaque container.

4.) Prepare 0.6M potassium iodide in borate-iodate solution
   - 9.96g KI per 100mL borate-iodate solution

5.) Measure iodide-iodate-borate solution temperature in degrees Celsius. (T)
6.) Measure absorbance at 300nm (A_{300}) and 450 nm (A_{450i})
7.) Irradiate with UV under desired geometry.
8.) Measure absorbance at 450 nm (A_{450f})

CALCULATIONS

Quantum yield determination:

$$\Phi = 0.75\ [1 + 0.02\ (T-20.7)]\ [1 + 0.23\ (C-0.577)]$$

where: Φ = quantum yield (mol/einstein)

T = solution temperature in degrees Celsius

C = molar concentration of iodide = [KI] = $A_{300}/1.061$

Fluence determination:

$$H' = \frac{4.72 \times 10^5 \cdot \Delta A_{450} \cdot V \cdot 1000}{\varepsilon_{450} \cdot \Phi \cdot A}$$

where: H' = Fluence (mJ/cm^2)

ΔA_{450} = change in absorbance at 450 nm (cm^{-1}) = (A_{450f} - A_{450i})

V = solution volume (L)

ε_{450} = molar absorption coefficient of triodide at 450 nm = 1600 (M^{-1} cm^{-1})

Φ = quantum yield (mol/einstein)

A = area irradiated (cm^2) = π * (radius of dish)^2

$4.72*10^5$ = converting einsteins to joules

1000 = converting J to mJ

Analysis of H_2O_2

Solution A:

500ml	Potassium hydrogen phthalate (KHP)	10g
	+ Distilled water (DW)	

Solution B:

500ml	KI	33g
	NaOH	1g
	Ammonium molybdate tetrahydrate	0.1g
	+DW	

Analysis:

Wavelength	351nm
Zero	DW
Blank	2.5mL of each solution A and B
	dilute with DW in 10mL volumetric flask
Sample	2.5mL of each A and B
	0.5 of sample
	dilute with DW in 10mL volumetric flask

Calculation:

Peroxide (ppm) : $(Abs_{Sample}-Abs_{Blank})*10*D/(0.7776*S)$

D is additional dilution (1 if none), S sample volume (=0.5mL)

Measurement of Alkalinity

Alkalinity measurement was conducted according to the Standard Method 2320 B (Titration Method). A few (2-3) droplet of bromocresol green indicator solution, pH 4.5 indicator, were dropped in a 100 mL sample solution with stir bar. Sulfuric Acid (H_2SO_4, standard solution 0.02 N) was added slowly until the color turned from blue to yellow.

The amount of acid used was read and alkalinity was calculated as below:

$$Alkalinity\ (mg\ CaCO_3) = \frac{A * N * 50000}{mL\ Sample}$$

Where A is the volume of the acid used (mL) and N is the normality of the acid (0.02 N).

For alkalinities below 20 ppm ($CaCO_3$) , the low alkalinity method (SM 2320 B, 4.d) was used .

High Performance Size Exclusion Chromatography (HPSEC)

To obtain a better resolution and more clear peaks some modifications were performed on a previously applied HPSEC technique, as reported by Sarathy and Mohseni (2007). Sarathy and Mohseni (2007) used phosphate buffer (pH=6.8, Ionic strength= 0.1 M) however this eluent showed to be not appropriate for the column used in this work, and inappropriate calibration was obtained.

Therefore Sodium acetate was replaced the phosphate buffer; however experiments needed to bed one in order to find the best concentration giving the most clear resolution sand separation of peaks. The following figure shows the effect of solution concentration on the separation of the peaks in the BI and SR water chromatograms.

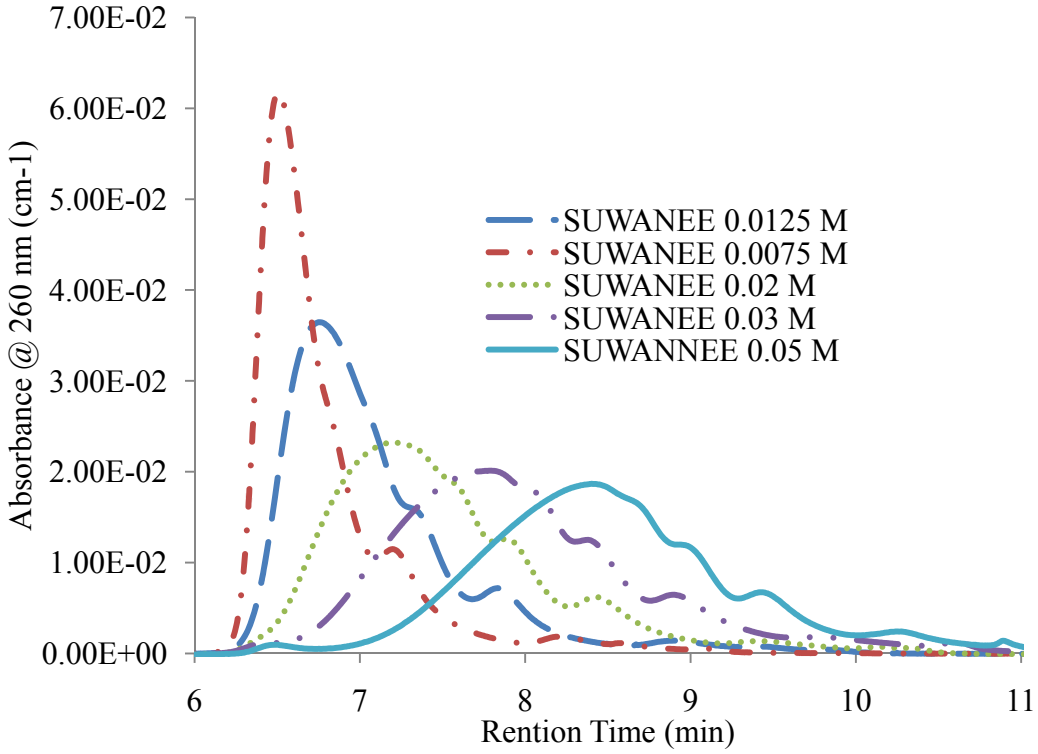

Figure B.1: Effect of different concentrations of eluent (Sodium Acetate) on separation/ resolution of SR NOM HPSEC chromatogram

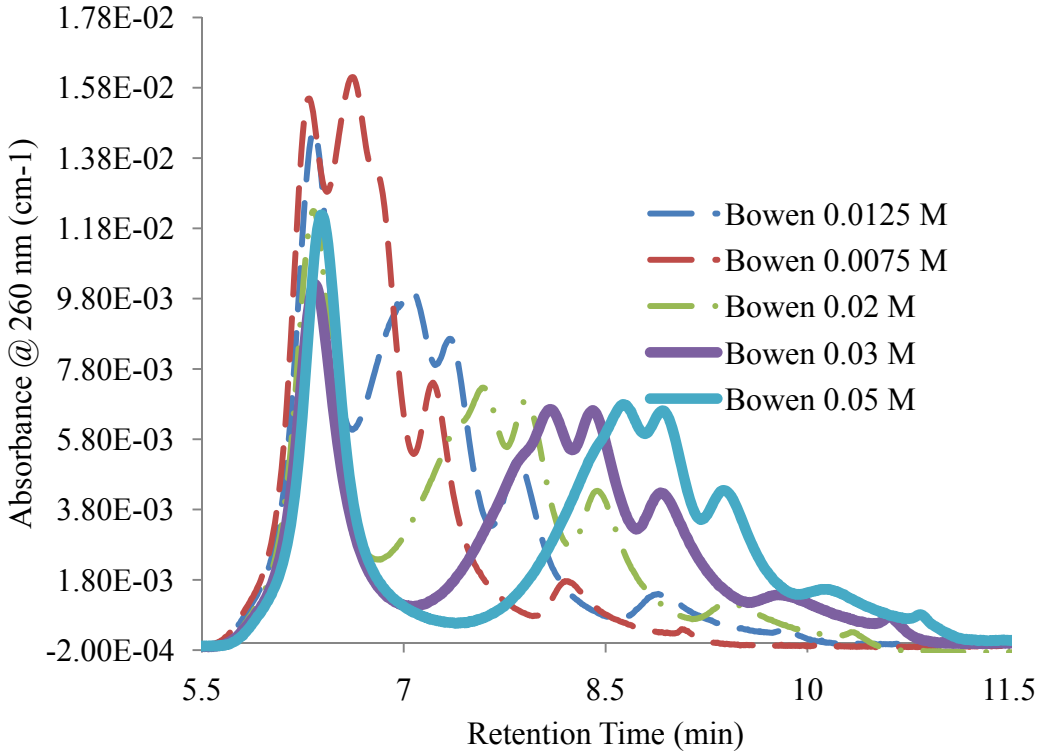

Figure B.2: Effect of different concentrations of elunet (Sodium Acetate) on separation/ resolution of BI NOM HPSEC chromatogram

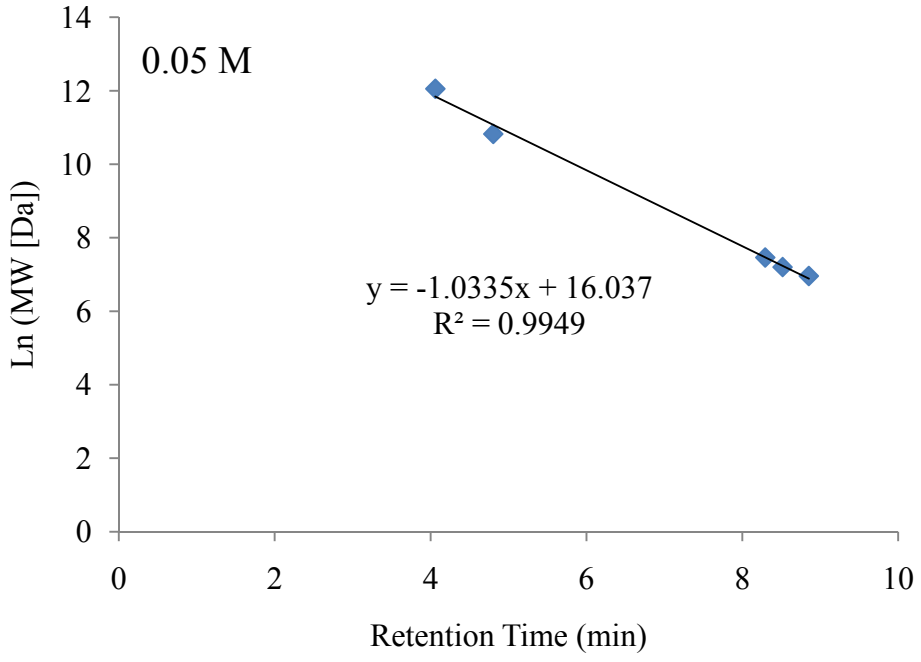

Figure B.3: Calibration curve used to convert retention time to AMW of NOM

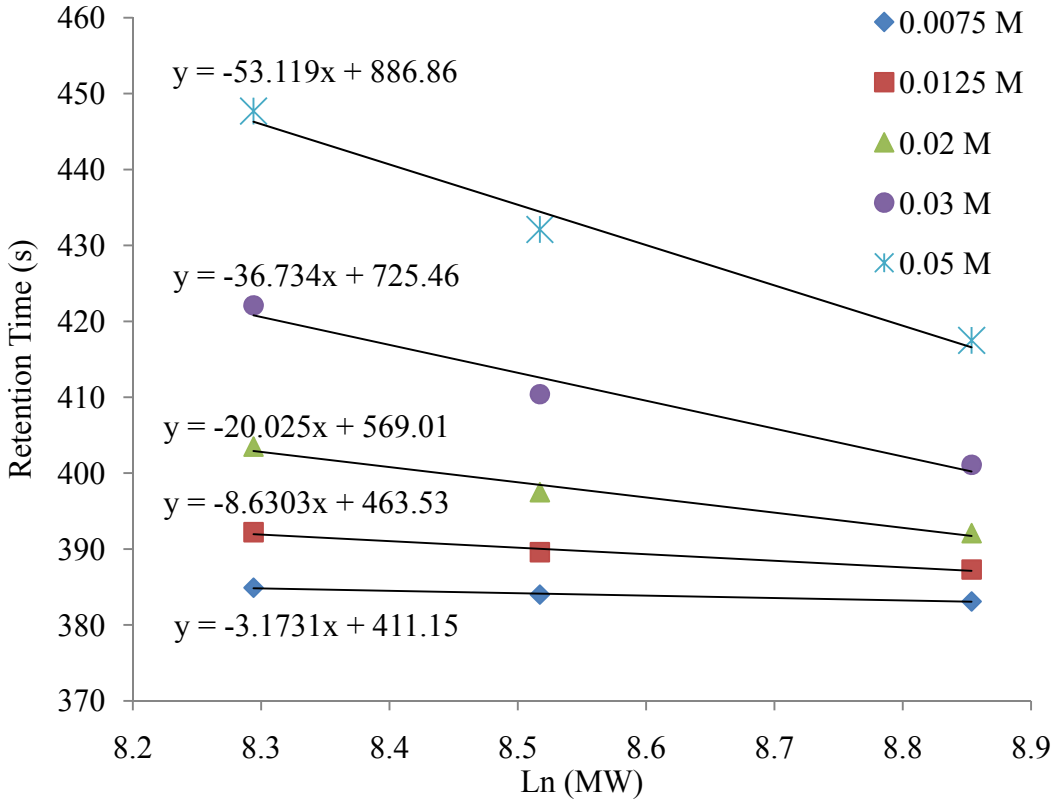

Figure B.4: Different calibration curve obtained for standard polymers using different concentration of sodium acetate

References

Rahn RO. Potassium Iodide as a Chemical Actinometer for 254 nm Radiation: Use of Iodate as an Electron Scavenger. *Photochemistry and Photobiology*. 1997;66(4):450–455.

Rahn, R. O., P. Xu, and S. Miller.. Dosimetry of room-air germicidal (254 nm) radiation using spherical actinometry. *Photochem. Photobiol*. 1999;70:314–318.

Rahn, R. O., M. Stefan, J. R. Bolton, E. Goren, P-S. Shaw, and K. R. Lykke. Quantum yield of the iodide-iodate chemical actinometer: dependence on wavelength and concentration. *Photochem. Photobiol*. 2003;78:146–152.

Klassen, N.V., Marchington, D. & McGowan, H.C.E. (1994) H_2O_2 Determination by the I3-Method and by KMnO4 Titration. Analytical Chemistry, 66, 2921-2925.

Nissinen TK, Miettinen IT, Martikainen PJ, Vartiainen T. Molecular size distribution of natural organic matter in raw and drinking waters. *Chemosphere*. 2001;45(6-7):865-873.

Appendix C Effect of UV/H_2O_2 on AMW Distribution of SR NOM

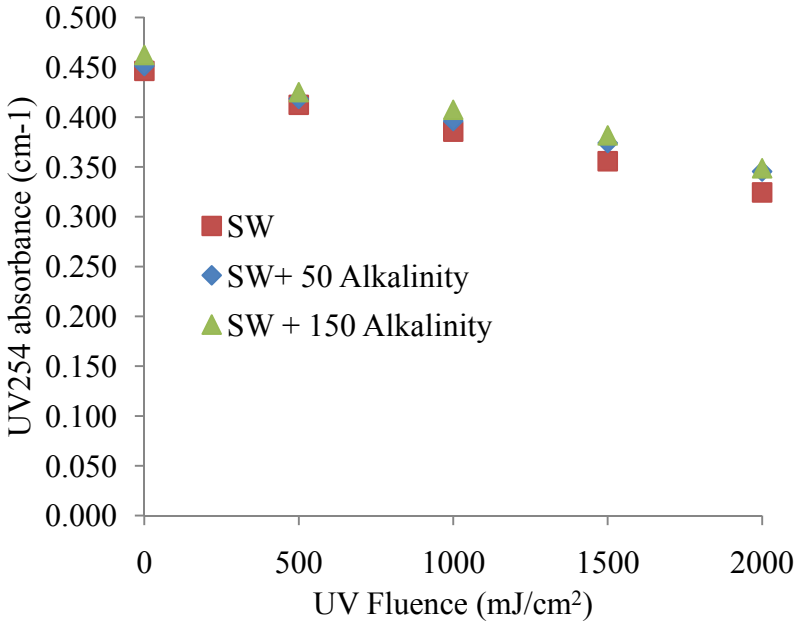

Figure C.1: UV_{254} profile of SR water (TOC~ 10 ppm) during UV/H_2O_2 treatment, [H_2O_2] ~10 ppm.

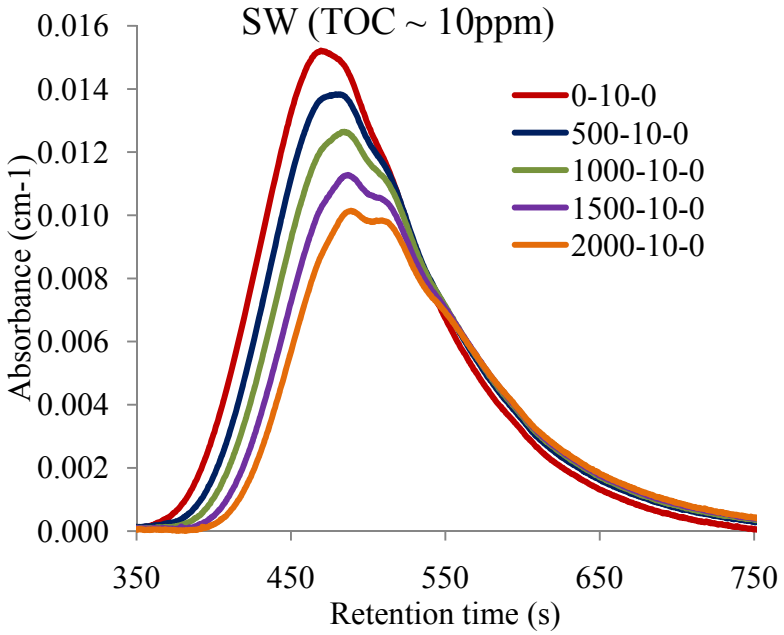

Figure C.2: AMW Distribution of SR NOM water (TOC~ 10 ppm, 0 Alkalinity) during UV/H_2O_2 treatment

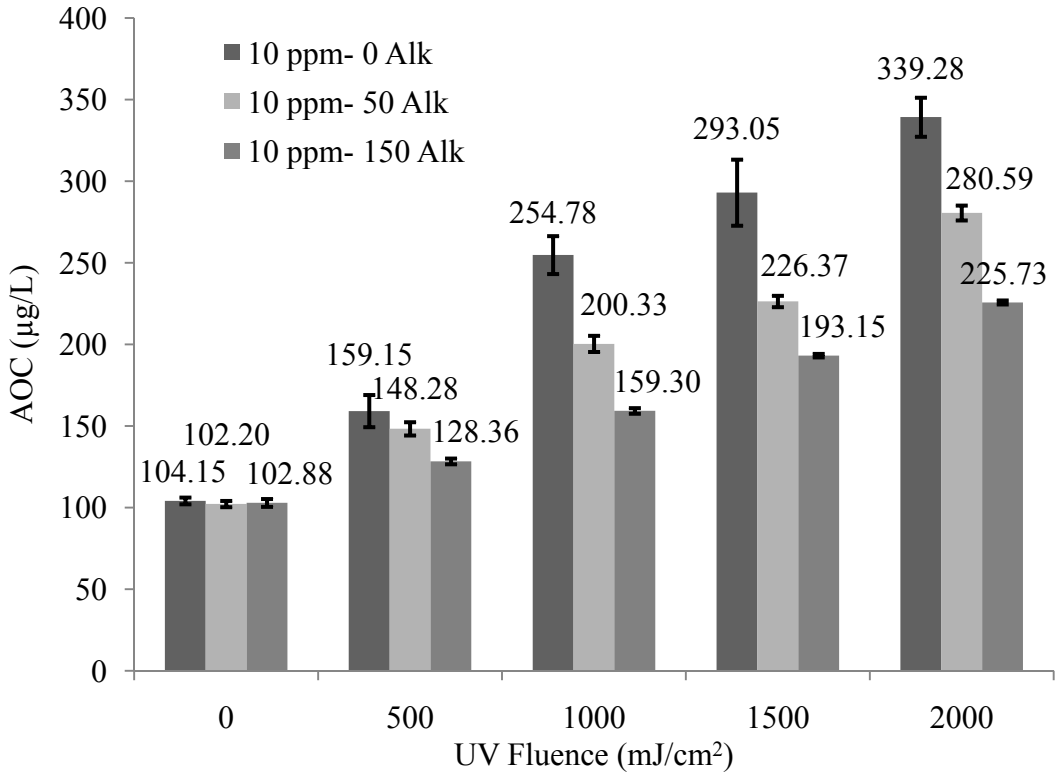

Figure C.3 : AOC profile of SR water (TOC ~ 10 ppm) with different alkalinities during UV/H_2O_2 treatment

Appendix D Statistical Analysis of the Correlation between AOC and BDOC

Table D.1: Results for the pilot plant study

	Coefficient	Std. Error	t	p
y_0	0.0485	0.0519	0.9344	0.3624
a	0.0034	0.0005	7.3699	<0.0001

Table D.2: Results for the UV/H_2O_2 study

	Coefficient	Std. Error	t	p
y_0	-0.0908	0.0606	-1.4988	0.1648
a	0.0055	0.004	12.5237	<0.0001

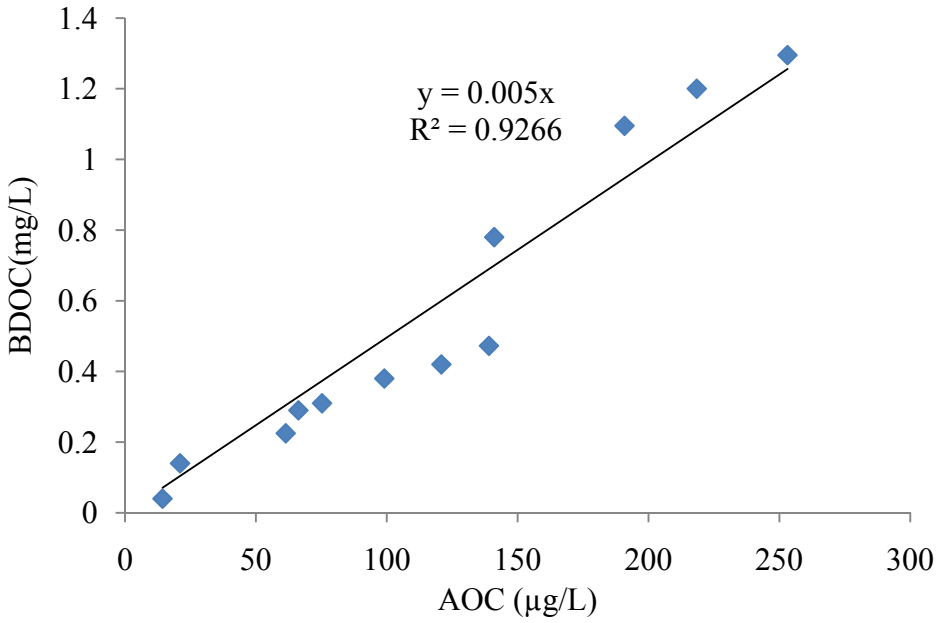

Figure D.1: BDOC vs. AOC of UV/H_2O_2 treated surface waters (b=0)

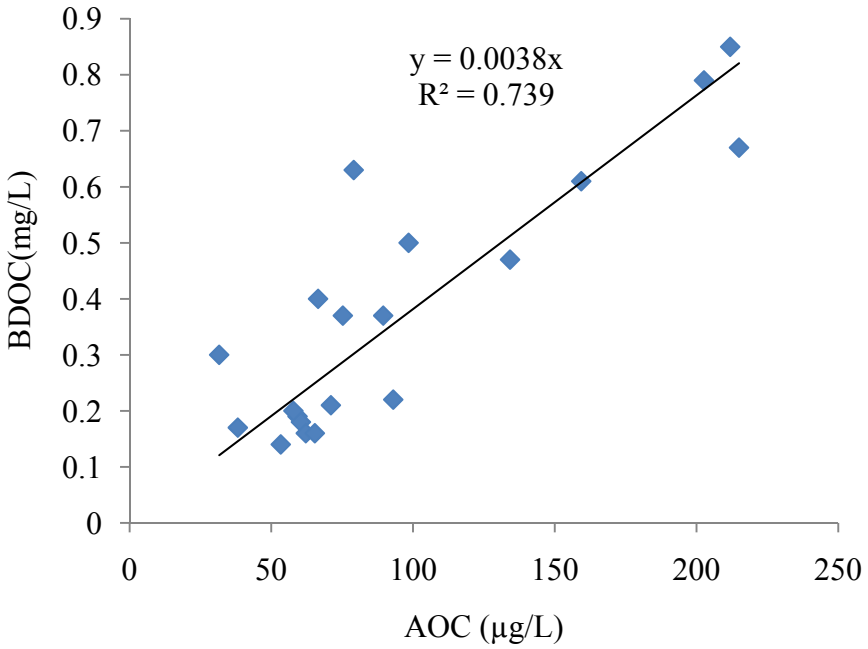

Figure D.2: BDOC vs. AOC of the pilot plant study (b=0)